Environmental Controls on Calving in Grounded Tidewater Glaciers

Susan Jennifer Cook

Submitted to Swansea University in fulfilment of the requirements for the Degree of Doctor of Philosophy

Swansea University

2012

Abstract

The calving of icebergs is an important mass loss process in many glaciers worldwide, including the Antarctic and Greenland Ice Sheets. Despite its importance, calving is still relatively poorly reproduced in ice sheet models, largely due to the complexity of the processes involved. In this thesis a new grounded tidewater glacier model is presented using a physically realistic calving criterion, based on the penetration of crevasses in the ice, applied in a two-dimensional, vertically-resolved ice flow model using the finite element software Elmer. This is the only tidewater glacier model so far developed which can been used to model individual calving events, allowing a detailed analysis of calving at the terminus of the glacier. The model is tested with four environmental variables which have been thought to affect calving rates: water depth in crevasses, basal water pressure, undercutting of the calving face by subaqueous melt and backstress from ice mélange. Of the four variables, only crevasse water depth and basal water pressure were found to have a significant effect on terminus behaviour when applied at a realistic magnitude. This is in contrast to previous modelling and observational studies, which had suggested that ocean temperatures could strongly influence the calving front.

The apparent contradiction in results is likely to be caused by either the feedback processes linking air and ocean temperatures, or by the fact that floating ice is likely to respond more strongly to subaqueous melt and backstress than grounded ice. The lack of basal elevation data makes it difficult to distinguish grounded and floating ice in many regions. The results presented highlight the importance of good basal elevation data in interpreting glacier behaviour. They also raise the possibility that Greenland outlet glaciers could respond more strongly than previously thought to the recent trend of increased surface melt observed in Greenland, as surface ablation can strongly affect calving dynamics through both the pooling of water in crevasses and changing water pressure at the glacier bed.

Declaration

This work has not previously been accepted in substance for any degree and is not being concurrently submitted in candidature for any degree.

Signed ..... (candidate)

Date .....

Statement 1

This thesis is the result of my own investigations, except where otherwise stated. Where correction services have been used, the extent and nature of the correction is clearly marked in a footnote(s).

Other sources are acknowledged by footnotes giving explicit references. A bibliography is appended.

Signed ..... (candidate)

Date .....

Statement 2

I hereby give consent for my thesis, if accepted, to be available for photocopying and for inter-library loan, and for the title and summary to be made available to outside organisations.

Signed ..... (candidate)

Date .....

Contents

Acknowledgements

First and foremost, thanks go to my two supervisors, Tavi Murray and Ian Rutt. Without their help, guidance and encouragement this thesis would never have been completed. Also to Thomas Zwinger, who generously gave his time to help me get to grips with Elmer and solve the many problems encountered during the model development, and his family who kindly looked after me on trips to Helsinki.

This PhD has been supported by funding from a number of bodies. It could not have been performed without a studentship from Swansea University. Additional funding for travel and computer resources was provided by HPC - Europa2 project (project No. 228398) with the support of the European Commission Capacities AreaResearch Infrastructures Initiative and resources from CSC - IT Center for Science Ltd. I would also like to thank the IOP for providing conference funding during my studies. This research forms part of the GLIMPSE project funded by the Leverhulme Trust Research Leadership Scheme.

Modelling work relies heavily on data from other sources, and thanks are due to Shad O'Neel and the US Geological Surveys Climate and Land Use Program for the data provided from Columbia Glacier, as well as some very valuable discussion on the nature of tidewater glaciers. The data from Helheim Glacier was kindly provided by Adrian Luckman, Nick Selmes, Tim James, Anne Goldsack and Yoann Drocourt of Swansea University. Thanks to them all for helping patiently with all my most unreasonable requests. Last and not least, thanks go to all my friends and family for their patience during the writing process.

List of Figures

List of Tables

List of Notation

Vectors

$\{x, y, z\}$ Coordinate system x along flowline, y across flow, z vertical (m)

$\mathbf{u}$	2D velocity vector (m a^{-1})
u_b	Basal velocity (m a^{-1})
$\boldsymbol{\sigma}$	Cauchy stress tensor (kg m^{-1} a^{-2})
$\boldsymbol{\tau}$	Deviatoric stress tensor ((kg m^{-1} a^{-2})
τ	Second invariant of deviatoric stress tensor ((kg m^{-1} a^{-2})
τ_b	Basal shear stress (kg m^{-1} a^{-2})
$\dot{\epsilon}_{ij}$	Strain rates kg m^{-1} a^{-2})
$\mathbf{p}$	Pressure (kg m^{-1} a^{-2})

Scalars

ϕ	Ice flux (m^3 a^{-1})
μ	Viscosity (kg a^{-1} m^{-1})
T	Ice temperature (K)

s	Surface elevation (m)
H	Ice thickness (m)
W	Channel width (m)
L	Glacier length (m)
M	Surface mass balance (m a^{-1})
U_C	Calving rate (m a^{-1})
ϕ_C	Calving flux (m^3 a^{-1})
H_f	Flotation thickness (m)
H_o	Height over flotation thickness (m)
H_m	Mean ice thickness (m)
D	Depth of the bed below sea level (m)
P_w	Basal water pressure (kg m^{-1} a^{-2})
N	Effective pressure (kg m^{-1} a^{-2})
R_b	Roughness parameter
λ	Distance between obstacles (m)
a	Characteristic obstacle size (m)
A_s	General tunable sliding parameter
D_w	Depth of water in crevasses (m)
F_f	Force acting on calving face (kg m^{-1} a^{-2})
M_f	Melt rate at the calving face (m a^{-1})
σ_{crit}	Fracture toughness of ice (kg m^{-1} a^{-2})
d	Damage variable

Constants

g	Gravitational acceleration (m a^{-2})
ρ_i	Ice density (m kg^{-3})
ρ_{sw}	Salt water density (m kg^{-3})
ρ_{fw}	Fresh water density (m kg^{-3})
A	Arrhenius factor ((m kg)$^{1/2}$ a^{-2})
A_0	Arrhenius constant (m)
Q	Creep activation energy (J)
R	Universal gas constant (J mol^{-1} K^{-1})
n	Glenn's coefficient

For any variable the subscript t indicates the value of that variable at the terminus. The subscript i indicates the value at a specific mesh node (with one exception, where ρ_i indicates density of ice at any and all nodes). The subscript n is used to indicate the value at a specific timestep.

Chapter 1

Introduction

The calving of ice as icebergs is an important process in tidewater glaciers worldwide, in locations such as Svalbard (Blaszczyk et al., 2009), Alaska (O'Neel et al., 2003; Larsen et al., 2007) and Patagonia (Venteris, 1999). It is also a significant mass loss contributor for both the Greenland and Antarctic Ice Sheets (Church et al., 2001; Rignot and Thomas, 2002), where outlet glaciers drain ice into the ocean.

Quantifying mass loss by calving is particularly important as recent studies show that tidewater glaciers can be strongly sensitive to climate change (Howat et al., 2007; Larsen et al., 2007). Recently, many tidewater glaciers are observed to have entered a period of marked retreat, such as those in in Alaska (Krimmel, 2001; O'Neel et al., 2003) and the Antarctic Peninsula (Cook et al., 2005). Fluctuations in terminus position have also been observed in many Greenland outlet glaciers, with concurrent surface lowering and acceleration (Howat et al., 2007; Luckman et al., 2006). Such changes can lead to significant mass loss from the ice sheets by dynamic thinning (Pritchard et al., 2009). Increases in mass loss by changes in calving have the potential to significantly increase the contribution of tidewater glaciers and ice sheets to global sea level rise, and a good understanding of tidewater processes is key to making accurate predictions of future mass loss from both tidewater glaciers and ice sheets.

Figure 1.1: Photograph of calving front of Helheim Glacier, showing the dense distribution of transverse crevasses around the terminus which leads to calving. Photo: N. Selmes

1.1 Calving Processes

Calving occurs via the fracturing of ice, with sections of a marine-terminating glacier breaking away from the glacier body. The nature of calving events can vary significantly depending on the type of glacier. In ice shelves, motion is opposed solely by drag from the sides of the shelf. In this case, calving normally takes the form of large tabular icebergs, which may measure many kilometres across. These icebergs form as large, isolated rifts in the ice propagate laterally some distance behind the ice front (Joughin and MacAyeal, 2005).

For narrower tidewater glaciers, the process occurs on a much smaller scale. Here calving events generally occur within one or two ice thicknesses of the front (Hughes, 1992), separating along one of the many crevasses in the highly fractured terminus region (see Fig. 1.1). There are a number of ways in which this calving can take

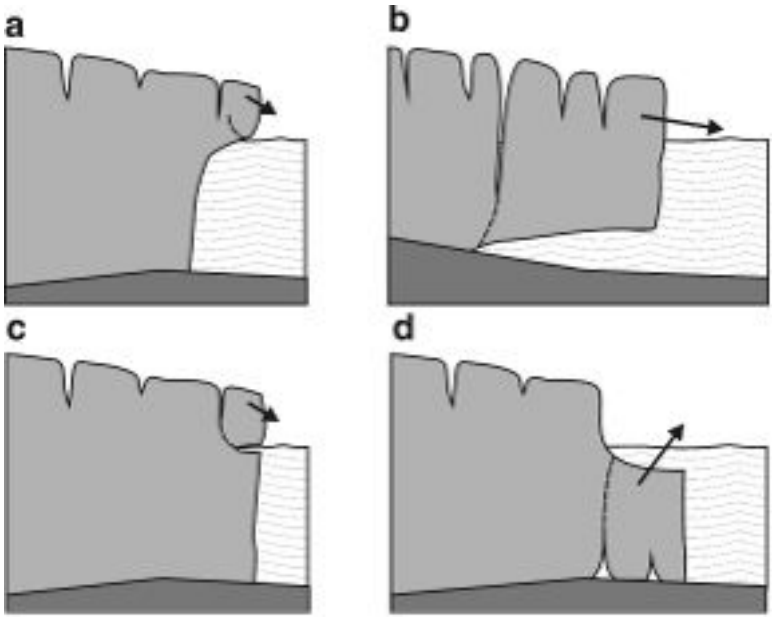

Figure 1.2: Main calving processes at a grounded calving front: (a) Launch of serac. (b) Calving at deep surface crevasse. (c) Undercutting by melting at waterline. (d) Break away of ice foot. Figure from van der Veen (2002)

place, with some of the main mechanisms identified by Kirkbride and Warren (1997) illustrated in Figure 1.2. The glacier can lose ice in small calving events by the launch of subaerial seracs (Figure 1.2a). Alternatively, large icebergs may be produced when separation occurs along a deep crevasse reaching to the glacier bed (Figure 1.2b). Both processes are controlled by the depth of crevasses in the ice surface. These crevasses are caused either by longitudinal strain arising from a velocity gradient along the glacier, or, near the front, crevasses can be caused by the imbalance of hydrostatic and lithostatic pressures. The rate of calving by this method is also affected by surface melting; crevasses which fill with water tend to penetrate deeper as the water pressure helps to oppose the ice overburden pressure (Benn et al., 2007b). The calving process may also be enhanced by the undercutting of ice at the front of the glacier, which can leave the surrounding ice unsupported hence increasing fracturing (Figure 1.2c).

As ice calves above the waterline, some glaciers build up a block of ice below the surface of the water, which is highly susceptible to buoyant forces, as it is less

dense than the water around it. Eventually torque from these buoyant forces causes sections of the foot to break away (Figure 1.2d). This process is inherently of a lower order than those above, because the build up of such an ice foot is limited by the rate of ice loss above the waterline (Benn et al., 2007b). If a glacier has a floating tongue, the buoyancy forces acting on the floating ice section mean that basal crevassing becomes increasingly important, with tidal action flexing the floating tongue and causing fracturing of the ice.

The calving processes acting in different glaciers can have very different natures, and therefore to simplify the problem, this thesis is restricted to consideration of tidewater glaciers with grounded termini. This restricts the range of mechanisms which need to be explored, although ultimately there will be a discussion of how the results could be extended to floating ice. Calving from marine-terminating glaciers is usually quantified by the calving rate, defined as the difference between velocity at the glacier's terminus and the change in its length over time:

$$U_c = u_t - \frac{dL}{dt}, \tag{1.1}$$

where U_c is the calving rate, u_t is the velocity at the terminus and L is the glacier's length. Predicting the calving rate for a glacier is complicated by the feedback between calving and wider glacier dynamics, and also the action of external environmental processes on fracturing in a tidewater glacier, which can strongly affect the calving rate.

1.2 Tidewater Glacier Behaviour

1.2.1 Calving and glacier dynamics

Many tidewater glaciers have been observed to be in a stable position, meaning that the average calving front position remains at the same location over long periods of

time, although since calving will occur frequently the exact position may vary. It is when the glacier retreats or advances from this position that the behaviour becomes particularly interesting with complex feedback between calving and glacier dynamics occurring. The link between calving and glacier dynamics was first thoroughly investigated by Meier and Post (1987). They suggested that loss of ice at the calving front can decrease back stress up-glacier, causing an increase in velocity. Likewise an increase in velocity around the front increases longitudinal strain rates, increasing crevassing and therefore increasing calving rates. This suggests there may be a positive feedback effect between changes in calving rate and glacier velocity.

On long timescales, the cause of tidewater glacier retreat is often attributed to surface thinning by ablation, which can trigger retreat from a stable terminus position (for example van der Veen (1996) at Columbia Glacier and Pritchard and Vaughan (2007) on the Antarctic Peninsula). Other tidewater glaciers show a variable terminus position on a timescale too short to be caused by long-term trends in surface mass balance, such as Greenland outlet glaciers (Joughin et al., 2008b) and Svalbard tidewater glaciers (Mansell et al., 2012), which show significant annual variations in terminus position. In this case the glaciers are hypothesized to be responding to short term changes in climate variables such as atmospheric and ocean temperatures.

There are two hypothesized mechanisms for these short time-scale tidewater glacier terminus variations. The first, as proposed by van der Veen (2002) is that retreat is triggered by an increase in the speed of the glacier, which thus increases calving rate. This could occur by two mechanisms: firstly, if velocity increases more strongly down-glacier there will be an increase in longitudinal strain which will increase fracturing; secondly, if the glacier increases in speed this will cause dynamic thinning, which can make the terminus region unstable (prone to retreat). The relevance of this mechanism is supported by observations of seasonal speed-up in Greenland glaciers which indicate surface meltwater penetrates to the bed of outlet glaciers, effectively lubricating motion by increasing the basal water pressure (Zwally et al., 2002).

Alternatively, retreat may be caused by changes at the calving front; if calving rates undergo a sudden increase, the loss of ice at the terminus will reduce backstress, hence causing an increase in velocity and thinning up-glacier. Potential causes of increases in calving rate include pooling of surface melt water in crevasses, undercutting of the terminus by subaqueous melt and a decrease in backstress from a proglacial ice mélange. This is the likely mechanism for the retreat of Jakobshavn Glacier, where the retreat and acceleration was preceded by the break-up of a floating tongue (Joughin et al., 2004; Thomas, 2004), attributed to ocean warming by Holland et al. (2008). The different environmental variables which can affect calving rates are discussed in more detail below.

1.2.2 Ocean forcing

Ocean temperature may have an effect on calving dynamics via changes in subaqueous melt, which can undercut the calving front. Undercutting is thought to change the stress distribution around the calving front and enhance fracturing (Benn et al., 2007b). This is confirmed by modelling work by O'Leary (2011), indicating that undercutting can displace the stress field around a glacier terminus by up to four times the horizontal extent of the undercut cavity. If calving is controlled by the stress distribution in the ice, this could displace the calving location and hence increase calving rates. It had previously been considered that undercutting was only significant for glaciers with a low calving rate, allowing sufficient time for melting to work at the face between calving events (Vieli et al., 2001). However recent studies using measurements of water temperature and velocity to estimate heat flux to the calving face of tidewater glaciers have revealed that subaqueous melt rates may be sufficiently high to affect even fast flowing tidewater glaciers (Motyka et al., 2003; Rignot et al., 2010). This is supported by observations in East Greenland that retreat of tidewater glaciers in the early 2000s coincided with a period of increased water temperature, with undercutting being a likely mechanism for enhanced retreat (Murray et al., 2010; Seale et al., 2011).

Another effect of increased ocean temperatures is important in polar glaciers with narrow fjords. Here, the build up of a mixture of sea ice and calved icebergs in the proglacial fjord is referred to as an ice mélange, which is thought to have a significant effect on calving in outlet glaciers. The mélange is thought to be able to significantly inhibit calving rates by providing backstress acting on the calving face (Amundson et al., 2010). It may also have an effect in two other ways: firstly, in the case of a glacier with a floating terminus, by suppressing ocean waves and thus decreasing flexing acting on the calving front. Secondly, by protecting the fjord waters from wind, decreasing mixing and therefore suppressing melt rates which require convection in the water to be significant. Observational evidence has linked the break-up of a proglacial ice mélange to increases in calving rate in various Greenland outlet glaciers (Reeh et al., 2001; Joughin et al., 2008c).

1.2.3 Effects of air temperature

Increases in air temperature will affect tidewater glaciers by increasing surface ablation and meltwater availability. This can affect the glacier by causing meltwater to pool in surface crevasses, which can increase the penetration of the crevasses through the ice and thus enhance calving rates. If the meltwater penetrates to the bed of the glacier it can also enhance basal water pressure, causing an increase in the glacier velocity. If the glacier velocity increases this can cause an increase in calving rate and potentially terminus retreat (van der Veen, 2002). Changes in basal water pressure have been found to be significant in tidewater glaciers in Alaska (Meier and Post, 1987; Kamb et al., 1994) and Svalbard (Vieli et al., 2000). Seasonal increases in velocity caused by changes in basal water pressure have been observed in Greenland, but are proportionally much higher in land-terminating glaciers than for tidewater outlet glaciers (Joughin et al., 2008a; Andersen et al., 2011; Seale et al., 2011). Previous modelling work on Helheim Glacier, East Greenland by Nick et al. (2009) also found that perturbations in basal lubrication and surface ablation had a far less significant effect on modelled glacier dynamics than perturbations in lon-

gitudinal stress at the calving front. In some cases, increased penetration of water to the bed of a glacier has also been linked to a decrease in basal water pressure, as the nature of the subglacial drainage system changes to drain more efficiently (*e.g.* Bartholomew et al., 2010)). Thus the link between surface ablation and calving rate has a complicated nature.

Another possible effect of air temperatures is that increased glacial runoff can enhance circulation of waters in the proglacial fjord, driving increased exposure of the calving front to warm oceanic waters and enhancing melting (Motyka et al., 2003). Studies of subaqueous melt on grounded tidewater glacier termini by plume modelling have also shown that increased subglacial discharge can enhance melting rates at the calving face (O'Leary, 2011; Xu et al., 2012).

1.2.4 Role of modelling

Although the effects of air and ocean temperatures on calving have been hypothesized, it is difficult to determine their relative importance from observational data, as the highly active, crevassed regions around the terminus of a tidewater glacier make a difficult working environment. Most observational data are sourced from satellite images, which are often adversely affected by cloud cover, meaning that repeat measurements are often infrequent or absent during the dark winter months. Making comparisons between different glaciers under particular climatic conditions is also prone to difficulty as in most cases accurate basal topography is not available, and bed slope is thought to be one of the most significant factors behind any particular glacier's response to forcing (Howat et al., 2008; Nick et al., 2009). Little is also known about the conditions at the bed of most tidewater glaciers. The nature of the bed will have have a significant effect on glacier sliding and the response to changes in basal water pressure, which can be crucial factors in a tidewater glacier's behaviour.

The inter-related nature of the environmental processes discussed above and the

difficulty of obtaining sufficient data on tidewater glaciers mean that causes of terminus change are difficult to identify observationally. The use of ice flow models of tidewater glaciers provide an experimental environment in which each variable can be examined individually. The types of model which have been used previously are discussed in detail in Chapter 2. Each has its own successes and failures, but at present no model has successfully coupled a time-evolving ice flow model to a physically realistic calving law with a detailed implementation of all relevant physical processes. The development of such a model to include a full range of environmental processes is an important area of research if we are to build an understanding of how tidewater glaciers are likely to respond to future changes in climate. Because of the wide variety of processes involved in calving there has been some doubt as to whether a universal calving model (able to represent calving in all glaciers) is possible (*e.g.* Bassis, 2011). The work in this study is restricted to calving in grounded tidewater glaciers to simplify the problem, although the extension to floating termini is also discussed.

1.3 Summary

The calving of ice is a significant process in many ice masses around the world, with important consequences for future sea level rise. An understanding of calving behaviour, and its effect on wider glacier dynamics, is important for accurately predicting glacier behaviour. However, calving in tidewater glaciers is a complicated process, governed by complex fracturing within the ice and potentially affected by a wide variety of environmental factors. Trying to distinguish the processes behind fluctuations in glacier termini observationally is a difficult task given the low temporal resolution of most observations available, the inter-related nature of some of the forcing variables and the fact that basal topography is likely to be the most important factor controlling glacier behaviour over short timescales. Numerical modelling is a key tool for understanding the behaviour of such systems, as a model allows the key processes to be isolated and investigated individually to further the under-

standing of calving and ice flow in tidewater glaciers. Previous tidewater glacier models have been limited in the physical processes they represent, and developing these modelling techniques further is key to understanding how tidewater glaciers are likely to respond to future changes in climate.

1.4 Thesis Aims and Outline

This thesis presents a new tidewater glacier model designed to investigate calving processes and the response of grounded tidewater glaciers to external variables. The aims of the work are as follows:

- To produce a tidewater glacier model which improves on the range of physical processes previously included in modelling experiments.
- To investigate the sensitivity of the model to various environmental forcing factors.
- To analyse the relative importance of these factors and make conclusions about the sensitivity of tidewater glacier systems to climatic change which may be used in application in wider research contexts.

A secondary aim is to examine the calving behaviour produced by the model under different environmental forcings. If the model produces a significantly different mean size and frequency of calving event when different environmental variables are applied, this could be compared to observed calving events on tidewater glaciers to contribute to conclusions about the dominant processes acting on the glacier.

The different methods by which calving may be modelled, and the previous work on the topic are discussed in Chapter 2, identifying the limitations of previous work and the areas in which it may be improved upon. The model developed in this thesis is described in Chapter 3, which discusses the numerical implementation used, the selected boundary conditions and the method chosen for implementing calving.

Although the work uses finite element software previously established for use in ice flow modelling, the development presented here is an entirely new application with the code being extended in numerous areas in order to be applied to a tidewater glacier.

The model is applied to two tidewater glaciers. The first application presented in Chapter 4 uses data from Columbia Glacier, Alaska. The chapter investigates the sensitivity of the model to changes in crevasse water depth. The second application, using the automated calving method, uses data from Helheim Glacier, East Greenland. The model is first tested for its sensitivity to changes in the various input parameters as presented in Chapter 5, allowing conclusions to be made about the sensitivity of the model to poorly known input variables, and the potential uncertainty in results.

Four key environmental forcing factors are identified to be investigated at Helheim Glacier; depth of water in crevasses, basal water pressure, subaqueous melt rate on the calving front and back stress from proglacial ice mélange. Chapter 6 presents results of sensitivity testing using each of these variables applied constantly to the model over a 5 year period. A more realistic seasonal pattern of forcing is then applied in Chapter 7. In each case the results are analysed by examination of the modelled terminus evolution and the size and frequency of calving events. This analysis allows conclusions to be drawn about the relative importance of the four environmental forcing factors and their effect on modelled calving behaviour. Chapter 8 draws together discussion from each of the previous four results chapters, identifying the model's strengths and weaknesses, its sensitivity to the various forcing factors applied and drawing comparisons to previous modelling work. Any new conclusions which may be important to our knowledge of tidewater glacier behaviour are summarized in Chapter 9.

1.5 Publication from this thesis

Some of the methods and results of this thesis are published as Cook et al. (2012). Published material includes:

- A model description and methodology
- Background to Columbia Glacier and results from modelling
- Discussion of the effects of water in crevasses on the model

Chapter 2

Calving Models

The behaviour of tidewater glaciers is important for understanding the likely future evolution of ice masses around the world, and the calving of ice is a key control on it, but as yet it is not well understood. The many processes involved in calving are complicated by the wide range of environmental factors which may influence the calving rate of a glacier. This means that it is difficult to distinguish the different processes involved and their relative importance by observation alone. To this end, scientists create models of the system, in order to create a controlled environment in which experiments may be performed to test the response of a model glacier to input variables, and thus to improve understanding of the dynamics of the system. This chapter lays out the principles of ice flow modelling, the different methods by which calving may be represented in a model, and discusses some of the modelling work already performed on the topic, with its successes and failures. It also introduces the model used in this thesis, and the ways in which it improves on those used in previous studies.

2.1 Ice Flow Modelling

2.1.1 Mathematical basis

An ice flow model is the basis on which any calving law or model must be superimposed. An ice flow model uses the geometry of a glacier, and the forces acting upon it, to model the stresses within the ice. By knowledge of the material properties of the ice, this can be used to calculate the rate at which the glacier deforms. This information can then be used to predict the change in elevation of the surface and terminus position.

When considering a three dimensional ice flow problem, there are nine stresses acting on an infinitesimal ice element within the glacier:

$$\begin{pmatrix} \sigma_{xx} & \sigma_{yx} & \sigma_{zx} \\ \sigma_{xy} & \sigma_{yy} & \sigma_{zy} \\ \sigma_{xz} & \sigma_{yz} & \sigma_{zz} \end{pmatrix} . \tag{2.1}$$

These axes are typically defined with x pointing down glacier, y perpendicular to this across the width of the glacier and z being vertical. The stresses can be divided into three normal stresses (σ_{xx}, σ_{yy}, σ_{zz}) and six shear stresses. In glaciological contexts it is normal to assume that opposing shear forces are balanced such that $\sigma_{ij} = \sigma_{ji}$ (using standard summation notation). Some important stresses discussed in this thesis are σ_{xy}, the lateral shear stress arising from drag at the side boundaries of the glacier and σ_{xx} the longitudinal stress in the x direction. Of the other stress, σ_{zz} arises from the action of gravity on the ice and σ_{xz} from basal drag, while the lateral stresses σ_{yy} and σ_{yz} arise from changes in the width of the glacier but are likely to be less significant than the other terms.

The conservation of momentum (given that acceleration in the system is negligible) requires that:

$$\nabla . \boldsymbol{\tau} - \nabla \mathbf{p} = \rho_i \mathbf{g} \, , \tag{2.2}$$

where $\boldsymbol{\tau}$ is the deviatoric stress tensor, $\mathbf{p}$ the pressure, ρ_i the density of ice and $\mathbf{g}$ the external gravitational force. This leads to the well known Navier-Stokes equations:

$$\frac{\partial \sigma_{xx}}{\partial x} + \frac{\partial \sigma_{xy}}{\partial y} + \frac{\partial \sigma_{xz}}{\partial z} = 0 \ , \tag{2.3}$$

$$\frac{\partial \sigma_{xy}}{\partial x} + \frac{\partial \sigma_{yy}}{\partial y} + \frac{\partial \sigma_{yz}}{\partial z} = 0 \ , \tag{2.4}$$

$$\frac{\partial \sigma_{xz}}{\partial x} + \frac{\partial \sigma_{yz}}{\partial y} + \frac{\partial \sigma_{zz}}{\partial z} = \rho_i g \ . \tag{2.5}$$

These are given in terms of the full (or Cauchy) stresses acting on the glacier, which can be split into two components: the mean normal stress and the deviatoric stress τ_{ij}

$$\sigma_{ij} = \tau_{ij} + \frac{1}{3}\sigma_{kk}\delta_{ij} \ , \tag{2.6}$$

where δ_{ij} is the Kronecker delta and σ_{kk} (the mean normal stress) is related to the isotropic pressure:

$$p = \frac{\sigma_{kk}}{3} = \frac{\sigma_{xx} + \sigma_{yy} + \sigma_{zz}}{3} \ . \tag{2.7}$$

The deviatoric stress τ_{ij} may be linked to the strain rate $\dot{\epsilon}_{ij}$ via the constitutive relation, which depends on the material properties of the medium. The constitutive relation used in glaciology is usually referred to as Glen's flow law (Glen, 1955; Nye, 1957), and relates the stress acting on an element to its rate of deformation. This deformation rate depends non-linearly on the applied stress, as well as varying with temperature:

$$\dot{\epsilon}_{ij} = A\tau^{n-1}\tau_{ij} \ , \tag{2.8}$$

where τ is the second invariant of the deviatoric stress tensor

$$2\tau^2 = \sum_{ij} \tau_{ij}^2 \ , \tag{2.9}$$

and A is the Arrhenius factor, a constant at given temperature. Even this is an approximation, as true deformation rates will also depend on impurities or bubbles in the ice and the size and orientation of ice crystals.

The strain rate tensor

$$\dot{\epsilon}_{ij} = \frac{1}{2}\left(\frac{\partial u_i}{\partial x_j} + \frac{\partial u_j}{\partial x_i}\right) \tag{2.10}$$

may then be used in conjunction with the conservation of mass

$$\nabla.\mathbf{u} = 0\ , \tag{2.11}$$

to find the velocity within the glacier.

In many applications, in order to simplify the problem, some of these stresses laid out in equation 2.1 are neglected. For example, in the shallow ice approximation the lateral shear stress τ_{xy} is neglected (Hooke, 2005). This approximation is valid (as the name suggests) in ice masses which are much broader than they are tall with relatively shallow surface and bed slopes, such as ice sheets. For tidewater glaciers, all the stress components may be considered significant, especially around the calving front. However, a model including all stress components (usually referred to as full-Stokes) is a complex problem, so in many cases some simplifications are made. The simplifications used in previous modelling work are discussed in Section 2.3.

2.1.2 Numerical solutions

The equations above cannot be solved analytically for a real glacier geometry, and therefore a numerical model is required to provide a solution. A numerical model solves continuous partial differential equations by approximating the solution at points on a discretized spatial grid, and also at discrete points in time. There are many methods by which the solution can be approximated at these points, but most tidewater glacier model use one of two methods: finite element or finite difference.

The finite difference method splits the mesh into discrete points, with the solution based on a local Taylor expansion at each point, approximating the gradient in local variables. The finite element method splits the mesh into polygons (or polyhedra in three dimensional problems) and fits a trial function within each element which best represents the original equations. Each numerical scheme may be judged based on its stability and convergence. In an unstable model errors grow uncontrollably, while in a convergent model the difference between the modelled and exact solutions shrinks to zero as the mesh size tends to zero. The two methods have different strengths and weaknesses, with both capable of providing a stable and convergent solution. The different schemes that have been used in calving models and their performance are discussed in Section 2.3.

2.2 Calving Models

As discussed in the Introduction, there are a number of different processes by which calving can occur, but it may be said generally that the controlling mechanism is the fracture of ice, itself depending on the local stress distribution. This process is complicated by variations in the material properties of the ice, the various forces acting around the glacier front, including the effects of tides and sea ice, and the non-linear feedback between fracturing and the stress distribution itself. The combination of all these processes is presently beyond our ability to represent in a model, but there have been a number of attempts to formulate a simplified method of representing calving for inclusion in ice flow models. Some have taken a theoretical approach, trying to represent the most significant underlying physical mechanisms, while others side-step the complexities of the problem and attempt to find an empirical relation between calving and external forcing factors. They may be roughly divided into three categories: empirical calving laws, relating calving rate to external factors by observation, theoretical calving criteria, which use a physical model of the calving process to predict where calving will occur and statistical calving models which use the statistical properties of frontal behaviour to create a framework for other calving

laws, which may be either empirical or physical in nature. Only calving models and laws which are applicable to grounded glaciers are considered, as these are the focus of this study.

2.2.1 Empirically derived models

Water depth model

One of the earliest approaches to the problem was to use observational data to find relationships between calving rate and other external variables. In a study of 12 tidewater glaciers in Alaska, Brown et al. (1982) observed a strong linear relationship between calving rate and water depth at the terminus. This result was confirmed by Pelto and Warren (1991) who extended the range of glaciers studied, including sites from West Greenland and Svalbard as well as Alaska and using glaciers of grounded temperate, polar and floating polar types. They derived the following relationship between water depth and calving rate:

$$U_C = 70 + 8.33 D_t \quad ma^{-1} \, . \tag{2.12}$$

Similar relationships were found by other studies for freshwater-terminating glaciers (Funk and Röthlisberger, 1989), as well as many other marine sites around the globe (see Figure 2.1).

The water-depth model was widely used to describe calving front behaviour for many years, but as can be seen from Figure 2.1 the exact nature of the relationship depends on many factors including region, glacier type and whether the glacier terminates in fresh or salt water. It can also vary for a particular glacier over time, as measurements of the retreat of Columbia Glacier show that seasonal variations in calving rate occurred even when water depth at the terminus remained constant (van der Veen, 2002).

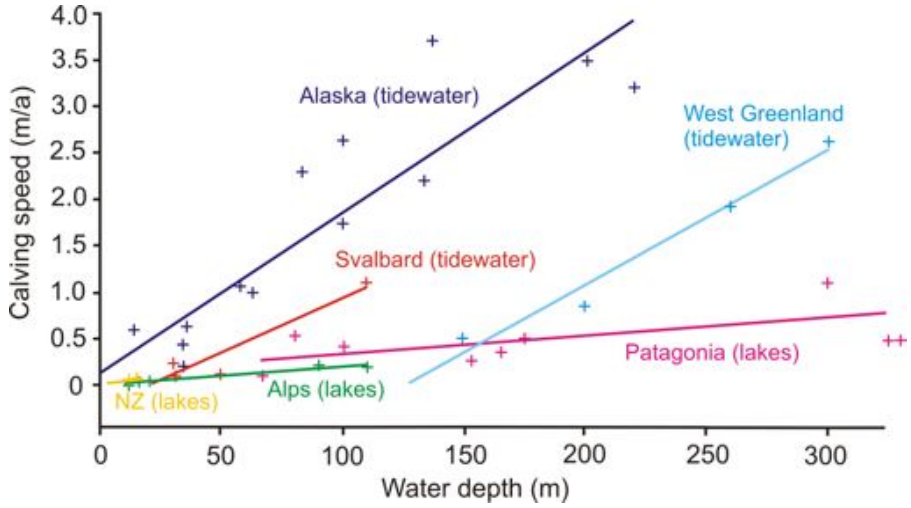

Figure 2.1: Variation of calving rate with water depth for tidewater and freshwater calving glaciers in different regions. Figure adapted from Haresign (2004).

It was realised by van der Veen (1996) that the glaciers used to build these relationships were all in, or close to, steady state. He proposed that the results do not represent a fundamental causal connection between calving rate and water depth, but rather small scale adjustments to environmental conditions. As an example to disprove the theory, he used data from the retreat of Columbia Glacier over the period 1983-1984. During this time the calving rate increased despite a decrease in water depth, suggesting that under some circumstances the relationship can break down entirely.

Flotation model

After exposing the flaws in the water depth model, van der Veen (1996) proposed an alternative approach. He focused on the factors controlling the position of the calving front, rather than the calving rate, and favoured the hypothesis that an outlet glacier calves such that the ice thickness at the terminus has a fixed relationship to the flotation thickness, an idea first proposed by Sikonia (1982). Through observations at Columbia Glacier, he found that the calving front was generally located where the height of the ice cliff above buoyancy was $H_o \approx 50$ m. This leads to the calving relation:

$$H_o = H_t - \frac{\rho_{sw}}{\rho_i} D_t \ , \tag{2.13}$$

where H_t is the ice thickness at the terminus, D_t the depth of water at the terminus and ρ_{sw} and ρ_i are the salt-water and ice densities.

Although the precise details of this relationship are empirically derived, it does have a physical basis in the concept first put forward by Meier and Post (1987) that if the ice is too weak to support a floating tongue, as flotation is approached sections of ice will break away, constraining the terminus location. This model qualitatively explains behaviour observed in the retreat of Columbia Glacier between 1980 and 1992 (van der Veen, 1996), Hansbreen in Svalbard in the year 1990-1991 (Vieli et al., 2002) and several temperate Patagonian glaciers (Venteris, 1999).

However, the basic premise of the approach, that most glaciers will not develop a floating tongue is flawed. It has long been known that a floating tongue is possible in cold regions, but it has now also been shown that temperate glaciers may develop a floating section (Walter et al., 2010). Aside from this point, the validity of the approach has also been called into question by further modelling work (Nick and Oerlemans, 2006). In a numerical ice flow application it was found that although the height-over-flotation approach qualitatively described the cycle of advance and retreat in a calving glacier, it tended to underestimate the equilibrium length of the glacier as the law inhibits advance into deep water. They concluded that "this model is not adequate to describe a full cycle of glacier length variations".

Mass continuity model

A conceptually similar model was proposed by Amundson and Truffer (2010), where not only a fixed height at which calving occurs was suggested, but also a fixed ratio between ice thickness before and after calving. When combined with simple equations of mass continuity, this leads to a calving law:

$$U_C = \frac{(M + H_t\dot{\epsilon}_{zz})\nabla H}{|\nabla H|^2} \,, \tag{2.14}$$

where ∇H indicates dH/dx, the surface gradient around the terminus and M is a combined mass balance term including both surface and bottom melting. The two ice thicknesses (before and after calving) may be represented by any function, thus allowing the model to be applied to different calving scenarios and providing the possibility for other calving models to be incorporated.

This calving law produces a calving rate governed by ice thickness, thickness gradient and vertical strain rates ($\dot{\epsilon}_{zz}$)at the terminus. This approach to calving is much more versatile than the other empirical calving laws presented here, and unlike them it may be applied to both floating and grounded ice. However, the problem remains of the most appropriate way to model the two ice thicknesses, before and after calving, with no obvious rigorous approach apparent.

2.2.2 Physically derived models

Elastic beam model

While others approached the problem from an empirical view, Hughes (1992) attempted to derive a calving relation from physical principles. He based his model on the idea that an imbalance between lithostatic pressure and hydrostatic pressure at the calving front is the main driver of calving. Thus calving is controlled by local bending moments and shear forces, and can be described by an elastic-beam model. This was backed by the observation that calving events at Jakobshavn Glacier, Greenland were often associated with the appearance of new crevasses within one or two ice thicknesses of the front rather than older crevasses formed further upstream.

Testing a range of parameters in the model, Hughes was able to produce agreement between modelled calving rates and observations by Brown et al. (1982) of 12 Alaskan glaciers. However, observations during the retreat of Columbia Glacier

show that calving rates increased as the glacier retreated into deeper water and approached the flotation point (van der Veen, 1996). This is in exact opposition to Hughes's theory, which would suggest that as the glacier approaches flotation the imbalance between lithostatic and hydrostratic pressure should decrease, hence lowering calving rates. It is now generally considered that stretching associated with longitudinal velocity gradients is the more important cause of strain, and therefore fracturing, in grounded glaciers.

Crevasse depth models

As calving must primarily be controlled by the fracture of ice, this has been the focus of most theoretical methods. One of the first attempts to model calving by explicitly modelling fracture rates of ice was made by Iken (1977). This study modelled the ice cliff at Grubengletscher, using a finite element model of the stress distribution around the front to predict the speed and direction of fracture propagation, and hence the size and location of iceberg calving. However, the implementation of fracturing was basic, relying on arbitrarily chosen fracture criteria, and the concept was not pursued after the initial study.

The idea of using an ice fracture model to define a calving point was picked up by Benn et al. (2007a), who proposed a modified method of modelling calving by crevasse depth. They suggested that dominant mechanism of calving in tidewater glaciers is triggered by the downwards propagation of crevasses in the surface of the ice. Calving occurs when crevasses reach the base of the glacier, but in the highly fractured regions around the terminus it is reasonable to assume a hydraulic connection to surrounding water, therefore the critical point will be reached as the crevasse reaches sea level. At this point, the influx of water will necessarily force penetration to the bed. The location of the terminus is thus determined by the position along the glacier at which this criterion is satisfied.

Benn et al. (2007a) suggest a scheme whereby the interaction between crevasses and the surrounding ice is neglected. The model is thus applied to a glacier geometry of

solid, unfractured ice (which is easy to model) and the stress distribution calculated is used to predict crevasse depth. This is then in turn used to model whether calving will occur, and where the new terminus will be located. This allows a much more wide ranging model than that of Iken (1977), which attempted to model the short-timescale physical displacement and evolving stress distribution of a single ice block during the calving process. The simplified approach suggested by Benn et al. (2007a) can more feasibly be included in a tidewater glacier model examining calving over long periods of time.

The Benn et al. (2007a) approach may be applied to both grounded and floating ice, though consideration of basal crevassing will also become important as a floating tongue develops. It provides an easy-to-understand physical model of the calving process, which is somewhat simplified but represents the likely dominant mechanism active in iceberg calving. It relies only on the stress distribution in the glacier, a variable which is available axiomatically in ice flow models, and is therefore conceptually easy to apply. This is the approach I have chosen to pursue in this work.

Damage mechanics model

A different approach to calving was developed by Pralong et al. (2003), using damage mechanics to track weaknesses in the ice. Cracks and fissures in the ice are represented by a damage variable d, which is a value between 0 and 1 representing the level of fracturing. The property d is advected with the ice, with additional sink and source terms related to the stress field allowing for opening and closing of cracks. The damage variable is used to adjust the ice flow properties, creating new stress and strain rate tensors and a new viscosity representing the change in rheological properties with increasing material fracturing. Highly fractured regions have a very low viscosity, allowing ice blocks above to slide quickly over the damaged area, in effect producing calving (see Fig. 2.2).

Two-dimensional ice flow models including damage mechanics have been used successfully to model crevasse opening and the calving of an ice block (Pralong and

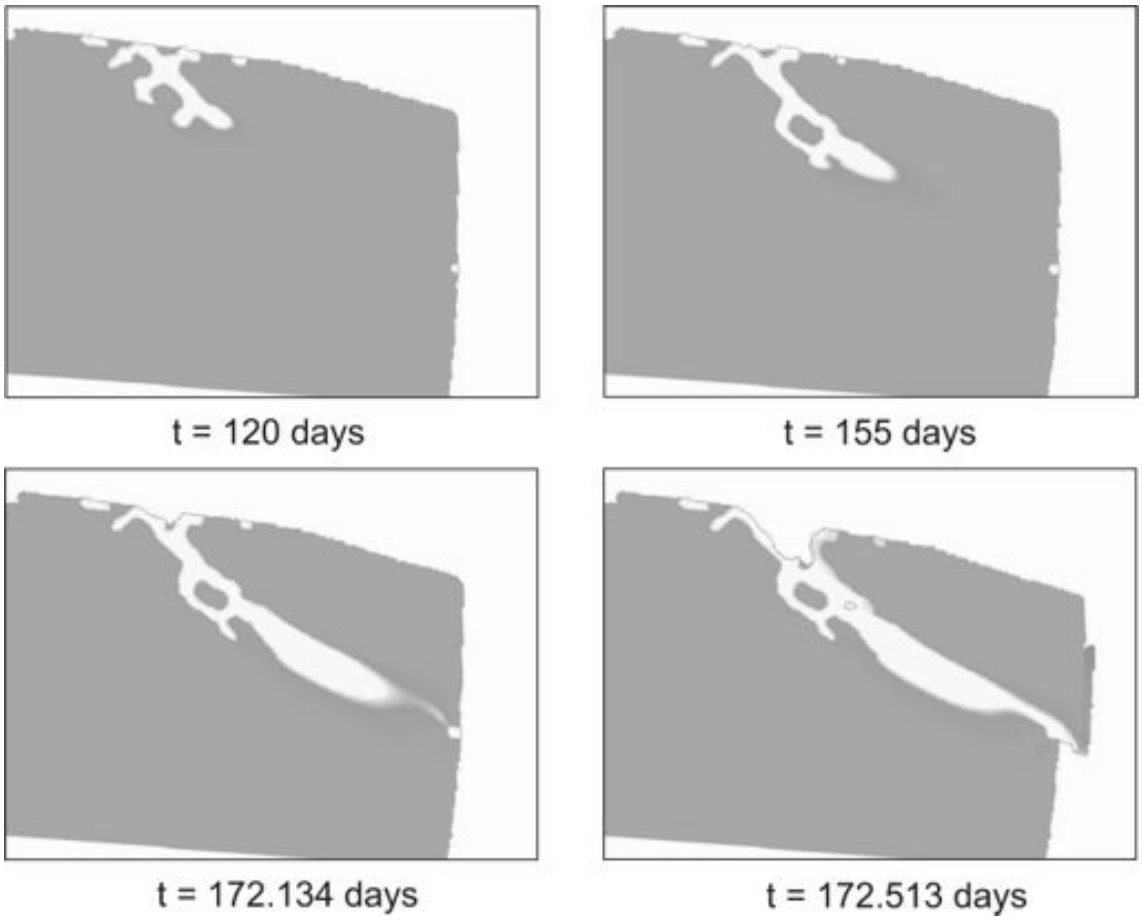

Figure 2.2: Damage mechanics approach to calving. Dark grey shading represents undamaged ice and white areas have a damage variable of 1. The model run is initialised with entirely undamaged ice, but fractures quickly develop as stresses exceed the fracture threshold. The fracture development eventually leads to the calving of an ice block. Figure from Jouvet et al. (2011)

Funk, 2005; Jouvet et al., 2011), although validation is largely based on a subjective similarity to observed calving events. The method depends heavily on the implementation of crack growth and healing processes (the stress conditions under which the ice will fracture, or fractures will close) which are not yet well understood in glaciers. At present the approach has not been applied any further than a single calving event, nor combined with any model of wider glacier dynamics, largely due to the extremely high spatial resolution required for model runs, but it does have great potential to provide a physical calving implementation of higher sophistication than that of Benn et al. (2007a).

The damage mechanics method has also been developed in a separate application to ice shelves, using a glacier ice flow model coupled to a damage mechanics model to produce a first-order estimation of calving rate (Levermann et al., 2012). In this work, strain rates and material properties (depending on the damage variable) at the calving front are used to infer an average calving rate. This provides a physically realistic estimation of calving rate, although it does not distinguish individual events as the previous applications aimed to. The approach has been applied successfully to several Antarctic ice shelves (Martin et al., 2011; Levermann et al., 2012) and although it has not yet been applied to grounded ice, there is potential that a similar relationship between strain and calving rates could be found.

2.2.3 Statistical calving models

A different framework for calving was developed by Bassis (2011), based on statistical mechanics methods, likening the behaviour of a calving front to a random walk system. This approach is designed to bypass the complexities of trying to determine calving from various internal parameters around the ice front, and instead provide a macroscopic equation which can predict the changes in terminus position over longer time scales. The model works by defining "transition rates" *i.e.* the probability of the terminus advancing or retreating at a given time. Forward transition rates may be fixed by the glacier velocity, while the probability of retreat must be explic-

itly specified, and may be a function of various internal or external variables. By methods standard in statistical mechanics, these are converted to a master equation describing the most likely evolution of the terminus over long timescales

This calving law is universal, and may be applied to any calving situation, but its precise form depends on the transition rates used, which will differ significantly between different calving regimes. To this extent it may be classified with the empirical approaches which require tuning to each calving scenario. A physical framework for determining transition rates from fracture mechanics may be found. However, at present this method requires some further development before it is ready to be included in ice flow models and thoroughly tested.

2.2.4 Summary

Each type of model has different strengths and weaknesses. Empirical models may currently be the best approach to including calving in ice sheet models, which generally have neither the detailed mesh density or full stress calculations required to adequately represent fractures and crevasses in the ice, although advances are being made in both these areas (e.g. Larour et al. (2012)). These empirical calving models should be validated against more detailed models of calving provided by theoretical approaches, and there is also the possibility of coupling a large ice sheet model to separate small scale detailed models of outlet glaciers to provide a more accurate overall model. The theoretical approach to calving can include the effects of a wider variety of environmental forcing factors, and has greater potential to increase our understanding of calving.

2.3 Previous Tidewater Glacier Models

There have been relatively few studies in which the full behaviour of a calving model (any of those listed above) has been tested by inclusion in an ice flow model. As

described in the Introduction, it only by representing fully the interaction between calving and ice dynamics that the behaviour of tidewater glaciers can be adequately modelled, therefore this area is of particular interest.

There have been three main approaches used in tidewater glacier models, each using a different set of approximations and also in general using different numerical methods to solve the ice flow equations:

- Minimal calving model; making large simplifications of glacier physics (Oerlemans and Nick (2005, 2006))
- Vertically averaged; these flowline models tend to use finite difference methods, and can include parameterisations of lateral processes (Nick et al. (2007b, 2009, 2010))
- Full-Stokes; these 2D or 3D models provide a full-Stokes solution with no depth averaging, but require substantial computer resources for 3D processes (Vieli et al. (2001, 2002), Otero et al. (2010))

2.3.1 Minimal calving model

A minimal model, as discussed here, is one that has no spatial resolution, considering only the evolution of state variables such as the overall length of a glacier or mean ice thickness. They provide a simple way to investigate the general response of a glacier to changes in input variables.

A minimal model was used to investigate calving by Oerlemans and Nick (2005, 2006). The basic assumption of their model was that the mean ice thickness is simply related to the glacier length:

$$H_m = \alpha_m L^{1/2} \,, \tag{2.15}$$

The evolution of the glacier can be determined from conservation of mass:

$$\frac{d(H_m L)}{dt} = M + F_C \,, \tag{2.16}$$

where F_C is the calving flux, calculated using the water depth model discussed in Section 2.2.1. The two equations can be combined to determine the change in glacier length over time:

$$\frac{dL}{dt} = \frac{2(M + F_C)}{3\alpha_m} L^{-1/2} \, . \tag{2.17}$$

This type of model has obvious limitations. By working only with state variables, there is no possible information on the evolution of the surface, and it would not be suitable for use with any of the theoretical types of calving model. However, work by Nick and Oerlemans (2006) showed that the minimal model exhibited qualitatively the same advance/retreat behaviour as more complex finite difference models. It is extremely simple to write and adapt, and may be used as a learning tool, or method to experiment swiftly with some of the governing principles of calving glacier dynamics. For example, Oerlemans and Nick (2005) used the minimal model to deduce a high dependency of model behaviour on bed profile.

2.3.2 Vertically averaged models

The first record of a flowline model of a tidewater glacier that the author has found is a study by Bindschadler and Rasmussen (1983) which uses the finite difference method to model ice flow in the lower 14 km of Columbia Glacier, coupled to a water depth type calving law. The model was essentially one dimensional, being both depth and width averaged with a parameterised width used to account for lateral drag and lateral spreading of ice. The model also lacked any longitudinal stresses. The work was able to produce a predicted period of surface lowering and retreat for Columbia Glacier. However, it lacked any detailed investigation of the the performance of the water depth calving law and the work does not appear to have been continued beyond a single study.

The next appearance of such a tidewater glacier model was Nick and Oerlemans (2006), using finite difference code developed by Oerlemans (2001). The purpose was to test the performance of the water depth and height-above-flotation calving

laws (see Section 2.2) over a full range of glacier variation, starting from a land terminating glacier, advancing into water and then retreating again. In this case, the velocity of the glacier was vertically averaged, and the effects of longitudinal stress gradients and lateral drag were neglected, although lateral spreading of ice was made possible by a parameterisation of the glacier width. It was found that the flotation model inhibited advance into deeper water.

The model was developed in further applications to Columbia Glacier (Nick et al., 2007b) and Helheim Glacier (Nick et al., 2009) to include longitudinal stress gradients and lateral drag. The work showed that glaciers are highly sensitive to changes in their terminus boundary conditions and dynamically adjust extremely rapidly, with the nature of the adjustment depending strongly on the bed geometry. The model has also more recently been adapted to include the Benn type calving criterion (Nick et al., 2010) demonstrating that this type of calving law can reproduce typical cycles of seasonal advance and retreat, unlike the height-above-flotation calving model. This model has also been applied to to Jakobshavn Glacier, West Greenland (Vieli and Nick, 2011), again demonstrating high sensitivity to changes at the terminus, and also to the depth of water in crevasses.

The Oerlemans (2001) finite difference model was also adopted by Lee et al. (2008) for a model of Marian Cove, King George Island, Antarctica, coupling the ice flow model to a height-above-flotation calving law and also a more advanced surface mass balance model. Results corresponded well to the observed retreat at Marian Cove over the 1956-2005 period.

These models have demonstrated a high sensitivity to bed profile and rapid response to changes at the terminus, lending weight to the idea that changes in tidewater glaciers are triggered at the calving front, rather than by an increase in speed further up-glacier. Vertically averaged, flowline models have been the main method used so far to investigate tidewater glacier behaviour. The main advantage of this type of model is the ease of writing the required code, which means that it may be adapted to include many different physical processes. An effectively one-dimensional model

(vertically integrated along a flowline) may be adapted to include the effects of lateral drag and lateral spreading of ice, hence it may represent the effects of a large drainage basin, without the need for a large, computationally expensive three-dimensional mesh.

However, the vertically integrated nature of these tidewater glacier models means that they are not best suited for use with the theoretical type of calving model described in Section 2.2.2, which require a good calculation of stress distribution with depth for an accurate result. The difficulty of writing the numerical code increases dramatically for a fully two dimensional model, with a mesh which can vertically resolve variables, and such a project would require a substantial input of time and effort.

2.3.3 Full-Stokes models

The first example of a vertically resolved model of a tidewater glacier was produced by Sikonia (1982) as part of an extensive study of Columbia Glacier, Alaska. A flow model of the lowest 14 km of Columbia Glacier was produced, using a calving law depending on H_o, the height over flotation (the first instance of such a calving law). This model successfully predicted that Columbia Glacier was about to begin a dramatic retreat, showing a remarkable example of successful model prediction.

The first such model to use a full tidewater glacier length, linking calving front behaviour to glacier dynamics was created by Vieli et al. (2001) and tested on data on Hansbreen by Vieli et al. (2002). Vieli used a modified version of the flotation criterion to calculate terminus position:

$$H_t = \frac{\rho_{sw}}{\rho_i}(1+q)D_t \ . \tag{2.18}$$

In this version of the flotation model q can be adjusted for different glaciers. This factor depends on the glacier geometry and will be smaller for glaciers that are thin-

ner or less heavily crevassed. The study used a two-dimensional flowline geometry, with no inclusion of lateral processes. The results of the studies demonstrated a high dependence of terminus behaviour on basal topography, but the model has not been developed beyond the initial studies.

The crevasse-depth criterion for calving has been tested in a three-dimensional diagnostic (non-time evolving) model by Otero et al. (2010), who found that it predicted well the terminus position of Johnsons Glacier, a small glacier on Livingston Island, Antarctica. This is the only calving model so far produced with a three-dimensional geometry, which is important to allow the robust inclusion of lateral effects, and also has the benefit of being able to model the evolution of a calving bay rather than treating calving as a process which necessarily occurs across the entire glacier width. However, the chosen glacier is in a stable position with very slow velocities and low water depth at the terminus. Therefore it does not fully test how the model would perform in a more active outlet glacier situation. The choice of location was made as their model is currently only able to handle diagnostic problems.

As noted above these vertically resolved two- and three-dimensional problems require a more substantial and complicated numerical code, and in most cases studies use a multi-purpose modelling package for the numerical solution, which in most cases use finite element methods. The advantage of this is that a numerical solution of the Navier-Stokes equations (Equations 2.11:2.5) may be quickly achieved on a fine 2D or 3D grid, producing a full velocity and stress result without the need to write new code, and the package will already have been thoroughly tested so may be assumed to produce reliable, consistent results.

The disadvantage in using multi-purpose software is that the physics involved may be considered to be fixed, so for example a parameterisation of lateral spreading may not be easily included in a flowline model. The finite element method also requires that the elements within the discretized mesh are of roughly equal size in all dimensions, which means that in general the number of elements required is high, with corresponding high memory and CPU requirements. This is a particular

problem in Glaciology, where the high length of most glaciers compared to their height make them ideally suited to a finite difference type grid, where elements may be created of similar aspect ratio to the overall glacier. If the issues of memory and CPU requirement can be overcome, the advantage of high resolution stress modelling in the crucial areas around a glacier terminus gives these finite element modelling packages a significant advantage over other model types for investigating the behaviour of physically-derived calving models.

2.4 Calving Model Used in This Thesis

The work presented in this thesis expands on previous work using a crevasse-depth-based calving criterion included in an ice flow model. As discussed above, there have already been two models to use this approach. One, by Vieli and Nick (2011) uses an established finite difference code (Nick et al., 2007a, 2009) and applies the crevasse-depth calving criterion. However, the finite difference model used is vertically integrated and is not best suited to the crevasse-depth calving approach, which relies on an accurate modelled stress distribution.

This problem was addressed by Otero et al. (2010), who presented a 3D full-Stokes model of Johnsons Glacier, Antarctica. However, this application provided only a diagnostic (snap-shot) solution. A full investigation of the performance of the crevasse-depth criterion requires a model of a typical, fast-flowing tidewater or outlet glacier, with prognostic (time-evolving) solutions and a full-Stokes analysis of the stresses acting within the ice. This is the aim of this thesis: I use the finite element software package Elmer/Ice to provide a two-dimensional full-Stokes solution of glacier flow, coupled to a crevasse-depth based, physically-derived calving criterion. Details of the model used are discussed in the next chapter.

Chapter 3

Methodology

The intention of this work is to investigate iceberg calving by incorporating a physically-derived calving model in an ice flow model of a glacier. The combination of the two models is important, as there is significant feedback between calving and glacier dynamics. As the flow of a glacier changes, and its terminus retreats and advances, there is a resulting change in calving. And as calving events occur, the change in geometry of the glacier will affect its velocity around the terminus, with this change also eventually propagating further up-glacier. This chapter lays out the details of the two models used, and how they are coupled. In this thesis the model is applied to two glaciers: Columbia Glacier in Alaska, and Helheim Glacier in East Greenland. The features that the two experiments have in common are discussed, along with examination of some of the minor differences. Larger differences will be laid out in the relevant chapters on each individual experiment.

Both experiments use two-dimensional (2D) geometries, therefore many of the equations below are only valid for this space, and would have to be extended for three dimensions. Although the two-dimensional geometry has some limitations and drawbacks, such as missing the effects of tributaries and lateral spreading in channel widenings, it is the only practicable method for these experiments at the current time. Firstly, for the calving law to be applied an accurate model of the stress act-

ing around the front of the glacier is needed, which requires a fine mesh. For a 3D glacier model this fine mesh density would cause the memory and CPU requirements of model runs to be impractically high. Secondly, in many cases 2D data are more readily available than 3D, and bed elevation measurements are often made along a designated flowline, missing the edges of the glacier. Thirdly, and perhaps most important, at the current time no adequate scheme has been devised to implement calving in 3D. This requires us not only to model the calving location at one point, but the new 3D shape of the terminus, which is an extremely difficult problem on an unstructured mesh as required by the modelling software.

3.1 Numerical Model

3.1.1 Mathematical basis

The equations used to model ice flow are laid out in section 2.1, but cannot be solved analytically, so a numerical model is required. In this application they are solved using the Finite Element Method (FEM) code Elmer/Ice (http://elmerice.elmerfem.org). Elmer/Ice is particularly suitable for this type of experiment, as it has been used extensively for ice modelling work (e.g. Zwinger et al. (2007); Zwinger and Moore (2009)). The numerical solution of the ice flow equations has also been tested against other models in the ISMIP-HOM experiments, designed as a benchmark for testing glacier models (Gagliardini and Zwinger, 2008). Although for real geometries there is no analytical solution of the equations, to which the output can be compared, the results from Elmer/Ice were very close to those of the other full-Stokes model tested (Pattyn et al., 2008) giving a high confidence in the validity of the numerical solution.

Once again we begin with the Navier-Stokes equations:

$$\nabla.\mathbf{u} = 0 \ , \tag{3.1}$$

the conservation of momentum (given that acceleration in the system is negligible):

$$\nabla.\boldsymbol{\tau} - \nabla\mathbf{p} = \rho_i\mathbf{g} \ , \tag{3.2}$$

and the constitutive relation:

$$\dot{\epsilon}_{ij} = A\tau^{n-1}\tau_{ij} \ , \tag{3.3}$$

For a numerical solution of these equations, the non-linear constitutive relation introduces possible instabilities into the system, requiring an iterative solution. Improved performance is given by inverting the constitutive relation (Equation 3.3) and re-formulating it in terms of a strain-rate dependent viscosity:

$$\tau_{ij} = 2\mu\dot{\epsilon}_{ij} \ , \tag{3.4}$$

where

$$\mu = A^{1/n}\dot{\epsilon}_{ij}^{\frac{1-n}{n}} \ , \tag{3.5}$$

which combined with Equations (2.11), (2.4) and (2.10) may once again be solved for velocity.

The Arrhenius factor A differs in the two cases used in this thesis. Columbia Glacier is temperate, therefore a fixed value of $A = 5.6 \times 10^{-15}$ s^{-1} (kPa)$^{-3}$ is used. This is an average of two experimentally observed values for temperate ice, both measured in situ on glaciers (Paterson, 1994). Helheim Glacier has a variable temperature structure (as can be inferred from the polythermal structure of the ice sheet (Dahl-Jensen et al., 1998) and modelling on other outlet glaciers (Funk et al., 1994)), and A depends on the temperature of the ice according to the Arrhenius equation:

$$A = A_0 e^{-Q/RT} \ , \tag{3.6}$$

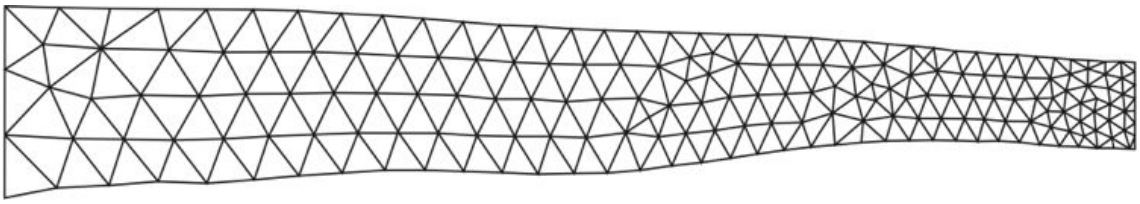

Figure 3.1: An example of the type of unstructured mesh used in model simulations

where $A_0 = 3.985 \times 10^{-4}\text{s}^{-1}\ (\text{kPa})^{-3}$ is a constant, R is the universal gas constant, and Q is the creep activation energy, which may take two values depending on the temperature:

$$Q = \begin{cases} 60\ \text{kJ}^{-1}\ \text{mol}^{-1} & \text{where} \quad T < -10°\text{C} \\ 139\ \text{kJ}^{-1}\ \text{mol}^{-1} & \text{where} \quad -10 \leq T < 0°\text{C} \end{cases} \tag{3.7}$$

These constants are standard values taken from Paterson (1994). The values used for the ice temperature are discussed in Section 5.4.

The strain rate tensor may then be used to find the velocity:

$$\dot{\epsilon}_{ij} = \frac{1}{2}\left(\frac{\partial u_i}{\partial x_j} + \frac{\partial u_j}{\partial x_i}\right) , \tag{3.8}$$

3.1.2 Numerical solution

The numerical solution of the above equations is achieved using the Finite Element Method code, Elmer/Ice. The geometry of the glacier is represented by an unstructured grid of triangular elements. The geometry is produced from bed and surface digital elevation models (DEMs), and filled by an unstructured triangular mesh using the finite element mesh generator gmsh (http://geuz.org/gmsh/). This geometry can also be set with a variable mesh size to allow for higher resolution in areas of interest, such as the calving front (e.g. Fig 3.1).

The quality of the modelled solution depends strongly on the accuracy of the DEMs used in creating this mesh. Previous work has shown that models are sensitive to surface elevation uncertainty in the DEM (Zwinger and Moore, 2009), leading

to inaccuracy in the simulated velocity field and surface evolution. This effect is normally counteracted by an initialization period, during which the model is run forward until the surface reaches a steady state, smoothing out any DEM errors. However, the nature of dynamic tidewater glaciers means that they are inherently unstable, and it is rare to find them in a steady state, unless the front is pinned for a length of time on a local bedrock maximum. The effect of this highly variable nature on the results and conclusions is discussed in more detail in each results chapter.

As well as the equations governing flow discussed above, for a numerical solution we also require boundary conditions.

3.1.3 Upper boundary conditions

For prognostic (time-evolving) model runs, the evolution of the glacier's surface must also be considered. The surface of the glacier acts as a free boundary, with no stress acting on it. The continuity equation used for calculating change in height acts as a kinematic boundary condition:

$$\frac{\partial s}{\partial t} + u_x \frac{\partial s}{\partial x} = u_z + M \ , \tag{3.9}$$

where s is the surface elevation and M the surface mass balance (the cumulative effect of accumulation and ablation acting on the glacier).

3.1.4 Basal boundary conditions

One important contributor to the speed of a glacier is basal motion, which can take place by one of two processes:

1. Sliding over the bed
2. Deformation of underlying till.

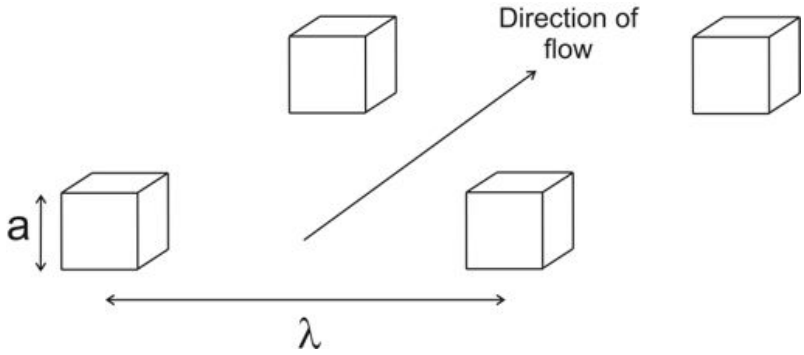

Figure 3.2: Arrangement of objects on solid bed in Weertman sliding formulation, indicating definitions of a (size of controlling obstacles) and λ (distance between basal obstacles).

Sliding occurs on hard, rock beds (impermeable and undeformable), while till deformation tends to occur where the bed is made up of sediment saturated with water. Each bed type produces a different style of sliding, with a different relationship between driving stress and basal motion.

Solid beds

One of the first attempts to define a relationship between driving stress and velocity at the bed was made by Weertman (1957). This formulation assumes a hard bed covered with obstacles of fixed size and separation (Figure 3.2). The ice can overcome these obstacles by creep deformation of ice or melting and refreezing. It also assumes that there is a thin, lubricating layer of water such that the interface between ice and rock does not support shear stresses. This leads to a relationship of the form:

$$u_b = A_s \left(\frac{\tau_b^{1/2}}{R_b} \right)^{n+1} , \tag{3.10}$$

where u_b is the basal velocity, τ_b the basal shear stress and $R_b = a/\lambda$ can be regarded as a roughness parameter (see Figure 3.2). A_s is a sliding parameter, which can be tuned to fit the modelled velocity to observed values.

Control of flow by objects on bed is still the basis of most sliding laws, though many use a controlling wavelength rather than discrete objects. One of the first major developments on the theory was the inclusion of water-filled cavities at the bed (Lliboutry, 1958). A power law formation of Weertman sliding was promoted by

Budd and Keage (1979), Bindschadler (1983) and Fowler (1987) and used in some experiments *e.g.* Nick et al. (2007a) to include the effects of basal water pressure:

$$u_b = A_s \left(\frac{\tau_b^q}{N^p} \right) , \tag{3.11}$$

where the exponents p and q must be tuned to observed data and N, the effective basal pressure, depends on the basal water pressure P_w:

$$N = \rho_i g H - P_w . \tag{3.12}$$

Further developments and improvements have been made by a number of studies e.g. Schoof (2005); Gagliardini et al. (2007). However, an entirely satisfactory sliding law has yet to be found, as the problem of feedback between friction from objects of the controlling size and the erosion of those objects has not yet been fully addressed.

The work by Gagliardini et al. (2007) has already been implemented in Elmer/Ice, and provides an improvement over the simplified theory of Weertman, with a form very similar to that of Schoof (2005). Its most significant development is the inclusion of cavity effects, which inhibit the unbounded increase of basal shear stress with sliding velocity or effective pressure present in Weertman and Budd-type sliding laws. The Gagliardini model is an empirical equation, where three parameters are set to tune the model to fit ideal results on numerically modelled glacier beds.

The sliding law is expressed as a function (Fig. 3.3)

$$\frac{\tau_b}{CN} = f \left(\frac{u_b}{CNA_s} \right)^{1/n} , \tag{3.13}$$

where A_s is the sliding parameter without caviation and C is the maximum value reached by τ_b/N (see Figure 3.3). At low water pressures the sliding law follows the same behaviour as Weertman sliding. As water pressure increases, caviation begins and τ_b/N reaches a maximum value (which is independent of the Glen power-law exponent n). After this peak, as water pressure increases the friction law decreases

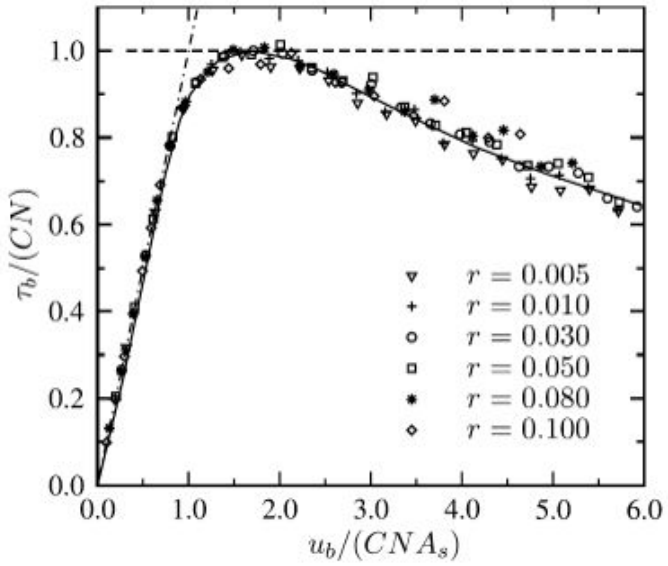

Figure 3.3: Plot of Gagliardini sliding law; dash-dotted line represents sliding with no caviation, data points represent modelled sliding relationship with varying obstacle size (source: Gagliardini et al., 2007).

and τ_b/N is bounded by the maximum bedrock slope in the area of ice-bed contact. This leads to a sliding law of the form:

$$\frac{\tau_b}{N} = C\left(\frac{\chi}{1+\alpha\chi^q}\right)^{1/n} , \tag{3.14}$$

where

$$\chi = \frac{u_b}{C^n N^n A_s}^{1/n} , \tag{3.15}$$

and

$$\alpha = \frac{(q-1)^{q-1}}{q^q} . \tag{3.16}$$

The sliding law for a particular model configuration is determined by setting A_s, q and C, where C is a positive value, less than the maximum bed slope, which is always constant for a fixed geometry and q controls the post-peak decrease of the friction law.

The Gagliardini sliding formation is used for work at Helheim Glacier. Little is known about the bed properties of the Greenland outlet glaciers, however Joughin

et al. (2008a) states bedrock under Helheim and Kangerdlugssuaq Glaciers can support high basal shear stresses and work by Smith and Andrews (2000) indicates low rates of sediment deposit in East Greenland fjords, which may imply low levels of sediment at the glacier bed. With so little data available for the bed conditions at Helheim, the use of this sliding law is reasonable as it includes all the major features of any sliding law - increased sliding with increased driving stress, basal water pressure and is tuned to the observed surface velocities before use.

Deformable bed

A bed formed of deformable till is often associated with fast basal motion. It is generally considered that the till deforms in a shallow layer near the surface in a plastic fashion *i.e.* the till will only support stresses up to the limit of its strength, after which it fails and provides no more resistance to flow. Columbia Glacier is known by borehole experiments to have a deformable till of varying thickness at the bed (Humphrey et al., 1993), and the till strength was found to be 5.5 - 13 kPa, although this will change with variations in basal water pressure. This is much smaller than the driving stress acting on the till; therefore it has been suggested by Cuffey and Paterson (2010, p281) that the driving stress is largely opposed by sticky spots (areas of exposed bedrock) on the bed of the glacier and that basal drag may be best represented by a form similar to that of the Weertman equation:

$$\tau_b = AN u_b^{1/n} \, . \tag{3.17}$$

All of the sliding equations rely on some knowledge of basal water pressure, used to calculate the effective pressure N. This variable can be hard to determine, as to collect the data from the field requires laborious and expensive borehole drilling. We use an approximation of basal water pressure depending on D, the depth of the bed below sea level:

$$P_w = \begin{cases} 0 & y_i \geq 0 \\ \rho_{sw} g D & y_i < 0 \end{cases} . \tag{3.18}$$

This represents a physical minimum level, with observed basal water pressure often being higher due to additional water input from basal melting of the glacier or the conduit of surface meltwater to the bed via crevasses and moulins.

Sliding parameters All of the sliding laws discussed above use at least one sliding parameter, which may be tuned to provide a best fit of modelled to observed velocities. This may be done using a single sliding parameter for the entire glacier, or by using different parameters for different sections of the glacier's bed to account for the fact that basal properties are likely to vary significantly in different areas under the glacier. When the bed is divided into sections with different sliding properties, finding a best fit to observed velocity becomes more time consuming and one possible solution is to use inverse methods to infer the sliding velocity from the surface velocity and glacier geometry. This requires accurate knowledge of the glacier's geometry and internal ice temperature structure and a good coverage of surface velocity measurements. In the experiments performed in this thesis it was felt that the observations available were insufficient for inverse methods to improve the basal sliding parameterisation significantly and the basal sliding parameters were determined by hand as described in the relevant results chapters.

Lateral boundaries

As both of the models discussed in this thesis use only a two-dimensional geometry, technically there are no lateral boundary conditions to apply. However, there are two disadvantages to such a setup: first, it cannot take into account the effects of lateral spreading or constricting of ice as the fjord/valley widens or narrows, or the effect of tributary glaciers meeting the main flowline. Second, given the setup of equations in Elmer/Ice it will not include a term for lateral drag from the sides of the glacier. This is a particular drawback as it has been suggested to have a stabilising

effect on glacier termini (O'Neel et al., 2005). There is little that can be done to address the effect of tributaries without switching to a 3D geometry, but in the Helheim Glacier experiments presented in Chapters 5, 6 and 7, parameterisations of lateral drag and flux contribution from changes in channel width are used. In each case a trapezoidal channel shape is assumed, with a flow width at the bed 66% narrower than at the surface. A constant lateral velocity gradient is also prescribed, with the speed at the channel walls half that at the central flowline. This leads to a flux term for lateral spreading of:

$$\phi = -\frac{5}{8}\frac{HU}{W}\frac{\partial W}{\partial x} \ , \tag{3.19}$$

where W is the channel width at the surface. This is then applied as an additional mass balance term. For the experiments on Helheim Glacier presented in this thesis a parameterization of lateral drag is also included in the model. To do this, a force is imposed on each element in the glacier body, opposing flow, with the following form:

$$F = \frac{1}{2w(z)}\left(\frac{1}{2A}\frac{u_x}{w(z)}\right)^{\frac{1}{3}} \ , \tag{3.20}$$

where $w(z)$ is the channel width at an elevation z and u_x the velocity along flowline. This parameterisation is reached by integrating the horizontal shear stress over the channel width, using the geometrical assumptions listed above.

This is only a simple representation of the lateral processes in the glacier, which is unable to take into account the full 3D geometry , the lateral variations in velocity, or the effect of the lateral crevassing common in fast flowing glaciers which will affect the ability of the ice to transmit lateral resistive stresses to the centreline. This could be greatly improved by using a full three-dimensional model. However, such a model is beyond the capability of this study due to the large requirement in computing resources, and the technical developments required to implement calving in three dimensions, as finding the new shape of a calving bay after a calving event

takes place is far from a trivial problem.

3.1.5 Other boundary conditions

In the Columbia Glacier experiments presented in Chapter 4, the model geometry reaches back towards an ice divide, in which case one can specify that horizontal velocity is zero at the rear boundary. In the Helheim Glacier model presented in Chapters 5, 6 and 7 the model geometry is cut down-stream of the ice divide. In these experiments an ice velocity is prescribed at the inflow boundary.

At the calving front, the boundary is allowed to move freely in the horizontal direction, according to the velocity profile: each node i moves a horizontal distance

$$\Delta x_i = u_{xi}.\Delta t \tag{3.21}$$

at each timestep. This method is also adapted in some experiments to provide a representation of melting at the calving face. The nodes are then also moved backwards horizontally by an amount representing the melting rate, M_f, at the face:

$$\Delta x_i = u_{xi}.\Delta t - M_f.\Delta t \ . \tag{3.22}$$

A stress boundary condition is also applied on the calving face to represent the pressure applied by the surrounding sea water. Where $z_i < 0$ the force on the calving face, F_f, is

$$F_f = \begin{cases} 0 & z_i \geq 0 \\ \rho_{sw} g z & z_i < 0 \end{cases} \ . \tag{3.23}$$

The force is inversely proportional to depth below sea level, where the negative sign indicates that it acts against the glacier flow. In other experiments a backstress simulating sea ice is also applied to the calving face. This backstress is simply

added to F_f and can also be spatially variable, applying to the entire calving face or a narrow band around the waterline representing the vertical extent of the ice mélange.

3.1.6 Mesh update

The mesh is updated at each timestep in a prognostic (time-evolving) solution. The upstream inlet boundary is fixed, and the upper surface and front boundaries move as described in the sections above. The bed should be fixed, but the mesh nodes on the boundary need to be allowed to move along the bed profile so that mesh elements do not become significantly distorted during a run. This is achieved by allowing each node to move horizontally according to the basal velocity using Equation (3.21). The node is then adjusted vertically to match the bed profile at this location, as defined either by a polynomial equation (Columbia Glacier experiments) or by linearly interpolating between points in an array of bed values (Helheim Glacier experiments). The internal mesh nodes are shifted elastically at each timestep to keep a roughly uniform mesh distribution within the glacier, and to prevent significant mesh distortion.

3.2 Calving Model

We use the calving scheme suggested by Benn et al. (2007a) whereby the location of the terminus may be predicted by the location at which crevasses penetrate to sea level (discussed in section 2.2.2). This scheme requires crevasse depths to be predicted, for which there are a number of methods.

3.2.1 Crevasse-depth model

The first model designed to predict the crevasse depth in glaciers was developed by Nye (1955, 1957). This model works from the principle that a crevasse will extend to the point where longitudinal tensile strain rate, arising from downstream velocity gradients, is balanced by the ice overburden pressure. Considered in terms of the full (or Cauchy) stress this means crevasses reach to the point where:

$$\sigma_{xx} = 0 \ . \tag{3.24}$$

This approach is valid for a field of closely spaced crevasses, as in this case the stress concentration around the tip of the crevasse is minimised. As proposed by Benn et al. (2007a), this equation can be modified to include the effects of the fracture toughness of ice by adding a critical value of strain rate, which must be exceeded for fracturing to occur. In the work presented here this has been neglected. The effect of pressure from surface meltwater pooling in crevasses can also be considered, leading to the modified equation:

$$\sigma_{xx} + D_w \rho_{fw} g = 0 \ . \tag{3.25}$$

The weaknesses of the model, as identified by van der Veen (1998), are that it does not account for the differing density found in the normal ice profile due to snow and firn cover, and it does not account for stress concentration around the tip of the crevasse. More advanced models of crevassing use linear elastic fracture mechanics to include these effects. This approach was first applied in glaciology by Smith (1976), and developed further by van der Veen (1998).

In this study I choose to apply the Nye approach to crevassing, due to its ease of implementation. Although the LEFM formulation may be more thorough, the region around the terminus of a fast flowing glacier is in general highly crevassed, therefore the close crevasse spacing assumption is a reasonable one. We also focus on

the ablation zone near the front of the glacier, where firn and snow cover are likely to be negligible for much of the year, hence the assumption of constant ice density is valid. Testing of the two models is challenging, as there are many difficulties to measuring crevasse depths; the crevassed regions of any glacier are a dangerous and difficult working environment and the steep-sided, narrow shape of crevasses makes them difficult to observe remotely. One of the few studies to compare modelled and observed crevasse depths (Mottram and Benn, 2009) found that if the crevasse spacing is not implicitly specified, the two methods produce similar results.

Following Otero and others (2010), strain rates are calculated along the flowline (x-direction) rather than in the direction of the vector of maximum longitudinal strain rate. The latter method is more accurate, but was found to give no appreciable difference in calculated crevasse depth, and suffers from a higher computational cost. One disadvantage of this method is that the depth of crevasses is calculated instantaneously using the local stress field, and therefore there is no allowance for the advection of fractures downstream with the ice.

3.2.2 Python wrapper

The calving model is implemented outside Elmer/Ice using a Python wrapper code, which due to the complexity of the code involved was developed largely by Dr. Ian Rutt. This code loads Elmer/Ice and applies the calving model to the output. A flowchart outlining the work process is shown in Figure 3.4.

First, the ice flow model is run in Elmer/Ice for a fixed number of timesteps (n). At the end of the Elmer/Ice run the code examines the output file, reading in coordinates and stress values for each node and determining whether at any time during the run crevasses have penetrated below sea level according to the Nye formulation. If they have not, then Elmer/Ice is restarted from its finishing position and run for another n timesteps and the process repeated. If calving does occur, then the code will identify the new terminus position (the point furthest upstream where

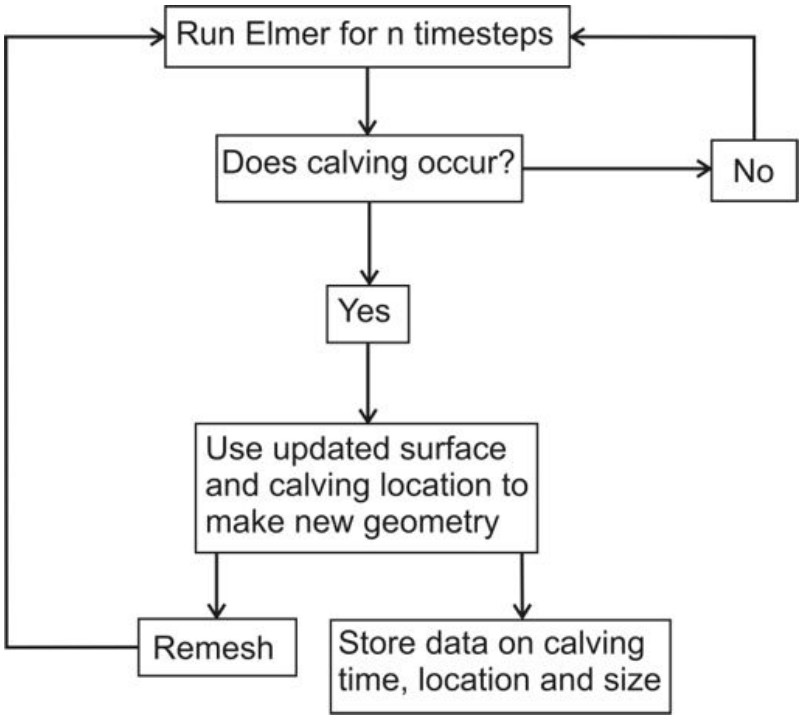

Figure 3.4: The process of the Python wrapper code, which tracks calving events during a model run

crevasse penetrate below sea level), and use the coordinate information to define a new geometry. This information is used to create a new mesh and input file for Elmer/Ice, and the model runs are begun again. This process continues recurrently, producing a file consisting of the timesteps at which calving has occurred, the size of the calving event and the updated terminus location.

The first experiments at Columbia Glacier were made before this wrapper code was completed, and therefore the process of identifying calving was performed visually using Paraview output visualisation software (see Fig. 3.5). The new mesh files were then also created by hand. In both cases experiments were performed using supercomputing resources provided by CSC- IT Center for Science via the HPC-Europa2 funding project. Using the manual calving process, a model run of one year took approximately one week, while with the automatic calving script a 5 year model run took between 20 and 200 hours depending on the timestep used.

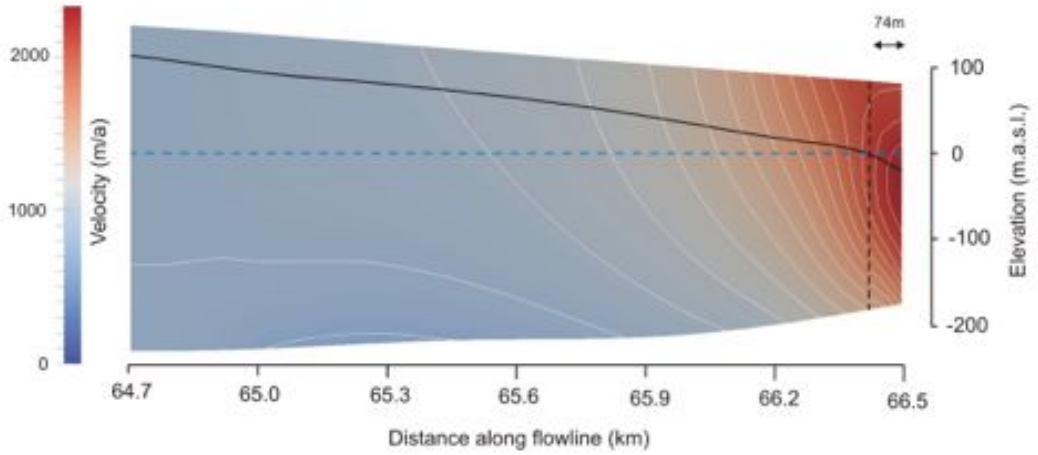

Figure 3.5: An example of how the calving location is located. Contours represent horizontal velocity, solid black line the bottom of the crevasse field, dashed blue line sea level. Where the crevasses cross sea level calving occurs, in this case producing a change in terminus position of 74 m

Chapter 4

Columbia Glacier Experiments

4.1 Introduction

The new calving model presented in this thesis is the first implementation of the crevasse-depth calving criterion to allow the prediction of discrete calving events, with the potential to provide insight into calving behaviour statistics. As discussed in Chapter 2, the crevasse-depth calving criterion has been applied in a number of glacier models (Otero et al., 2010; Vieli and Nick, 2011), but the model presented in this thesis is the first depth-resolved, prognostic model to use a crevasse-depth calving criterion.

The intention of the experiments in this chapter is to test the behaviour of the new calving model outlined in Chapter 3, to investigate the style of calving behaviour produced (size and frequency of calving events) and to investigate its sensitivity to water applied in crevasses, which has been found to have a potentially significant effect on calving behaviour by previous modelling work (Vieli and Nick, 2011). In order to apply the crevasse-depth criterion with a realistic stress distribution, the model is applied to flowline data from Columbia Glacier, Alaska. However, rather than attempting to reproduce the behaviour of this glacier, the work is aimed at understanding the behaviour of the new model and the sensitivity of the crevasse-

depth criterion to a key controlling parameter, the depth of water in crevasses. This work has been published as Cook et al. (2012).

Columbia Glacier is a large, temperate tidewater glacier on the south coast of Alaska (Figure 4.1). The glacier was for a long time pinned on a large moraine shoal near Heather Island, the top of which reached to around 20 m below sea level, while further up-glacier the glacier sat in a basal overdeepening of up to 500 m below sea level. In the mid-seventies it was realised that this precarious situation meant that Columbia may have been about to begin a rapid retreat, raising concerns over the effect of icebergs on nearby shipping lanes. This led the U.S. Geological Survey (USGS) to begin an intensive study involving aerial photography and ground-based and boat-based fieldwork. Fears proved to be correct, and in the early 1980s the glacier began a dramatic retreat which has lasted to the present day. The glacier has retreated around 18 km over this period, while observation by the USGS has continued, providing a uniquely long and detailed record of glacier behaviour in retreat. This comprehensive data record with accompanying bed elevation measurements makes Columbia Glacier particularly suitable as a test case for a tidewater glacier flow model.

4.2 Data

This work uses a dataset composed of repeat aerial photography from which measurements of glacier length, surface elevation and speed have been made (Krimmel, 2001; O'Neel et al., 2005). Glacier length is measured along the flowline defined in Figure 4.1. The standard error in the surface altitudes measured by this photogrammetric method is estimated to be 2.5 m by Rasmussen and Meier (1985), determined by comparison with 58 ground truthing points. Velocities are calculated by feature tracking of surface crevasses and seracs, with 4-6 repeat flights being typically made per year. The error in displacement vectors is estimated to be 4 m (Krimmel, 2001), leading to an uncertainty in velocity of up to 50 $\mathrm{m\,a^{-1}}$, although this does not take

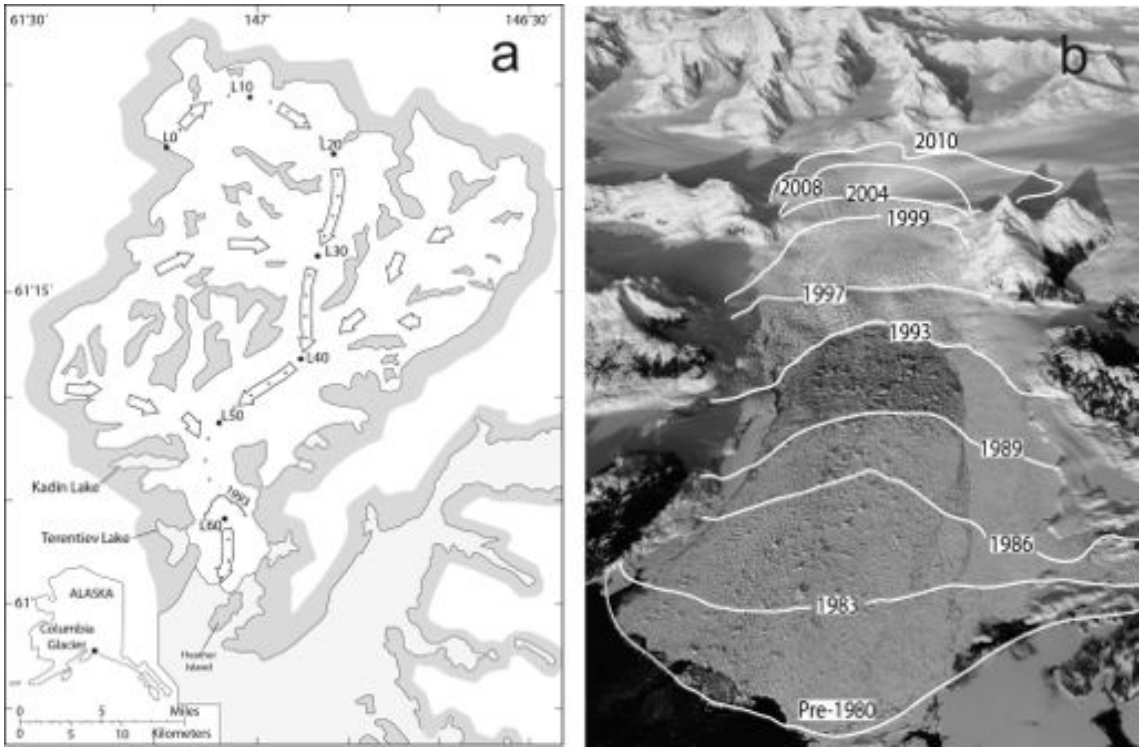

Figure 4.1: (a) Map of Columbia Glacier (source: USGS). Thick arrows and dotted line show the location of the central flowline used in this model. Location of 1993 calving front marked. (b) Oblique photograph of Columbia Glacier, with front marked to show retreat (source: R. M. Krimmel).

into account the short term velocity fluctuations which will necessarily be averaged out by this observation method.

Basal topography measurements are taken from two sources; downstream of approximately the 2003 terminus, measurements are taken from a ship-borne survey by the US National Oceanographic and Atmospheric Administration (NOAA) using side-scan sonar, which provides the bathymetry on a 5-meter grid (Noll, 2005). Upstream of this region, a continuity-based model (Rasmussen, 1989; O'Neel et al., 2005; Engel, 2008) constrained by airborne radar measurements provides basal topography. In the downstream regions covered by bathymetry, basal elevations are accurate to ± 20 m, while in the region of continuity estimates, errors are on the order of 25% (100 m). Although the glacier was observed temporarily to have a floating tongue between 2007 and 2009 (Walter et al., 2010), the bed topography and surface geometries show that the glacier remained grounded for the majority of its retreat, meaning that for the majority of the retreat the effects of floating ice in the model do not need to be considered.

4.3 Model Set-up

A two-dimensional (2D) model of Columbia Glacier was created using the observed bed topography and surface elevation from 1993 on an idealised flowline along the approximate centre of the glacier. The path of the flowline is shown in Figure 4.1, and the 1993 bed and surface elevation in Figure 4.2 (b). Flowline locations used in this chapter reflect the horizontal distance (km) from the ice divide. The 1993 start time was chosen as it represents a point mid-way in Columbia Glacier's retreat, characterising the dynamics of Columbia Glacier during a period of rapid frontal change. General details of the model used are discussed in Chapter 3, with specific forcing parameters outlined here.

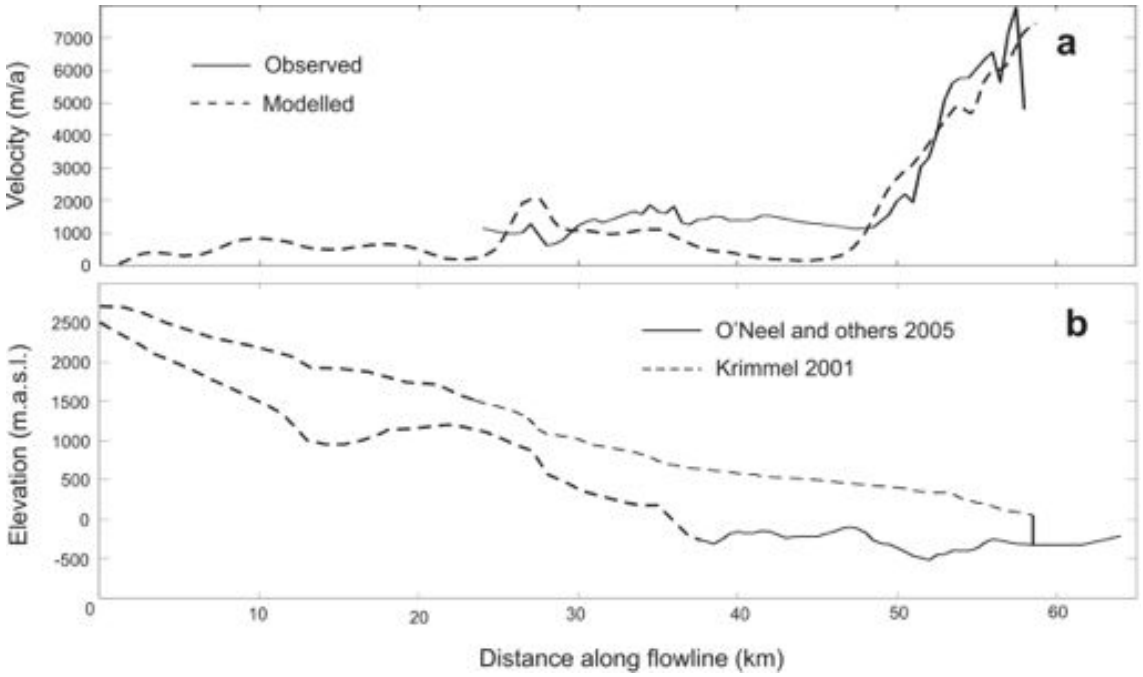

Figure 4.2: (a) Comparison of observed and modelled horizontal flow velocity. (b) 1993 surface and bed elevation data along the central flowline of Columbia Glacier, showing different data sources.

4.3.1 Mass balance

Accumulation and ablation data were taken from Tangborn (1997), who parameterized surface mass balance as a function of altitude using low-altitude precipitation and temperature observations and the area-altitude distribution of the glacier. The annually-averaged surface mass balance profile over the period 1949-96 is approximated by the empirically fit equation:

$$M = 3.2\ln(s) - 22.5 \text{ ma}^{-1} , \tag{4.1}$$

where M is the surface mass balance and s is elevation in metres above sea level. The summer of 1993 had a mass balance very close to this average.

Table 4.1: Error in surface velocity of Columbia Glacier model associated with different sliding parameters.

	A_0 $(\mathrm{m\,kg})^{1/2}\ \mathrm{a}^2$	A_1 $(\mathrm{m\,kg})^{1/2}\mathrm{a}^2$	r.m.s. full length $(\mathrm{m\,a}^{-1})$	r.m.s. 53km+ $(\mathrm{m\,a}^{-1})$
	2.9×10^{14}		2275.0	4995.8
	5.0×10^{14}		2219.4	4797.0
	1.0×10^{15}		2055.1	4414.2
	5.0×10^{15}		1404.3	2541.1
	1.0×10^{16}		1083.4	1261.7
	5.0×10^{16}		2774.2	5900.5
Initial	5.0×10^{16}	1.0×10^{15}	836.4	360.9
a	1.0×10^{17}	1.0×10^{15}	967.4	824.1
b	1.0×10^{15}	1.0×10^{15}	911.1	1276.2
c	5.0×10^{16}	5.0×10^{15}	2166.6	4691.1
d	5.0×10^{16}	5.0×10^{14}	900.9	1033.5
Final	7.2×10^{16}	9.1×10^{14}	-	249.0

4.3.2 Basal sliding

As discussed in Chapter 3, Columbia Glacier has been observed to have a significant deformable sediment layer at the bed. Additionally, measured flow speeds at Columbia Glacier demonstrate that sliding is the dominant component of surface motion (Meier and Post, 1987; O'Neel et al., 2005), and borehole water pressures confirm low values of effective pressure (Meier et al., 1994). However, measurements of till strength indicate that it would be unable to support the high driving stresses of Columbia Glacier, leading to the conclusion that basal drag is dominated by areas of exposed bedrock. Thus the adapted power law described in Equation (3.17) was used.

The basal sliding parameter A_s was determined by an iterative trial and error process, refining the parameter to find a best fit to observed data by minimising the

r.m.s. error. The starting point was the value used by Nick et al. (2007a) $A_s = 2.9\times10^{14}$ $(\mathrm{m\,kg})^{1/2}\mathrm{a}^2$. Fits using a single sliding parameter are detailed in Table 4.1 and shown in Figure 4.3. Although the observed surface velocity profile shows a down-turn in velocity near the terminus, in the modelled velocity profile this occurs further upstream (around km 55) which leads to underestimated velocity at the terminus. This corresponds with a region of reversed bed slope towards the front of the glacier (km 52-62, see Figure 4.2 (b)). The discrepancy between modelled and observed velocities in this area was probably caused by 3D effects neglected in the flowline model. To account for the difference, in this region (down-glacier from km 55) sliding was enhanced by decreasing the sliding coefficient, creating two regions of different sliding coefficient in the model. The two sliding coefficients were varied, with the associated r.m.s. errors detailed in Table 4.1 and the fits shown in Figure 4.4. From this stage only r.m.s. errors in the region from km 53 to the terminus were considered, as this is the region most relevant to terminus dynamics, and also the area least likely to be affected by 3D effects, as the width of the glacier is fairly constant. Refinement by iteration continued to produce a best fit of $A_0 = 9.1\times10^{14}$ $(\mathrm{m\,kg})^{1/2}\mathrm{a}^2$ (up to km 55) and $A_1 = 7.2\times10^{16}$ $(\mathrm{m\,kg})^{1/2}\mathrm{a}^2$ (km 55 to terminus). These values produced an r.m.s. error of 249 $\mathrm{m\,a}^{-1}$, which is relatively small compared to absolute velocity values of 7000 $\mathrm{m\,a}^{-1}$ around the front. The final fit of modelled to observed velocity can be seen in Figure 4.2(a).

4.3.3 Lateral effects

The experiments in this chapter were performed without any additional 3D contributions to flow. Figure 4.1 shows several regions where this assumption would be expected to fail: convergent flow at km 35 and 50 where tributary glaciers join the main trunk, and km 53 where the valley narrows. Lateral drag is also considered to have a stabilising effect on glacier termini (Benn et al., 2007a; O'Neel et al., 2005), but should only have a significant effect on the stress balance around the terminus if there are large along-flow gradients in flow width. Neglecting these 3D processes

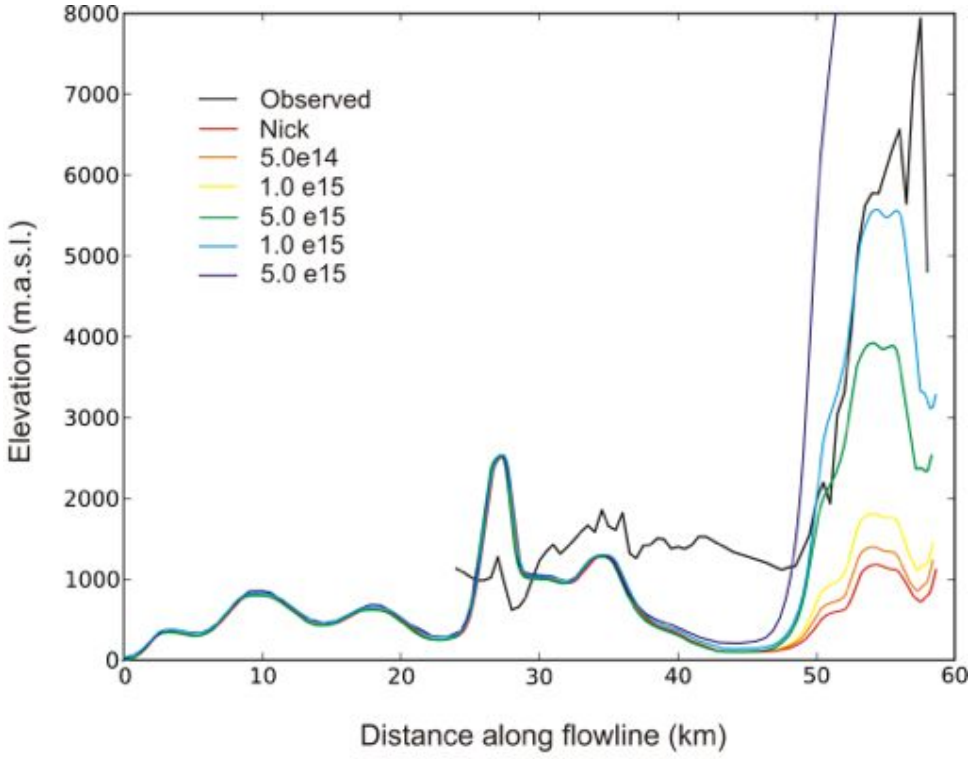

Figure 4.3: Fit of modelled to observed surface velocity using a single basal sliding parameter

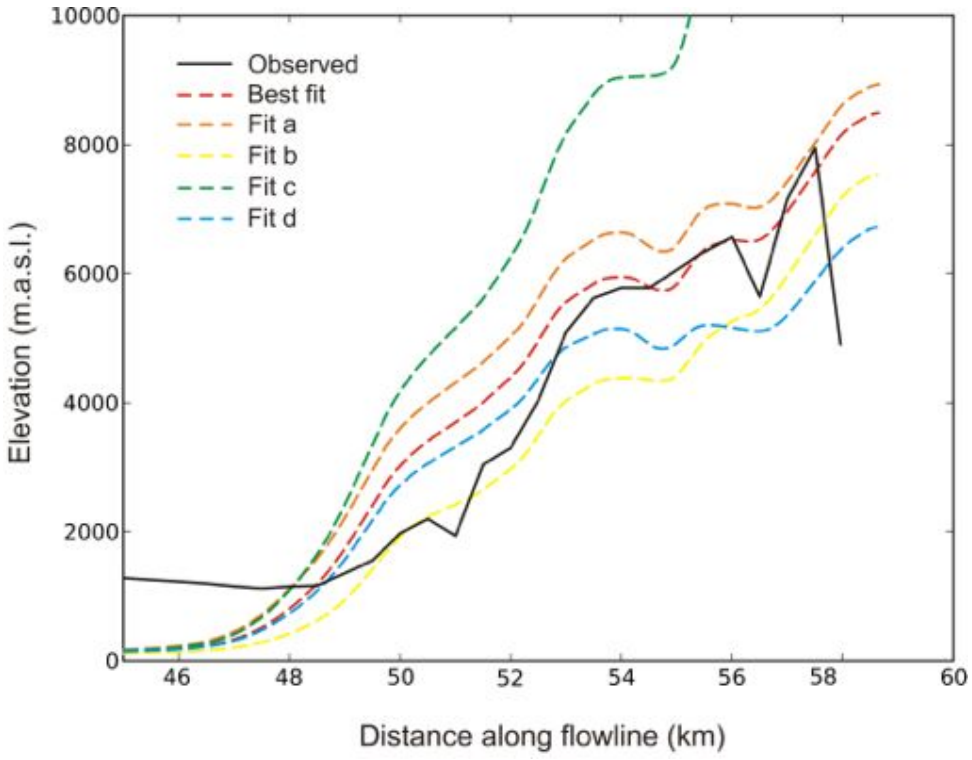

Figure 4.4: Surface velocity fits using two sliding parameters. Details of sliding parameters used in fits a-d are given in detail in table 4.1.

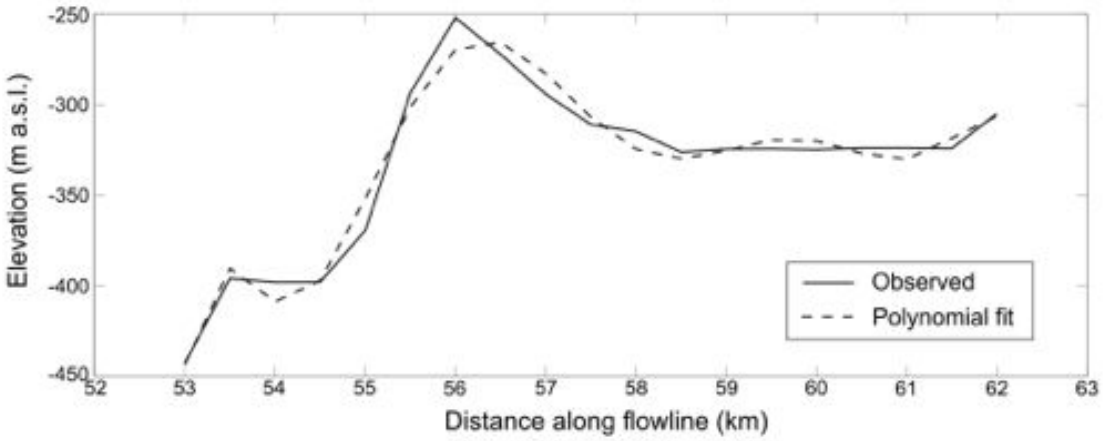

Figure 4.5: Bed interpolation used for advancing front experiments.

is possible because of the broad and constant channel width (5-6 km) upstream of the 1993 terminus in the region of interest (km 55-60, Fig 4.1).

4.3.4 Bed sensitivity

The 1993 start time was chosen as it characterizes the dynamics of Columbia Glacier during its retreat, which is a period of particular interest. The associated length change and surface lowering in a time of retreat prohibited the use of an initialization (spin-up) period before model runs began. Full-Stokes computations result in long model run times, which also prevented the execution of an initialization period in the glacier's steady state position 15 years prior to 1993. This lack of initialization makes the model sensitive to errors in the bed and surface DEMs (Zwinger and Moore, 2009), which could lead to inaccuracy in the simulated surface evolution. Despite this source of inaccuracy, the mid-retreat set-up is sufficient to provide a realistic glacier geometry in order to perform sensitivity testing, as it is not intended to produce an accurate model of observed glacier retreat.

As mentioned in Section 3.1.6 the bed around the front of the glacier was approximated by a polynomial function, plotted in Figure 4.5. The bed polynomial has an r.m.s. error of 13.8 m, less than the uncertainty in the observed bed data.

4.4 Model Experiments

The implementation of the crevasse-depth calving criterion in this model allows the prediction of discrete calving events. Whether or not the glacier calves depends on the stress profile around the front, and a sufficiently short time-step will ensure multiple time-steps occur between calving events. This is important as, in such a scheme, calving at every time-step would produce a spurious dependence of calving rate on the time-step chosen. Therefore, the time-step of model runs was selected in to ensure that calving did not occur at every time-step.

Prognostic model runs were carried out with lengths of 0.5 and 1 year, starting in each case from the 1993 geometry. To test sensitivity of the model to the input variable, a variety of different crevasse water depths (D_w) were used, ranging from 0 to 10 m. Results using crevasse water depths over 10 m were rejected as they led to calving occurring at every time-step. Although 10 m may be a relatively small amount of water compared to the depth of crevasses, it is sufficient to reproduce a wide range of glacier behaviour. For most of the model runs, a time-step of 0.005 year (1.8 d) was found to produce reliable results, with multiple time-steps occurring between calving events. The experiment with 10 m water depth used a 0.001 year (0.4 d) time-step, which was found to be the maximum time-step still to produce periods with no calving. Model runs on such short time-steps take a significant time to complete, so this experiment was only run over 0.5 year, compared to 1 year for the others.

4.5 Results

4.5.1 Sensitivity tests

The first experiment performed was to test the dependency of model results on the mesh density used. The observed geometry was used to create a variable mesh of

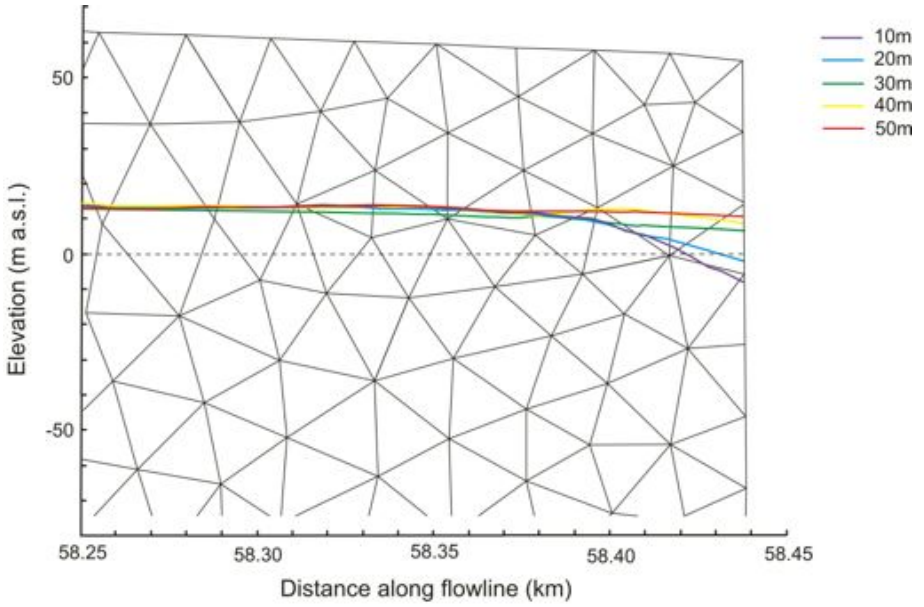

Figure 4.6: Testing the influence of mesh density on model output. Coloured lines represent the base of the modelled crevasse field, showing that calving occurs for grid sizes below 30 m.

size 70 m towards the upper boundary, shrinking nearer the terminus to produce a more accurate result. The model was tested with a range of grid sizes at the front, from 10 m to 50 m. The effect of grid size was also tested with a range of crevasse water depths. There are two cases in which mesh size might have an effect. Firstly, in the case of calving does it affect the size of calving event observed? Second, does a smaller grid size pick up calving events which are not observed on a coarser grid?

Firstly, a typical calving event was examined, using a model snapshot towards the beginning of the experiment with 7 m crevasse water depth (t = 0.2 a). In this situation the largest difference in outcome occurred between 10 m and 50 m mesh density cases, with a difference of 13 m in the size of calving event observed, a change of 2.7%. If the crevasse water depth was increased at this point to 10 m, the discrepancy reduced to only 10.1 m or 2.1%. Both of these changes are small compared to the overall size of calving event observed, and would be expected to have minimal effect on the overall results of the experiment.

Secondly, the initial state of the glacier was used as an example of a case where on

a 50 m grid no calving event was observed. At 0 m crevasse water depth, there were some minor differences in the depth of the crevasse field around the front, but none of the different mesh densities produced calving. Figure 4.6 shows the case with 5 m crevasse water depth. Here, in the cases of 10 m and 20 m grid size crevasses began to cross the water line around the terminus, producing respectively calving events of 14.6 m and 5.2 m. Lastly, the set-up was tested with 10 m crevasse water depth. In this case, the results using 10 m and 20 m mesh size again produced calving events, this time of size 20.1 m and 15.7 m, while coarser meshes did not show calving. In the model runs, events of under 20 m do not have a significant effect on the glacier behaviour, and are at the limit of the mesh resolution to represent accurately. Therefore it can be said that a smaller mesh size will only produce additional calving events of negligible size, and will not significantly effect the size of larger events, and a larger grid is used for the sake of reducing the memory required for model runs.

To test if the calculated calving rate was dependent on the time-step used, the experiment with 9 m water depth was run again with time-steps ranging between 0.002 and 0.005 years. Each experiment reached a slightly different final terminus position, with a maximum deviation of 19.6 m (less than the mesh size) and a standard deviation of 5.9 m which represents 1.3% of the overall change in terminus position. This difference is sufficiently small that the 0.005 year time-step is used for all further experiments in order to minimise the duration of model runs.

4.5.2 Calving behaviour

Previous calving models have used two approaches; using a calving law to define either a calving rate or the position of a glacier's terminus. However, in both cases this calving law has been applied at every timestep so that the terminus position of the glacier is predicted over time, but no information is gained about the calving events produced *i.e.* their size and frequency. The advantage of the calving criterion presented here is that it can predict whether calving will occur on a given

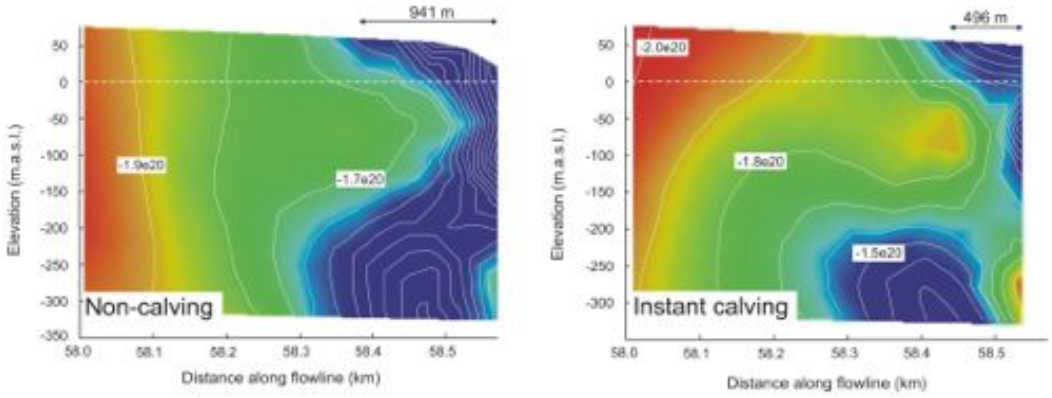

Figure 4.7: Modelled longitudinal deviatoric stress profiles, showing lower longitudinal stress in non-calving situations. Stress measured in $\mathrm{kg\,m^{-1}a^{-2}}$ with contour intervals of 0.1 $\mathrm{kg\,m^{-1}a^{-2}}$. Distance shown between the terminus and peak in longitudinal deviatoric stress.

timestep and if so where the new terminus location will be. In general, a time-step can be chosen which ensures that there are multiple time-steps of glacier advance between each calving event, thus providing information about the size and frequency of calving events which can be compared to observed data.

The fact that calving does not occur on many timesteps is likely to be because the maximum horizontal deviatoric stress is located some distance behind the calving face, as noted previously by Hanson and Hooke (2000, 2003), which is not the area of lowest surface elevation. Hence a period of surface lowering is required before calving occurs again. Figure 4.7 shows the modelled stress profiles when the glacier is just about to calve, and at the beginning of a long period without calving. In the calving situation, longitudinal deviatoric stresses are higher around the terminus, and the peak occurs closer to the front of the glacier, where surface elevations are lower. The precise timing of calving events in these situations would also be likely to be affected by the advection of crevasses downstream from the point of peak longitudinal deviatoric stress towards the calving front, but at present the model is not capable of representing this process.

Table 4.2: Modelled and observed rates of retreat and advance (retreats negative) in 1993. Modelled retreats calculated excluding the initial 10 calving events. Observed retreat rate calculated from most advanced position. Calving rates in km along flowline, calculated using the average size of, and time between, each calving event in the model run to indicate different styles of calving behaviour. Average size of calving events shown below.

D_w	0 m	5 m	7 m	8 m	9 m	10 m	Observed
Retreat rate ($\mathrm{km\,a^{-1}}$)	+3.53	+3.03	+2.69	-0.12	-0.12	-1.91	-0.64
Calving rate ($\mathrm{km\,a^{-1}}$)	0.000	0.096	0.190	0.470	0.570	0.700	-
Mean event size (m)	-	37.8	64.3	221.6	215.4	88.7	-

4.5.3 Response to water in crevasses

The model was also used to test the sensitivity of the modelled calving rate to the imposed crevasse water depth. To this end, a number of experiments were run with varying water depth as described in Section 4.4. Overall, the results show that the behaviour of the calving model depends strongly on the crevasse water depth (Figure 4.8). With no surface water in crevasses, the model glacier does not calve at all but steadily advances. Over the length of the model runs, for small crevasse water depths (5-7 m) the model glacier advances significantly, while for larger depths (8-10 m), after an initial advance, the model glacier retreats (Table 4.2). The observed retreat rate in 1993 of 0.64 $\mathrm{km\,a^{-1}}$ (Krimmel, 2001) falls between the values modelled with crevasse water depths of 9 m and 10 m. At the end of the experiment, the different water depth scenarios, although showing a similar surface evolution, reach significantly different end points in terminus position (Figure 4.9).

Throughout the experiments the models also exhibit significantly different calving behaviour. Examining the calving rates (Table 4.2, Figure 4.10) it can be seen that calving rate increases with crevasse water depth, as would be expected given the calving criterion used. Model runs with 5 m and 7 m water exhibit infrequent, relatively small calving events. For greater crevasse water depths the calving events are not only more frequent, but also tend to be larger; generally between 200 and

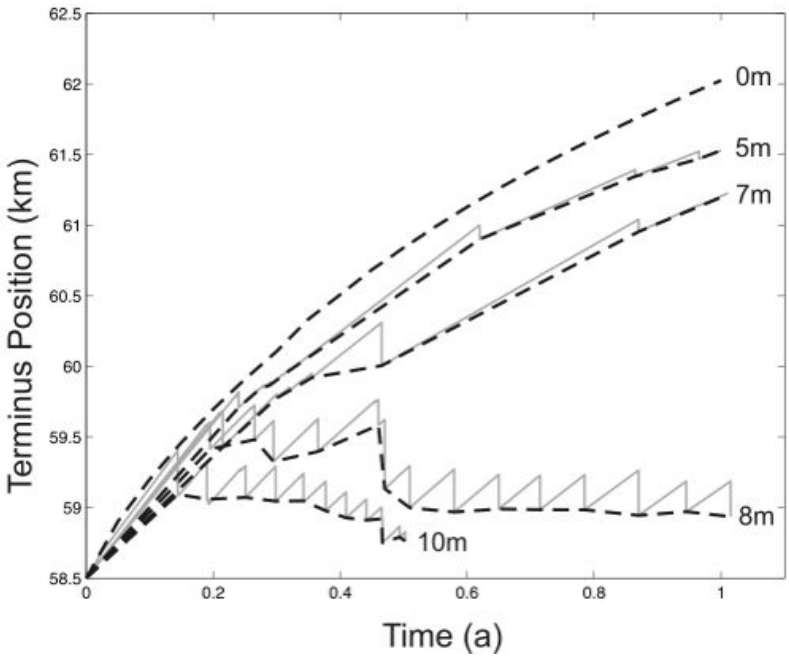

Figure 4.8: Computed evolution of terminus position over time for different depths of water in crevasses. Pale grey lines show the size of calving events, dashed lines show the position after each calving event to highlight the overall trend of retreat/advance (events less than 20 m in size are excluded). Lines for 9 m water depth are not shown as they do not significantly differ from those for 8 m.

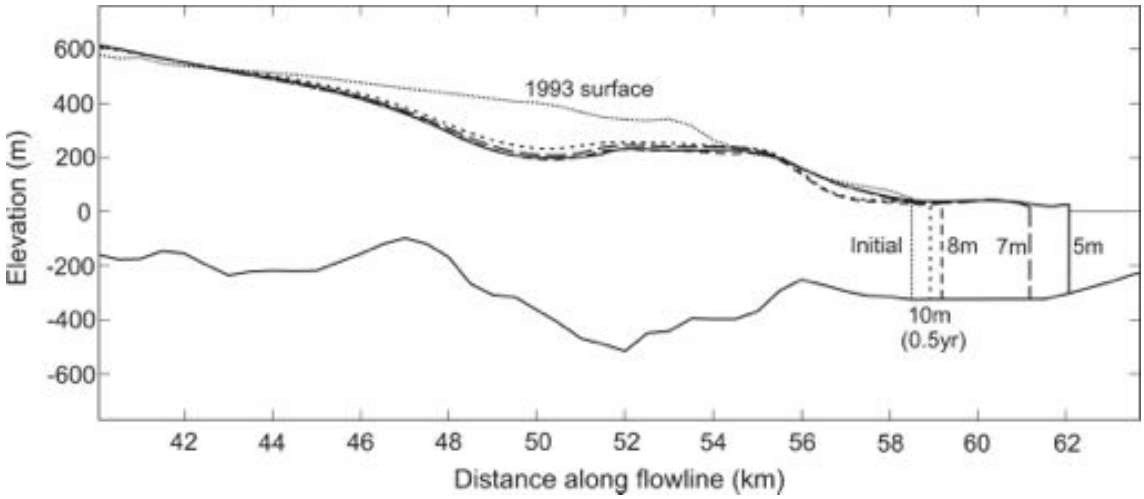

Figure 4.9: Glacier surface profiles for the initial model geometry in 1993, and at the end of each model run for different values of crevasse water depth (for 10 m the model run is only 0.5 year, compared to 1 year for others).

300 m, whereas the 5 m and 7 m experiments show an average calving event size of 54 m. The exception is the 10 m experiment, which showed a high frequency of both large and small calving events, hence the lower average size.

4.6 Discussion

The results show that modelled calving rate is highly sensitive to changes in crevasse water depth. Results were only reliable (with multiple time-steps between calving events) for crevasse water depths ranging between 0 and 10 m. Within this range there is a wide disparity in terminus behaviour, ranging from a 3.5 km a^{-1} advance to 1.9 km a^{-1} retreat. The range of crevasse water depths used is small compared to the depth which crevasses may reach in a glacier, but in this model is was sufficient to cause a significant difference in terminus behaviour. This effect is likely to be due to the low surface gradient around the glacier terminus, as seen in Figure 4.9. These areas of low surface slope also exhibit a shallow crevasse depth profile, so that small changes in crevasse depth can lead to large horizontal shifts in calving position. This is also the likely reason for the threshold in terminus behaviour between crevasse

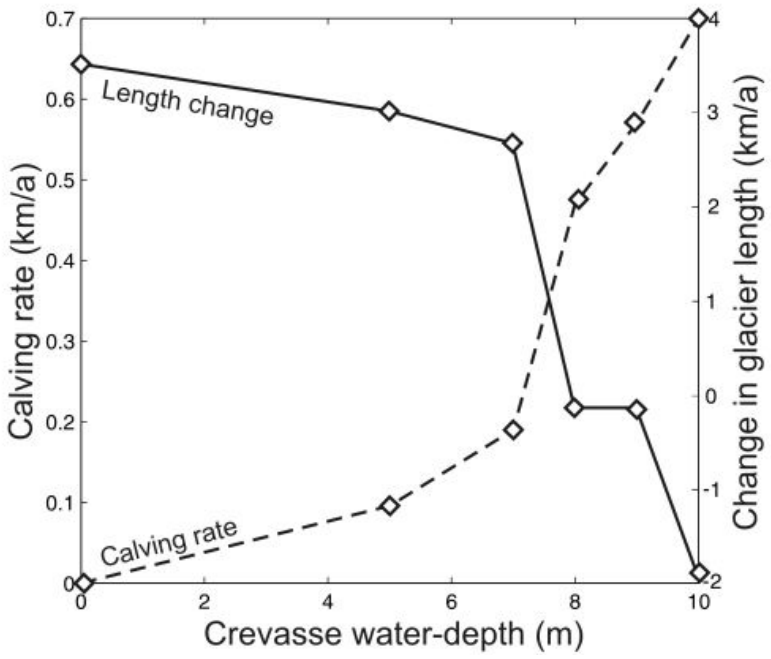

Figure 4.10: Modelled calving rates and final terminus position. Calving rates calculated using the average size of, and time between, each calving event in the model run. Glacier length change calculated over length of each run, and in case of retreat after initial 10 events.

water depths of 7 and 8 m. The shallow terminus is more pronounced in the modelled surface elevation than the observed, and may be partly due to the lack of a lateral drag term, as lateral drag will tend to impede horizontal spreading around the glacier terminus. However, a flat tongue is a feature of many glaciers, although less pronounced at Columbia Glacier in 1993, so the result may still be considered interesting from a general modelling perspective.

One particular feature of the sensitivity to meltwater is the change in behaviour between 7 and 8 m crevasse water depth, suggesting that the calving rate can be extremely sensitive to relatively small changes in this variable. This sensitivity to crevasse water depth may make the crevasse-depth calving criterion difficult to implement in a predictive ice-flow model. A 1 m change in crevasse water depth will produce a significant effect on the stress, in turn affecting crevasse depth and calving rate, but it is likely to be small compared to any potential measurement errors. Crevasse water depth is an inherently difficult property to measure, as the crevassed regions of any glacier are a dangerous and difficult working environment and the steep-sided, narrow shape of crevasses makes them difficult to observe remotely. It is also a difficult property to estimate using surface mass balance models, which would require estimates of crevasse width and length, and also an idea of the rate at which water drains from the crevasse. Drainage rates are likely to be high in the extensively fractured regions around a calving face.

Sensitivity to crevasse water depth had been indicated in previous modelling work (Vieli and Nick, 2011) and is an effect that may be expected, as many calving glaciers exhibit a strong seasonal cycle of winter advance and summer retreat, which may be explained in part by the presence of more surface meltwater in the summer months. As many studies have previously focused on the ocean warming as a potential trigger for glacier retreat (e.g. Holland et al. (2008); Murray et al. (2010)) the result may also be interesting in highlighting the potential for atmospheric warming to cause glacier retreat by the mechanism of increased crevasse penetration and calving, rather than by increased velocity as meltwater penetrates to the bed (Zwally et al., 2002).

The modelled increase in calving rate with crevasse water depth is characterised by a general increase in both frequency and size of calving events. This is the opposite behaviour to that expected from observation (Walter et al., 2010) and theory (Amundson and Truffer, 2010), where small icebergs calve frequently while large calving events happen only infrequently. This apparent contradiction can be explained by considering the simplifications made in formulating the calving model. Each calving event in the model should be considered as a rapid change of terminus position within one timestep (roughly one day), which could occur by the release of an individual large iceberg, or a disintegration into many smaller blocks. In many cases the region downstream of the calving point is also crevassed below sea level, so may be expected to disintegrate rather than break off as a single berg. It should also be noted that one would not expect a uniform crevasse field in a real glacier, and stochastic variations in crevasse depth will control the exact timing at which an iceberg is released. Consequently, the model simulates typical calving behaviour rather than being able to identify the release of individual icebergs. Nevertheless, the frequency of modelled calving events is physically meaningful, and the size distribution of events could best be compared to high frequency repeat measurements of terminus position from satellite images. The model establishes event-driven models as a potential method to investigate short-time scale physics at the tidewater margin.

4.7 Chapter Summary

Previous modelling work (Nick et al., 2009) suggests that penetration of surface meltwater to the bed of a calving glacier (causing increased basal water pressure and therefore increased sliding velocity) is unlikely to force observed levels of acceleration and retreat. The results presented here suggest that acceleration and retreat could be triggered by surface meltwater, via enhanced fracturing and deepening of crevasses. This input increases calving rates, allowing higher air temperatures to play a key role in initiating retreat and dynamic instability.

The strong dependence of the modelled calving rate on crevasse water depth is likely to cause difficulty in applying the method to predictive glacier and ice sheet models. Results may be significantly influenced by poorly constrained input data. However, the ability to simulate glacier calving as a sequence of individual, physically-meaningful events means that it has potential to investigate the physics controlling calving under a variety of environmental conditions. Potential exists to greatly enhance our understanding of the complex interactions between calving and ice dynamics, but this requires longer model runs with a larger dataset of modelled calving events for analysis to be rigorous. The further work presented in the following chapters addresses this issue.

Methodological improvements are also needed to switch from the kind of sensitivity experiment presented in this chapter to an accurate representation of glacier behaviour. Future improvements should accommodate lateral drag in the modelled stress distribution, as well as seasonality in the input variables (such as crevasse water depth, which may be expected to vary with surface ablation). A realistic calving model should also represent other processes affecting calving, such as submarine melt and resistive stress from sea ice that may alter the stress profile around the terminus. These improvements are addressed in the next chapter.

Chapter 5

Helheim Glacier: Sensitivity Analysis

5.1 Introduction

After the work presented in Chapter 4 was performed, the calving model was developed by Dr. Ian Rutt to include an automated process of identifying calving locations and updating the model's mesh (details are discussed in Section 3.2.2). This development meant that model runs could be performed much more rapidly, allowing a broader range of experiments to be undertaken. In the previous chapter, the time required for performing model runs meant that extensive testing of the model's sensitivity was not possible. In this chapter a sensitivity analysis of all the input parameters and boundary conditions is presented, examining the effect of changes in input variables on model results.

The sensitivity analysis experiments were performed using a model of Helheim Glacier, South-East Greenland rather than Columbia Glacier as before. The change of location was driven by the wider variety of environmental forcings thought to be active in South-East Greenland, making it a more interesting focus for future study. This is discussed in more detail in Sections 5.2 & 6.1.

5.2 Study Location

Helheim Glacier is the fastest flowing glacier on Greenland's eastern coast, with a large drainage basin of 48100 km^2 (Rignot and Kanagaratnam, 2006)(see Figure 5.1). The terminus location of Helheim Glacier was relatively stable throughout the late 1980s and early 1990s, although annual variations of up to 3 km were not uncommon (Bevan et al., 2012). After a period of thinning in the 1990s (Abdalati et al., 2001), the front began to retreat in 2001. Over the period 2001-2005 the front retreated by 6 km and the main trunk sped up by around 3.0 $km\,a^{-1}$ and experienced thinning of 40 m (Howat et al., 2005). By 2006, thinning had stopped near the front and the glacier slowed and began once again to advance (Howat et al., 2007). It has experienced a relatively stable frontal position between 2007 and the present day, though with significant seasonal variation (see Figure 5.2). Although annual variation in terminus position is common, the rapid retreat of 2001-5 was exceptional and was also paralleled in many glaciers in the region. The cause of this synchronous retreat is still widely debated, with potential triggering by high air and sea temperatures hypothesized. Modelling work has the potential to shed light on the mechanisms which might cause high temperatures to lead to a retreat. Previous work by Nick et al. (2009) has indicated that a sudden decrease in backstress from ice mélange could have sufficient effect to cause the changes observed, while further work by Vieli and Nick (2011) shows melting at the glacier surface and pooling of water in crevasses may also be significant. This interesting history of frontal variation, the availability of data both from the glacier and the proglacial fjord and the fact that Helheim seems often to be grounded at the front, unlike many other Greenland glaciers, led to its choice as the location for modelling work.

5.3 Data

Modelling work on Helheim Glacier became possible with the publication of bed data by CReSIS (Center for Remote Sensing of Ice Sheets), measured in April 2009

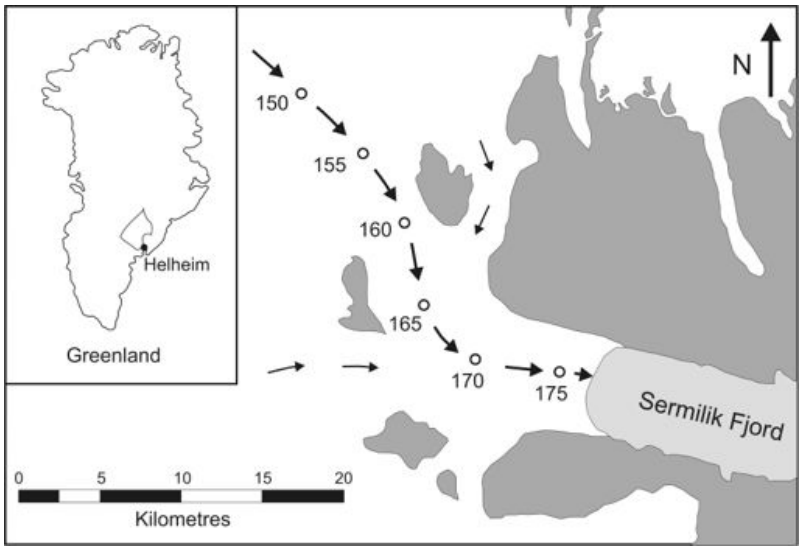

Figure 5.1: Location of Helheim Glacier and flowline used for modelling. The main flow line and significant tributaries are marked with arrows. Points along the flowline are marked with distance in km from the ice divide. Inset shows location of glacier and extent of drainage basin.

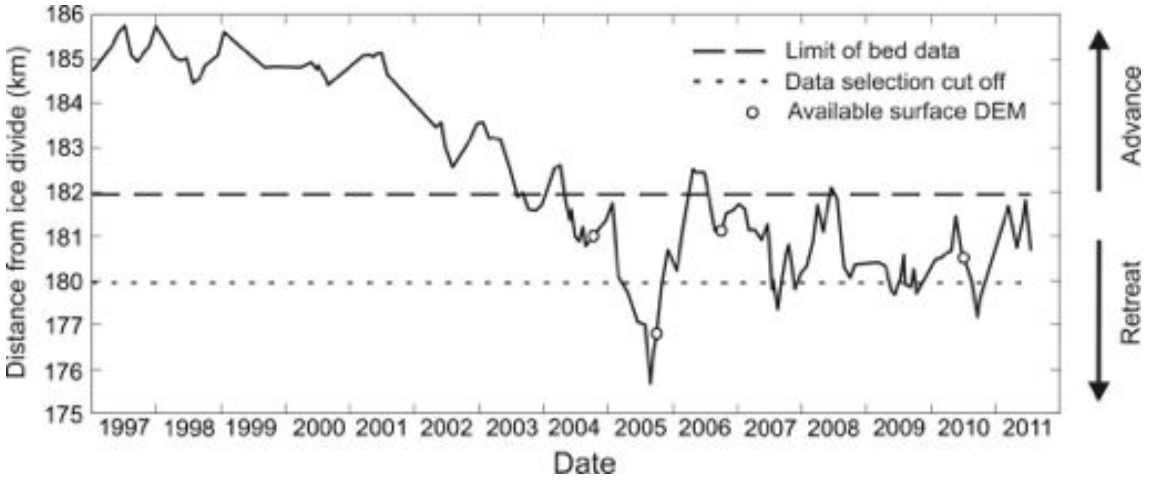

Figure 5.2: Helheim frontal position 1997-2011, showing criteria used for selecting data. Data from Anne Goldsack, Swansea University (personal communication, Nov 2011).

using an airborne radar depth sounder (Leuschen et al., 2011). This provides a bed elevation map of Helheim Glacier from the 2009 ice front up to around 45 km inland with a horizontal resolution of 500 m and vertical error of around 20 m in areas of good bed signal, while areas of poor quality return use an interpolated bed with higher associated error. In areas outside the reach of this bed product, the model uses data from Bamber et al. (2001), as provided by the National Snow and Ice Data Center DAAC, University of Colorado, Boulder (NSIDC). These are measured from an extensive campaign of airborne radar flights and interpolated onto a 5 km grid.

Surface elevation in the outlet glacier region was taken from a pair of ASTER images, with photogrammetry providing a DEM with 15 m horizontal resolution and a vertical accuracy of 15 m (data provided by Nick Selmes, Swansea University (personal communication, Oct 2011)). The date chosen for modelling was constrained by the availability of surface elevation data and the horizontal extent of the bed data. Ideally the terminus location at the time of measurement should allow at least 2 km of bed data for the model to advance into, to allow investigation of all types of glacier behaviour. Figure 5.2 shows the limit of the bed data and the available ASTER image pairs (those with sufficiently little cloud cover to be useful for producing a DEM), showing that July 2005 was the only suitable date. The ASTER DEM extends around 45 km inland from the glacier terminus, further upstream data were taken from the Geoscience Laser Altimeter System/ICESat 1 km Laser Altimetry Digital Elevation Model of Greenland (DiMarzio et al., 2007) also provided by the NSIDC (see Figure 5.3).

The surface velocity in the model was compared to velocity data measured by feature tracking between pairs of Landsat satellite images, selected approximately a month apart (data provided by Adrian Luckman, Swansea University (personal communication, Jan 2012)). Three pairs of images were found in summer 2005, and the results of feature tracking are shown in Figure 5.4(a). As can be seen, there was a large degree of scatter in this raw data, caused by incorrect identification of surface features by the automated tracking software. Data were selected by filtering on grounds of along-flowline velocity gradient, removing data points with a velocity

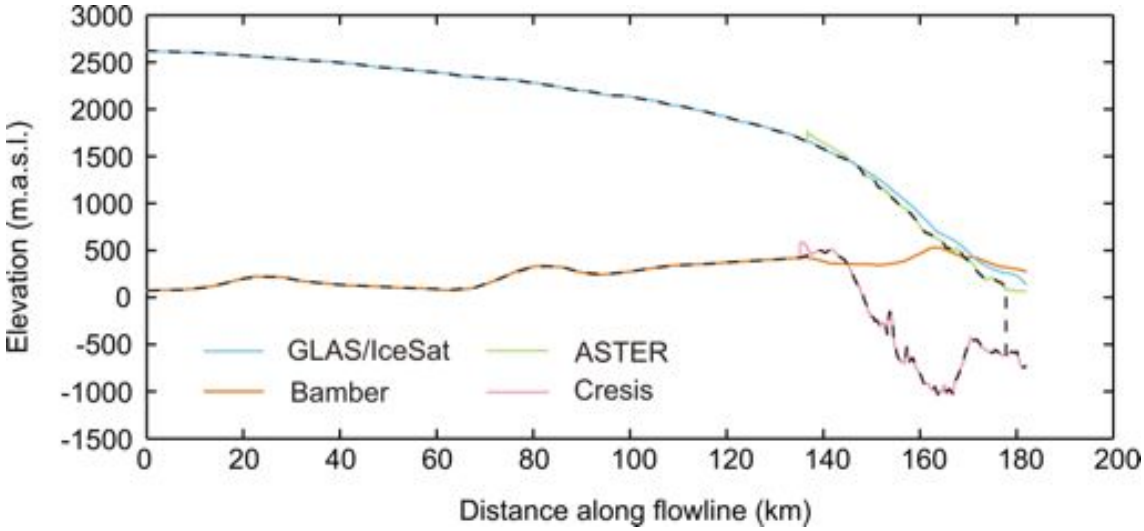

Figure 5.3: Surface and bed elevation data available from different sources. Black dashed line indicates data used in creating model geometry for July 2005.

gradient more than twice the average between them. The highest quality data were from the 29/08/05-21/09/05 pair, while some values from the other image pairs were used to fill data gaps. This means that the majority of the velocity data were measured around two months after the surface elevation DEM. The filtered data is shown in Figure 5.4(b). Errors on the selected velocity data arise largely from errors in geolocation of images and changes in the shape of tracked crevasses as they evolve between the two images and are likely to be less than 350 $\mathrm{m\,a^{-1}}$. All data were extracted along a flowline identified by Dr. Luckman (see Figure 5.1), this was identified using velocity data and surface debris features, and a flowline was selected as near to centre as possible.

5.4 Model Set-up

5.4.1 Geometry

In the previous model of Columbia Glacier it was possible to use the full extent of the flowline, as the channel was of roughly constant width along its entire length. The

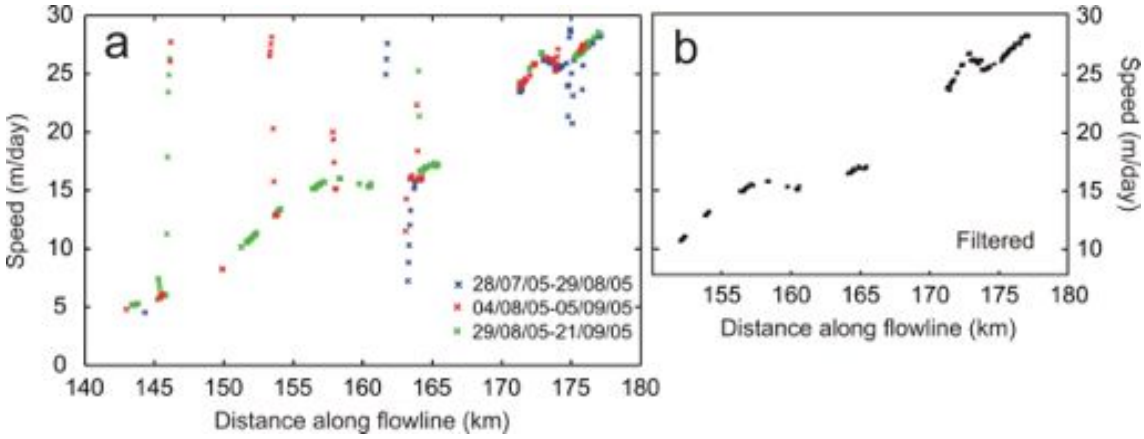

Figure 5.4: Surface velocity for Helheim Glacier, measured by feature tracking on Landsat image pairs (dates shown in key). (a) Raw data (b) Filtered data.

geometry of Helheim Glacier is very different, as can be seen in Figure 5.1, because the glacier drains a wide basin. In regions where the glacier joins the Greenland ice sheet a two-dimensional flowline geometry provides a very poor model of ice flow, as flow is strongly convergent. Therefore, a point was identified where the behaviour of the glacier changes from ice-sheet type, funneling ice from a wide range of angles, to an outlet glacier where the flow is channelised and the velocity vectors are roughly parallel; the two-dimensional model was limited to locations downstream of this point. This location was selected at 152 km along the flowline. As can be seen from Figure 5.5, downstream of 152 km the flow is largely bounded by nunataks and the fjord walls. Upstream of the chosen cut-off location the trough in the bed bifurcates, hence flow will necessarily diverge. The surface velocity in Figure 5.5 (b) shows a narrow stream of high ice velocity in all regions downstream of the chosen cut off location.

5.4.2 Englacial temperatures

There have been very few studies of englacial ice temperatures in Greenland outlet glaciers, as this would require a high budget drilling programme which is logistically difficult in the highly crevassed conditions that cover the surface of the majority of outlet glaciers. Instead, the model's englacial temperature profile was based on a

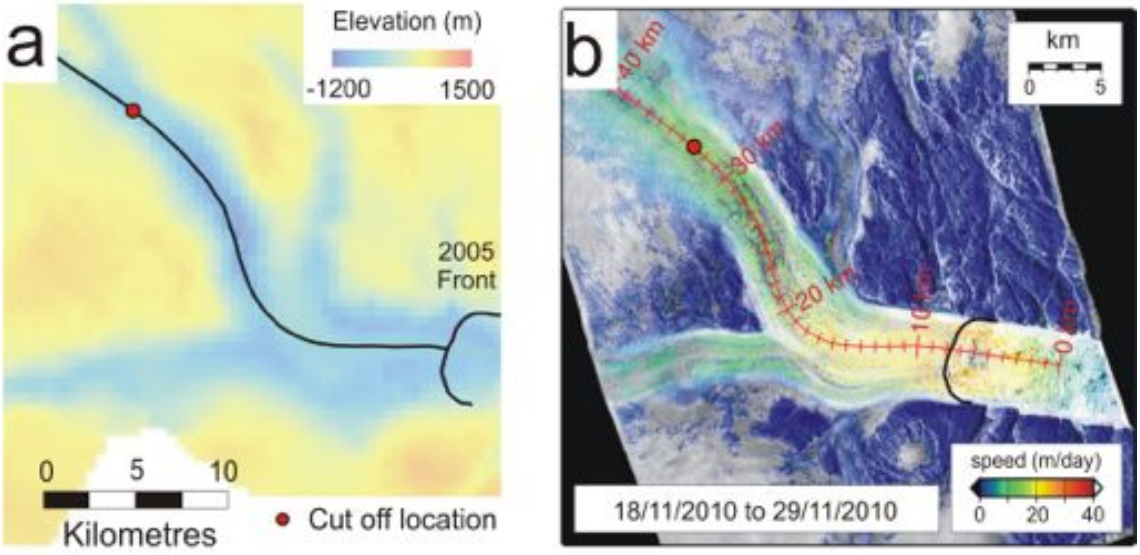

Figure 5.5: (a) Basal elevation of Helheim Glacier, showing bifurcation of basal trough above cut-off location. (b) Surface velocities from November 2010, showing channelised flow in regions downstream of cut-off. Black lines indicate the flowline and July 2005 calving front. Velocity image from Adrian Luckman, Swansea University (personal communication, Jan 2012).

previous modelling study of Jakobshavn Isbræ, a similar glacier on the West coast of Greenland (Funk et al., 1994). The study uses a thermo-mechanical ice flow model to estimate the ice temperature profile along the entire length of the glacier (Figure 5.6). At the upper end, modelled temperatures correspond well with the type of temperature profile measured from drilling projects at the ice divide (Johnsen et al., 1995), providing some validation of the results.

The modelled temperature profiles in Funk et al. (1994) show peaks in temperature at the bed and surface, with a minimum in the centre of the glacier. The high temperatures at the bed are caused by pressure heating of the ice, while the warm surface temperatures around the terminus are due to conduction of heat from the relatively warm surrounding air. The cold ice in the centre of the model is advected from upstream, where the majority of the ice sheet is known to be at very low temperatures, and is sufficiently thermally removed form both sources of heat to maintain its low temperature. The temperature profile in the bottom half of the

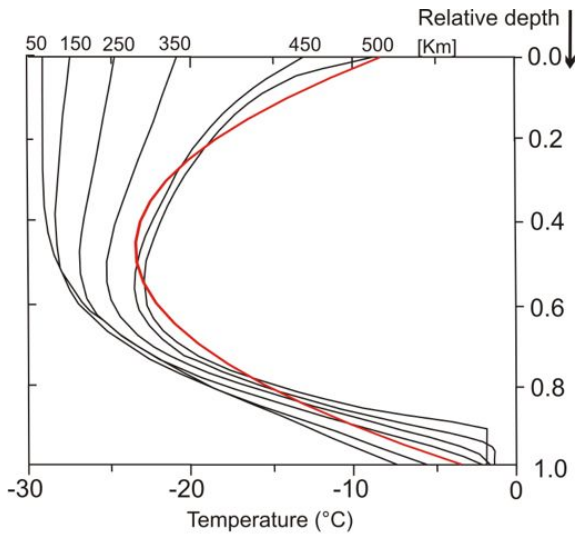

Figure 5.6: Modelled englacial temperatures from Funk et al. (1994) for Jakobshavn Glacier, with lines showing different points along the glacier's length. Red line shows values used in this model.

glacier's thickness is similar along the entire length of the glacier, but the surface temperature changes significantly depending on the location of the profile. The Helheim Glacier model was limited to a region up to approximately 25km from the calving front, therefore all of its extent fell in the range covered by 450-500 km in Figure (5.6). The temperature data cannot be read directly into Elmer/Ice, therefore the profile was approximated by fitting a quadratic curve, shown in red on the figure.

Temperatures in Funk et al. (1994) are also given with respect to a normalised ice depth, and the significant changes in ice thickness along the glacier's length mean that there is a complex temperature distribution within the glacier. For implementation in Elmer/Ice only local rather than global variables may be used to preset ice properties (*i.e.* we may use the coordinates, but not the ice thickness). Therefore, the ice thickness used to calculate englacial temperatures had to be estimated along the flowline at the beginning of the model run, and experiments in which the surface evolved a long way from the original profile will have additional errors in the temperature profile. The resulting distribution of temperatures inside the modelled glacier is shown in Figure 5.7. The large number of approximations made in implementing ice temperatures mean that this is a potentially high source of error in the model.

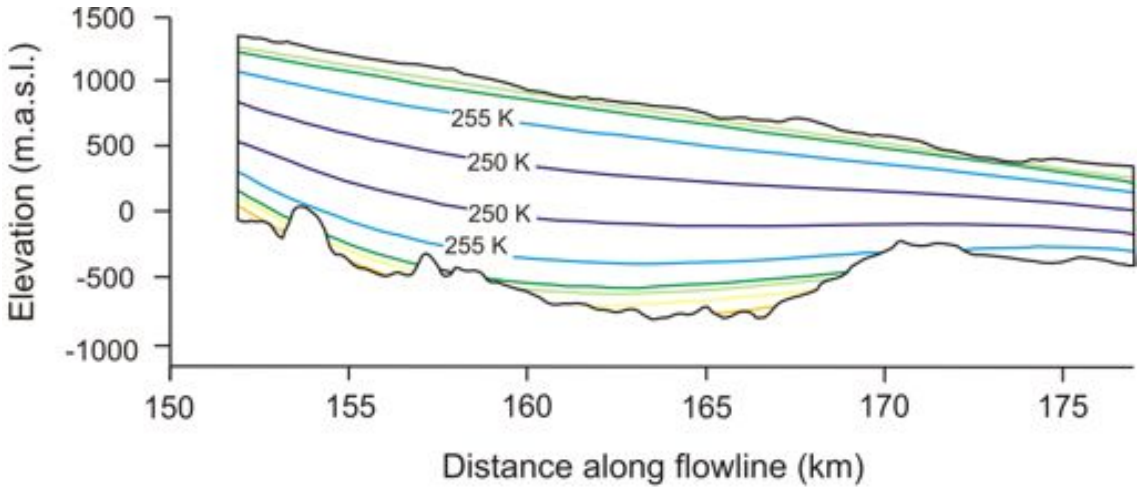

Figure 5.7: Temperature distribution used in model of Helheim Glacier, showing isothermal lines with 5 K interval.

This could be improved by using a full thermo-mechanical ice model, however the large CPU requirements of the more simple model used prohibited the use of more advanced temperature calculations. If the model were adapted to run in parallel this could be a useful area to improve upon.

5.4.3 Lateral drag

Lateral drag was applied by the method discussed in Section 3.1.4. In this case some slippage of ice at the walls of the glacier was accounted for, assuming that along flow velocity at the margins was roughly half that in the centre of the glacier, an estimate taken from velocity measurements from feature tracking on satellite images by Suzanne Bevan and Adrian Luckman (personal communication, Mar 2012). The bed data published by CReSIS are available in 3D, giving information on channel cross section which was approximated by a trapezoid with a width at the bed two thirds of that at the surface.

5.4.4 Influx boundary condition

As discussed above, unlike the Columbia Glacier model, the chosen geometry in this case did not extend to the ice divide, meaning that an inflow velocity had to be prescribed for the upstream boundary. As a starting point a model run was performed using the entire available geometry right back to the ice divide. This was then used to find an approximate velocity profile with depth at the cut-off location. Unfortunately the model currently only allows a single velocity input at the inflow boundary, rather than allowing the velocity to change with height. Therefore a value of 3500.0 $\mathrm{m\,a^{-1}}$ was used, an average between the observed surface velocity of 4001.6 $\mathrm{m\,a^{-1}}$ and 3000.0 $\mathrm{m\,a^{-1}}$, the modelled sliding velocity when using the entire glacier length. Using a single input velocity rather than one varying with height produces some error in the results, but this should be small since the sliding velocity around 152 km (where the model geometry begins) is high and the source of the error is well removed from the calving front, which is the main area of interest in a calving model. Developing the model to allow a varying inflow velocity profile is an area which should be addressed in future work.

5.4.5 Mass balance

There are two sources of surface mass balance input in the model, one arising from climatic forcing and the other from a parameterisation of lateral flux applied as a mass balance term. The first was estimated using mass balance data from two different sources, a coarse grid mass balance product modelled by Box et al. (2004) for the ice sheet region, and in the outlet glacier region observations by Andersen et al. (2010). In ice sheet regions an average over the period 1996-2000 was used, which is somewhat before the model's starting date but the trend of increasing mass loss at high elevation on the Greenland Ice Sheet is relatively small (Fettweis, 2007), and the average over 5 different seasons should be sufficient to remove the effects of any unusual years. In addition the mass balance at these elevation should have

minimal impact on the calving front on the timescales over which the model is run.

The data from Andersen et al. (2010) is directly observed from stakes placed over two consecutive melt seasons in 2007 and 2008. The stakes were placed in the ablation zone (*i.e.* on bare ice) for two months over the summer, and hence do not provide an annual mass balance. However, in comparison to annual values calculated by Sorensen et al. (2011) by mass balance modelling, the ablation values are high, and therefore it seems reasonable to use them as an approximation of overall surface mass balance.

Data from the two sources were combined and a polynomial curve was fit to the data (see Figure 5.8), leading to the equation:

$$M = -4.593x10^{-10}s^3 + 1.442x10^{-6}s^2 + 4.182x10^{-4}s - 2.3\ . \tag{5.1}$$

Although the polynomial fits the data well at high and low elevations, in the middle of the range at around 1500 m.a.s.l. the mass balance predicted by Box et al. (2004) is much higher than than the polynomial values. This is the region where the outlet glacier begins to show very different behaviour from the surrounding ice sheet, and it is likely that the coarse grid of the model used by Box et al. (2004) begins to break down in this area. Errors in this region, which is well removed from the terminus, are unlikely to have a significant effect on calving behaviour in the model.

The second contribution to the model's surface mass balance term is a parameterisation of lateral flux. The method of calculation is discussed in Section 3.1.4, and this was applied at each timestep.

5.4.6 Surface relaxation

The aim of a surface relaxation is to produce a good fit to both the observed surface velocity and elevation profiles. In this case, a perfect fit was impossible to achieve because of errors in the bed DEM, in the approximated parameterisation of 3D structure, and in the time which elapsed between surface elevation and velocity

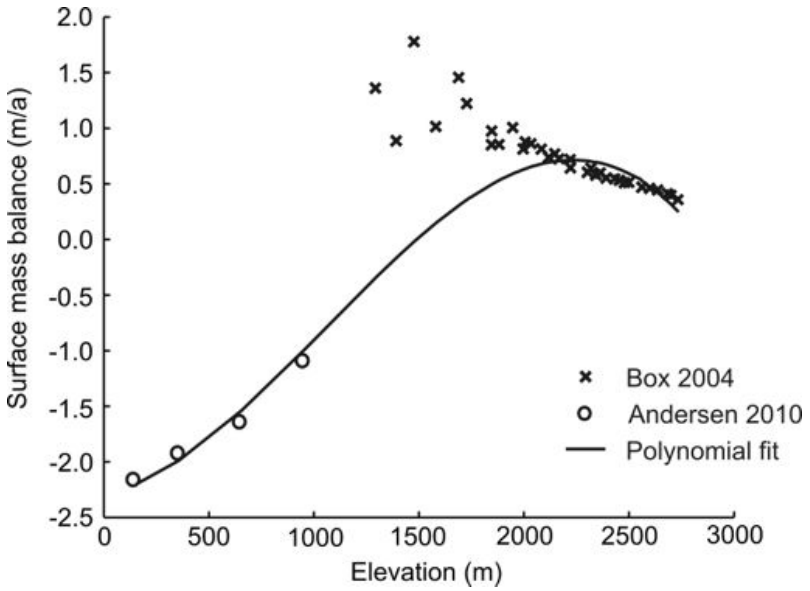

Figure 5.8: Surface mass balance data for Helheim Glacier, showing polynomial fit used to approximate mass balance in the model.

measurements. In the surface relaxation, the surface was allowed to evolve for a period of time while the terminus position was kept fixed. The majority of the surface elevation change occurred in the first 0.1 a of the relaxation, and it was run for 0.5 a, after which the change in surface elevation came into line with the observed surface mass balance. At the end of the relaxation, the surface was somewhat higher than observed around the inflow boundary and at around 170 km along flowline (see Figure 5.10), however the overall shape was similar, especially around the calving front where any change in geometry will have the largest effect. The relaxed geometry was then used as the starting point for all further model runs. The differences in geometry between the relaxed model and observation mean that the model is unlikely to be able to reproduce exactly the behaviour of the glacier in summer 2005, but it will respond in a physically realistic way to changing inputs, and may be used as a test case to investigate principles of tidewater glacier behaviour.

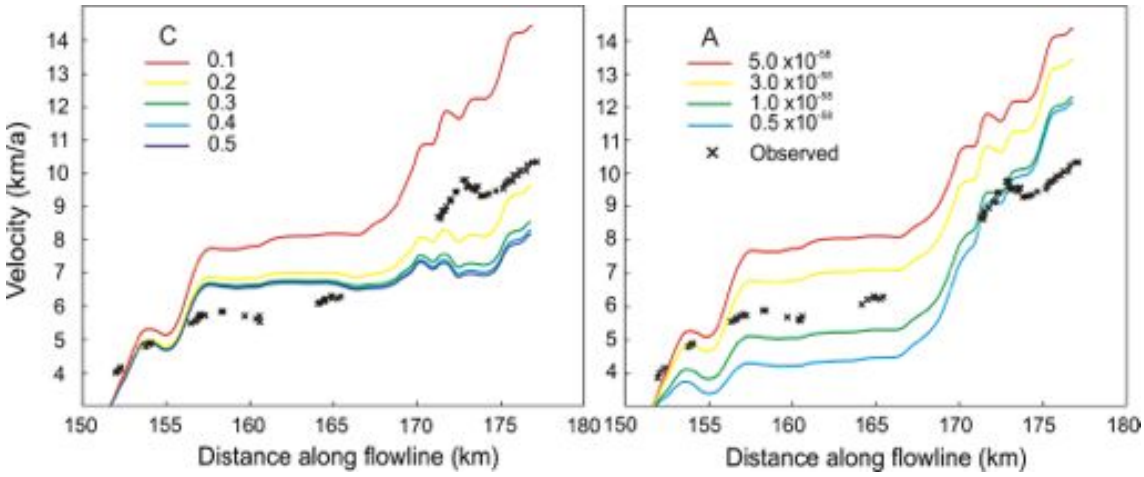

Figure 5.9: Velocity fitting performed on Helheim Glacier model. The two coefficients C and A are varied individually to fit modelled to observed surface velocity.

5.4.7 Basal sliding

In this application, the Gagliardini type of sliding law was used, as described in Section 3.1.4. This method provided two variables that could be adjusted in order to fit the modelled surface velocity to observed values: C, the maximum bed slope and A, the sliding coefficient. The other parameter q, the post peak exponent, made little difference to the modelled surface velocity when altered. A single value of each variable was used along the entire bed, and initially A and C were adjusted individually, keeping the other fixed, as shown in Figure 5.9.

Varying A had the effect of shifting the velocity profile vertically, while altering C changed the shape of the profile, with lower values enhancing the velocity around the front of the glacier. The r.m.s. errors for each fit are laid out in Table 5.1.

The shape of the graph best fit the observed velocity profile with $C = 0.149$ and the sliding parameter was then altered iteratively to find a best fit, as judged by the r.m.s error given in Table 5.1. The velocity fit was performed after a relaxation of 0.1 a since at this time the majority of surface elevation change had already occurred, as discussed in Section 5.4.6. This method allows the best possible fit to both surface elevation and velocity in the relaxed model. The final fit of modelled to observed

Table 5.1: Error between modelled and observed surface velocity associated with different sliding parameters.

C	A	r.m.s. error
	$(\mathrm{m\ kg})^{1/2}\ \mathrm{a}^2$	$(\mathrm{m\,a^{-1}})$
0.1	3.0×10^{-58}	2648.5
0.2	3.0×10^{-58}	789.9
0.3	3.0×10^{-58}	1647.9
0.4	3.0×10^{-58}	2069.3
0.5	3.0×10^{-58}	2295.2
0.2	1.0×10^{-58}	2736.8
0.2	2.0×10^{-58}	1528.5
0.2	3.0×10^{-58}	789.9
0.2	4.0×10^{-58}	494.2
0.2	5.0×10^{-58}	810.2
0.149	2.49×10^{-58}	321.9

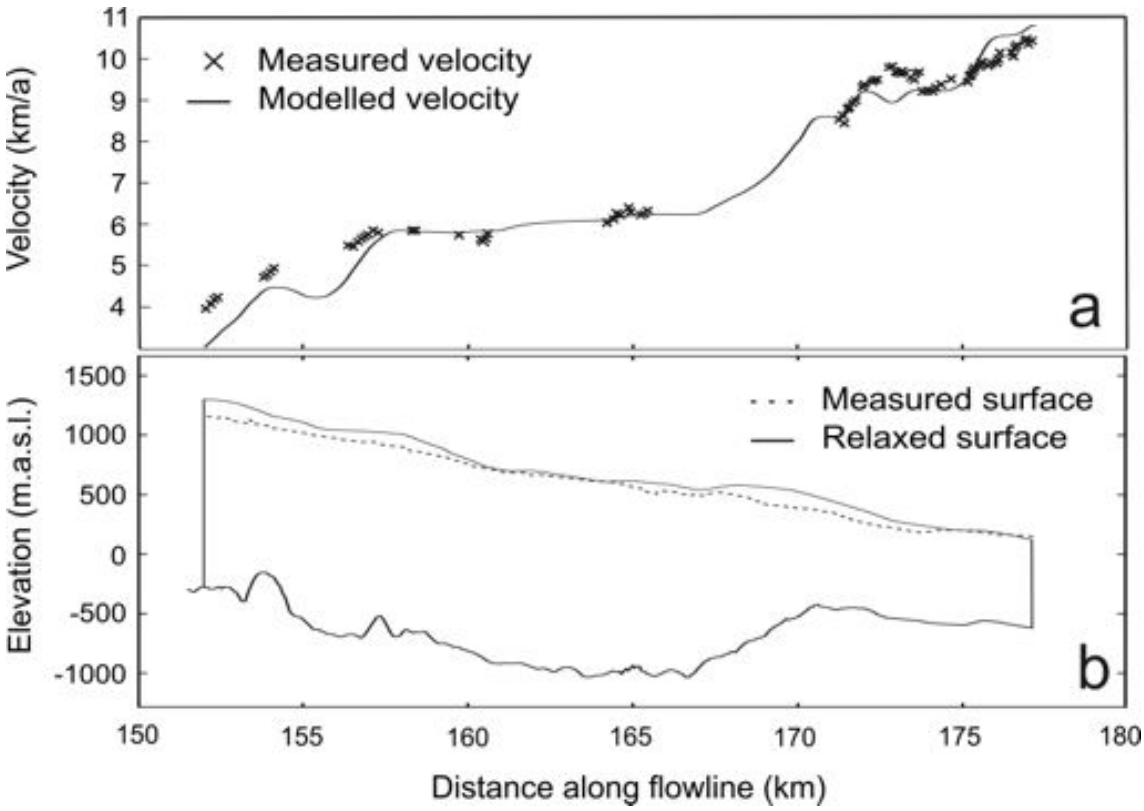

Figure 5.10: (a) Final fit of modelled to observed surface velocity. (b) Modelled glacier surface after 0.5 a relaxation, compared to observed elevation.

surface velocity is shown in in Figure 5.10, and has an r.m.s. error of 321.9 m a^{-1}.

5.5 Results: Sensitivity Analysis

The intention of this chapter is to perform a sensitivity analysis of the model by testing the effect of changes in each input parameter on model results. This will test the robustness of the model, by testing the impact on results of uncertainty in the input variables, and provide a context for understanding potential errors in future model results. The first tests are used to select the most appropriate timestep and mesh size for model runs. Further tests are then performed using each of the input variables and boundary conditions: relaxation period, DEM errors, lateral drag parameterisation, englacial temperature profile, inflow velocity, application of basal water pressure in the sliding law and surface mass balance. The previous section

describes the model set-up used as a standard case, a range in each of the input variables is then selected around this standard case as the input for the sensitivity analysis.

To test the sensitivity thoroughly, three crevasse water depth (D_w) scenarios were identified to cover a full range of glacier behaviour: advancing ($D_w = 0$ m), steady ($D_w = 10$ m) and retreating ($D_w = 40$ m). These crevasse water depths are used in most of the sensitivity testing in this chapter, with model runs typically of 5 years. In each case, to test the effect of changes on the model, the evolution of the terminus is examined and also the size and frequency of calving events produced. Comparison of the calving behaviour is performed by comparing the average size of calving event using the independent samples t-test where data are normally distributed and the Wilcoxon-Mann-Whitney test where they are not. Unlike the t-test the Wilcoxon-Mann-Whitney test compares not only the median event size in the two samples but also the width of the distribution.

5.5.1 Mesh sensitivity

Initial model experiments were performed to determine the most appropriate mesh density and time step for the work in this chapter. The model results would be expected to converge as the timestep and mesh size tend towards zero, but finer grids and short time steps also have a much higher computational cost. The aim is to identify a timestep and mesh density which will produce an acceptable running time, with results not significantly different model runs with a smaller timestep and grid size.

Firstly, the initial state of the glacier was examined, comparing the stress profile and crevasse field depth given different mesh densities. As can be seen in Figure 5.11, calving occurred for three cases with mesh density between 10 m and 50 m, while for lower densities the grid size was not sufficient to be able to detect this calving event. This indicates that a mesh density of at least 50 m is required to resolve

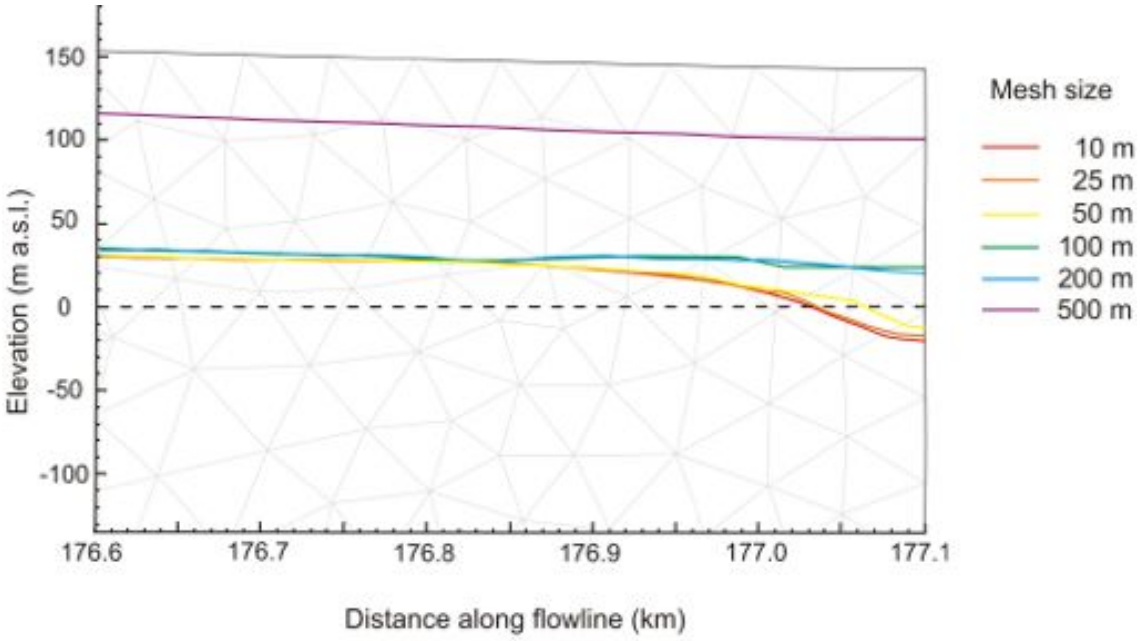

Figure 5.11: Modelled calving location using a range of mesh densities around the calving front. The coloured lines show the depth of the crevasse field in the different cases, indicating that calving is detected using mesh sizes of 50 m and below.

calving events.

There is a limit to the mesh density that may be used for a calving run. At the time of these experiments, the code could only be run in serial (not split between parallel processors) therefore experiments were limited by the memory available to a single processor. This limitation meant that 30 m was the finest mesh density on which calving experiments were possible. To further refine the mesh sensitivity testing, calving runs of 1 year were performed with mesh densities of 30 m, 40 m and 50 m. The results are laid out in Table 5.2, and show that the results for a 40 m mesh did not differ significantly from those with a 30 m mesh, whereas those for 50 m had a larger difference. Therefore in all following experiments a grid with 40 m mesh density around the front was used.

Table 5.2: Response of calving behaviour to changes in mesh density around the calving front over a 1 year model run. Percentage changes are calculated with respect to the 30 m mesh density example, which provides the most accurate results.

Mesh density	30 m	40 m	50 m
Number events	16	15	14
Average size (m)	420.7	421.6	450.9
Final terminus (km)	177.88	177.89	177.83
% diff in size	-	0.21	7.2
% diff in advance	-	1.3	6.4

5.5.2 Timestep sensitivity

To test the effect of chosen timestep on the results, model runs for 0, 5 and 10 m crevasse water depths were performed with a range of timesteps from 0.001 to 0.01 a. As the timestep was altered, the calving behaviour of the model changed quite significantly (see Figure 5.12), however in all cases the final terminus position changed by less than 1.0%. No clear choice of timestep emerged from these results. The ideal would probably to use a timestep even shorter than those presented here, however the CPU resources required for these runs were already very high and insufficient resources were available to use any shorter timesteps. Therefore the majority of further experiments used a timestep of 0.003 a (1.1 days), the results for which differed relatively little from the 0.001 a case. For some experiments, notably those with a crevasse water depth in the range 20 to 30 m, calving occurred at every timestep when using 0.003 a, therefore the timestep was reduced to the point at which periods without calving began to occur. A table of all the timesteps used is shown in Table 5.3.

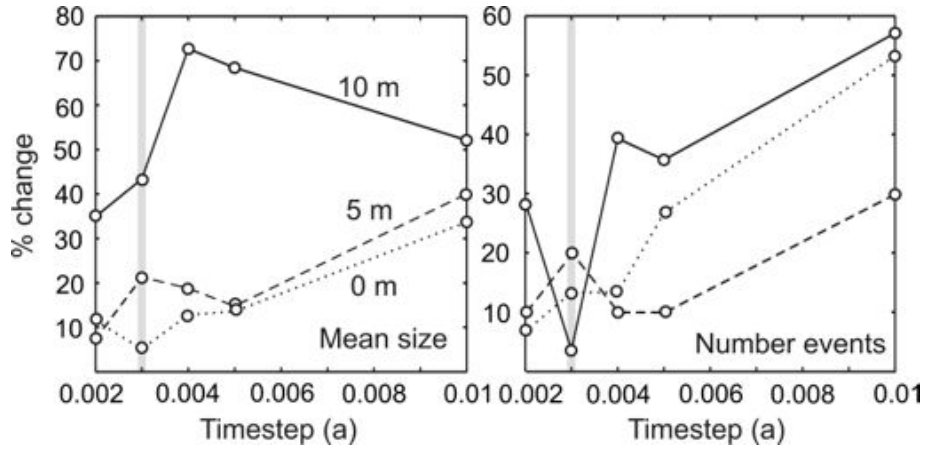

Figure 5.12: Percentage change in mean event size and number of events over a model run of 1 year using a range of timesteps and crevasse water depths. The base for comparison is a run with timestep 0.001 a and the grey shaded lines indicate the timestep chosen for further experiments.

Table 5.3: Timesteps used with different crevasse water depths in the Helheim Glacier model runs.

Crevasse water depth (m)	Timestep (a)	Crevasse water depth (m)	Timestep (a)
0	0.003	30	0.001
5	0.003	35	0.001
10	0.003	40	0.001
15	0.001	45	0.001
20	0.0005	50	0.001
25	0.0005		

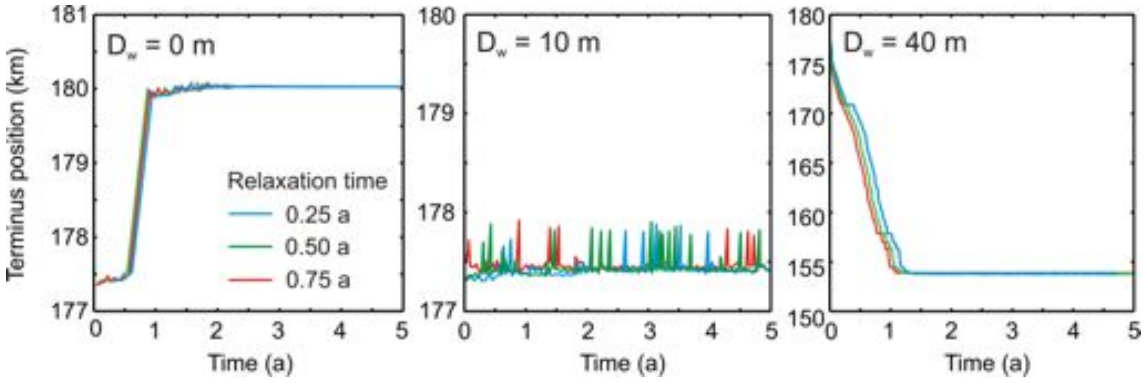

Figure 5.13: Effect of altering the initial relaxation period on modelled terminus evolution.

5.5.3 Surface relaxation sensitivity

Errors in the DEMs used mean that the glacier model was not in balance when initialised from the observed geometry. Therefore an initial period of surface relaxation was used, during which the terminus position was fixed and the surface allowed to relax until the rate of elevation change was comparable to the observed mass balance. The chosen period of relaxation was 0.5 a, but the model's behavior should not depend strongly on the precise value. To test this assertion, two alternative relaxations of 0.25 and 0.75 years were performed.

In all three model scenarios (D_w = 0, 10, 40 m) there was very little difference in the modelled terminus evolution between the cases with different relaxation periods (Figure 5.13). There were some small differences in the number and size of calving events over the model runs (Table 5.4) but these were not statistically significant. Therefore the model results do not depend strongly on the chosen relaxation period.

5.5.4 Englacial temperature sensitivity

In order to test the sensitivity of the model to the choice of englacial temperature profile, the experiments with 0, 10 and 40 m crevasse water depth were repeated with adjusted temperature profiles (see Figure 5.14). Firstly, the entire temperature profile was shifted up and down by 5 and 10°C. To test the impact of changing the

Table 5.4: Effect of changing relaxation period on calving behaviour of Helheim Glacier model. Number is total number of calving events over a 5 year model run, size is the average size of each event in metres.

	Relaxation period	Number	Size
Retreat	0.25 a	801	86.6
(D_w=40 m)	0.50 a	810	87.4
	0.75 a	810	90.5
Steady	0.25 a	119	448.8
(D_w=10 m)	0.50 a	121	431.0
	0.75 a	107	468.1
Advance	0.25 a	126	481.2
(D_w=0 m)	0.50 a	126	480.0
	0.75 a	125	480.6

ice temperature in internal layers, the original temperature profile was also altered in shape to change the temperature in the centre of the glacier by ±5 and 10°C, keeping temperatures at the bed and surface fixed. In each case the velocity fitting of the model was performed again to create a best fit to the observed velocity profile before the model runs were carried out. Because of the approximated method used to apply the temperature profiles within Elmer/Ice, all the models had some regions of temperate ice near the bed, but the two warmest experiments (+5 and +10°C) had more significant regions of temperate ice. In the warmest experiment it became difficult to produce a good fit of modelled to observed surface velocity as the internal deformation rate was very high.

The modelled terminus evolution for the experiments is shown in Figure 5.15. In the retreating scenario (D_w = 40 m) all the models behaved very similarly; the ice temperature exhibited some control over the speed of retreat, with colder experiments tending to retreat faster than the warmer ones, but in all cases the model retreated to the same pinning point within one year. In the other two examples there were more significant differences between the experiments. In the advancing

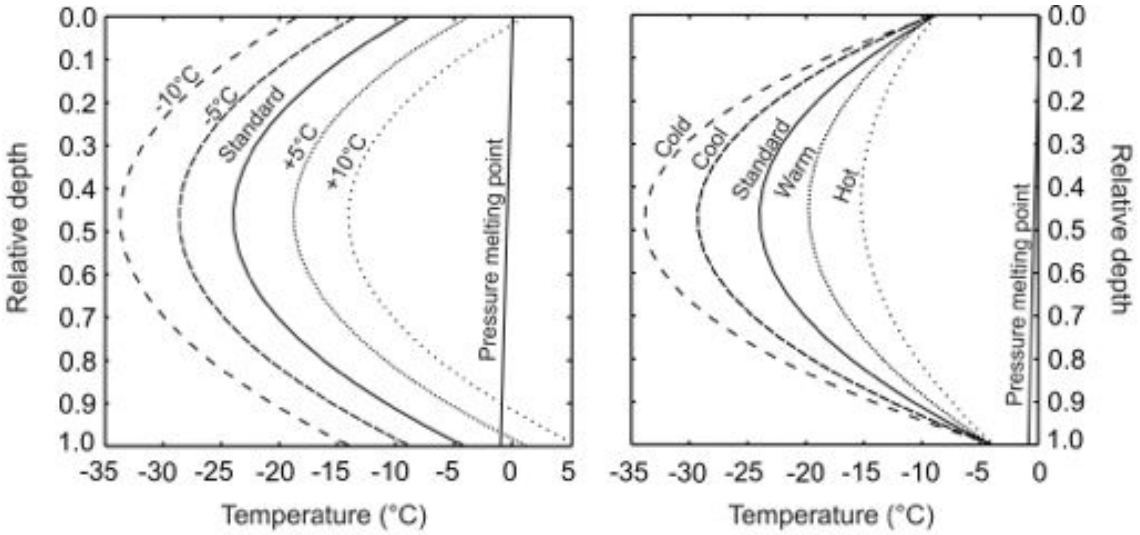

Figure 5.14: The range of englacial temperature profiles used to test model sensitivity to ice temperature, showing nomenclature used discussing results.

scenario ($D_w = 0$ m), cases with warmer ice at the bed advanced faster and further than the standard profile, while in cases with colder ice advance was inhibited and the coldest case showed a terminus retreat of around 2 km. Similarly, in the steady terminus scenario ($D_w = 10$ m) the models with coldest ice temperatures showed a retreat, while in the warmest cases the model advanced. In all cases the biggest change in terminus behaviour occurred when the temperature at the surface and bed was altered rather than just the internal ice temperature.

As would be expected given the large differences in terminus behaviour, the different englacial temperature profiles also caused a change in the modelled calving behaviour (Table 5.5). Comparisons should only be made between experiments with similar terminus behaviour, to separate the effects of the ice temperature from the effects of differing glacier geometry. Therefore statistical comparisons were run on all experiments in the retreating scenario, in the steady terminus scenario only those for the standard, warm, cool and -5°C temperature profiles, and in the advancing scenario the standard, warm and hot temperature profiles.

In the advancing scenario, the warm case (+5°C in the centre) was not significantly different from normal, but the hotter case (+10°C in the centre) did have a sta-

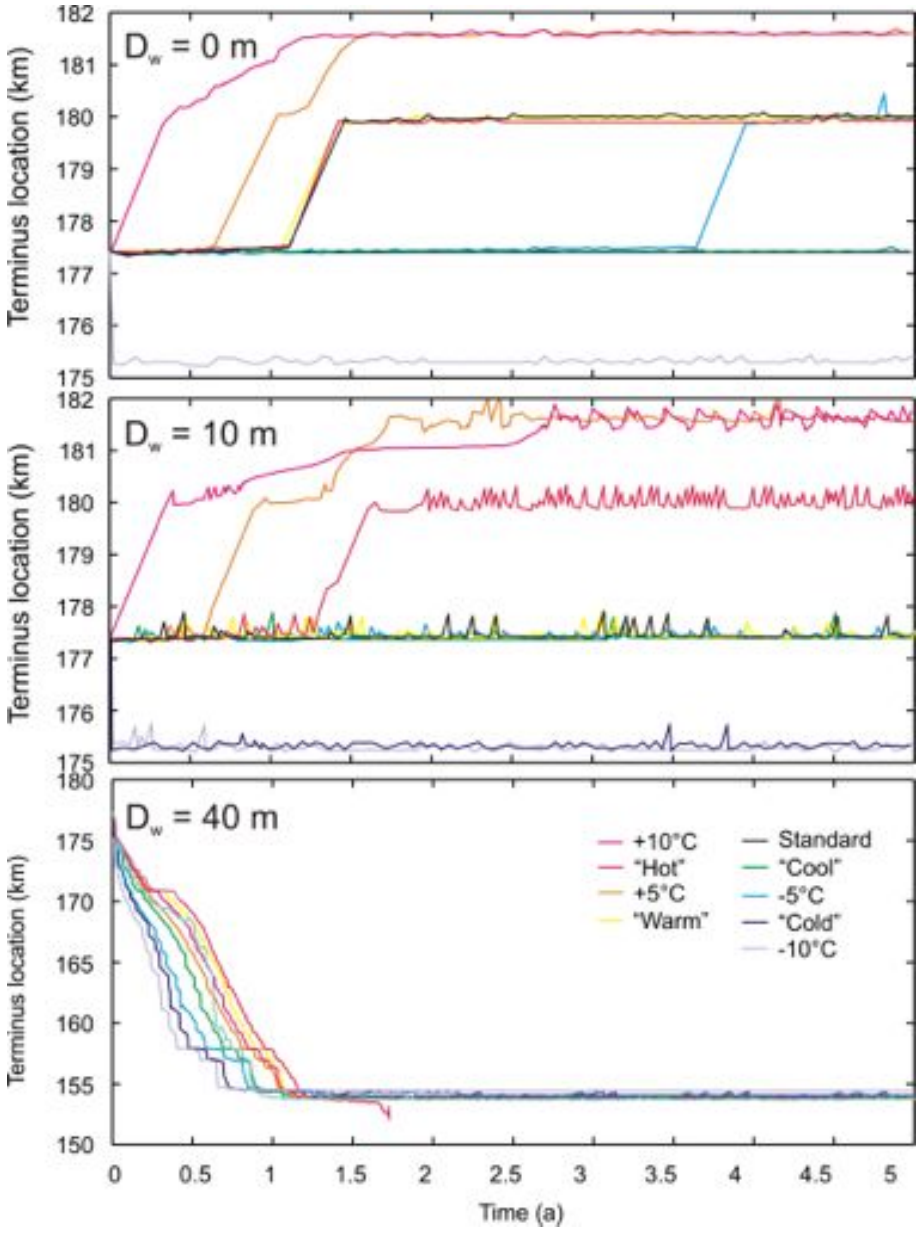

Figure 5.15: Response of modelled evolution of Helheim Glacier terminus to changes in englacial temperature profile.

Table 5.5: Effect of englacial temperature profile on the calving behaviour of the Helheim Glacier model. N is total number of calving events over a 5 year model run, $\overline{x}$ is the average size of each event in metres. Italics indicate that the run ended before the 5 year time limit, having reached the limit of the bed data. Red numbers are those where differences in calving behaviour are statistically significant from the standard model run (Norm). Grey numbers indicate those not included in statistical tests due to differing terminus behaviour.

D_w		-10°C	Cold	-5°C	Cool	Norm	Warm	+5°C	Hot	+10°C
40 m	$\overline{x}$	81.6	116.5	112.8	112.9	88.9	88.7	89.6	*129.8*	136.9
	N	771	572	588	616	807	854	810	*437*	537
10 m	$\overline{x}$	466.7	526.3	401.2	493.9	431.0	357.1	266.8	232.5	142.5
	N	114	103	129	104	121	149	173	235	378
0 m	$\overline{x}$	523.8	582.4	543.3	585.0	484.2	476.1	525.8	497.0	366.9
	N	101	88	86	87	107	107	80	102	115

tistically significant difference in calving event size. In the steady scenario, the "warm", "cool" and -5°C cases all produced significantly different calving behaviour to the standard case. In the retreating scenario, all the cases resulted in significantly different calving behaviour, apart from the "warm" and +5°C cases.

Since the difference in ice temperature between the most extreme cases was up to 20 °C, a difference in behaviour was expected, and this is one of the largest sources of error in the model. In some cases, experiments differing by 5°C did not produce significant differences in calving, but in most cases they produced either a difference in terminus evolution or calving event size. The internal ice temperatures of outlet glaciers are not well known, and from these experiments it can be seen that an error of 5°C may cause a significant change in glacier behaviour, causing a change from a steady to an advancing glacier terminus. Until more observational data become available, or the model is developed to include full thermo-mechanical processes these errors are unavoidable and must be considered when interpreting results.

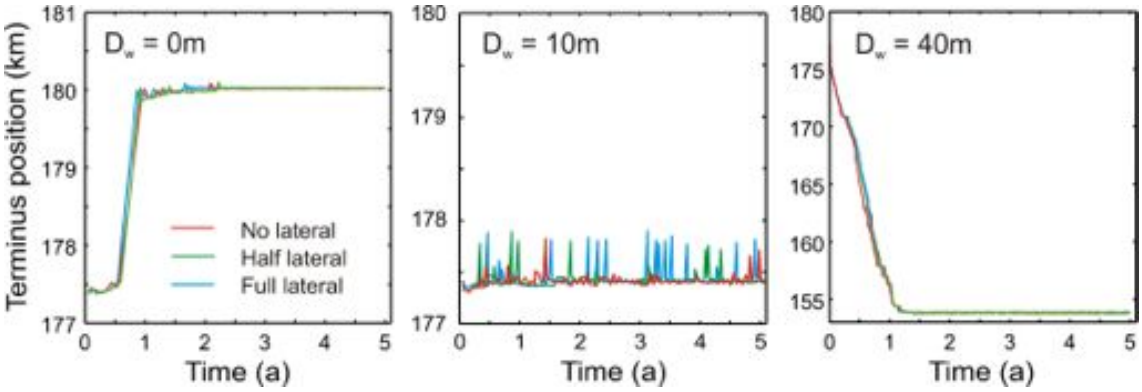

Figure 5.16: Response of Helheim Glacier model to changes in parameterisation of lateral drag.

5.5.5 Lateral drag sensitivity

The parameterisation of lateral drag in this model contains some significant approximations due to the assumptions made about the lateral velocity profile and the channel shape; therefore, sensitivity testing is important in this case. This experiment is also of some further interest as it has previously been suggested that lateral drag may have a significant impact on calving behaviour by stabilising the terminus. Two experiments were designed with the lateral drag applied in the model half the original value and reduced to zero. In each case velocity fitting was performed again to find a best fit of modelled to observed velocity before model runs took place (it may be noted here that errors in velocity fitting were lowest using the full lateral drag parameterisation).

The evolution of the terminus was nearly identical in all cases (Figure 5.16), and as can be seen from Table 5.6 the calving behaviour was also nearly identical. The case with no lateral drag differed very slightly from the standard case, with fewer events of somewhat larger size, however these differences were not statistically significant. It may be concluded that the parameterisation of lateral drag in the model does not have a significant effect on its behaviour, and this may be discounted as a significant source of error when analysing results. This also indicates that, contrary to previous thought, lateral drag does not have a significant effect on modelled calving behaviour

Table 5.6: Effect of changing lateral drag parameterisation on calving behaviour of Helheim Glacier model. Number is total number of calving events over 5 year model run, size is the average size of each event in metres.

	Lateral Drag	Number	Size
Retreat	Full	807	88.9
(D_w=40 m)	Half	818	89.5
	None	807	91.0
Steady	Full	121	431.0
(D_w=10 m)	Half	121	452.6
	None	110	467.5
Advance	Full	130	480.9
(D_w=0 m)	Half	130	489.3
	None	129	483.4

at the terminus of Helheim Glacier and there is no indication that lateral drag has the ability to stabilise a calving terminus. However, it may be important in other situations than Helheim Glacier, particularly in a glacier approaching flotation where it has been suggested that the effect of lateral drag opposing acceleration at the front of the ice may be the factor which allows a floating tongue to build up.

5.5.6 Inflow velocity sensitivity

The chosen geometry for the model of Helheim Glacier, which is cut around 25 km upstream of the calving front, means that the prescribed velocity on the upstream boundary becomes a potential source of error in the model. This is particularly important because the current model does not allow for the inflow velocity to vary with height above the bedrock as would be expected in a real glacier. To investigate the effect of this source of error on the model results the standard inflow velocity (3500 $\mathrm{m\,a^{-1}}$) was varied by $\pm 500\ \mathrm{m\,a^{-1}}$. The effect of these variations on the evolution of the glacier's terminus is shown in Figure 5.17.

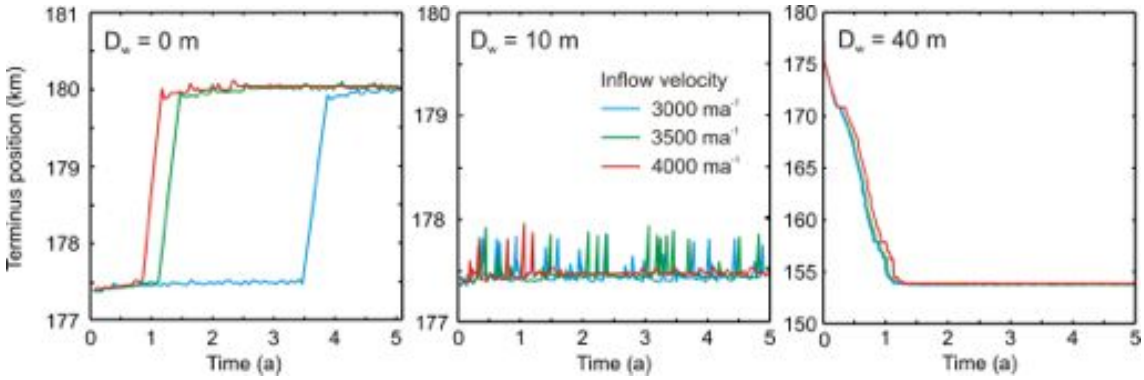

Figure 5.17: Effect of varying inflow velocity on modelled terminus evolution.

Table 5.7: Effect of changing inflow velocity on calving behaviour of Helheim Glacier model. Number is total number of calving events over 5 year model run, size is the average size of each event in metres.

	Inflow velocity	Number	Size
Retreat	3000 m a^{-1}	735	92.8
(D_w=40 m)	3500 m a^{-1}	818	88.9
	4000 m a^{-1}	879	89.9
Steady	3000 m a^{-1}	135	333.5
(D_w=10 m)	3500 m a^{-1}	121	431.0
	4000 m a^{-1}	118	507.7
Advance	3000 m a^{-1}	78	509.7
(D_w=0 m)	3500 m a^{-1}	107	484.2
	4000 m a^{-1}	126	490.8

Changing the inflow velocity did have an effect on the behaviour of the glacier. It would be natural to assume that these changes would be largest in the retreating scenario, where the calving front approaches the inflow boundary. However, the opposite was true. The difference between the retreating experiments was negligible, while for the other two scenarios an increase in inflow velocity produced a change in the glacier's behaviour. While for the steady scenario this did not lead to a change in the glacier's terminus behaviour, the difference in calving event size was statistically significant at the 99% confidence level (Table 5.7). The faster inflow velocities also caused a faster advance of the glacier terminus in the $D_w = 0$ m scenario (Figure 5.17). Due to this difference in terminus evolution the calving behaviour of the three advancing cases was not comparable.

The chosen inflow velocity is shown to affect the calving behaviour of the model, with the difference most striking in the scenario with an advancing glacier, but also with a statistically significant effect on calving behaviour in the steady terminus scenario. Unfortunately there is no way in which the estimate of this input parameter may currently be improved, as the model is currently unable to support a vertically variable velocity which would provide the most accurate model set-up. This is a key area for future improvement.

5.5.7 Basal water pressure sensitivity

The modelled glacier velocity will also be affected by the parameterisation of basal water pressure in the sliding law. Given the lack of observational data, the model uses a standard approximation of basal water pressure depending on the depth of the bed below sea level (see Section 3.1.4). However, studies have shown that changes in basal water pressure in tidewater glaciers can be large (*e.g.* Meier et al. (1994)), so the effect of errors arising from this approximation should be investigated. In order to do this the basal water pressure in the model was adjusted by changing the hydrostatic head by ± 50 m and ± 100 m. In each case the other sliding parameters were readjusted to produce a best fit of modelled to observed surface velocity as

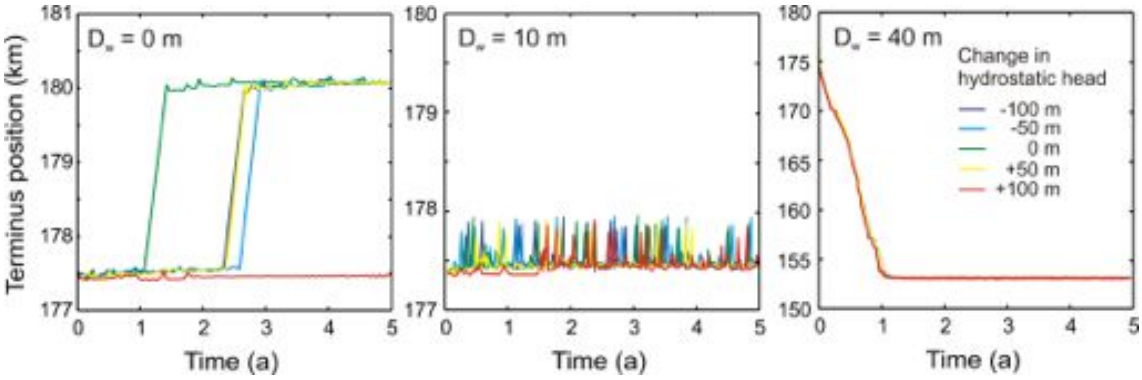

Figure 5.18: Response of Helheim Glacier model to changes in parameterisation of basal water pressure in sliding law.

the intention was not to investigate the effect of changing the glacier's velocity, but changing the nature of basal sliding.

Changing the implementation of basal water pressure in the model did have some effect on the calving behaviour. In the retreating and steady terminus scenarios it did not influence the glacier's terminus evolution, and although there was some change in the size and frequency of calving events these were not statistically significant, except in the case of +100 m in the steady state scenario. In the advancing scenario, the modelled behaviour of the terminus was affected by the modelled basal water pressure, with all new cases advancing later than that with a standard basal water pressure distribution. In the case of a change of +100 m in hydrostatic head no advance occurred at all. The differences in terminus behaviour in this scenario meant that the calving behaviour data were not directly comparable.

These results show that the implementation of basal water pressure in the model can have an effect on the model's behaviour. In the case of an advancing glacier terminus this had a significant effect on the the evolution of the glacier, but in all other scenarios the changes caused by altering basal water pressure did not produce a statistically significant effect on results. The implementation of basal water pressure can have an effect on results, and is an important area for future observational studies as little is known about the properties of the bed in Greenland outlet glaciers.

Table 5.8: Effect of changing basal water pressure on calving behaviour of Helheim Glacier model. Number is total number of calving events over 5 year model run, size is the average size of each event in metres.

Change in basal water pressure		-100 m	-50 m	0 m	+50 m	+100 m
Retreat	Number	823	811	807	790	792
(D_w=40 m)	Size	87.4	88.5	88.9	90.6	90.2
Steady	Number	136	132	121	114	152
(D_w=10 m)	Size	389.0	400.6	431.0	454.7	352.8
Advance	Number	97	96	107	98	97
(D_w=0 m)	Size	511.6	512.2	484.2	504.0	532.3

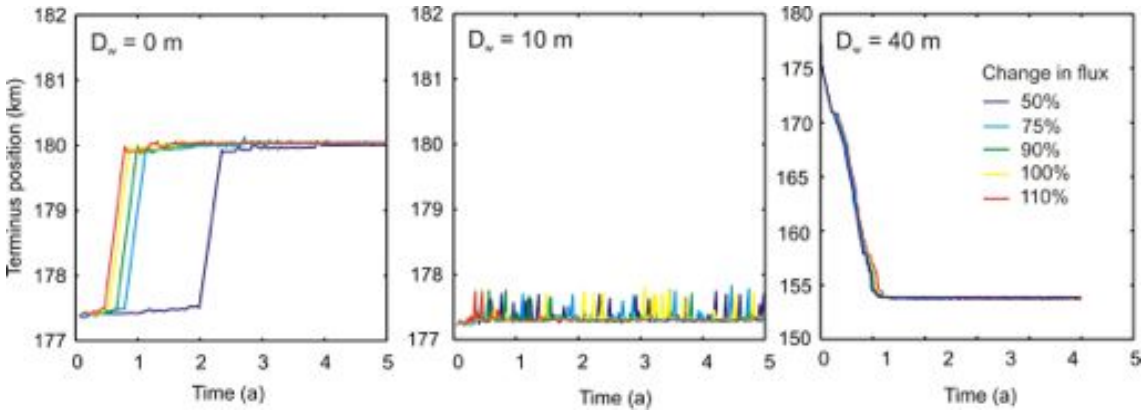

Figure 5.19: Effect of error in 3D flux correction on modelled terminus evolution.

5.5.8 Surface mass balance sensitivity

As discussed above there are two contributions to surface mass balance in the model of Helheim Glacier; meteorological ablation/accumulation and a 3D flux correction term. The latter is likely to have to largest associated errors due to the inherent assumptions about channel shape and lateral velocity profile, but the effect of errors in both should be tested.

Firstly, a series of experiments were conducted using a lateral flux correction of 50, 75, 90, 100 and 110% of the usual value. The effect of these variations on modelled terminus behaviour can be seen in Figure 5.19. In all scenarios the changes did

Table 5.9: Effect of changing 3D flux correction term on calving behaviour of Helheim Glacier model. Number is total number of calving events over 5 year model run, size is the average size of each event in metres.

Change in 3D flux		50%	75%	90%	100%	110%
Retreat	Number	798	821	814	818	832
(D_w=40 m)	Size	88.9	88.2	89.6	89.8	89.1
Steady	Number	148	123	114	121	108
(D_w=10 m)	Size	322.0	401.9	446.7	431.0	490.0
Advance	Number	96	121	126	130	132
(D_w=0 m)	Size	496.0	459.4	472.0	480.9	495.0

Table 5.10: Effect of changing surface mass balance on calving behaviour of Helheim Glacier model. Values shown are a percentage change compared to using the observed surface mass balance.

Change in smb (ma^{-1})	-2.0	-1.0	0.0	1.0	2.0
% change in number events	0.0	0.0	-	0.0	0.0
% change in mean size	6.8	3.4	-	3.4	4.5
% change in terminus	0.2	0.1	-	0.1	0.1

not have a significant influence on the modelled terminus evolution. The effect of the changes in surface mass balance on calving behaviour can be seen in Table 5.9. Although there were some differences in calving size and frequency in the retreating scenario these were not statistically significant. In the steady terminus scenario, the difference in calving behaviour was statistically significant at the 99% confidence level for the 50% experiment, but the other experiments did not differ significantly from the standard case. Likewise the differences in calving event size were not significant for the advancing experiments. Thus the implementation of the 3D flux correction does have the potential to affect the model results, but in most cases the changes in behaviour are not found to be statistically significant.

Next the model was tested with a range of values around the measured surface mass

balance. These tests were carried out only on the steady terminus scenario (D_w = 10 m), and the surface mass balance was altered by ±1 and 2 m a^{-1} from the observed values. Changing the surface mass balance on this scale had a negligible effect on the behaviour of the glacier, with little or no change in the behaviour of the terminus (see Table 5.10). There were some small changes in the average size of calving event, however they were not statistically significant.

5.5.9 Bed DEM sensitivity

The final source of error investigated in this chapter is not as easy to quantify as the others. As discussed in Section 5.3, the bed data available have reasonable errors in areas where a clear bed return was observed in the radar data (±20 m), but in other regions it is interpolated from nearby results which is likely to produce much higher errors. The results from previous sections also show that the terminus of the modelled glacier has a tendency to become pinned in particular regions of the bed, which are likely to be strongly controlled by the specific local bed geometry. In an attempt to quantify the model error associated with the errors in bed measurement, two alternative flowlines were selected, one either side of the original flowline but translated 100m north or south. This provided two bed profiles with roughly the same overall features as the original, but small areas of difference (mean difference from the original profile was ±20.7 m, equivalent to best estimates of measurement error, and maximum elevation difference was 145 m).

In all cases the terminus evolution of the models was almost identical to the standard case and therefore they have not been included in a figure here. There were some small differences in the calving behaviour (see Table 5.11), but none were statistically significant. The model is not sensitive to small changes in the basal elevation profile, but it is likely that if there are larger errors in the bed then these will have a significant effect on the glacier's behaviour. This would need to be taken into account if the glacier's evolution were compared to that observed in the real world.

Table 5.11: Effect of changing bed DEM on calving behaviour of Helheim Glacier model. Number is total number of calving events over 5 year model run, size is the average size of each event in metres.

	Flowline	Number	Size
Retreat	North	814	88.2
(D_w=40 m)	Standard	807	88.9
	South	814	88.2
Steady	North	119	420.3
(D_w=10 m)	Standard	121	431.0
	South	119	420.3
Advance	North	90	478.9
(D_w=0 m)	Standard	107	484.2
	South	91	478.8

5.6 Chapter Summary

The results of the sensitivity testing show that the largest source of error in the model is the implementation of englacial ice temperatures. A change of ±5°C in the glacier ice can produce a significant difference in the calving behaviour of the glacier and also on the modelled evolution of its terminus. Currently there is little that can be done to improve the accuracy of the model's ice temperature profile, which would require improved field observations of ice temperature, but in future the model could be extended to include full thermo-mechanical processes.

The next largest source of error in the model is the prescribed inflow velocity at the upstream boundary. In its current state the model does not allow this be varied with elevation, introducing a source of error as the internal deformation velocity is a significant contributor to ice flow at this point. The sensitivity tests show that errors in this velocity can produce a statistically significant change in calving behaviour, and in some cases can also alter terminus behaviour, although the changes are not

as large as those associated with varying englacial ice temperatures.

Other sources of error which have potential to affect the behaviour of the glacier are changes in basal water pressure and the parameterisation used to correct for 3D flux, however in these experiments relatively few cases showed any statistically significant change so they are unlikely to have a significant impact on the validity of model results. Other sensitivity experiments examining the response of the model to changes in the period of surface relaxation, surface accumulation/ablation, lateral drag and small alterations in the bed DEM showed no statistically significant difference in glacier behaviour and are not likely to be a significant source of error in the model results. One caveat should be added here, that large errors in the bed DEM would be expected to have a significant effect on model results, due to the nature of modelled glacier behaviour with the glacier terminus pinning on features on the glacier bed.

Chapter 6

Helheim Glacier: Environmental forcing

6.1 Introduction

The work on Columbia Glacier presented in Chapter 4 demonstrates the potential of the calving model to provide insight into the calving of tidewater glaciers; however, the physical processes represented in the model have so far been limited. It has been suggested by other studies that oceanic forcing may be important in the behaviour of tidewater glaciers, by the effect of undercutting by subaqueous melt at the calving face and backstress from an ice mélange in the fjord around the terminus (see Section 1.2). In this chapter, the model of Helheim Glacier is extended to include these oceanic forcings, and the sensitivity of the model to a wider range of environmental variables is investigated, examining the effects of water in crevasses, basal water pressure, undercutting by subaqueous melt at the calving face and backstress from ice mélange.

6.2 Model Experiment Set-up

The model experiments in this chapter focus on investigating the relative effect of different environmental forcing factors on the model of Helheim Glacier. A range in each variable is applied individually to the Helheim Glacier model described in Section 5.4, and model runs are carried out for a period of 5 years. As in the previous chapter, the model output is analysed by examining the change in terminus position and the average size and frequency of calving events. The average sizes are compared by the Wilcoxon-Mann-Whitney test. In experiments with significantly different terminus behaviour statistical tests were not run as it is then impossible to separate the effects of the variable from the influence of the changing geometry. Each model run is also checked regularly for floating ice, which the model is unable to accurately represent. These checks occur at least every ten timesteps (0.03 a), and once the model reaches the flotation point, subsequent changes in geometry are considered to be unreliable. The range of values used for each forcing factor is discussed below.

6.2.1 Crevasse water depth

The model is first tested with a range of crevasse water depths (D_w) from 0 to 50 m. Surface ablation near the terminus of Helheim Glacier is roughly 2 m a^{-1} (Andersen et al., 2010), and annual precipitation rates are roughly 1200-1800 mm a^{-1} (Mernild et al., 2010). The spacing of crevasses on the surface is highly variable, but from observations it is possible to determine that a spacing of 200 m is fairly typical. This means that water availability to each crevasse may be up to 724 m^2 per unit glacier width annually. If we assume a crevasse water depth of 50 m the crevasse would have to have a mean width of 14.5 m. This is somewhat narrower than would be expected of crevasses around the terminus, but it means that the upper limit of 50 m crevasse water depth is at least physically plausible and likely to represent an upper limit of water depth, as wider crevasses and leaking of water from the crevasse

would be expected to make true values somewhat lower.

6.2.2 Basal water pressure

The first of the new environmental forcing variables applied to the model in this chapter is variation in basal water pressure. During the melt season, water produced by surface ablation may penetrate to the bed via crevasses and moulins, adding to the water at the bed arising from basal melting. The consequent increase in basal water pressure may increase the glacier's speed, which has been suggested to increase calving rates by changing the terminus geometry (van der Veen, 2002). Observations made in Greenland have linked basal water pressure to increases in velocity at the ice sheet margin (Zwally et al., 2002). This is also observed at Helheim Glacier, with a study by Andersen et al. (2010) finding a correlation between observed velocity and estimates of melt water availability from surface mass balance modelling. The relationship between surface meltwater and velocity is complicated, as the basal water pressure also depends on the type of drainage system at the bed. If sufficient water is added to the system it may trigger a change from a distributed to a more efficient channelised drainage system, thus decreasing basal water pressure (Bartholomew et al., 2010; Howat et al., 2010). Generally, summer velocity increases seem to be higher on the ice sheet than in outlet glaciers, but even outlet glaciers show seasonal variations in speed of up to 15%, thought to be caused by changes in basal water pressure (Joughin et al., 2008a). This scale of acceleration was concluded to be insufficient to be a likely cause of observed glacier retreat. This conclusion has been backed up by modelling work, showing basal water pressure to have relatively little effect on terminus behaviour in a tidewater glacier model (Nick et al., 2009). Nevertheless, the data are sufficiently unclear to make some study of the effect of basal water pressure in the calving model worthwhile.

Experiments with varying basal water pressure are applied in the three different scenarios used throughout Chapter 5; advancing ($D_w = 0$ m), steady ($D_w = 10$ m) and retreating ($D_w = 40$ m). Changes in basal water pressure are measured by the

change in hydrostatic head, with a maximum change of ±75 m from the standard case, and an interval of 25 m. The maximum observed change in velocity of 15% (Joughin et al., 2008a) is produced in the model by a change in hydrostatic head of 50 m. It was also noted previously that if the type of drainage system at the bed changes, this may decrease the basal water pressure. Therefore the range of experiments includes those with reduced basal water pressure to investigate the effect that this would have.

6.2.3 Subaqueous melt

Melting at the calving face has been thought to be able to affect calving by removing support from an overhanging block of ice, encouraging fracturing and calving (*e.g.* Benn et al., 2007b; O'Leary, 2011). Previously this had been thought to be most significant for smaller glaciers with low calving rates, which allow sufficient time for melting at the front to have a significant effect (Vieli et al., 2001). However, recent observations around Greenland suggest that subaqueous melt rates in this region may be sufficient to have an effect on calving. These studies use measurements of fjord temperature and water velocity to estimate the heat flux transported to the glacier terminus and use this to infer average melt rates across the calving face. This leads to estimates of 0.7 to 3.9 $\mathrm{m\,day^{-1}}$ (255 $\mathrm{m\,a^{-1}}$ to 1424 $\mathrm{m\,a^{-1}}$) for glaciers in West Greenland (Rignot et al., 2010) and an estimated range of 540 to 1238 $\mathrm{m\,a^{-1}}$ for Helheim Glacier (Sutherland and Straneo, 2012).

The vertical profile of the the melt rate will also be likely to affect the way in which melting at the front changes the stress distribution in the ice. Two studies have investigated the vertical melt profile using models of a plume of subglacial discharge and its interaction with the calving front. One by Xu et al. (2012) uses an idealised representation of a typical Greenland outlet glacier and its surrounding fjord waters to investigate melt rates, finding that melting requires some level of subglacial discharge to drive convection, after which melt depends linearly on water temperature and on the cubic-root of subglacial discharge. The modelled vertical

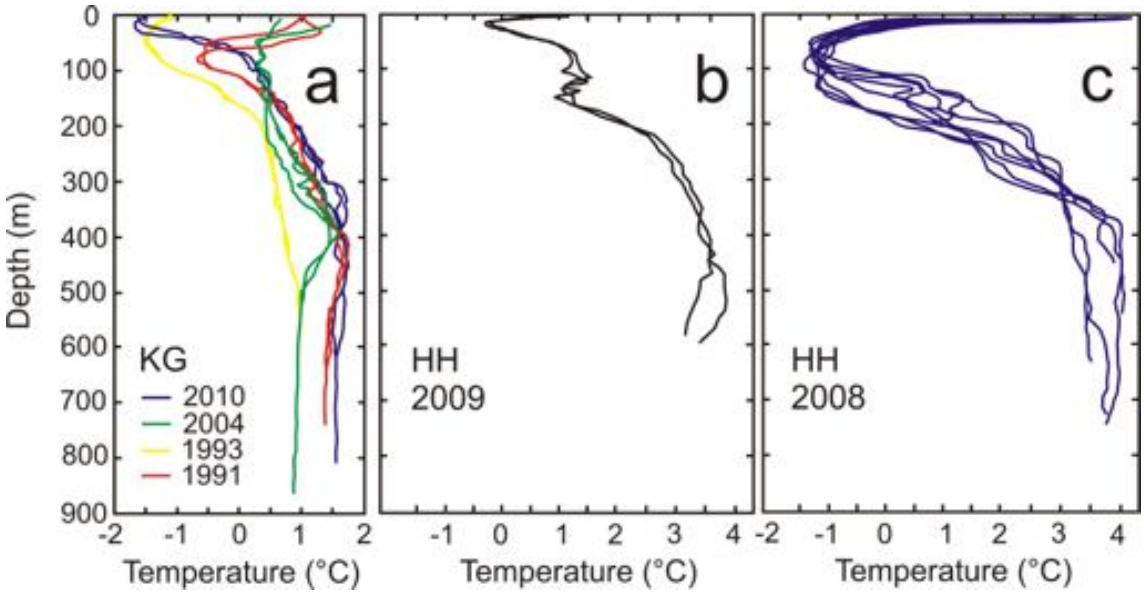

Figure 6.1: Measured water temperatures in Kangerdlugssuaq (KG) and Helheim (HH) fjords. (a) Water temperature in Kangerdlugssuaq fjord, measured in August/September (O'Leary, 2011). (b) Water temperature in Sermilik fjord, August 2009 (Sutherland and Straneo, 2012). (c) Water temperature in Sermilik fjord, July 2008 (Straneo et al., 2010).

melt profile follows roughly a parabolic shape with no melt at the waterline or bed, and typical melt rates are found to be in the region of 4 $\mathrm{m\,day^{-1}}$ water equivalent (w.e.) corresponding to 1605 $\mathrm{m\,a^{-1}}$ ice.

A second study by O'Leary (2011) uses a similar model to predict the melt rate on the calving front of Kangerdlugssuaq Glacier, East Greenland using observations of ocean temperatures and estimates of subglacial water discharge from surface mass balance modelling. The model indicates that the maximum melt rate occurs close to the base of the glacier, reducing to around zero at the water line, with estimated average summer melt rates of 1.3 to 2.7 $\mathrm{m\,day^{-1}}$ w.e. (540 to 1070 $\mathrm{m\,a^{-1}}$ ice melt) averaged over the entire calving face. This work takes into account the observation that Kangerdlugssuaq Fjord, like Helheim Glacier's Sermilik Fjord, has two layers of different water types, an upper layer of cold polar water and warm subtropical water underneath, which are likely to significantly affect the melting rate (Straneo et al., 2011). The water temperature profiles at Kangerdlugssuaq and Helheim Glaciers are very similar, but the warm water in the lower layers at Sermilik Fjord

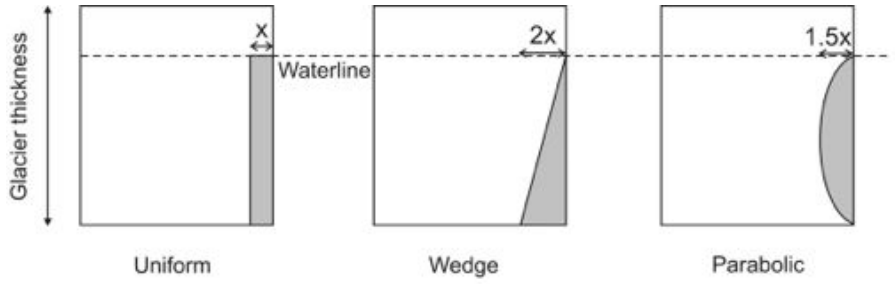

Figure 6.2: Different vertical melt profiles used for undercutting experiments. Bars indicate the maximum melt rates used so that each case removes an equal volume of ice, in terms of a factor applied to the mean melt rate x.

is much warmer than that at Kangerdlugssuaq Fjord (see Figure 6.1). In sensitivity testing performed by O'Leary on the plume model, this magnitude of temperature rise should increase maximum melt rates at the front from around 2.5 m day^{-1} w.e. (around 900 m a^{-1} ice) to 3.5 m day^{-1} w.e. (1400 m a^{-1} ice). Interestingly, both modelling studies indicate that the presence of the subglacial water plume is as important as surrounding water temperatures for determining melt rates.

Since there is still uncertainty about the vertical subaqueous melt profile at the calving face, undercutting experiments are run with three different shapes: uniform melt, wedge shape and parabolic shape (Figure 6.2). The range in summer melt rates found by previous studies of Greenland glaciers is 255 – 1605 m a^{-1}, averaged over the full calving face. The model is tested with a range of average subaqueous melt rates (M_f) from 0 to 5000 m a^{-1}, with an interval of 1000 m a^{-1}, in each case with no water applied in crevasses. Initially experiments with lower melt rates were considered but preliminary testing showed that the effect on calving was minimal. The different undercutting profiles lead to different volumes of ice loss, therefore the maximum melt rate is adjusted to ensure melt volume is comparable in each case; for the wedge shape maximum undercutting rate is twice that of the mean and for the parabolic profile 1.5 times the mean melt rate. It should be noted here that since the external water pressure on the calving face acts normal to the boundary, the stress interaction between the terminus and surrounding ocean water is generally well represented in the model. However, in the case of uniform undercutting

there is a shortage of mesh nodes on the horizontal undercut section, meaning that in this case the stress applied to the front around the waterline may be less well represented. This occurs because the horizontal displacement is applied between two nodes leaving the undercut section without any nodes to represent it. Although the water pressure is clearly zero at the waterline, the vertical spacing of 40 m between nodes means that some of the undercut section sits below the waterline and therefore should experience some external pressure which due to the lack of nodes will be unrepresented.

6.2.4 Ice mélange

Ice mélange in the proglacial fjord has been suggested to provide a resistive stress acting on the front of outlet glaciers, which may have a significant effect by stabilising the terminus and preventing calving in winter. One of the first studies to observe this effect in Greenland was Sohn et al. (1998), who found a strong correlation between the break up of ice in the fjord of Jakobshavn Glacier, West Greenland and the onset of summer calving, and hypothesized a reduction in backstress as a possible cause. These results are supported by similar observation made by Reeh et al. (2001) at Nioghalvfjerdsfjorden Glacier, North-East Greenland, Joughin et al. (2008c) at Jakobshavn Glacier, and Walter et al. (2012) at Store Gletscher, West Greenland. The potential effect of backstress on tidewater glaciers is confirmed by modelling studies which have found that perturbations in the variable are able to cause model retreat (Nick et al. (2009), Vieli and Nick (2011)).

Relatively little is known about the mélange due to the difficulties in performing studies in the proglacial fjord environment. In order to include the effects of the ice mélange in the calving model we must know the thickness of the mélange and the stress it applies on the calving face. Using LiDAR data from July 2007, the ice mélange in front of Helheim Glacier is measured to have a typical freeboard of 10-20 m, discounting isolated larger icebergs (personal communication, T. James (2012)). The stress applied on the calving face is less easy to measure. The only

Table 6.1: Stress acting on the calving front, assuming a force as calculated by Amundson et al. (2010) sufficient to prevent calving, applied over a number of different vertical ranges. Below, stress from water pressure at the bottom of the given depth range for comparison.

Depth range (m)	full-face	-303 to 40	-119 to 15	-7.6 to 1
Backstress (kPa)	16.3	36.4	93.6	1454
Water pressure (kPa)	6245	3062	1196	76.8

observational measurement made is by Walter et al. (2012), observing that in one melt season on Store Gletscher the break-up of the ice mélange was coincident with an acceleration in the terminus velocity of 15%, leading to an estimation that the ice was providing a backstress of 30-60 kPa.

A different approach was taken by Amundson et al. (2010), estimating the effects of the ice mélange on calving at Jakobshavn Glacier in West Greenland. They state that the melange has little effect on the velocity of the glacier front, but hypothesize that the stress applied may be sufficient to prevent an ice block from tipping, thus holding calved ice in place over the winter months. The estimated force required to prevent an ice block from tipping is roughly equivalent to the change in stress arising from tidal variation in water depth, *i.e.* around 1.25×10^7 Nm^{-1} in the case of Helheim Glacier, assuming a tidal range of 2 m. The corresponding stress from this force is calculated in Table 6.1 over a range of depths. The stress acting over the smaller areas is high, but is generally smaller than the stress arising from water pressure at the bottom of the depth range. In previous ice flow modelling work an estimated backstress of 40 kPa was used acting over the entire calving face Vieli and Nick (2011), which is high compared to the Amundson et al. (2010) force estimate.

Since neither the magnitude of backstress from proglacial ice mélange nor the vertical range of the mélange is well known a range of experiments is run with forces (F_f) from 0.25×10^7 Nm^{-1} to 5.0×10^7 Nm^{-1} acting on the calving face over a range of vertical extents. The experiments are laid out in Table 6.2. The suite of experiments is performed in the three different scenarios identified previously; advancing ($D_w =$

Table 6.2: Backstress experiments performed on Helheim Glacier model. Backstress acting on calving face over stated ranges measured in kPa.

	Force ($\times 10^7$) Nm^{-1}				
Depth range (m)	1.0	2.0	3.0	4.0	5.0
Full-face	13.0	26.1	39.1	52.2	65.2
-303 to 40	29.2	58.3	87.5	116.6	145.8
-119 to 15	74.6	149.3	223.9	298.5	373.1
-7.6 to 1	1163	2326	3488	4651	5814

0 m), steady ($D_w = 10$ m) and retreating ($D_w = 40$ m). This is important because backstress is thought to have a stabilising effect on the terminus, therefore its effect may be more noticeable in cases where the glacier would normally retreat.

6.3 Results: Response to Climatic Forcing

6.3.1 Crevasse water depth

As expected from previous results at Columbia Glacier, the depth of water in crevasses had a significant effect on the evolution of the glacier's terminus (see Figure 6.3). Higher water depths tended to trigger a retreat of the terminus; examples of the changing geometry in the experiments are shown in Figure 6.4. The change in crevasse water depth also caused a change in calving behaviour of the glacier, in all cases the calving event size distribution was statistically significantly different from the case with $D_w = 0$ m. As crevasse water depth increased so did the number of calving events, up to a peak at $D_w = 20$ m, after which the number of events fell again and the median event size increased (Figure 6.5).

During the runs the model was seen to stick at pinning points, where the terminus oscillated until the surface profile changed sufficiently to drive further advance or retreat. The pinning points on the bed can be seen more clearly in Figure 6.6,

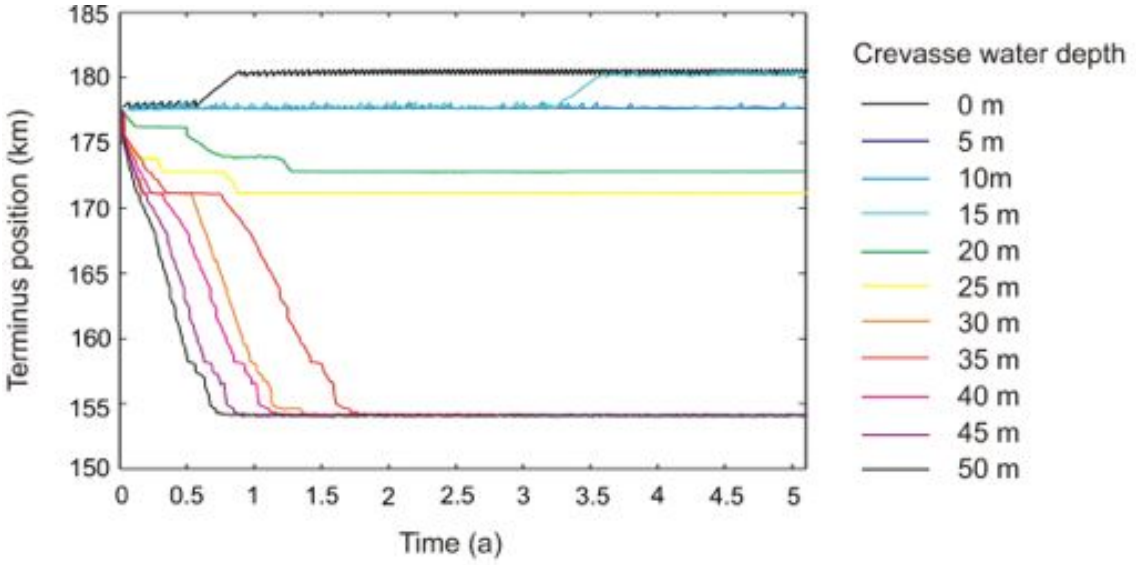

Figure 6.3: Response of Helheim Glacier model's terminus location to varying depth of water in crevasses.

showing that they generally occurred on or near peaks in bed elevation, with calving triggered as the terminus advanced into deeper water. The basal peaks were in some cases very small, indicating that small changes in bed elevation profile may in some cases have an effect on terminus behaviour. This behaviour qualitatively agrees with the flotation model of calving (described in Section 2.2.1), where calving is also triggered by advance into deeper water. This type of model was found by Nick and Oerlemans (2006) to inhibit advance into basal troughs, but in this example we see that after a period of surface evolution the glacier may begin to advance again.

The calving response of the glacier may be examined in more detail by plotting histograms of the event size (Figure 6.7). In low water depth experiments, calving events were mainly of a medium size (around 500 m). As water depth increased, calving became dominated by smaller events (less than 100 m). Then as water depth increased further, the larger events reappeared including some very large events of 1-2 km. The reason for these typical event sizes is examined in Figures 6.8 and 6.9. Figure 6.8 shows the depth of the predicted crevasse field in the initial state of the glacier, given different depths of water in crevasses. Given low crevasse water depths no calving occurs; in the middle range of crevasse water depth (D_w = 20, 25 m),

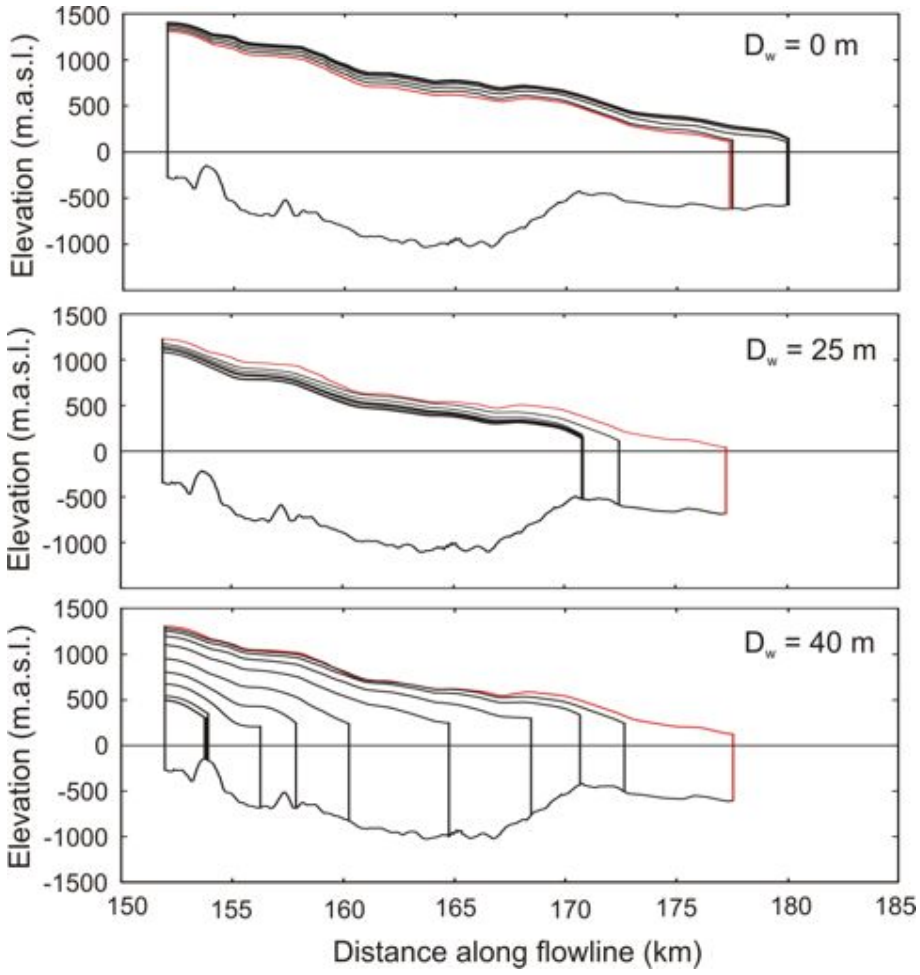

Figure 6.4: Surface geometry evolution of Helheim Glacier model with different crevasse water depths. Lines show model geometry at 0.5 a intervals over the 5 year model run, initial profile marked in red.

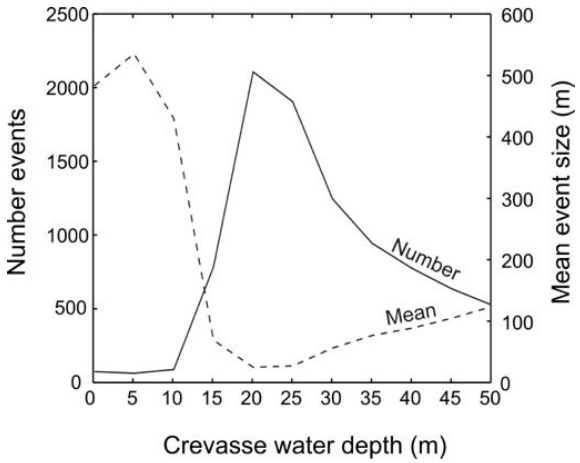

Figure 6.5: Response in calving behaviour of Helheim Glacier model to varying crevasse water depth, solid line indicated total number of calving events over a 5 year model run, dashed line shows mean calving event size.

small calving events began to occur around the calving front; while for larger water depths the crevasse field crosses the waterline further upstream creating a larger calving event. For the lower crevasse water depths experiments where no calving occurred in the initial state, the glacier surface had to evolve before a calving event took place (Figure 6.9). When calving eventually occurred, the event was of a large size ($\tilde{5}00$ m).

6.3.2 Basal water pressure

The response of the modelled glacier to changes in basal water pressure was found to depend on the state of the glacier (Figure 6.10). In the retreating scenario there was almost no difference between the different experiments. In the $D_w = 10$ m scenario, the model remained pinned with a steady terminus position in all experiments except for that with a decrease in hydrostatic head of 75 m, which advanced. This experiment reached flotation point at 3.85 a into the run: therefore, results after this point are excluded. In the advancing scenario, an increase in hydrostatic head tended to delay the timing of the model's advance, with the highest basal water pressure case remaining pinned in the initial position throughout the run.

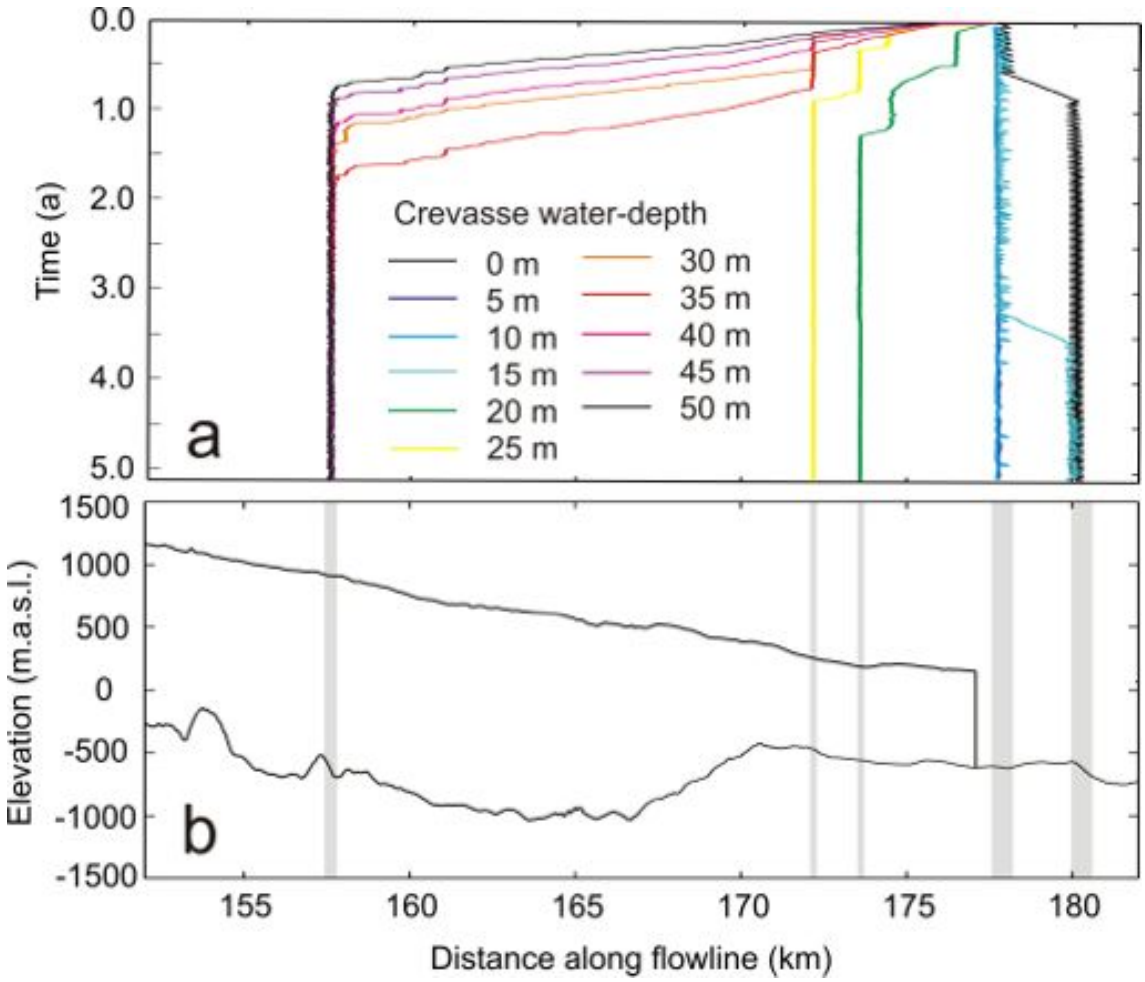

Figure 6.6: (a) Terminus evolution of Helheim Glacier model, given different depths of water in crevasses. (b) Observed glacier geometry (July 2005) showing pinning points on bed.

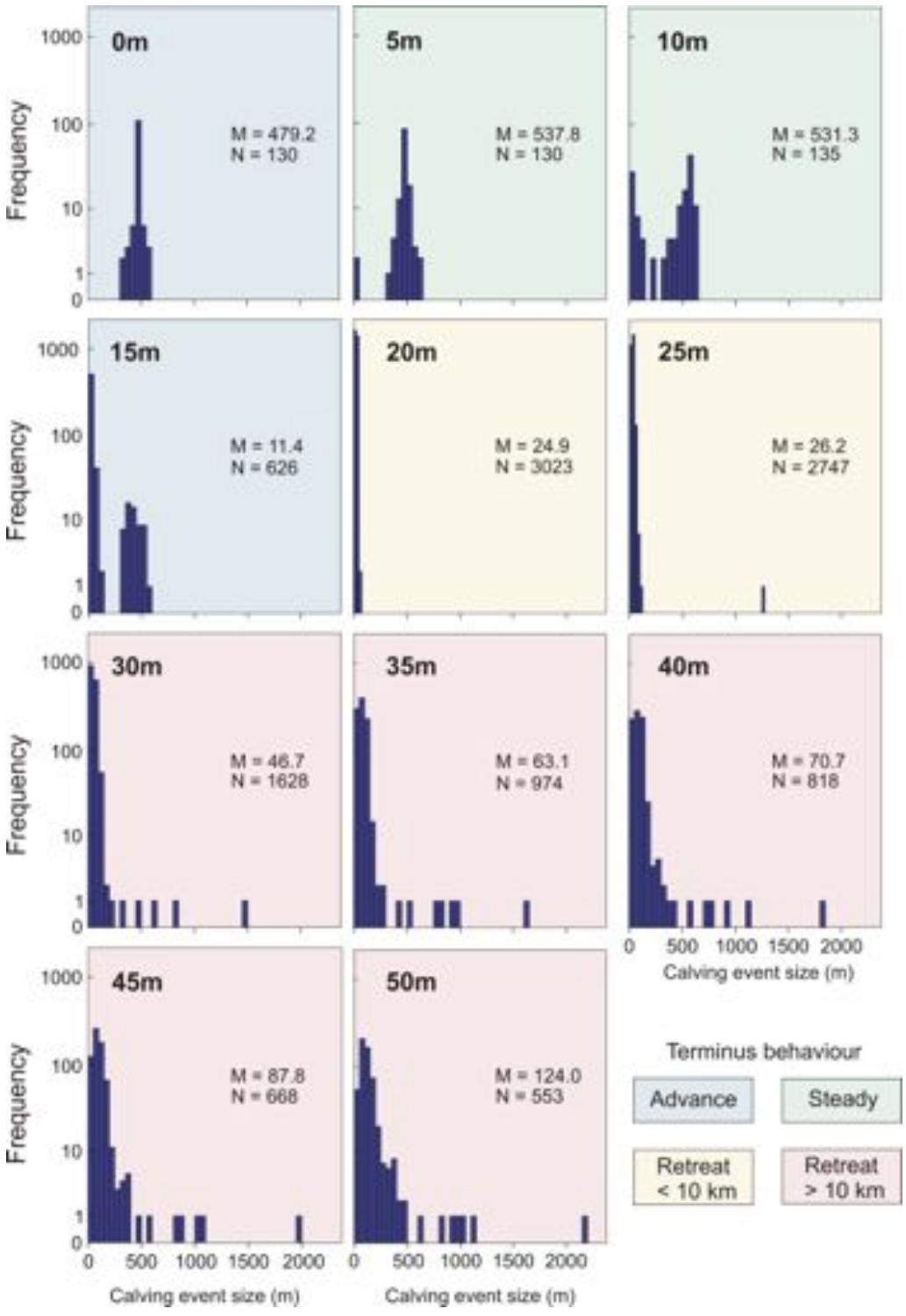

Figure 6.7: Calving behaviour of model given different crevasse water depths; histograms of calving event size against frequency given on a logarithmic scale. Graphs are colour-coded by the terminus behaviour in each case. M is median event size, N is the total number of events over a 5 year model run.

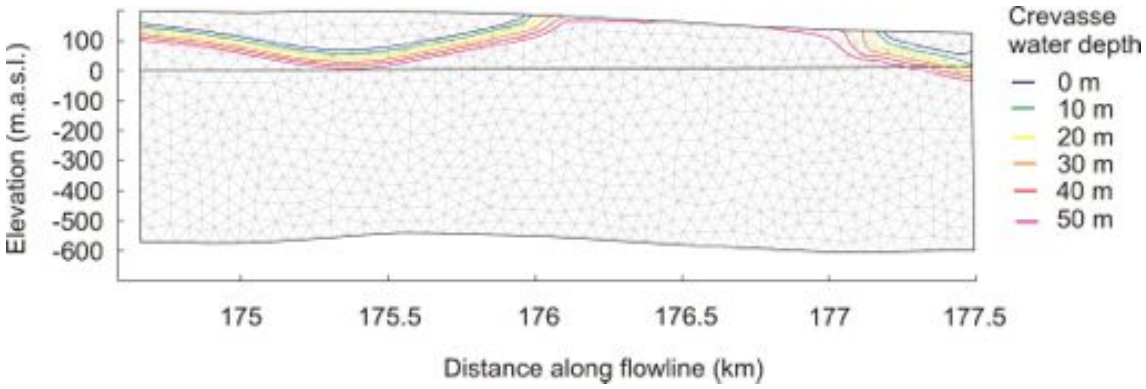

Figure 6.8: Depth of modelled crevasse field given different crevasse water depths, glacier model in initial state.

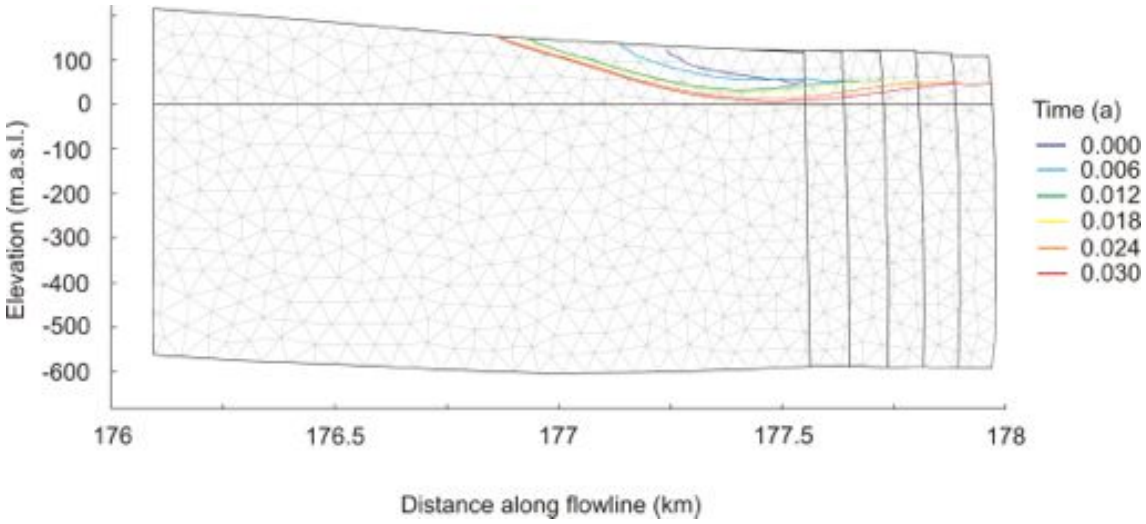

Figure 6.9: Glacier geometry and depth of crevasse field with no water in crevasses as model evolves over time. Snapshots shown at intervals of two timesteps (0.006 a).

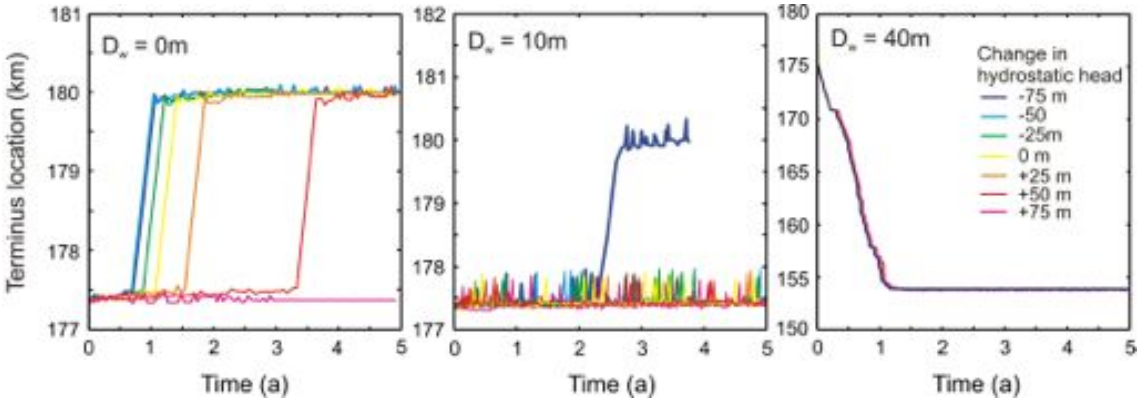

Figure 6.10: Modelled terminus evolution given different modelled basal water pressure, lines represent changes in hydrostatic head compared to standard basal water pressure. The three graphs show experiments with different applied crevasse water depth.

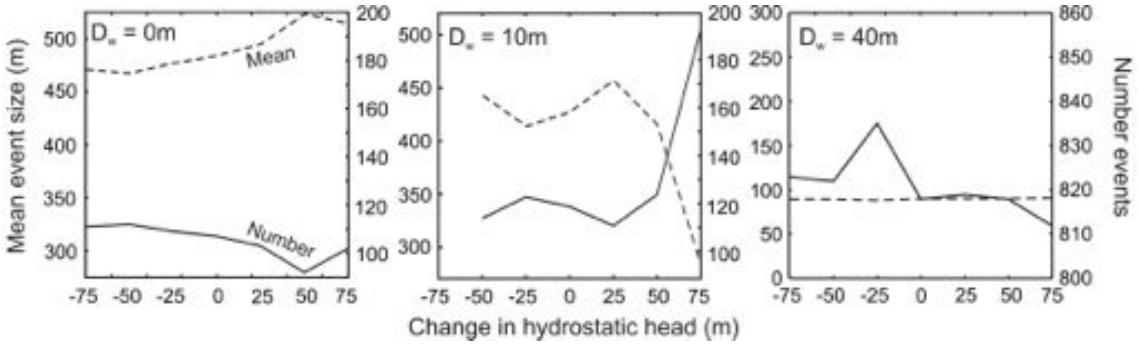

Figure 6.11: Effect of changing hydrostatic head of water acting at the bed of the glacier on modelled calving behaviour. Dashed lines show mean event size, solid lines show the total number of events over a 5 year model run. The three graphs show experiments with different crevasse water depth.

Examining the calving behaviour, an increase in hydrostatic head generally produced a decrease in the number of calving events and in some cases an increase in the mean size (Figure 6.11). In most cases there was not a statistically significantly difference in the calving event size distribution compared to the case with standard basal water pressure, although in experiments with significantly different terminus behaviour statistical tests were not run as it is then impossible to separate the effects of changing geometry from changing basal water pressure.

6.3.3 Subaqueous melt

As described in Section 6.2, experiments were run with a range of frontal melting rates over three different vertical melt profiles (see Figure 6.2). The response of the terminus to undercutting is shown in Figure 6.12. With no undercutting applied at the front, the terminus advanced quickly from its starting position to a location around 180 km along the flowline. The inclusion of undercutting at the calving face tended to inhibit this advance. In the case of uniform melt, as melt rates were increased the advance was delayed and in experiments with a melt rate over $3.0\,\mathrm{km\,a^{-1}}$ the terminus did not advance at all. The response to undercutting was even larger in the case of a wedge shaped melt profile, where rates of only $2.0\,\mathrm{km\,a^{-1}}$ inhibited glacier advance. For the parabolic profile the effect was also pronounced, with the melt rate of $5.0\,\mathrm{km\,a^{-1}}$ causing a mild retreat of the terminus.

The response in calving behaviour of the model is also shown in Figure 6.12. In all but three cases the mean event size was statistically significantly different to the no melt case at the 99% confidence level. Comparing the cases to each other, an increase in melting of $1000\,\mathrm{m\,a^{-1}}$ produced a statistically significant change in calving in approximately half of the comparable experiments (excluding comparisons with significantly different terminus behaviour). The terminus behaviour is indicated by the colour of graphs in Figure 6.13 to aid comparison. In the case of uniform undercutting the size distribution became less peaked and shifted towards smaller iceberg sizes as the undercutting rate increased. In the case of the wedge profile,

there is little pronounced trend in calving event size. In the two advancing cases an increase in undercutting rate results in a lower number of larger calving events, while conversely in the examples which have a steady terminus as undercutting increases there is a general decrease in calving event size and increase in number of events. In the case with a parabolic melt profile, there is little evidence of a trend in calving event size, but the higher undercutting rates do begin to exhibit very large calving events which are not observed in the other experiments. Although the experiments show that differences in calving event size and frequency can be significant for changes in subaqueous melt rate, the experiments presented here are not sufficient to pin down the causes of these differences. The calving event size depends not only on geometry of the calving face, but also on the terminus position and bedrock geometry, causing complicated feedback effects. To properly test the full effect of undercutting on calving event size, experiments should be performed on an idealised geometry allowing the two influences on calving to be separated.

The results of the undercutting experiments show that although melting at the calving face does have an effect on the terminus position and calving behaviour of the modelled glacier, the undercutting rate required to cause these changes is generally higher than those predicted for Greenland glaciers. Plotting the change in longitudinal deviatoric stress in each case may explain some of this lack of sensitivity. It has previously been assumed that melting below the water line will have the effect of removing support from the glacier terminus, increasing fracturing around the front of the glaciers. Figure 6.14 shows that in ice above the water line, undercutting makes relatively little difference in stress, highlighted in difference plots shown in Figure 6.15. This is because pressure from the supporting ice is replaced by a similar external pressure from the surrounding water body. In the case of uniform undercutting the lack of mesh nodes around the waterline means that the external water pressure is not well represented, which may explain why the distribution of modelled calving event sizes is more sensitive to changes in the subaqueous melt rate.

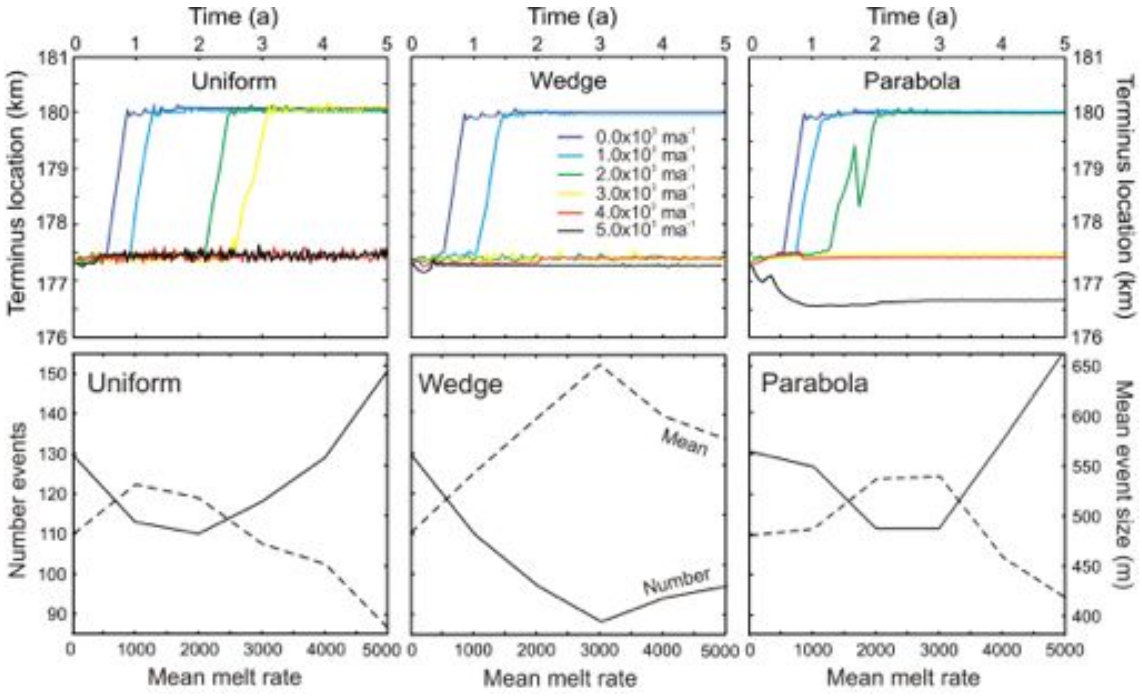

Figure 6.12: Response of Helheim Glacier model to varying melt rate at the calving face, using three different vertical melt profiles. Top row shows the terminus evolution in each case, bottom row of graphs shows the response in calving behaviour with dashed lines indicating mean event size and solid lines showing the total number of events over each 5 year model run.

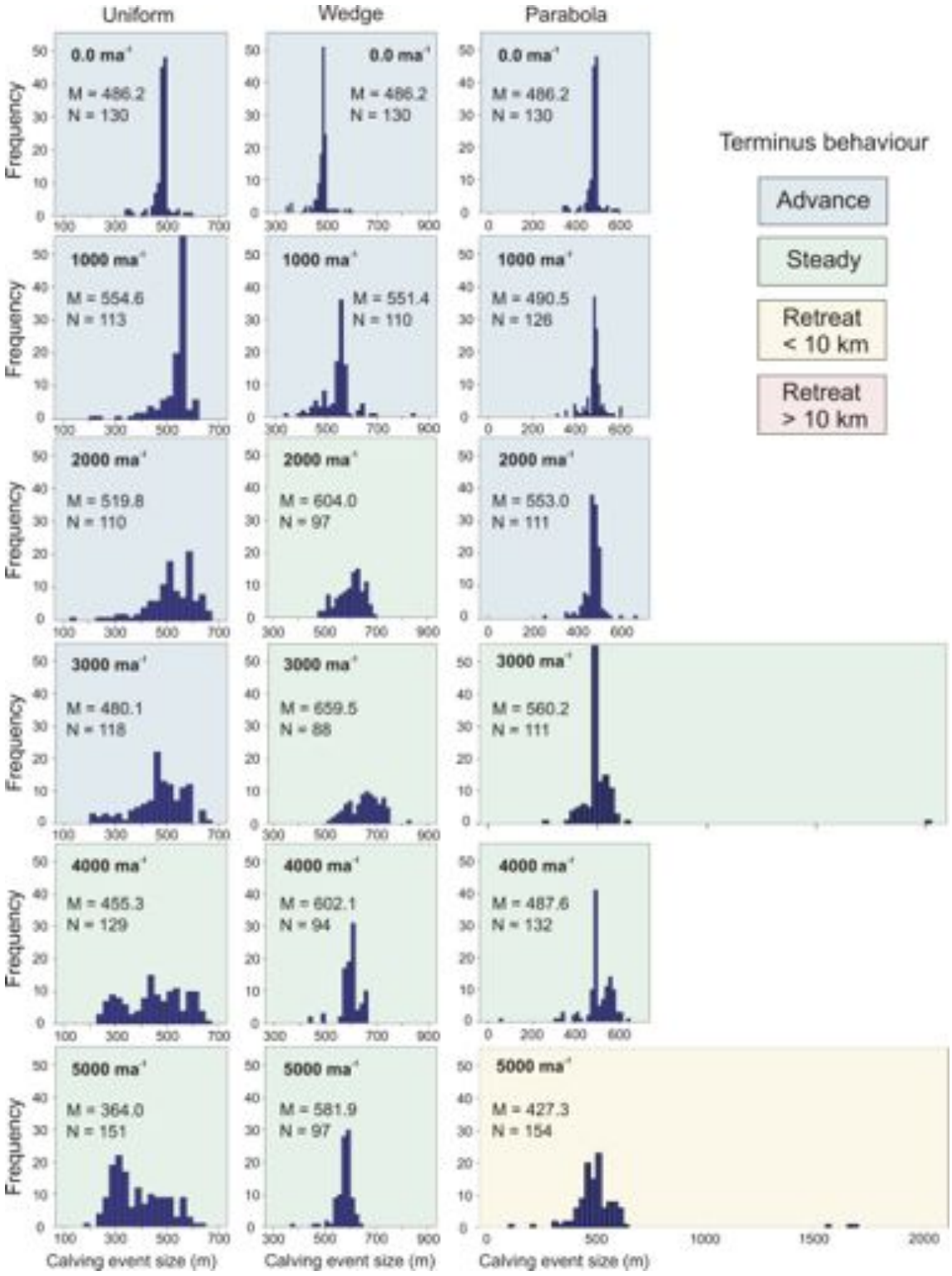

Figure 6.13: Response of modelled calving behaviour to varying melt rate at the calving face. Histograms show frequency against size of calving event for different vertical melt profiles and melt rates. Graphs are colour-coded to indicate terminus behaviour.

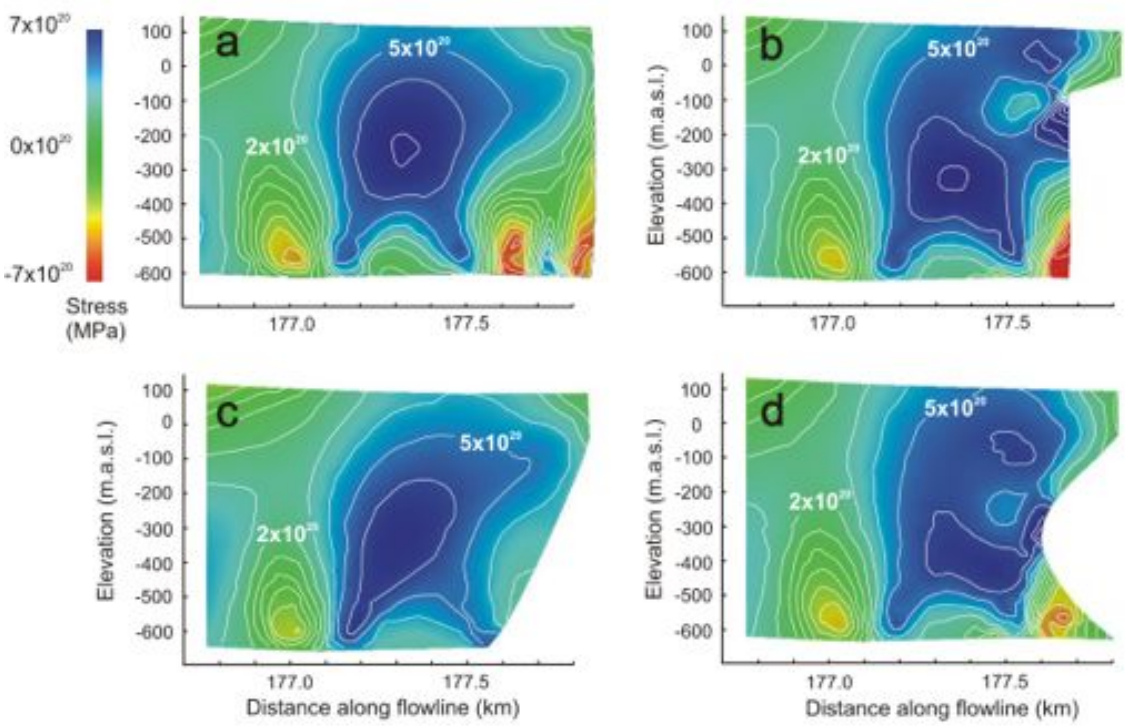

Figure 6.14: Longitudinal deviatoric stress distribution around the glacier terminus in different undercutting scenarios: (a) no undercutting (b) uniform (c) wedge (d) parabolic. Stress measured in MPa with contour intervals of 1.0 MPa. Positive values indicate longitudinal stretching, negative values show areas of compression.

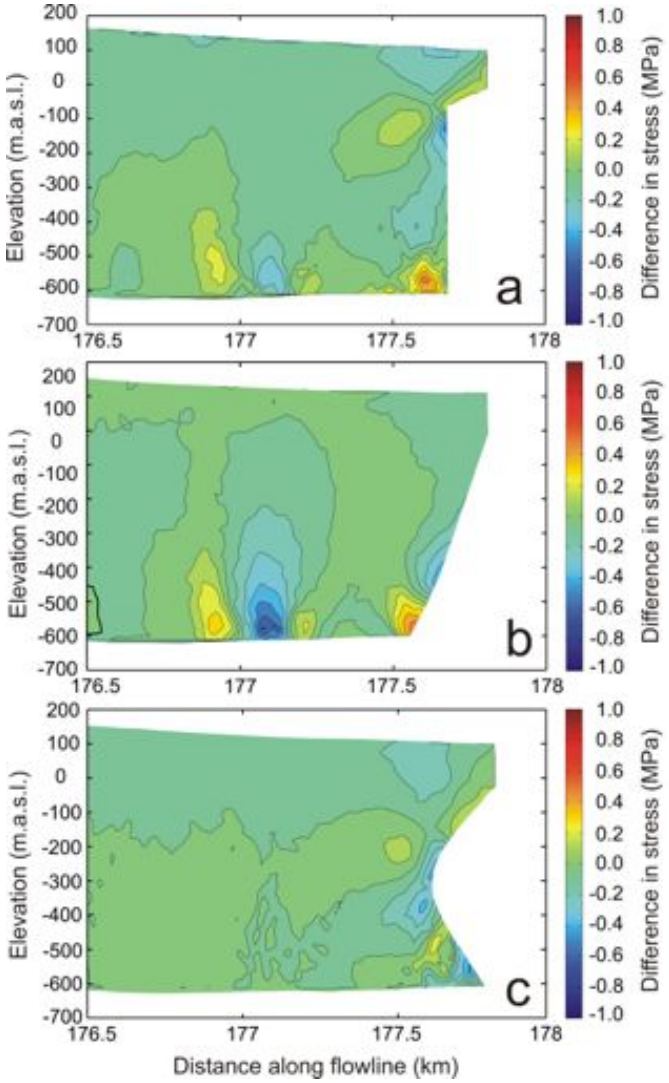

Figure 6.15: Difference in longitudinal deviatoric stress distribution around the glacier terminus in different undercutting scenarios: (a) uniform (b) wedge (c) parabolic. Difference calculated compared to the case with no undercutting. Stress measured in MPa with contour intervals of 1.0 MPa. Negative values indicate a higher stretching rate, positive values indicate more compression.

Table 6.3: Effect of changing backstress on terminus velocity of Helheim Glacier model, showing the percentage change in velocity at the terminus in each experiment compared to that with no backstress applied.

	Force ($\times 10^7$) Nm^{-1}				
Depth range (m)	1.0	2.0	3.0	4.0	5.0
Full-face	0.90	1.8	2.7	3.6	4.4
-303 to 40	0.39	0.79	1.0	1.6	2.0
-119 to 15	0.14	0.27	0.40	0.54	0.67
-7.6 to 1	0.00	0.00	0.00	0.00	0.00

6.3.4 Ice mélange

The response of the glacier terminus to varying backstress is shown in Figure 6.16. In the advancing scenario all the experiments show nearly identical terminus behaviour, although with the three highest stresses applied over the full calving face the model began to float approximately half way through the run: therefore, results after this point were excluded in these cases. In the steady scenario, in all but one case the terminus remained pinned in the starting position; only the experiment with a force of 5.0×10^7 Nm^{-1} acting over the full face of the glacier advanced from this position. In the retreating scenarios there was more of a difference in the terminus evolution, cases with a higher force acting on the terminus tended to retreat later in the model run, with the effect increasing as the force acted over a larger area of the calving face.

It has been stated by Amundson et al. (2010) that backstress from the ice mélange should not have a significant effect on the velocity of the glacier. To test this the terminus velocity at the beginning of the model run was examined for each backstress experiment. The change in terminus velocity compared to the case with no backstress is shown in Table 6.3. The effect on the velocity of the glacier was greater in experiments acting over a larger area of the calving face, with a maximum change of 4.4% in the case with 5.0×10^7 Nm^{-1} acting over the full face of the glacier.

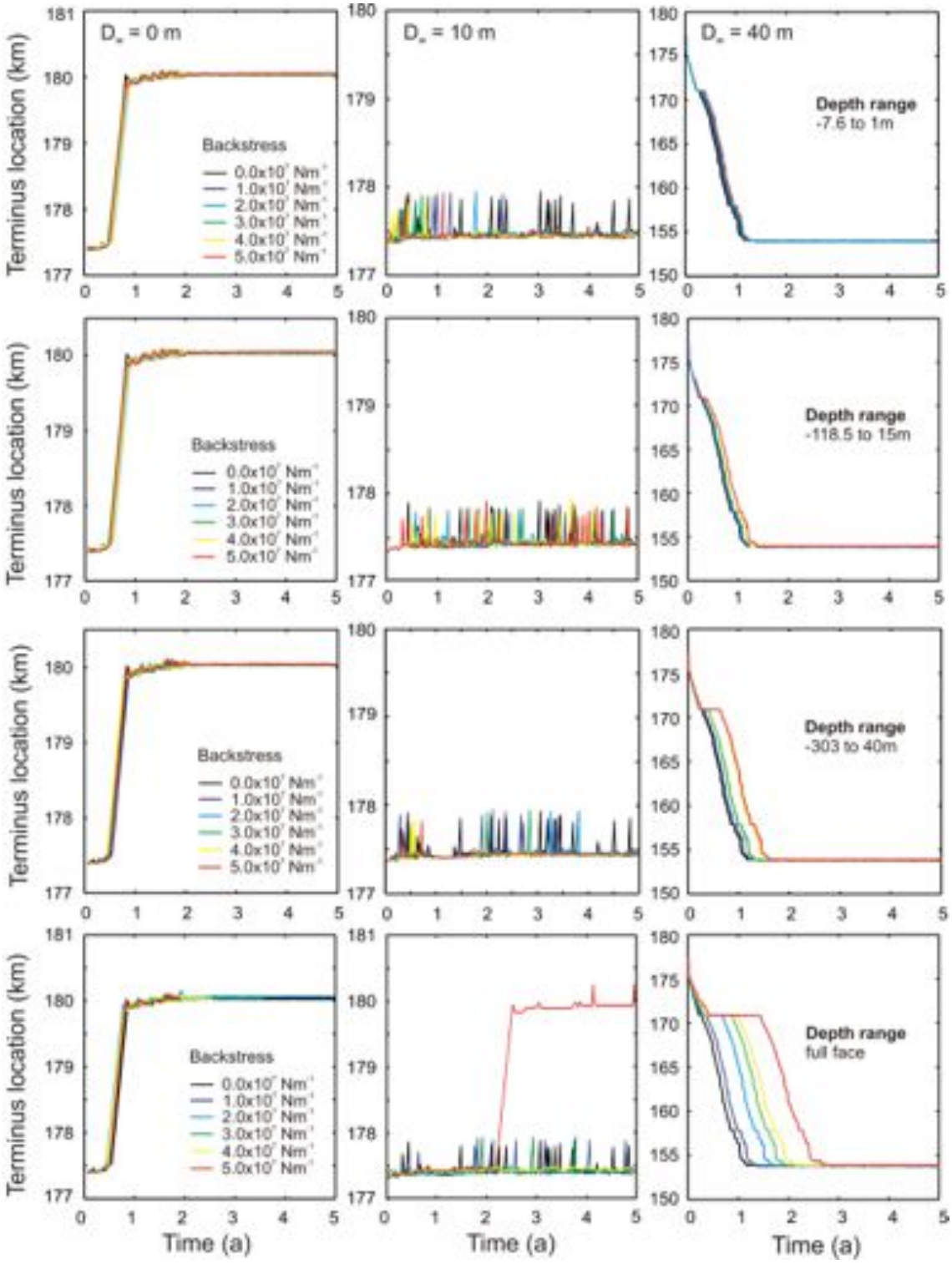

Figure 6.16: Response of Helheim Glacier model's terminus location to varying backstress at the calving face. Columns show response given different crevasse water depths, rows apply backstress over different vertical ranges.

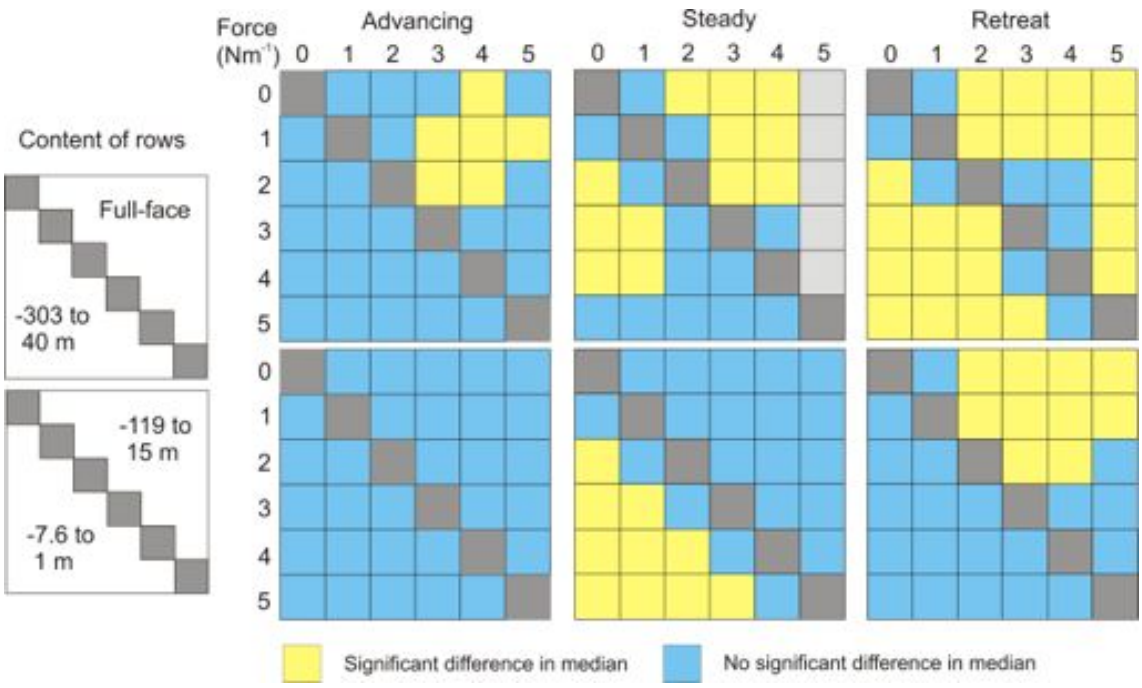

Figure 6.17: Statistical significance of changes in calving event size between experiments with different backstresses applied at the calving front. The columns show three different model scenarios, advancing ($D_w = 0$ m), steady ($D_w = 10$ m) and retreating ($D_w = 30$ m). The different rows show the different vertical ranges over which the backstress was applied. Blue squares indicate no statistically significant difference in calving event size between experiments, yellow show a statistically significant difference (95% confidence limit).

The hypothesis of Amundson et al. is contradicted by evidence from Walter et al. (2012) observing an increase in velocity of 15% at Store Gletscher on break-up of the ice mélange which indicates that it may provide sufficient backstress to affect the terminus velocity.

Although changes in backstress generally did not produce a change in the terminus behaviour of the glacier, in many experiments there was a change in the calving behaviour compared to the case with no backstress. To test this, the calving event size distribution was compared for each experiment using the Wilcoxon-Mann-Whitney test and results are laid out in Figure 6.17. In general the changes in calving event size were not significant for the advancing scenario, but many of the steady and retreating model runs showed significant changes in calving event size, particularly

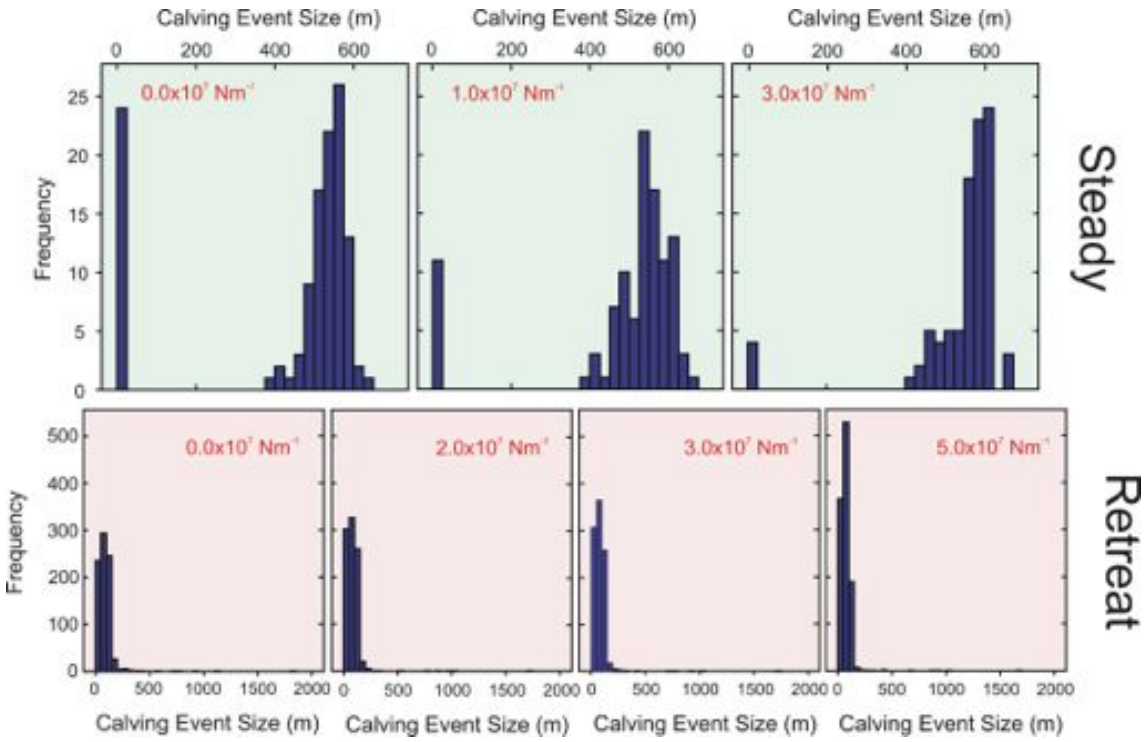

Figure 6.18: Histograms of frequency against calving event size for varying backstress applied over the full calving face in the steady (D_w = 10 m) and retreating (D_w = 30 m) scenarios. Force applied is indicated in red text in each graph.

at the upper end of the range of backstress. To examine this change in further detail, some typical histograms of calving event size are shown in Figure 6.18. There was no clear pattern of response to changes in backstress; in the steady scenario increases in backstress caused a decrease in smaller calving events (<100 m), while for the retreating scenario increasing backstress cause an increase in smaller events. Although backstress has the potential to affect calving behaviour, the change in calving event size also depends on the geometry changes in the glacier.

Given the insensitivity of the model's terminus behaviour to the range of backstresses tested so far, an extended range of backstresses was devised to test the model further, as laid out in Table 6.4. In these experiments the force was only applied over the vertical range considered most realistic, -118.5 to 15 m (Section 6.2.4). The force was not increased above 50×10^7 Nm^{-1} as higher values caused distortion in the mesh around the front, causing instability in the model. The effect of these larger

Table 6.4: Additional backstress experiments, with backstress applied to the terminus over a vertical range of -118.5 to 15 m. Below, percentage change in velocity at terminus in each experiment compared to that with no backstress applied.

Force ($\times 10^7$ Nm^{-1})	10	15	20	25	50
Backstress (MPa)	0.75	1.12	1.49	1.87	3.73
Velocity change (%)	3.8	5.6	7.4	9.1	17.5

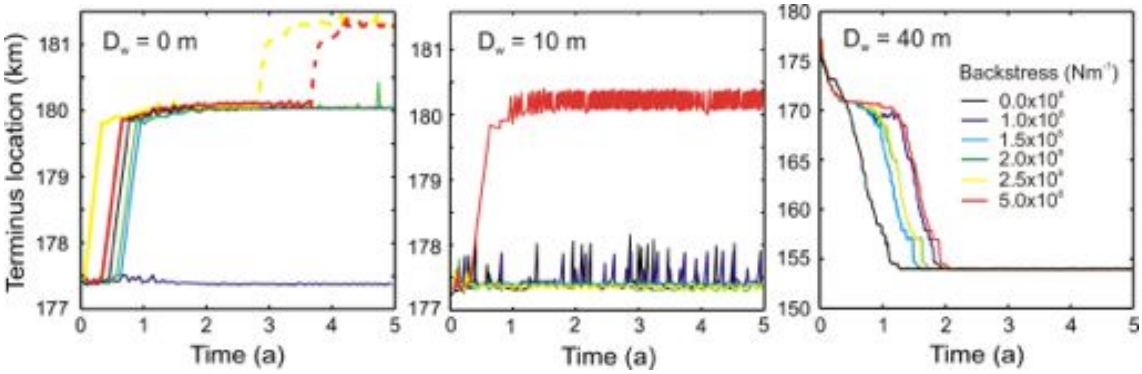

Figure 6.19: Response of modelled Helheim Glacier terminus location to varying backstress at the calving face, in all cases applied over a vertical range of -118.5 to 15 m. The three graphs show the effect given different crevasse water depths. Sections of dashed line for the two highest stresses indicate results which are unreliable as the model contains ice at the flotation point.

backstresses on the behaviour of the terminus can be seen in Figure 6.19, and their effect on the terminus velocity is given in Table 6.4. The highest backstress used produced a percentage change in terminus velocity similar to, though slightly larger than, that observed by Walter et al. (2012).

In these experiments the effect of backstress on the terminus was somewhat larger than before (Figure 6.19). In the advancing scenario, the two larger backstresses advanced further than the standard case, although during these advances sections of the modelled glacier reached flotation point so the subsequent results were excluded from analysis. In the steady scenario the highest backstress caused the terminus to advance, while the other experiments remained pinned. In the retreating scenario higher backstresses tended to delay the timing of the glacier retreat. When

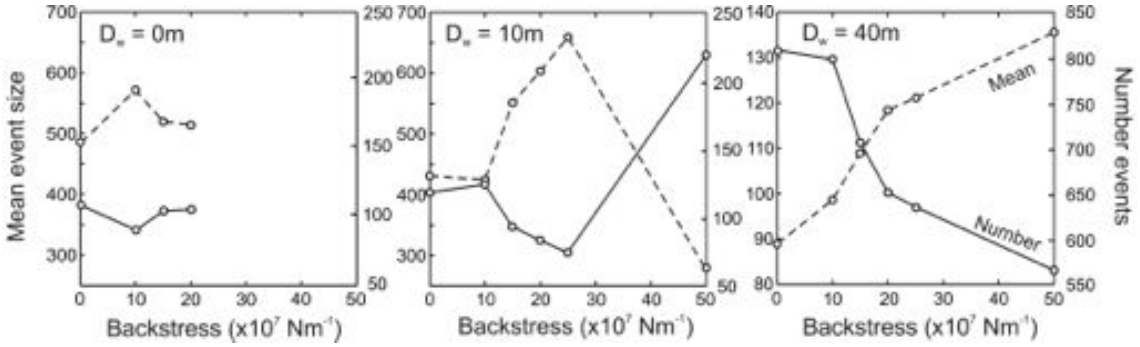

Figure 6.20: Response of Helheim Glacier model's calving behaviour to varying backstress at the calving face, in all cases applied over a vertical range of -118.5 to 15 m. Showing mean event size (dashed line) and total number of events over a 5 year run (solid line) in three applications with varying crevasse water depth.

the calving event sizes were compared for these experiments, in all but three cases a cross-comparison of experiments produced a statistically significant difference in calving event size. The three exceptions were: in the steady scenario, a comparison of the $F_f = 0$ and $10{\times}10^7$ Nm^{-1} experiments and in the advancing scenario, comparisons between $F_f = 15/20{\times}10^7$ Nm^{-1} and $F_f = 25/50{\times}10^7$ Nm^{-1}.

The change in number and mean size of calving events is shown in Figure 6.20. As with the previous experiments, the response of calving behaviour to changes in backstress depends on on the behaviour of the terminus. In the retreating experiments, an increase in backstress caused an decrease in the number of calving events and an increase in their average size. In the steady terminus scenario, excluding the $F_f = 50{\times}10^7$ Nm^{-1} case due to the change in terminus behaviour, increasing backstress caused a decrease in number of events and increase in their mean size. The results of the advancing experiments are unclear as the shorter run of the $F_f = 25$ and $50{\times}10^7$ Nm^{-1} experiments mean that their results are not directly comparable with the other experiments.

6.4 Discussion

6.4.1 Crevasse water depth

As with the results presented in Chapter 4, the depth of water in crevasses had a very large effect on the behaviour of the modelled glacier. At lower crevasse water depths the glacier model advanced, moderate values produced a steady terminus or a mild retreat and large values (>25 m) produced a significant retreat of over 10 km. The true levels of water in crevasses at Helheim Glacier are not well known; the nature of tidewater glaciers make them a difficult working environment to make direct observations. The water level in crevasses is also difficult to model as, given the highly fractured nature of a tidewater glacier terminus, it is likely that there will be significant leakage from crevasses. There is evidence that water levels can be high, even in regions around the glacier terminus, as water is observed to fill some areas of crevasses (see Figure 6.21). However, the depth of crevasses is also a poorly known variable and it is likely that water levels will be highly variable both spatially and temporally. The rough calculation presented in Section 6.2 indicates that a water-depth of 50 m is likely to be high, but is physically plausible. However, an improved method of predicting the depth of water in crevasses from meteorological data should be developed, or more observations in situ made, before we can know whether the numbers presented in this thesis are reasonable or not.

Previous modelling work by Vieli and Nick (2011) has also found a strong dependence of calving rate on the depth of water used in crevasses, in an application in Jakobshavn Glacier. It was hypothesized that this might be due to the low surface gradient around the terminus of Jakobshavn Glacier, which has a floating tongue. This was consistent with the work presented in Chapter 4, as the model of Columbia Glacier also developed a shallow profile around the terminus. The results from the Helheim Glacier model in this chapter indicate that even grounded glaciers without a particularly shallow terminus region may be sensitive to this variable. The dependence on crevasse water depth is unsurprising given the method by which calving

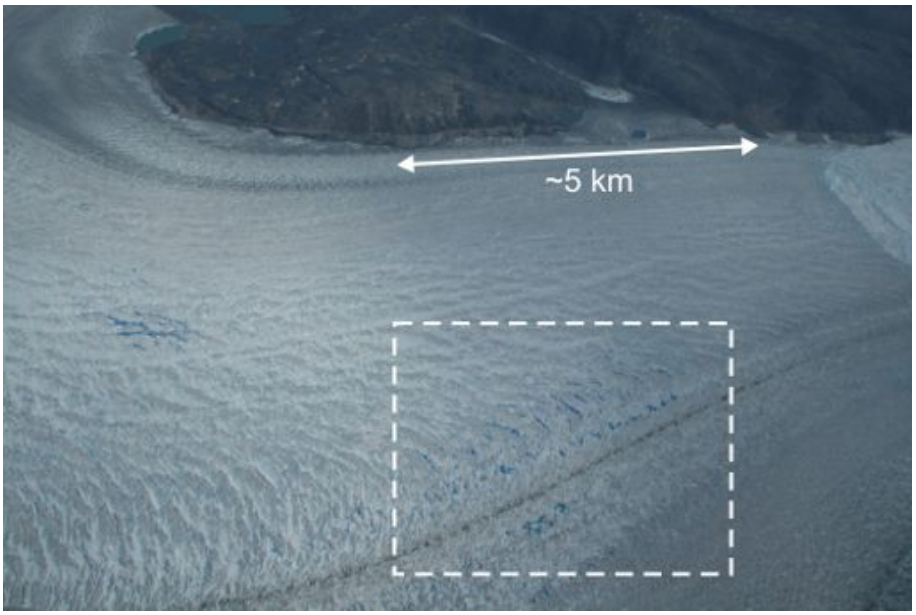

Figure 6.21: Terminus region of Helheim Glacier, July 2007, showing water-filled crevasses near the calving front (dashed box). Photo: T. James.

is implemented. The Nye formulation of crevasse depth strongly depends on the depth of water added to crevasses. The model is also particularly sensitive to this variable due to use of the Benn-type approach to calving, which is modelled to occur when crevasses penetrate to the waterline rather than to the bed. In most cases the height of the terminus above the waterline is a relatively small proportion of the full ice thickness. An alternative approach has been used by Nick et al. (2010), instigating calving only when crevasses penetrate the full ice thickness. The model of Helheim Glacier presented in this chapter remains grounded throughout the majority of model runs (the only exception being strongly advancing experiments) and the stresses near the base of the glacier are strongly compressive due to the high ice overburden pressure. If a full ice thickness calving approach were applied the model would not calve at all. In cases where a floating tongue develops, consideration of basal crevassing becomes very important and a full ice thickness calving criterion is more realistic. Future studies could use different calving criteria for the two different cases; requiring full thickness crevasses for calving in floating tongues, while grounded termini retain the waterline criterion.

The experiments also showed that the calving behaviour of the model changed significantly with varying crevasse water depth. For low water depth experiments calving event sizes followed a normal distribution around approximately 500 m. As water depth increased, the crevasse field near the terminus dipped below the water line causing more frequent, smaller calving events. As the water depth was increased further, the point at which the crevasse field crossed the waterline evolved further up-glacier and some significantly larger, but highly infrequent calving events began to occur on the scale of 1-2 km. In the model these calving events cause a dramatic retreat of the terminus, however in the real glacier we would expect the effect to be far less as such a large iceberg would be unable to tip over and would therefore need to be in a floating section of ice to be able to move away from the calving front. However, the model functions by identifying only the point furthest upstream from the calving front at which the crevasse field crosses the water line. If areas of the glacier further downstream are also deeply crevassed then the calving event may occur by the disintegration of the ice block into many smaller icebergs which would be able to move away from the ice front. There is little data available of observed calving event sizes to verify these results, however they do qualitatively agree with observations by Joughin et al. (2008b) that during the retreat of Helheim Glacier (2001-2005) retreat of the terminus occurred through large (0.5 to 1 km) episodes of calving several days or weeks apart.

6.4.2 Basal water pressure

The model was tested with a variety of basal water pressures around the standard case based on the bed depth, using three model scenarios to cover all types of glacier terminus behaviour; advancing ($D_w = 0$ m), steady ($D_w = 10$ m) and retreating ($D_w = 40$ m). The effect on terminus behaviour was strongest in the advancing scenario, where high basal water pressures suppressed the advance of the glacier. This is a result that would be expected from the hypothesis of van der Veen (2002) that changes in calving are caused by changes in the velocity of the glacier, with increases

in velocity causing an increase in calving. However, examining the calving behaviour statistics, in all cases with comparable terminus behaviour no significant change in mean calving size was found. In the steady and retreating terminus experiments there was very little effect of changing basal water pressure in either the modelled terminus evolution or the mean calving event size produced. A strong dependence on basal water pressure was not expected, as it has been found by previous modelling work not to have a significant effect on tidewater glaciers (Nick et al., 2009).

The experiments presented here use a highly simplified basal water pressure model, depending solely on the depth of the bed below sea level. This provides an effective minimum for basal water pressure, but true values are likely to be higher as additional water enters the system from basal melting and surface runoff. The Gagliardini type sliding law used leads to a non-linear relationship between basal drag, sliding velocity and basal pressure making it difficult to speculate how a more sophisticated basal hydrology model would affect the results. However, it is possible that if higher basal water pressures were used then small variations in the parameter would have a larger effect on velocities and hence on calving rates.

6.4.3 Subaqueous melt

The first oceanic forcing factor tested was the effect of subaqueous melt undercutting the calving face. A variety of melt rates were used, with a range of vertical profiles; uniform, wedge and parabolic shaped. Experiments with all three vertical melt profiles were found to affect the modelled terminus behaviour. The model was run with no water in crevasses, so in its natural state would advance. Higher subaqueous melt rates were found to prevent this advance, and in the highest melt experiment with a parabolic profile a mild retreat of the terminus occurred. The different experiments also showed significantly different calving behaviour. However, no clear pattern in the calving statistics emerged. In all three cases there seemed to be a peak in mean event size and minimum in number of events in the middle of the range of melt rates. Interestingly, the parabolic profile also began to produce some

anomalously high calving event sizes at higher melt rates, in the region of 1.5-2 km.

Although the modelled glacier behaviour was found to be sensitive to undercutting at the front of the glacier, it should be noted that the melt rates required to produce a change in terminus behaviour were much more than those predicted by previous studies. In general previous estimates of subaqueous melt have fallen in the range 255-1605 $\mathrm{m\,a^{-1}}$ for Greenland glaciers (see Section 6.2.3). In these experiments the minimum melt rate found to produce a significant change in terminus behaviour was 2000 $\mathrm{m\,a^{-1}}$. This relative insensitivity is in part due to the fact that all of the cases use zero melt at the waterline. Where ice is melted underwater, the support that had been provided by the ice is replaced by external water pressure and the undercutting does not have a very large effect on the stress profile around the front. If ice were melted above the waterline the overhanging ice block would be unsupported and this would cause significant additional fracturing. This effect has been observed at other glaciers (*e.g.* Vieli et al. (2001)) but evidence from models of melt indicates that melt near the waterline in Greenland outlet glaciers is minimal (O'Leary, 2011; Xu et al., 2012) and this is consistent with observations of very cold polar water in the upper parts of the Sermilik Fjord water column (Straneo et al., 2011). The modelled melt profile is therefore assumed to be realistic, although no direct observations are possible.

The relative insensitivity of the model to undercutting of the calving face is surprising in the context of previous work by O'Leary (2011), which finds that undercutting of the calving face has the potential to significantly affect calving, as the displacement of the stress field around the terminus due to undercutting is up to four times the length of the undercut region. This leads to the conclusion that undercutting had the potential to increase calving rate by up to 4 times the subaqueous melt rate. The O'Leary model found a linear relationship between the length of the undercut cavity and the displacement of the stress field around the waterline, however in all cases the terminus was kept in a fixed position. In order to investigate this, the 5000 $\mathrm{m\,a^{-1}}$ undercut run was examined at each timestep, measuring the length of the undercut cavity and the displacement of the stress field at the waterline ap-

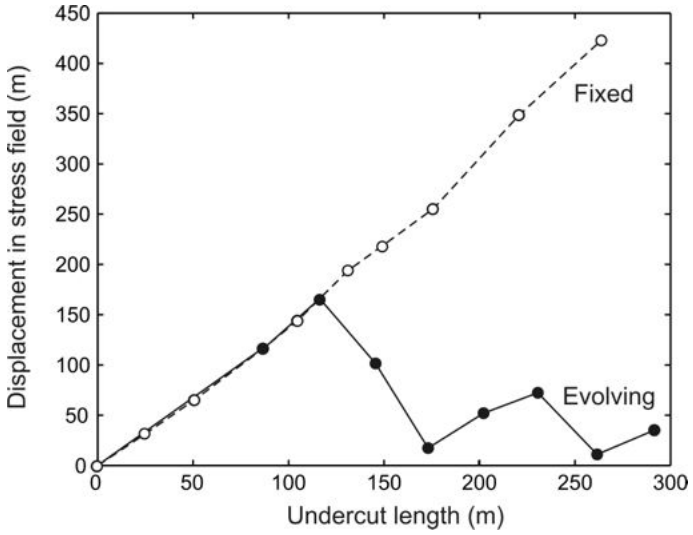

Figure 6.22: Horizontal displacement in stress field associated with varying undercut length. Dashed line shows results with a fixed terminus, solid line shows results allowing the terminus to evolve.

proximately one ice thickness upstream of the calving front. This experiment was then compared to a parallel experiment in which the terminus was kept fixed and the undercutting rate was varied in order to change the cavity length. Results are shown in Figure 6.22. The model showed the same behaviour as the O'Leary model when the terminus was fixed, with the stress displacement increasing linearly with the undercut length. However, when the terminus was also allowed to evolve the stress displacement showed no clear relationship to the undercut length, however for larger undercutting lengths the stress displacement was significantly less than for the fixed terminus example. It seems that the ice flow in the model has a counteracting effect to the undercutting, reducing its effect on the stress around the terminus.

6.4.4 Ice mélange

The first experiments were performed using backstress in the range of 0.0 to 5.0×10^7 Nm^{-1} over a variety of different vertical extents. Although in many cases these experiments produced a statistically significant change in calving event size, they made very little difference to the terminus behaviour of the glacier, with one exception in the experi-

ments applying backstress over the full face in a retreating scenario where increased backstress was found to delay the retreat of the model. It was decided to extend the range of backstress experiments to include the effects of force up to 50×10^7 Nm^{-1}. These additional experiments were carried out only on a vertical range of -118.5 to 15 m, thought to be the most physically realistic (see Section 6.2.3). In these experiments the backstress had a greater effect on the terminus evolution, with the highest values causing the advancing case to advance further than previously, and in the steady case causing the model to advance. Changes in backstress also had a significant effect on the modelled calving behaviour, but the response also depended on the behaviour of the glacier terminus. In the advancing and steady cases an increase in backstress generally caused the model to produce more frequent, smaller icebergs, while for the retreating experiments an increase in backstress caused more infrequent larger events.

The range of backstresses used in this chapter is greater than that used in any previous model, or predicted by previous observations. Previous values all lay in the range 20 to 60 kPa, which adjusted for the height of the calving face gives a force of 3.6×10^7 Nm^{-1}. In the extended experiments presented in the chapter the highest force used was 50×10^7 Nm^{-1}, an order of magnitude larger. Such a high force was used for two reasons; firstly, the intention was to investigate the value required to produce a change in terminus behaviour, which lower forces did not do. Secondly, the previous measurements of backstress are prone to high levels of uncertainty and the high forces used in the model experiments were found to produce a similar percentage change in terminus velocity to that observed by Walter et al. (2012), making it reasonable to extend the range of forces used to this level. Despite this, it seems unlikely that such a high backstress is physically realistic. The mixed nature of the ice mélange is likely to be much weaker than glacier ice, and limited by the shear strength of the weakest material: the sea ice binding the mélange together. The shear strength of sea ice has been measured to be around 550 ± 120 kPa (Frederking and Timco, 1984), suggesting that a mélange bound by sea ice would be unable to support stresses as high as those used in experiments here.

It appears from the results in this chapter that the model is not sensitive to changes in backstress on a realistic scale, this is in contrast to previous studies which have observed a correlation between terminus behaviour and sea ice cover (*e.g.* Sohn et al. (1998)) and modelling studies which have found a significant effect of backstress on calving (Nick et al., 2009; Vieli and Nick, 2011). Most of the evidence linking sea ice and ice mélange to changes in calving has been collected at glaciers with significant floating sections. In this case ice fracturing caused by tidal flexing is significant, and ocean waves may be damped by the presence of fast-ice, decreasing fracturing. In grounded glaciers such as those included in this study a significant proportion of the driving stress is supported by basal drag, and changes in lateral drag processes will be less significant.

6.5 Chapter Summary

The results presented in this chapter confirm the model's sensitivity to water in crevasses. This variable has the greatest effect on the modelled terminus behaviour. The other variable arising from atmospheric forcing is the basal water pressure, which affects the velocity of the glacier. This variable can have an effect on the modelled glacier terminus, but it is less significant than the effect of changes in crevasse water depth and it does not generally have a significant effect on the mean calving event size.

Of the two oceanic forcing factors, undercutting by subaqueous melt has the greatest effect. Increases in subaqueous melt rate have the ability to prevent the advance of the modelled glacier terminus, and also have a significant effect on the modelled calving behaviour. However, the values used to produce these changes are outside the previously predicted range of melt rates for Helheim Glacier. Applying backstress of physically realistic magnitude to the calving front of the model has very little effect on the terminus progression, although it can change calving behaviour. If the magnitude of the backstress is increased significantly, it can affect the modelled

terminus evolution. However, these values are unlikely to be realistic. It seems likely that backstress does not have a significant effect on grounded glaciers, as most observations linking it to ice dynamics were made at glaciers with significant floating sections.

These results show the sensitivity of the model to various forcing factors when applied continuously, however in the real world these variables would all vary seasonally which may produce different effects.

Chapter 7

Helheim Glacier: Seasonal forcing

7.1 Introduction

The results of the previous chapter give an indication of the model's sensitivity to climatic variables. However, each of these was applied constantly over a long period. While this gives some indication of model sensitivity, it does not provide a realistic model of glacier behaviour, as in reality each variable will vary both seasonally and inter-annually. The response of the model to seasonally varying input may be somewhat different to its response to constant forcing. In this chapter each of the environmental forcing experiments is adapted to include seasonal changes in input variables, and model sensitivity is investigated once again using this more realistic forcing. The experiments use the Helheim Glacier model once again, which is tested with four environmental forcing factors; water in crevasses, basal water pressure, undercutting by subaqueous melt and back stress from ice mélange.

7.2 Model Experiment Set-up

Experiments are carried out using the model of Helheim Glacier, as described in Section 5.4. Since the model is forced with seasonally varying inputs, the applied

mass balance described in Section 5.4 is altered to provide a seasonal mass balance. This is unlikely to affect the model's behaviour, as the model is not sensitive to small changes in mass balance (see Section 5.5.8); however, it should be adjusted for completeness. Using data from Andersen et al. (2010), surface lowering of around 2 m was found to occur near the front over the summer period, implying a summer melt rate of 6 $\mathrm{m\,a^{-1}}$ (assuming a 4 month summer season). The model geometry lies entirely in the ablation zone, therefore any snow accumulated over the winter months will be melted during the summer, rather than consolidating. The effects of snow and firn are neglected in the model, as they have very different physical properties but only contribute an extremely small fraction of the total ice thickness. Therefore winter accumulation is neglected in the model.

Two sets of experiments are performed for each of the input variables. First, each variable is altered individually with varying seasonal forcing. Then three sets of experiments are repeated using a crevasse water depth of 30 m in the summer season, which is selected as it gives a terminus which, although varying seasonally, is stable inter-annually. This provides a test of the other variables in a wide range of glacier behaviour to thoroughly test the model's sensitivity. The range of experiments performed is laid out in Table 7.1.

As discussed in Section 5.5.2, the timestep used depends on the crevasse water depth used in each experiment. In winter, with 0 m crevasse water depth, a timestep of 0.003 a is used. For summer periods, the timestep depends on the crevasse water depth being used as laid out in Table 5.3, with higher crevasse water depths requiring a shorter timestep. As in previous chapters, the model output is analysed by examining the change in terminus position and the average size and frequency of calving events. The average sizes are compared by the Wilcoxon-Mann-Whitney test. In experiments with significantly different terminus behaviour statistical tests were not run as it is then impossible to separate the effects of the input variable from changing geometry.

Table 7.1: Seasonal experiments performed. dP is the change in hydrostatic head applied to the basal water pressure, M_f is the maximum melt rate applied at the calving face and F_f is the force applied to the calving front over a vertical range of -118.5 to 15 m. In the second set of backstress experiments the seasons in crevasse water depth and backstress do not match, meaning that there is also an autumn season where both the crevasse water depth and the backstress are set at zero.

Experiment		Summer values		Winter values	
Crevasse water depth		$D_w = 0$, 10, 20 , 30 , 40 , 50 m		$D_w = 0$ m	
Basal water pressure	a	$dP = 50$ m	$D_w = 0$ m	$dP = 0$ m	$D_w = 0$ m
Basal water pressure	b	$dP = 50$ m	$D_w = 30$ m	$dP = 0$ m	$D_w = 0$ m
Subaqueous melt	a	$M_f = 0$,1,2,3,5000 m a^{-1}	$D_w = 0$ m	$M_f = 500$ m a^{-1}	$D_w = 0$ m
Subaqueous melt	b	$M_f = 0$,1,2,3,5000 m a^{-1}	$D_w = 30$ m	$M_f = 500$ m a^{-1}	$D_w = 0$ m
Backstress	a	$F_f = 0$ Nm^{-1}	$D_w = 0$ m	$F_f = 0$, 2, 5, 25, 50 Nm^{-1}	$D_w = 0$ m
Backstress	b	$F_f = 0$ Nm^{-1}	$D_w = 30$ m	$F_f = 0$, 2, 5, 25, 50 Nm^{-1}	$D_w = 0$ m

7.2.1 Crevasse water depth

The melt season at Helheim Glacier was analysed using an air temperature record measured at nearby Mittivakkat Glacier from 1998 to 2002 (published by NSIDC as Hasholt and Christiansen (2003)). The melt season is identified from a 5 day running average, which was found typically to exceed the freezing point from the middle of May to mid or late September. This agrees relatively well with data from Andersen et al. (2010) suggesting a melt season from early May to late September for Helheim Glacier.

For the crevasse water depth experiments, water-depth is set at 0 m over an 8 month winter period (Oct-May) and varied between 10 and 50 m over the summer period, with the model run lasting 5 years.

7.2.2 Basal water pressure

Previous observations have indicated that outlet glaciers accelerate by up to 15% in the summer months (Jun-Sep) (Joughin et al., 2008a). A change in the hydrostatic head providing basal water pressure of 50 m produces roughly this 15% change, and therefore the basal sliding parameters were adjusted so that the model velocity produced a best fit to observed summer values when this 50 m hydrostatic head was applied. In the seasonal basal pressure experiments, during the winter months (Oct-May) the basal pressure returns to the standard case, and the glacier velocity slows down, and in summer the basal pressure is increased by 50 m. The length of the summer season coincides with the observed annual surface melt period, as the source of additional water at the bed is likely to be from surface meltwater penetrating to the bed.

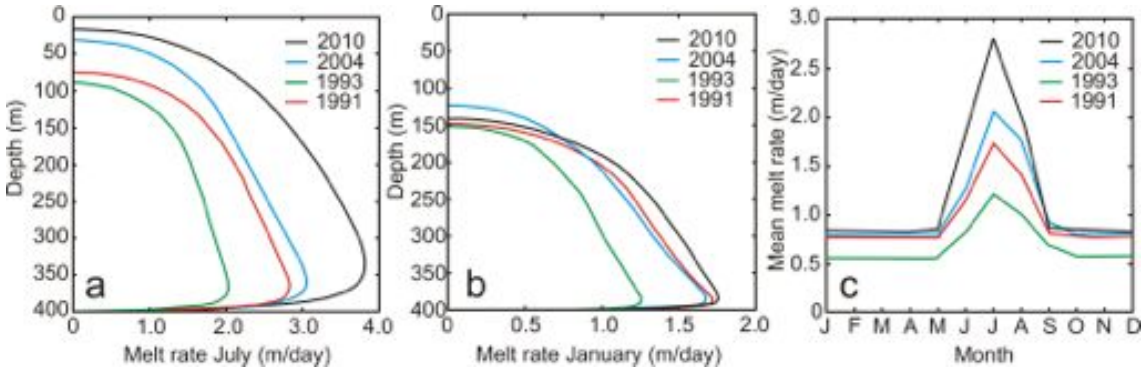

Figure 7.1: Modelled subaqueous melt rates for Kangerdlugssuaq Glacier, East Greenland taken from O'Leary (2011). Panels (a) and (b) show vertical melt profile in July and January. Panel (c) shows mean melt rate over the front throughout four different years.

7.2.3 Subaqueous melt

The only study providing information on likely seasonal variations in subaqueous melt rates is that by O'Leary (2011). As discussed in Section 6.2.3, this work uses observations of water temperatures and surface melt at Kangerdlugssuaq Glacier in conjunction with a model of subglacial discharge and its interaction with the surrounding ocean to predict subaqueous melt rates at the calving front. Modelled frontal melt rates are shown in Figure 7.1, with maximum summer melt rates ranging from 2 to 4 $\mathrm{m\,day^{-1}}$ w.e. (800 to 1600 $\mathrm{m\,a^{-1}}$ ice) and maximum winter melt rates of 1.2 to 1.7 $\mathrm{m\,day^{-1}}$ w.e. (480 to 680 $\mathrm{m\,a^{-1}}$ ice) acting over a reduced vertical range. The summer season lasts from around May to September, coinciding with the summer season in surface ablation as the increased availability of meltwater in the proglacial plume is the factor driving increased summer melt rates. The waters in Kangerdlugssuaq Fjord are somewhat cooler than those in Sermilik Fjord (see Section 6.2.3), therefore melt rates at Helheim Glacier are likely to be higher by a factor of around 1.5.

For the undercutting experiments, in all cases a wedge shaped profile of subaqueous melt is used, as it seems likely to be the most realistic. Although model results from O'Leary (2011) and Xu et al. (2012) show very low melt rates at the base of the glacier, any foot of ice developing here will be subject to very strong buoyancy

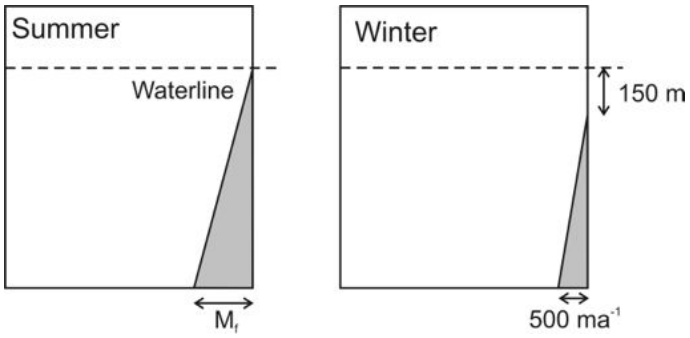

Figure 7.2: Vertical profile of melt rates used for seasonal undercutting experiments.

forces and is likely to quickly break away leaving a roughly wedge shaped cavity. In these experiments the melt rate is identified by the maximum melt rate rather than the average melt rate. Two different melt profiles are used in summer and winter, as shown in Figure 7.2. In summer (Jun-Sep) melt is applied right up to the waterline, with the maximum melt rate at the base varying between 1000 and 5000 m a^{-1}. In winter the top of the melt profile is lowered to 150 m below the waterline, and the maximum melt rate at the base of the calving face is set at 500 m a^{-1}. The length of the summer period is chosen to match the period of surface melt, as additional meltwater in the proglacial plume is the likely driver of increased subaqueous melt during the summer.

7.2.4 Ice mélange

In addition to data on the depth and strength of the ice mélange, data are also required on what period of the year it is frozen solid in order to apply seasonal forcing. Two studies of Greenland outlet glaciers have published data on this point; Howat et al. (2010) state that the ice mélange in West Greenland forms in January and February, achieves maximum coverage in late April, and then disintegrates rapidly in May or early June. Similarly Christofferson et al. (2012) find that Kangerdlugssuaq fjord is ice covered from January to June. These observations are consistent with observations from satellite images of Sermilik Fjord, where ice is present in the fjord throughout the entire year, but moves as a solid block from approximately January

to May (personal communication, Y. Drocourt, Mar 2012).

For the seasonal backstress experiments, the extended range of backstress from 0 to 50×10^7 Nm^{-1} presented in the previous chapter is applied over a vertical range of -118.5 to 15 m. This backstress is applied over a selected winter period of Jan-May with backstress reduced to zero during the corresponding summer season (Jun-Dec). It should be noted that this is a different seasonal cycle to the other experiments presented in this chapter.

7.3 Results: Seasonal Experiments

7.3.1 Crevasse water depth

As would be expected given the sensitivity results presented previously, the varying summer crevasse water depths produced a significant difference in terminus behaviour (Figure 7.3a). These experiments were more prone than any others to floating ice; for $D_w = 10$ m flotation occurred after 4 years, for 20 m after 3 years, for 30 m after 2.7 years, for 40 m after 2.5 a and for 50 m after 1.5 a. Although the model generally became grounded again after each of these points, subsequent results should not be considered reliable and were excluded from the statistical tests performed.

The real glacier advanced much more quickly than in any of the experiments presented here, then oscillated over a number of years around 180 km along flowline (Figure 7.3b). The variation in observed terminus position is around 3 km in magnitude, which is somewhat more than the $D_w = 20$ m experiment but comparable to the $D_w = 30$ m experiment, although this model initially retreats so the oscillations take place around a different mean terminus position. In general it may be said that none of the model experiments provided a good fit to the observed terminus behaviour.

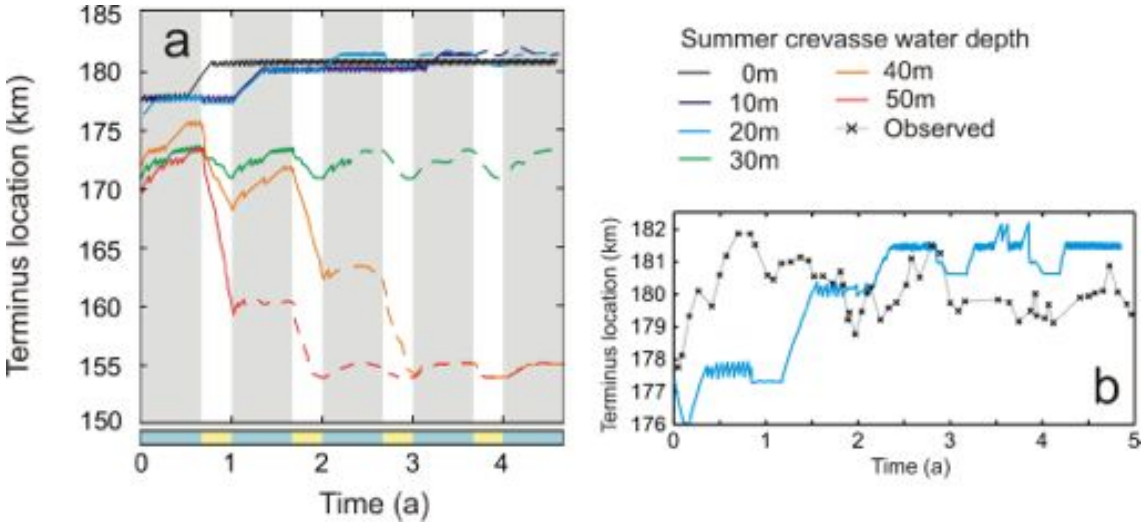

Figure 7.3: (a) Modelled terminus evolution in case of seasonally applied crevasse water depths of different magnitudes. Blue/grey shading indicates winter periods and yellow/white shading is used for summer. Sections of dashed line indicate unreliable results after the model reached flotation point. (b) Comparison of 20 m experiment to observed terminus position.

Changes in calving behaviour were examined by statistical comparisons of calving event size distribution, using summer season data for the different experiments. The difference between event size in all experiments was significant when cross-tabulated, apart from in one case when the 20 m and 50 m experiments were compared. Histograms of summer calving events are shown in Figure 7.4, using only data from before the model reaches the flotation point. The histograms of calving event size are qualitatively similar to those presented in the previous chapter. With no water in crevasses the iceberg sizes followed a normal distribution centered around 500 m. As crevasse water depth was increased to 20 m, smaller calving events (<100 m) began to dominate the distribution, with the frequency of events increasing dramatically. As the crevasse water depth increased further, the frequency of events began to drop again, and although the majority of calving events were still less than 200 m in size, the number of larger calving events began to increase again with the appearance of extremely large events (>1000 m).

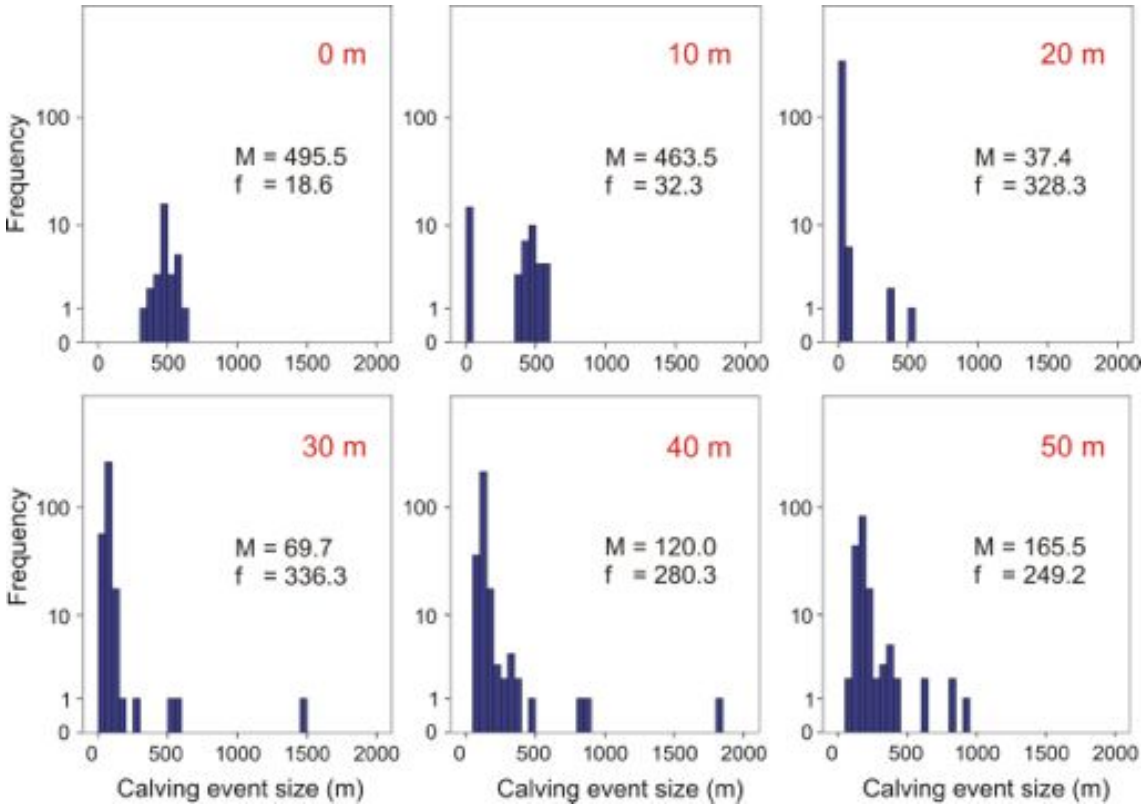

Figure 7.4: Modelled calving behaviour in case of seasonally applied crevasse water depths of different magnitudes, showing histograms of summer calving event size against frequency measured on a log scale. M is the median event size, f is the frequency of events measured per annum in the summer periods of each model run.

7.3.2 Basal water pressure

A change in hydrostatic head of 50 m was applied seasonally to basal water pressure in the $D_w = 0$ m model. The change in basal water pressure produced an increased velocity in the summer months of between 10 and 15 % compared to the case with no change in hydrostatic head (Figure 7.5b). The modelled terminus evolution was then compared to the case with no change in basal water pressure (using sliding parameters from the standard experiments, rather than the winter values in these experiments). When the basal water pressure was varied seasonally, reducing the velocity of the model over winter, the modelled terminus advanced further than in the case of fixed basal water pressure (Figure 7.5c), although after 2.1 a the model developed some areas of floating ice so subsequent results were not reliable. The problem of floating ice midway through the run meant no statistical analysis of the calving events produced was performed, since the number of calving events was too few for a robust analysis and the comparison would be affected by the changing geometry during the model's advance.

A second experiment was performed, using the same basal water pressure forcing, but with a crevasse water depth of 30 m during the summer season. In this case the basal water pressure had an even larger effect on the behaviour of the model terminus (Figure 7.6). Using the standard basal water pressure throughout the entire run, the model made a significant retreat of around 5 km and then experienced large seasonal variations in terminus position of around 2 km. When the basal water pressure was varied seasonally, the slower winter velocities caused an advance of the terminus, with much smaller subsequent variations in terminus position. It is likely that the reduced size of seasonal variations in terminus position in the advancing model are caused by the basal topography. The retreating experiment varies around 171-173 km along flowline, which is a region of shallow bed slope, while the advanced position stops at approximately 180 km along flowline, where there is a steep drop in the bed which prohibits further advance (Figure 6.6). The difference in terminus behaviour means that the calving behaviour in the two experiments is

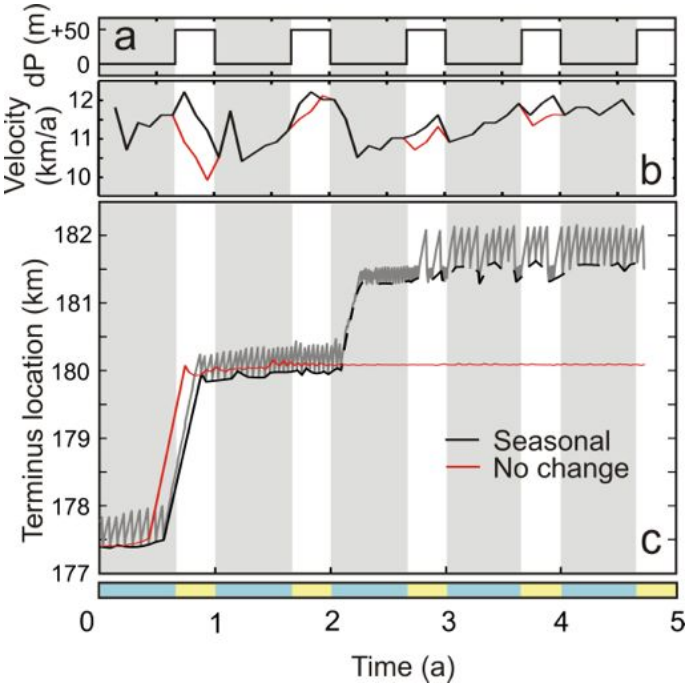

Figure 7.5: (a) Seasonal basal water pressure, measured by change in hydrostatic head. (b) Velocity at glacier front, with and without seasonal change in basal pressure. (c) Modelled terminus evolution, with and without seasonal change in basal pressure. The dashed section in the seasonal experiment indicates results after the model reached flotation point. Blue/grey shading indicates winter periods and yellow/white shading is used for summer.

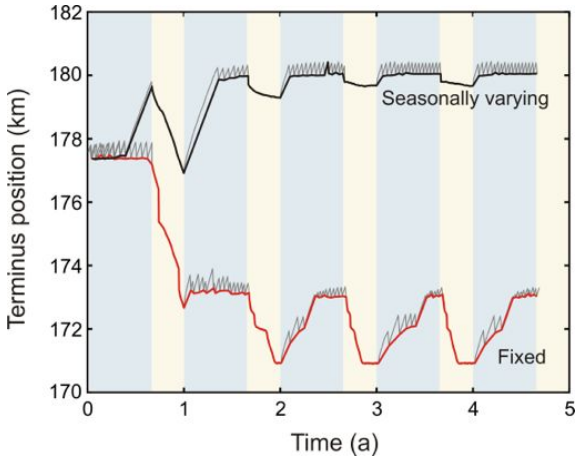

Figure 7.6: Modelled terminus evolution in cases of seasonally applied basal water pressure and fixed basal water pressure, using a summer crevasse water depth of 30 m. Blue/grey shading indicates winter periods and yellow/white shading is used for summer.

not comparable and in this case the difference between summer and winter calving behaviour is not examined because it would also be influenced by the changing crevasse water depth.

7.3.3 Subaqueous melt

Experiments were performed using a seasonally varying undercutting rate, with maximum summer melt rates of 1000 – 5000 m a^{-1}. Previously published estimates of subaqueous melt lead to an expected range of 1090 – 2560 m a^{-1} in maximum subaqueous melt rate for Helheim Glacier (see Section 7.2). The modelled terminus evolution showed only a small response to the varying undercutting rate (Figure 7.7). The higher undercutting rates showed a delay in the advance of the terminus, but in all cases the terminus advanced to 180 km along flowline within the first two years of the model run.

No statistically significant difference in calving event size was found between the summer and winter periods in any of these undercutting experiments (data from second year was excluded to remove the effects of geometry change during the glacier advance). Comparing calving event size distribution for the summer period of each

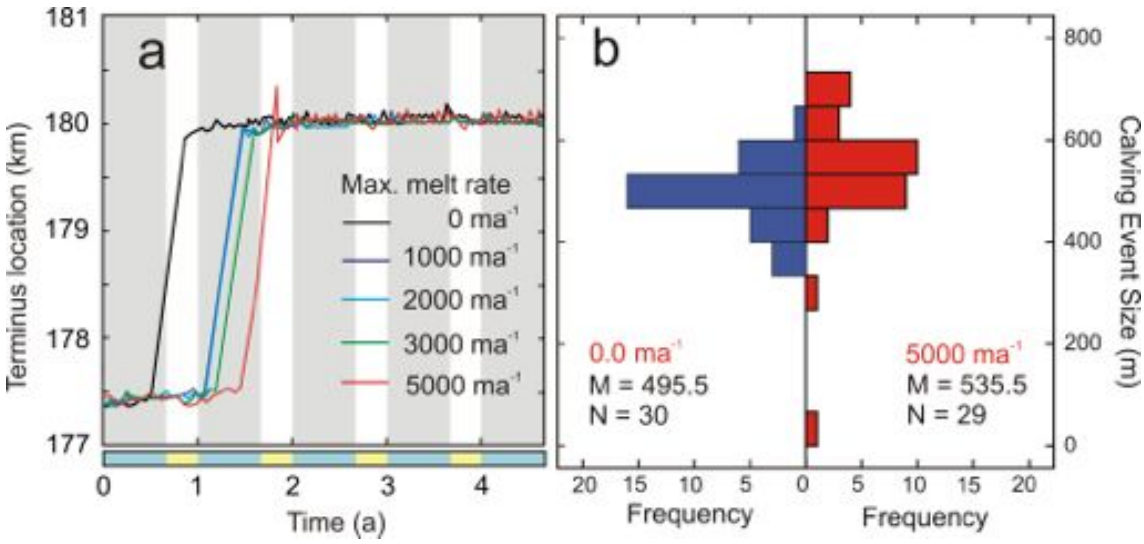

Figure 7.7: (a) Modelled terminus evolution in case of seasonally applied melt at the calving face of different magnitudes, with no water in crevasses. Blue/grey shading indicates winter periods and yellow/white shading is used for summer. (b) Histogram comparing calving event sizes between 0.0 and 5000 m a^{-1} undercutting experiments.

experiment, the only statistically significant difference was between the lower undercutting experiments and that with undercutting of 5000 m a^{-1}: two example histograms are shown in Figure 7.7. The number of calving events over the summer period was similar in all cases, but the experiment with undercutting of 5000 m a^{-1} had a higher median event size than the others.

A second experiment was performed using the same range of seasonal undercutting rates but with a summer crevasse water depth of 30 m. The modelled terminus evolution was nearly identical in each of these experiments (Figure 7.8). As may be expected given the very similar terminus behaviour, there was also no statistically significant difference in the calving event size distribution between any of these undercutting experiments.

Since the undercutting rates used in the seasonal experiments had relatively little effect on the terminus evolution and calving behaviour of the model, a further set of experiments was designed to determine the undercutting rate required to trigger a glacier retreat. In each case the model geometry at the end of the first winter

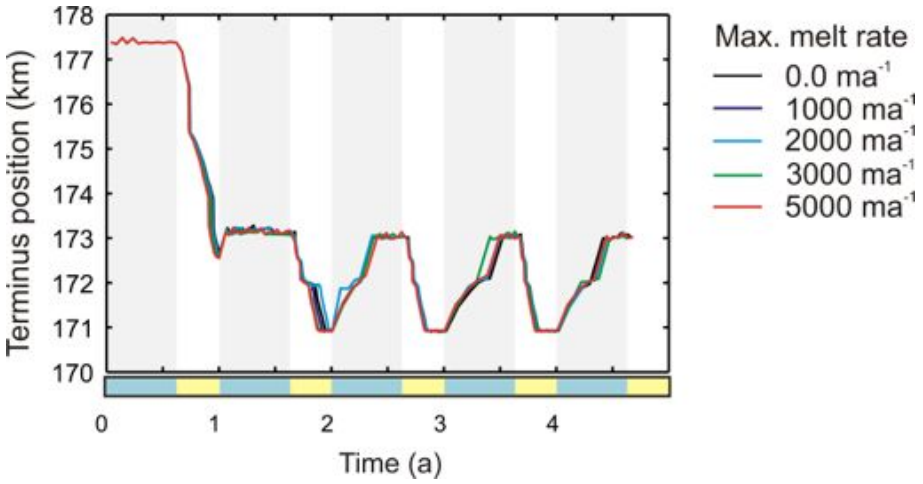

Figure 7.8: Modelled terminus evolution in case of seasonally applied basal undercutting at the calving face, using a summer crevasse water depth of 30 m. Blue/grey shading indicates winter periods and yellow/white shading is used for summer.

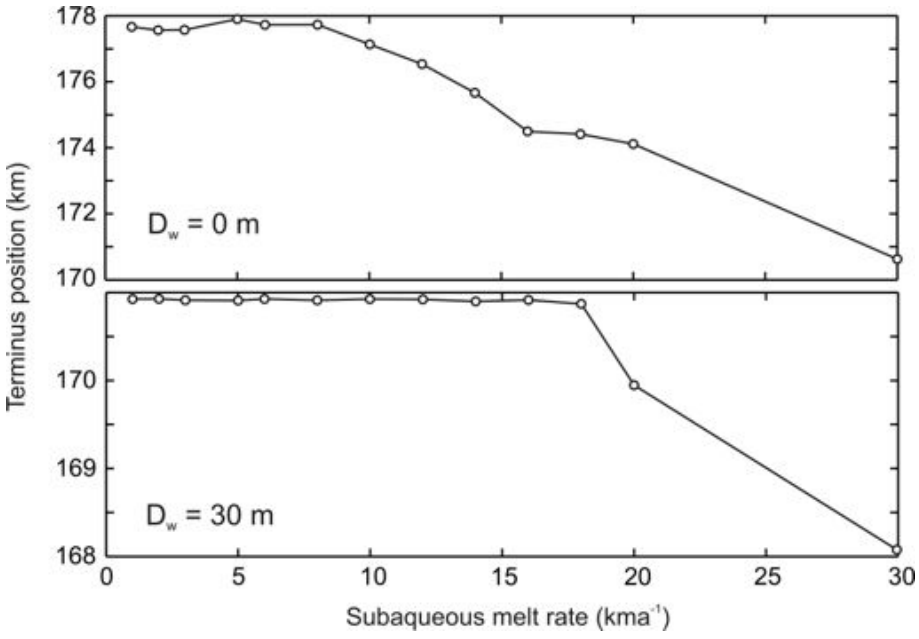

Figure 7.9: Terminus position of Helheim Glacier model at the end of first summer period in two experiments with different crevasse water depth during the summer, forced with varying rates of undercutting by subaqueous melt.

season was used as a starting point, and the model was run for a single summer period. Two sets of experiments were performed, using crevasse water depths of 0 and 30 m. The terminus positions of the model at the end of the summer period are shown in Figure 7.9. In the case with no water in crevasses, there was a gradual change in terminus behaviour with retreat beginning at a maximum melt rate of approximately 10000 m a^{-1}. In the case using a crevasse water depth of 30 m, there was a sharp change in terminus behaviour between 18000 and 20000 m a^{-1} as the undercutting became large enough to trigger retreat.

7.3.4 Ice mélange

Experiments were performed using a backstress of between 2.0 and 50×10^7 Nm^{-1}, applied over a 5 month winter season. The only experiment to produce a change in modelled terminus evolution compared to the case with no backstress was that with F_f = 50×10^7 Nm^{-1}, which advanced further than the other experiments (Figure 7.10a), although it was found to develop some areas of floating ice after 3.0 a so results after this point were not reliable. Comparing the difference in calving event size between the different backstress experiments (using only winter data and excluding the 50×10^7 Nm^{-1} experiment because of its different terminus behaviour), the only experiment to produce a statistically significant difference in calving event size distribution compared to the case with no backstress was the F_f = 25×10^7 Nm^{-1} experiment, with example histograms shown in Figure 7.10 for comparison. Although this experiment did not produce a change in the number of calving events over the winter periods, the median calving event size was 88.1 m larger than for the experiment with no backstress applied.

The seasonal backstress experiments were repeated using a crevasse water depth of 30 m during the summer period. Given the disparity between the timing of summer ablation and the formation of a consolidated ice mélange in the fjord, there were effectively three seasons in these experiments: summer when there is water in crevasses, winter with no water in crevasses and backstress acting on the front,

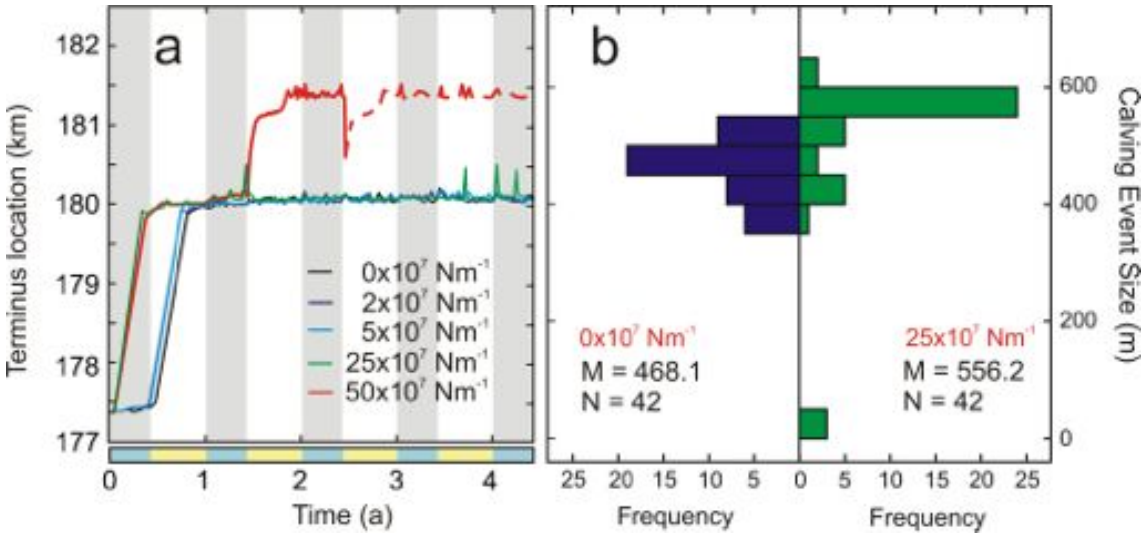

Figure 7.10: (a) Modelled terminus evolution in case of seasonally applied backstress at the calving face of different magnitudes. Dashed section indicates unreliable model results after some sections reached flotation point. Blue/grey shading indicates winter periods and yellow/white shading is used for summer. (b) Histogram showing calving event size distribution for $M_f = 0.0$ and $25{\times}10^7$ Nm^{-1} experiments.

and autumn when no surface water is available but neither is there backstress from ice mélange. These experiments also showed little change in the modelled terminus evolution until the backstress was increased to $50{\times}10^7$ Nm^{-1} which is sufficient to prevent the model from retreating (Figure 7.11a). In the experiment with $F_f = 5.0{\times}10^7$ Nm^{-1} the model reached flotation point at 3.4 a; therefore, subsequent results were neglected for this experiment. Comparing the winter calving event size between these experiments, in all cases the difference was not statistically significant, although the $50{\times}10^7$ Nm^{-1} was excluded because of the difference in terminus evolution.

An alternative conception of how backstress can affect calving was presented by Amundson et al. (2010), suggesting that a relatively small force acting on the calving front may prevent any block of ice that has separated from the main glacier body from tipping and moving away from the calving front. This would hold calved ice in contact with the front and thus provide a significant effect on dynamics during the winter months. To test whether this type of mechanism would have a greater effect

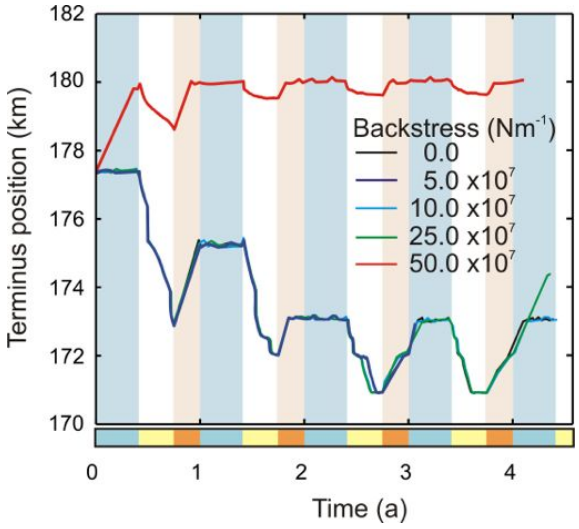

Figure 7.11: Modelled terminus evolution in case of seasonally applied backstress of varying magnitude, using a summer crevasse water depth of 30 m. Blue shading indicates winter periods where backstress is applied, yellow/white shading is used for summer when water is applied in crevasses, orange shading indicates an autumn period when there is neither water in crevasses nor backstress from ice mélange.

on the calving front an additional model run was performed with calving switched off over winter. This model run quickly advanced beyond the limit of the bed data available, and in advancing so far and so fast the surface also evolved significantly below the flotation point meaning that results were beyond the model's limit of accurate representation. However, by switching off calving over winter there was an obvious and significant effect on terminus behaviour - the glacier advanced much further and more quickly than previously. This indicates that although backstress did not have a significant effect on ice dynamics and stress profile when applied to the calving face, if it were able to prevent calving via another mechanism it would have the potential to significantly affect calving dynamics.

7.3.5 Checking the effect of ice temperature

In Chapter 5 it was shown that the modelled terminus behaviour was affected strongly by the chosen ice temperature profile. The results presented in the pre-

vious chapter and this one indicate a lack of sensitivity to oceanic forcing which was unexpected given previous modelling results (*e.g.* (Vieli and Nick, 2011)). In order to check that the results do not depend on the ice temperature profile chosen, another suite of experiments was performed, repeating some tests of oceanic forcing using different ice temperatures. Out of the variety of ice temperature profiles tested in Section 5.5.4 two were chosen which were within a physically realistic range of ice temperature and still produced noticeably different results from the standard temperature profile. The two selected were those shifted by ±5°C from the standard profile.

Subaqueous melt

Using the results from Chapter 6 as a guide, a range of subaqueous melt rates was selected to cover a full range of glacier behaviour. The selected melt rates (M_f = 0, 1, 2, 5 km a^{-1}) are an average over the entire calving face, equivalent to maximum melt rates of 0, 2, 4, and 10 km a^{-1} on the wedge-shaped vertical profile. The undercutting was applied constantly in a variety of vertical profiles over a model run of 5 years, using the three different ice temperature profiles. The modelled terminus evolution in each case is shown in Figure 7.12. In the standard case, the terminus shows a small change in behaviour at M_f = 1 km a^{-1}, a more significant change at M_f = 2 km a^{-1} and a distinct change at M_f = 5 km a^{-1}. In the case where ice temperature is increased by 5°C, the response to undercutting is very similar, though in the case of a parabolic undercutting profile there is a more significant retreat at M_f = 5 km a^{-1}. In the case with ice temperature lowered by 5°C the terminus is steady in most cases, showing only a later advance in the experiments with no undercutting and once again a significant retreat in the case with a parabolic profile and M_f = 5 km a^{-1}. Examining the terminus behaviour alone, there is no strong evidence that the changes in ice temperature change the model's sensitivity.

Differences in calving behaviour between experiments were also examined in cases with similar terminus behaviour. Table 7.2 shows the significance and magnitude of

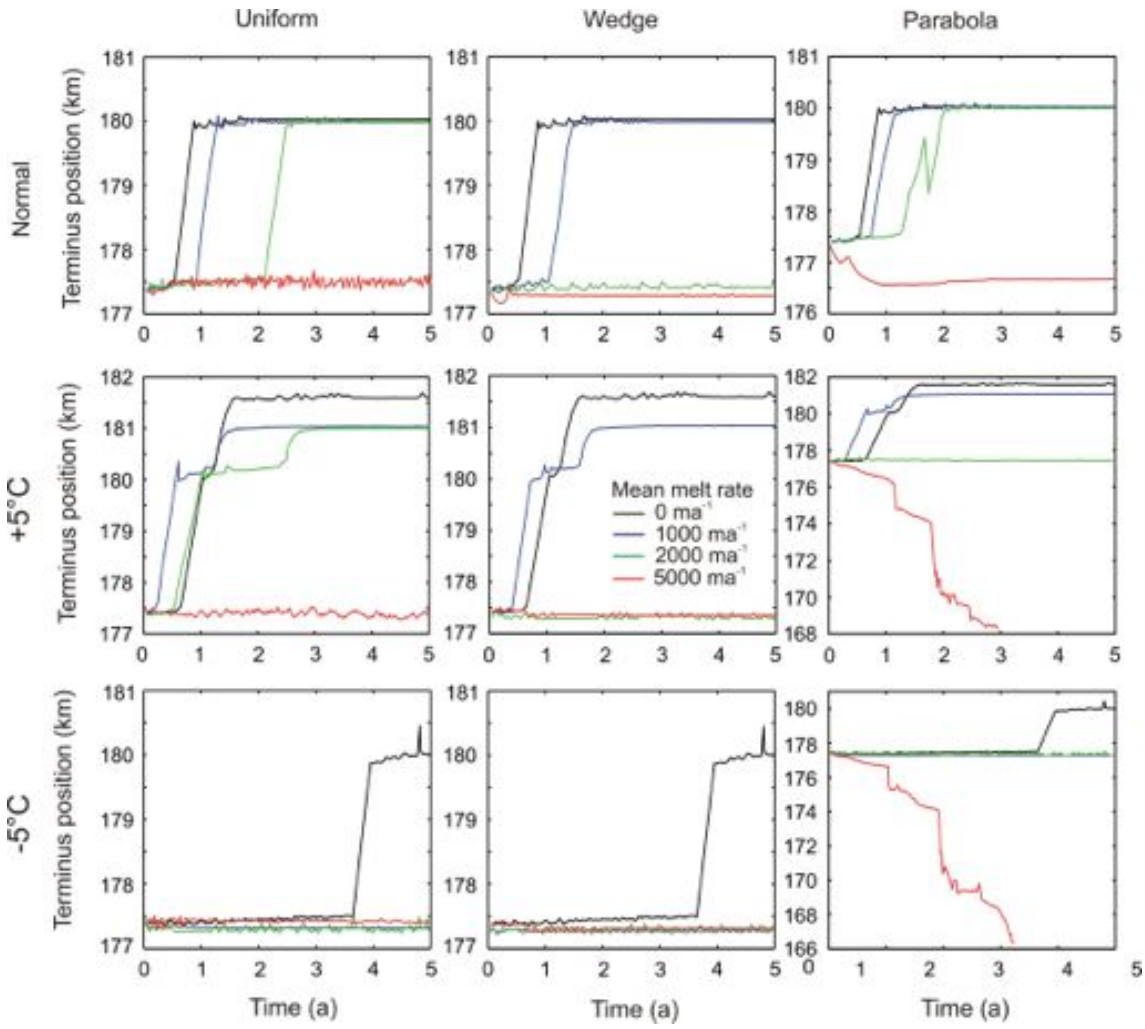

Figure 7.12: Modelled terminus evolution using three different ice temperature profiles and a range of mean undercutting rates with three different vertical undercutting profiles.

these differences. In many cases the difference in calving event size was larger in the experiments with an increased ice temperature. For example, comparing the M_f = 0 and 1.0 km a^{-1} experiments, with a normal temperature profile the differences in event size were 68.4, 65.2 and 4.3 m while for an ice temperature change of +5°C the same experiments led to differences of 476.7, 478.8 and 448.4 m. There was no clear difference between results from the standard temperature profile and experiments with decreased ice temperature.

Table 7.2: Difference in calving event size between experiments with different ice temperature and vertical undercutting profiles. ΔM is the difference in median calving event size between experiments and α is the significance of the difference. Grey text indicates that the difference in median is not statistically significant at the 95% confidence limit. Missing values occur where terminus behaviour was significantly different in the two experiments.

Undercut profile	Melt rates	+5°C		Normal		-5°C	
	(kma^{-1})	α	ΔM	α	ΔM	α	ΔM
Uniform	0 : 1	0.000	476.7	0.000	68.4	-	-
	0 : 2	0.000	478.8	0.000	33.6	-	-
	1 : 2	0.228	2.1	0.406	34.9	0.000	39.8
Wedge	0 : 1	0.000	477.3	0.000	65.2	-	-
	2 : 5	0.000	176.8	0.000	22.1	0.000	129.1
Parabola	0 : 1	0.000	448.4	0.036	4.3	-	-
	1 : 2	-	-	0.000	62.5	0.000	47.4

Ice mélange

To test the effect of chosen ice temperature on the sensitivity of the model to backstress, experiments using forces of 0, 15, 25 and 50×10^7 Nm^{-1} were repeated using three different crevasse water depths (D_w = 0, 10, 40 m) and three ice temperature profiles (standard and ±5°C). In the advancing experiments (D_w = 0 m), for the normal temperature profile the experiments with 25 and 50×10^7 Nm^{-1} showed a greater advance than the others (Figure 7.13). With an ice temperature decrease of 5°C, only the $F_f = 50\times10^7$ Nm^{-1} experiment showed an earlier terminus advance, while for a temperature increase of 5°C all experiments behaved very similarly. In the steady case (D_w = 10 m), an advance occurred for the 50×10^7 Nm^{-1} experiment in the normal temperature profile case, for 25 and 50×10^7 Nm^{-1} in the experiments with increased ice temperature and in none of the experiments for the cooler ice case. In the retreating experiments (D_w = 40 m) all three ice temperature profiles produced very similar results in terminus behaviour.

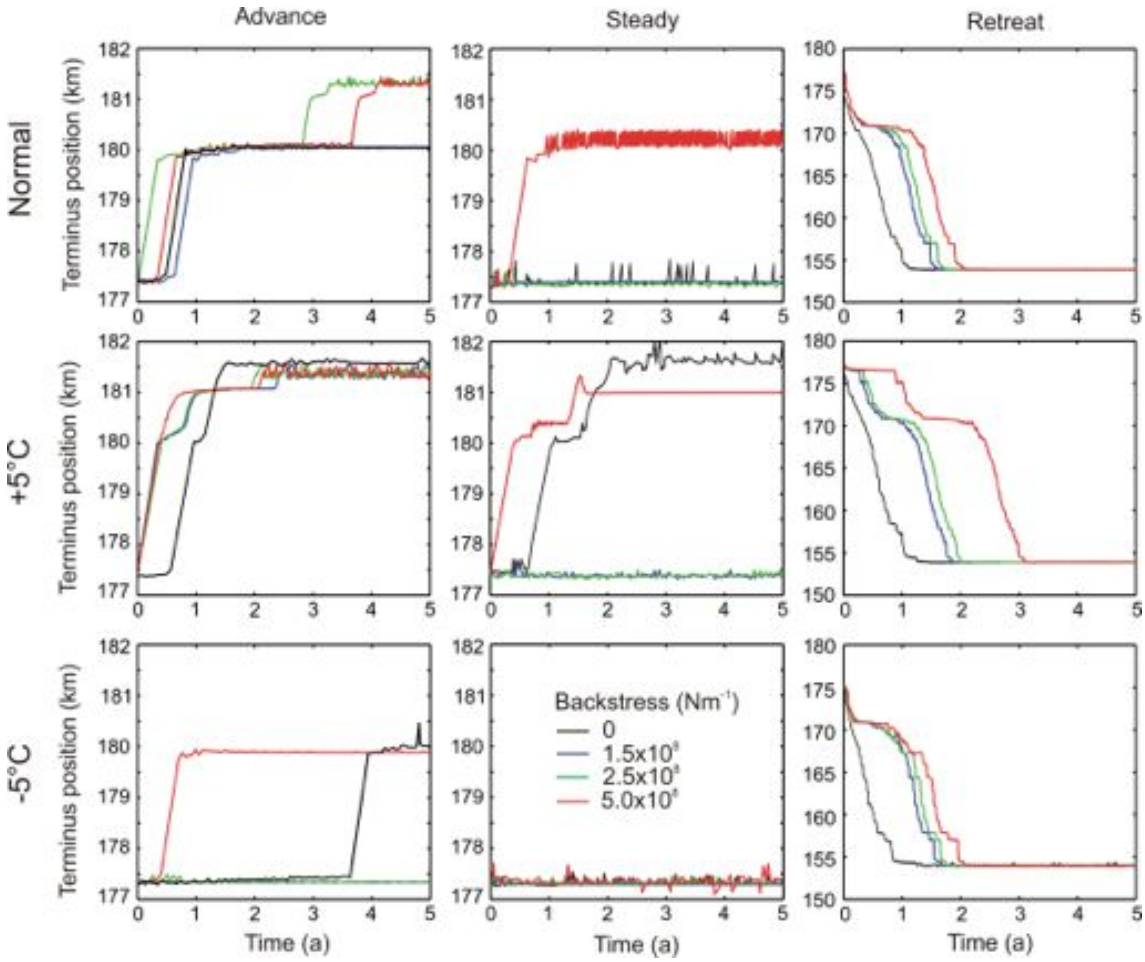

Figure 7.13: Modelled terminus evolution using three different ice temperature profiles. The columns show the response to a range in backstress at the calving face in three different model scenarios; advancing ($D_w = 0$ m), steady ($D_w = 10$ m and retreating ($D_w = 30$ m)
.

The calving behaviour of the different experiments was also compared in cases where there was similar terminus behaviour, with the difference in median calving event size and the significance of the result shown in Table 7.3. The experiments using a change in temperature profile of -5°C were more likely than the the other experiments to produce a change in calving event size which was not statistically significant. Comparing the other two temperature profiles, in the retreating case the results were very similar, but in the steady and advancing scenarios, the +5°C temperature profile tended to produce a larger difference in median event size.

Table 7.3: Difference in calving event size between experiments with different ice temperature and backstress. ΔM is the difference in median calving event size between experiments and α is the significance of the difference. Grey text indicates that the difference in median is not statistically significant at the 95% confidence limit. Missing values occur where the terminus behaviour was significantly different in the two experiments.

D_w	Backstress	+5°C		Normal		-5°C	
	($\times 10^7$ Nm^{-1})	α	ΔM	α	ΔM	α	ΔM
0 m	0.0 : 1.5	0.000	408.5	0.000	65.3	0.250	12.2
	2.5 : 5.0	0.196	1.3	0.084	50.8	-	-
10 m	0.0 : 1.5	0.000	311.9	0.000	41.4	0.279	18.2
	0.0 : 2.5	-	-	0.000	154.5	0.186	15.0
	1.5 : 2.5	-	-	0.000	113.1	0.253	3.2
	2.5 : 5.0	0.000	262.3	-	-	0.000	43.8
40 m	0.0 : 1.5	0.000	30.2	0.000	14.5	0.000	11.7
	0.0 : 2.5	0.000	40.6	0.000	32.4	0.000	14.0
	0.0 : 5.0	0.000	51.2	0.000	45.8	0.000	13.6
	1.5 : 2.5	0.000	10.4	0.000	17.9	0.117	2.3
	1.5 : 5.0	0.000	21.0	0.000	31.3	0.021	1.9
	2.5 : 5.0	0.000	10.6	0.000	13.4	0.420	0.4

7.4 Discussion

7.4.1 Crevasse water depth

Once again, the model was found to be sensitive to changes in crevasse water depth, in terms of both terminus behaviour and calving event size and frequency (Section 7.3.1). Greater crevasse water depths caused the terminus to retreat (Figure 7.3), and also changed the calving behaviour towards more frequent, smaller calving events, although at the highest crevasse water depths very large calving events (>1 km) also began to occur (Figure 7.4). The data from these experiments were compared to observed frontal records and the terminus was found to match seasonal variations best with a crevasse water depth of 30 m (Figure 7.3), although none of the experiments matched the observed behaviour well, as the real glacier advanced rapidly from summer 2005. This difference in the behaviour of the terminus is disappointing but not unexpected as the precise terminus behaviour is likely to be strongly controlled by the bed topography, and in the area of the terminus the errors in measured bed elevation are likely to be high. The observations of not only topography but also ice temperature are not yet sufficient to produce a model which is accurate enough to be expected to reproduce observed behaviour well, but the model is sufficiently close to the observed system that it may reasonably be expected to respond in a similar manner to external forcing.

The experiments performed using seasonally varying crevasse water depth proved to be more susceptible to the model reaching the flotation point. This is a phenomenon that the model in its current form cannot represent, as it contains no implementation of buoyancy forces acting on the glacier body. The analysis presented used only data from the model run up to the point at which flotation first occurred, after which model results were considered unreliable. However, it is interesting to note that this was much more common in the seasonal experiments. It seems likely that this is due to the rapid retreat and subsequent abrupt alteration in forcing in many of the experiments. It has been suggested previously than when advancing into deeper

water glaciers develop a floating section initially, and then as ice flux from further upstream reaches the front the glacier terminus becomes grounded again (Howat et al., 2007; Joughin et al., 2008b). The model results presented here support the theory that, after a rapid retreat, when ice beings to advance again it is likely to reach flotation point, although it was also found that in some cases the model was able to advance into deeper water without reaching the floating point as discussed in Section 7.3.1.

7.4.2 Basal water pressure

Unlike the results from the previous chapter, the model showed a strong sensitivity to seasonal changes in basal water pressure (Section 7.3.2). In the experiment with no water in crevasses the changes in basal water pressure caused the model to advance beyond the standard case, although as it advanced the model became subject to some areas of floating ice making further results unreliable . The lack of modelled calving events due to this early failure of the model meant that no statistical comparison of calving events could be made. With a seasonally varying crevasse water depth, the change in basal water pressure changed the behaviour of the model from a strong retreat of 5 km to an advance of around 2.5 km (Figure 7.5). In these seasonal experiments, the slower winter pressures used led to a slow down of the glacier model, a reduction in calving and a consequent advance of the terminus. These results confirm the hypothesis from van der Veen (2002) that advance and retreat of the calving front is controlled by the velocity of the glacier via flow-induced changes in the terminus geometry.

The result that terminus behaviour was affected strongly by the seasonal change in basal water pressure was surprising in the context of the results from Chapter 6 and previous modelling work by (Nick et al., 2009), neither of which indicated a strong dependence on basal water pressure. However, it is considered important in other tidewater glacier systems. It has been found to have a significant effect on velocity in tidewater glaciers such as Columbia Glacier (Meier and Post, 1987; Kamb et al.,

1994) and to be important in previous modelling work on tidewater glaciers (Vieli et al., 2000). The seasonal experiments presented in this chapter were run using a single value for the change in basal water pressure, 50 kPa equivalent to a 10-15% change in terminus velocity. This is in line with observations by Joughin et al. (2008a) on West Greenland Glaciers, but somewhat more than meltwater induced velocity changes of 2 – 4% observed by Andersen et al. (2011) on Helheim Glacier and it is likely that the results presented here show a greater effect of subglacial hydrology than would be observed in real life. However, it does indicate that, in contrast to some previous modelling work, subglacial hydrology can be an important factor in the calving dynamics of Greenland outlet glaciers and should be an area of future study.

7.4.3 Subaqueous melt

The seasonal undercutting experiments were performed using melt rates up to twice that expected from previous studies. However, when applied seasonally the variable made very little difference to the terminus behaviour or the typical calving event size of the model, particularly in the experiments which used a seasonally varying crevasse water depth as well as undercutting (Section 7.3.3). In an additional experiment to test the undercutting rate required to cause the model to retreat during the first summer period it was found that, in the case with no water in crevasses, a rate of at least 10 $\mathrm{km\,a^{-1}}$ would be required, while with a crevasse water depth of 30 m an even higher undercutting rate of 18 $\mathrm{km\,a^{-1}}$ would be required (Figure 7.9). The range of physically realistic melt rates for Helheim Glacier derived from previous studies is 1090 - 2560 $\mathrm{m\,a^{-1}}$ (Section 7.2.3). Although, as demonstrated in the previous chapter, undercutting has the potential to change the stress profile around the terminus of the glacier, it seems that when applied in conjunction with ice dynamics the effect does not have a significant impact on the model's terminus behaviour.

7.4.4 Ice mélange

A range of backstresses from 2 to 50×10^7 Nm^{-1} were applied seasonally to the model using summer crevasse water depths of 0 m and 30 m. The only backstress which affected the terminus behaviour of the model was 50×10^7 Nm^{-1} , although in some cases lower backstresses produced a statistically significant change in calving event size (Section 7.3.4). As discussed in Section 6.4.4, although this magnitude of backstress causes a change in velocity which may be physically plausible, it is very unlikely that a mélange of glacier ice and sea ice would be able to support such stresses without failing.

Another possibility is that the backstress does not affect the front directly via changing the ice dynamics, but affects other processes occurring around the ice margin. It has been hypothesized by Amundson et al. (2010) that ice mélange may affect tidewater glaciers by preventing the tipping of ice blocks away from the glacier front and thereby holding them in place over the winter months. When the model was tested by suppressing calving during the winter period it unsurprisingly had a very large effect on the terminus of the glacier. This mechanism has the potential to have a large impact on the glacier's behaviour. However, insufficient data are available to implement it in the model at present. It can be seen from terminus records of Helheim Glacier that calving events do occur in winter and therefore determining the proportion of calving events that ice mélange would be able to prevent via this mechanism would need to be an area of further study before it could be implemented fully in a tidewater glacier model.

7.4.5 Effect of ice temperature

The results presented here, showing a relative insensitivity of the glacier model to oceanic forcing, were unexpected. Previous modelling work had indicated that tidewater glacier models could be sensitive to both undercutting and backstress (Nick et al., 2009; Vieli and Nick, 2011). Although the second of these studies

was applied to Jakobshavn Glacier, which has a floating section, the former was performed on Helheim Glacier and the difference in results was unexpected. The greatest source of error in the model as identified in Chapter 5 is the applied ice temperature profile, therefore further testing was performed to see if this could be affecting the sensitivity of the results.

Two alternative ice temperature profiles were selected, shifting the temperature of the ice by ±5°C, and a selection of undercutting and backstress experiments were repeated using them. Although the changes in ice temperature did in some cases lead to different results in the terminus behaviour of the model, they did not have an obvious effect on the sensitivity of the terminus behaviour to either undercutting rate or backstress (Figures 7.12 & 7.13). Examining the difference in calving event size distribution, the experiments with increased ice temperature showed greater changes in calving event size between both undercutting and backstress experiments and in some cases the cooler temperature profile showed a less significant difference in calving event size. It may be concluded that using a warmer temperature profile can make the model more sensitive to changes in calving event size arising from oceanic forcing, but that these do not lead to a significant change in terminus behaviour.

7.4.6 Calving statistics

One of the aims presented at the beginning of this thesis was to identify a response in the calving event size distribution to external forcing, which when compared with observational data could identify the cause of observed tidewater glacier retreat. The seasonal experiments presented in this chapter provide the most realistic model scenario for making these comparisons. It was found that crevasse water depth had the strongest effect on the modelled calving event size distribution (Figure 7.4). Amongst the other environmental forcing variables, there were insufficient data to perform the analysis for basal water pressure, but in the previous chapter it was not found to have a significant effect on calving event size. Undercutting and backstress both made a difference to the calving event size distribution in some

cases, the highest rate of undercutting produced somewhat larger calving events, as did the largest comparable magnitude of backstress. However, the majority of experiments showed no significant difference in iceberg distribution to the standard experiment with no forcing. This is unsurprising since the two forcing variables were also observed not to have a significant effect on terminus behaviour. Of the two variables which did have significant influence on the model's terminus position, only crevasse water depth showed a significant change in calving distribution and it is possible that this could be a means of distinguishing glacier retreat triggered by acceleration due to raised basal water pressure and retreat caused by increased calving rates from pooling of water in crevasses.

7.5 Chapter Summary

The four environmental variables previously identified as important to tidewater glacier systems (crevasse water depth, basal water pressure, subaqueous melt and backstress from ice mélange) were applied to the model of Helheim Glacier using seasonally variable values. Once again, the model was found to be sensitive to changes in crevasse water depth, in terms of both terminus behaviour and calving event size and frequency. Unlike the results from the previous chapter, the model showed a strong sensitivity to changes in basal water pressure. Using lower basal water pressures in winter (hence causing the glacier to slow down) changed the model's behaviour from a retreat of around 5 km to an advance of around 3 km. It also had the effect of decreasing the seasonal change in terminus position, although this factor may be more strongly controlled by the basal topography.

The seasonal undercutting experiments were performed using melt rates up to twice that expected from previous studies. However, when applied seasonally the variable made very little difference to the terminus behaviour or the typical calving event size of the model. In an additional experiment to test the undercutting rate required to cause the model to retreat during the first summer period it was found that a rate

of at least 10 km a^{-1} would be required. The range of physically realistic melt rates derived from previous studies is 1090-2560 m a^{-1}. As previously, the only backstress which affected the terminus behaviour of the model was 50×10^7 Nm^{-1} , although in some cases lower backstresses produced a statistically significant change in calving event size.

The results indicate that the model is much more sensitive to changes in atmospheric forcing than oceanic variables. To test that this result did not depend on the ice temperature profile used in the experiments, the oceanic forcing variables were tested again using two different ice temperature profiles. Although experiments with warmer ice temperatures did show a greater response in calving event size there was no obvious effect on the sensitivity of the terminus behaviour to either undercutting rate or backstress.

Chapter 8

Discussion

The aim of the thesis was to produce a realistic grounded tidewater glacier model which can adequately represent the tidewater glacier system and its interaction with its environment, and to investigate the sensitivity of the model to various environmental forcing factors. The new model presented is the first full-Stokes, time-evolving model of a tidewater glacier to include a calving criterion based on crevasse penetration. It is also the first tidewater glacier model to represent individual calving events. The model was tested with four environmental variables thought to influence calving rates: water depth in crevasses, basal water pressure, undercutting of the calving face by subaqueous melt and backstress from ice mélange. The results show that the model is not sensitive to either subaqueous melt rate or backstress at the terminus when applied within realistic ranges, while basal water pressure and crevasse water depth are shown to be much more significant. This stands in contradiction to previous assumptions about Greenland outlet glaciers, except in the respect that water in crevasses can significantly affect calving and terminus dynamics, which was also found in previous modelling work by Vieli and Nick (2011). In this chapter, these results are examined in the context of previous studies on the topic.

8.1 Comparison to Previous Modelling Approaches

Tidewater glacier models presented previously have used a number of different approximations, as laid out in Section 2.3. Some studies, such as those by O'Leary (2011) and Otero et al. (2010), use diagnostic models, which are able to provide some insight into the calving process, but are unable to make firm predictions about calving rates. There have been a number of studies using prognostic (time-evolving) models, most of which have used one of the empirical calving models described in Section 2.2.1. As discussed there, these empirical models have significant limitations in their ability to represent the full range of tidewater glacier calving behaviour. Two previous studies have used a physically realistic calving mechanism similar to that adopted in this thesis, where calving is dependent on the penetration of crevasses through the glacier ice (Nick et al., 2010; Vieli and Nick, 2011). These studies provide an interesting insight into the full range of tidewater glacier behaviour, encompassing both grounded and floating ice dynamics. However, the ice-flow model used is vertically-integrated, which limits the accuracy of the modelled stresses acting within the ice. This is a particular problem because the calculation of crevasse depths relies on an accurate model of englacial stresses.

Earlier studies by Vieli et al. (2001) and Vieli et al. (2002) have used a vertically-resolved, time-evolving model, which is likely to represent ice dynamics better than the vertically-integrated model. However, these studies used a calving model based on height-above-flotation (described in Section 2.2.1), which is flawed as a representation of calving as it inhibits advance into deeper water (Nick and Oerlemans, 2006) and is unable to allow for floating ice sections. The model presented in this thesis combines the advantages of a vertically-resolved ice flow model, which is likely to provide the best representation of internal stress, with a physically realistic calving criterion based on crevasse depth. Although this particular implementation was not developed to account for floating ice, unlike the Vieli et al. (2001) model it is possible to extend the code to allow for a floating terminus in future.

The new calving model presented in this thesis also has the advantage that it is

the first tidewater glacier model to represent individual calving events. Whether or not the glacier calves depends on the stress profile around the front, and if a sufficiently short time-step is chosen, multiple time-steps will occur between calving events. The modelled calving events produced are not necessarily equivalent to an individual iceberg, as the model identifies only the calving point furthest upstream from the terminus. In many cases, areas downstream of this point are also crevassed below the water line, and the region of calved ice is therefore likely to disintegrate rather than break off as a single iceberg. It should also be noted that a uniform crevasse field would not be expected in a real glacier, and stochastic variations in crevasse depth will control the exact location and timing of calving. Consequently, the model simulates average calving behaviour rather than being able to identify individual calving events. With these caveats in mind, the model provides a new means of investigating the calving of ice on short time-scales and a potential means of examining in detail the effect of forcing on tidewater glacier termini.

8.2 Environmental Forcing of Tidewater Glaciers

Two hypotheses have been formed in previous literature as to the main mechanisms behind changes in the length of tidewater glaciers. The first is that changes are caused by alterations in the glacier velocity. If the acceleration is greatest near the terminus, this could increase longitudinal stretching and hence crevassing. Alternatively, the dynamic thinning caused by such an acceleration could make the ice at the terminus more unstable. This is the mechanism favoured by van der Veen (2002), with changes in basal water pressure being suggested as the likely mechanism behind short-term changes in velocity (*e.g.* Zwally et al., 2002).

The second hypothesis is that tidewater glacier retreat is triggered by changes in calving at the terminus, which has consequent effects on the velocity of the glacier. Three key environmental factors have been identified which may affect the rate of calving at the terminus on short timescales: water in crevasses, undercutting by

subaqueous melt and backstress from ice mélange. On longer timescales geometry changes caused by surface mass balance effects could also have an effect (*e.g.* Pritchard and Vaughan, 2007). Because both mechanisms for tidewater glacier retreat have effectively the same outcome (increased calving rate, increased velocity and retreat of the terminus), it is difficult to distinguish them by observations alone and therefore modelling is used to predict the likely sensitivity of tidewater glaciers to each variable individually.

8.2.1 Acceleration mechanisms

Changes in calving rate triggered by glacier acceleration are likely to be caused by changes in basal water pressure, which can arise either from changes in either the water availability at the bed, or the style of drainage in the subglacial hydrology system. Variations in basal water pressure have been observed to have a significant effect on ice dynamics in some tidewater glaciers. For example, at Columbia Glacier, variations in speed of 15-30% are thought to be caused by changes in basal water pressure (Kamb et al., 1994). Basal water pressure has also been found to have a significant effect on modelled tidewater glacier dynamics in a study by Vieli et al. (2000), where adjustments in the applied basal water pressure gradient were able to reproduce observed fast-flow events.

This mechanism has not generally been thought to be significant for tidewater glaciers in Greenland, as seasonal variations in ice velocity caused by changes in basal water pressure are much more significant on land-terminating areas of the Greenland Ice Sheet than in outlet glaciers (Joughin et al., 2008a; Sole et al., 2011). The observed velocity changes in outlet glaciers of up to 15% in West Greenland (Joughin et al., 2008a) and 2-4% at Helheim Glacier (Andersen et al., 2011) were concluded to be insufficient to be a likely cause of glacier retreat. This was confirmed by a modelling study of Helheim Glacier by Nick et al. (2009) which found that increases in basal lubrication were unable to cause a significant retreat of the model's terminus. However, at least one study of a Greenland outlet glacier has

concluded that subglacial hydrology could be important for ice dynamics (Howat et al., 2010), with observations that drainage of supraglacial lakes and water-filled crevasses resulted in substantial changes in speed (40 – 60%) on fast-flowing glaciers in West Greenland.

In this thesis, basal water pressure was applied as an input to the basal sliding law (Section 3.1.4) which adjusts the sliding velocity of the glacier. This cannot account for the complex relationship between basal water pressure and the subglacial drainage system, which means that additional water availability can actually trigger a decrease in basal water pressure as the drainage system becomes more efficient. The response of the glacier to changes in basal water pressure may be more complex than a simple acceleration, but the changes in basal sliding velocity applied in the experiments presented here represent the type of response that could be expected.

Changes in basal water pressure were applied to the model of Helheim Glacier both constantly (Chapter 6) and seasonally (Chapter 7). When applied constantly, six experiments were performed using a change in hydrostatic head of up to ± 75 m from the standard case. In cases with an advancing terminus, the higher basal water pressures were able to inhibit the advance of the model. However, in most experiments the change in basal water pressure did not make a significant difference to terminus behaviour or the typical calving event size.

The results from seasonally applied changes in basal water pressure made a strong contrast to this behaviour. When a seasonal change in hydrostatic head of 50 m was applied (equivalent to a velocity change of 10-15%, in line with results from Joughin et al. (2008a)) a significant change in terminus behaviour occurred. The slower winter velocities promoted advance of the glacier, even in cases where the standard experiment showed a distinct retreat. In these cases there were no examples in which the calving event size was directly comparable. The change in velocity used for the seasonal experiments is somewhat greater than has been observed at Helheim Glacier (Andersen et al., 2011) and therefore the response may be more marked than would be expected in the real glacier. The precise response of the calving model to

changes in basal water pressure will depend on the type of basal hydrology model used. In the experiments presented in this thesis the basal water pressure depended simply on the depth of the bed below sea level, which provides a minimum level for water pressure but is likely to underestimate the true value which will be spatially and temporally variable. The Gagliardini-type sliding law used leads to a non-linear relationship between basal drag, sliding velocity and effective pressure making it difficult to predict how a more accurate basal hydrology model would affect the results presented here. However, it seems likely that an improved hydrology model might be expected to improve the fit to observed seasonal velocity variations.

The reason for the difference between the constantly and seasonally applied experiments is unclear. It may be that the seasonal nature of the changes in velocity in the later experiments prevent the model from reaching a stable terminus position, thus enhancing the effect of the forcing variable. The two sets of experiments also use different sliding parameters. This is because the velocity fit is performed using data from July 2005. In experiments using a fixed basal water pressure, the velocity fit is performed using the standard basal water pressure profile. In the seasonally varying experiments, it became more appropriate to perform the fit using the summer basal water pressure profile - an increase of +50 m on the standard model. It is possible that the resulting difference in basal sliding parameters is the cause of the increased sensitivity to basal water pressure. Whatever the cause of the difference, the model results show that under some circumstances the model can be highly sensitive to changes in basal water pressure, and that this effect should be considered to be potentially important in tidewater glacier systems, including Greenland outlet glaciers.

The results presented in this thesis confirm previous results by Vieli et al. (2000) that changes in basal sliding velocity can have a significant effect on the behaviour of tidewater glacier models. The modelling work by Nick et al. (2009) which found little response in terminus position to changes in basal sliding was performed using a relatively simple, vertically integrated ice flow model. Both the work presented here and the study by Vieli et al. (2000) used a vertically resolved full-Stokes model

and found sensitivity to basal water pressure. It is possible that the insensitivity to basal conditions found by Nick et al. (2009) may be an artifact of the approximations used in their model. Previous studies had considered the observed seasonal velocity variations in Greenland outlet glaciers of up to 15% to be too small to have a significant effect on terminus behaviour (Joughin et al., 2008a). The work presented here indicates that velocity changes of this magnitude should not be considered insignificant and changes in velocity arising from changes in basal conditions may be more significant for Greenland outlet glaciers than previously assumed.

8.2.2 Direct effects on calving rate

Crevasse water depth

The most obvious factor which can affect calving rates at the terminus of a tidewater glacier is the extent of fracturing within the ice. The penetration of surface crevasses in the glacier will be strongly affected by the availability of surface meltwater because the presence of water in crevasses will tend to deepen them as the water pressure opposes the ice overburden pressure acting to close the crevasse. The type of calving model used in this study depends directly on the penetration of surface crevasses in the ice, and would be expected to depend strongly on the level of water in them, as has been shown by previous modelling work using a similar calving criterion (Nick et al., 2010; Vieli and Nick, 2011).

Water in crevasses was applied to the model of Columbia Glacier in Chapter 4 and to the model of Helheim Glacier using both constant (Chapter 6) and seasonally varying levels (Chapter 7). In all three cases, the depth of water in crevasses had a very large effect on the behaviour of the glacier, with the modelled glacier front advancing with no water in crevasses, while greater crevasse water depths were able to trigger a retreat of the terminus. Although the experiments performed on Columbia Glacier were too short to produce a large enough dataset of calving events for statistical analysis, the Helheim Glacier experiments revealed that the changes

in crevasse water depth also caused a change in the modelled calving event size and frequency. In both the constantly- and seasonally-forced experiments the same pattern in calving behaviour emerged. With no water in crevasses the iceberg sizes followed a normal distribution centered around 500 m. As crevasse water depth was increased to 20 m, smaller calving events (<100 m) began to dominate in the distribution, with the frequency of events increasing dramatically. As the crevasse water depth increased further the frequency of events began to drop again, and although the majority of calving events were still less than 200 m in size, the number of larger calving events began to increase with the appearance of extremely large events (>1000 m). This qualitatively agrees with observations at Helheim Glacier of distinct calving episodes days to weeks apart, during which the terminus retreated by 0.5 to 1 km (Joughin et al., 2008b), although a higher temporal resolution calving record would be required to fully validate the model output.

Since few data are available on true crevasse depths, or the water levels within them, it is difficult to determine to what extent the values used in this study are reasonable. However, the results indicate that surface ablation and pooling of water in crevasses can have a significant effect on calving rates and terminus behaviour of tidewater glaciers. This had previously been hypothesized to be particularly significant in glaciers with a shallow surface gradient (Vieli and Nick, 2011), as in this case a small vertical change in the stress profile can produce a large horizontal shift in the point where crevasses cross the water line. In both the model of Jakobshavn presented by Vieli and Nick (2011) and in the model of Columbia Glacier presented in this thesis the terminus region has a shallow surface gradient, and in each case a change in crevasse water depth of 1 m can have a significant effect on terminus behaviour. Another previous modelling study by Nick et al. (2010) uses an idealised geometry where changes in crevasse water depth on the scale of 20 m are required to change terminus behaviour. This is of a similar magnitude to the results from Helheim Glacier presented in this thesis, where a crevasse water depth of 30 m was required to produce a significant retreat. These results show that, although the scale of water level required to change terminus behaviour is much greater for glaciers without a

region of shallow surface gradient around the terminus, in all cases the application of water in crevasses can have a significant effect on glacier behaviour.

Subaqueous melt

Undercutting of the calving front by subaqueous melt is believed to be able to alter the stress field around the front, and hence affect fracturing (Benn et al., 2007b). This hypothesis is backed by a modelling study by O'Leary (2011) which found that undercutting of the calving front can displace the stress field around the terminus by up to four times the length of the undercut cavity. If calving is assumed to take place where surface crevasses cross the waterline, this means that the calving point could be shifted significantly upstream, thus increasing calving rates.

A number of studies have indicated that subaqueous melt rates, even in Arctic waters, are sufficiently high to have a significant effect on calving. In a study by Motyka et al. (2003) of Le Conte Glacier, Alaska, subaqueous melt was found to account for 57% of the total mass loss at the terminus. More recently, studies in Greenland have also found high rates of subaqueous melt. Estimates of subaqueous melt rates in West Greenland range up to 3.9 $\mathrm{m\,day^{-1}}$ (Rignot et al., 2010), compared to ice velocities of of 5.5 – 10.9 $\mathrm{m\,day^{-1}}$ in the region (Rignot and Kanagaratnam, 2006). Subaqueous melt rates at Kangerdlugssuaq Glacier, East Greenland have been estimated at up to 1525 $\mathrm{m\,a^{-1}}$, equivalent to 19% of flow speed (O'Leary, 2011). Changes in terminus position in East Greenland outlet glaciers have also been linked to changes in ocean temperature with one hypothesised mechanism being melting at the calving face (Murray et al., 2010; Seale et al., 2011). This relationship is backed by modelling work by Vieli and Nick (2011) on Jakobshavn Glacier which found that a modelled terminus retreat of approximately 9 km could be produced by a change in subaqueous melt rate of 20%.

In the results presented in this thesis, subaqueous melt was applied to the model of Helheim Glacier using both constant (Chapter 6) and seasonal forcing (Chapter 7). The constantly-applied experiments also used a variety of vertical melt profiles

(uniform, wedge, parabolic), all of which were found to be able to affect the modelled terminus behaviour, with higher subaqueous melt rates tending to delay the model's advance or even cause it to retreat. The different experiments also showed significantly different calving behaviour, however no clear pattern in the calving statistics emerged. In all three cases there was a peak in mean event size and a minimum in number of events in the middle of the range of melt rates. However, this range was much greater than has been predicted by previous work on Helheim Glacier, and melt rates of a realistic magnitude did not have a significant effect on the terminus.

In the seasonal experiments, undercutting of realistic magnitude was again found to have relatively little effect on the modelled terminus behaviour. Most of the experiments also showed no significant change in calving event size. To further test the model, the first summer season was re-run with an even greater range of undercutting rates to identify the point at which terminus behaviour began to change. In the $D_w = 0$ m experiment, the terminus began to retreat with a maximum undercutting rate of approximately 10 000 m a^{-1}, while for a crevasse water depth of 30 m terminus retreat did not begin until a melt rate of between 18 000 and 20 000 m a^{-1} was applied to the front. In general, previous estimates of subaqueous melt have fallen in the range 255 – 1605 m a^{-1} for Greenland outlet glaciers (see Section 6.2.3), suggesting that any realistic value of subaqueous melt is unlikely to have a significant effect on the glacier.

The insensitivity of the model presented here to undercutting of the calving face was unexpected in the context of previous modelling work, but the apparent contradiction may be explained. The study by O'Leary (2011) found that undercutting had a significant effect on the stress distribution in a tidewater glacier with a fixed terminus position. When the geometry of the model is allowed to evolve, this counteracts the effect of undercutting and the response in the surrounding stress field is significantly reduced. The model sensitivity to undercutting found by Vieli and Nick (2011) was performed using data from Jakobshavn Glacier which has a significant floating tongue. In this case, sensitivity to basal melt may be expected because it is well known that basal melt has a significant effect on the dynamics of floating

ice (*e.g.* Rignot and Jacobs, 2002). This is because the flow of floating ice sections is entirely opposed by lateral drag, therefore any thickness change will have a significant effect on the buttressing provided by the floating section (Pritchard et al., 2012). No previous studies have conclusively linked undercutting directly to changes in calving rate in grounded ice, and it seems likely from the model results presented here that it is not a significant factor. One possible exception is if the undercutting occurs at the waterline, as observed in some Svalbard glaciers (Vieli et al., 2002). In this case, the overhanging block will be unsupported and the increase in fracturing may be more significant. This is unlikely to be the case at Helheim Glacier, where the upper-most water layer in the fjord is very cold (Straneo et al., 2010).

Ice mélange

The calving front has also been thought to be affected by the presence of an ice mélange, which, when frozen solid, can exert stress on the calving face which may stabilize the terminus and inhibit calving (Amundson and Truffer, 2010). In many tidewater glaciers, onset of calving and retreat of the terminus have been seen to coincide with the break up of a proglacial ice mélange (*e.g.* Sohn et al., 1998; Reeh et al., 2001; Joughin et al., 2008c; Christofferson et al., 2012). A further study by Walter et al. (2012) on Store Gletscher, West Greenland found that the break up of the ice mélange also coincided with an acceleration in terminus velocity of 15%, suggesting that the effect of backstress from ice mélange on ice dynamics may also be significant.

These observations have been backed by previous modelling studies. Modelling work by Nick et al. (2009) on Helheim Glacier found that perturbations in backstress at the terminus had the potential to cause glacier retreat, while changes in basal water pressure did not have an effect on terminus behaviour. Further work by Vieli and Nick (2011) on Jakobshavn Glacier found that the model was sensitive to backstress at the front, with a decrease in the length of the ice mélange season of 2 months producing a retreat of around 6 km.

In the results presented in this thesis, backstress from ice mélange was applied to the model of Helheim Glacier, once again using both constant (Chapter 6) and seasonal forcing (Chapter 7). The first experiments performed used a range of backstresses from $F_f = 0.0$ to 5.0×10^7 Nm^{-1} over a variety of different vertical extents (Section 6.3.4). Although in many cases these experiments produced a statistically significant change in calving event size, they generally made very little difference to the terminus behaviour of the glacier. It was decided to extend the range of backstress experiments to include forces up to 50×10^7 Nm^{-1}. These additional experiments were carried out only on a vertical range of -118.5 to 15 m, thought to be the most physically realistic (see Section 6.4.4). In these experiments the backstress had a greater effect on the terminus evolution, with increased backstress promoting advance of the model's terminus, or delay of its retreat. Changes in backstress also had a significant effect on the modelled calving behaviour, but the nature of the response depended on the behaviour of the glacier terminus. In the advancing and steady cases an increase in backstress generally caused the model to produce more frequent, smaller icebergs, while for the retreating experiments an increase in backstress caused more infrequent, larger events.

The extended range of backstresses was also used for experiments with seasonally varying forcing. The backstress was then applied only over a hypothesized winter period of January to May, with the crevasse water depth either fixed at 0 m or varied seasonally with summer values of 30 m. In each experiment, the only backstress to affect the modelled terminus behaviour was $F_f = 50\times10^7$ Nm^{-1}, which caused the model to advance. Unlike the constantly applied forcing, in most seasonal experiments the change in backstress did not affect the size of calving events during model runs. Although backstress was found to affect the behaviour of the model in these experiments, the magnitude of force used is far beyond the range predicted in previous literature (*e.g.* Amundson et al., 2010; Walter et al., 2012). It is unlikely that the ice mélange would be able to support such high stresses, as the shear strength of sea ice has been measured at 0.55 ± 0.12 MPa (Frederking and Timco, 1984) while the stress applied to the front in the $F_f = 50\times10^7$ Nm^{-1} experiments is 3.73 MPa.

Previous modelling work had found that a backstress of only 40 kPa could have a significant effect on glacier dynamics (Vieli and Nick, 2011), while the results presented in this thesis found that a stress of 3.73 MPa was required to affect terminus behaviour in many cases. The apparent disagreement with previous modelling literature may be partially explained by the fact that the Vieli and Nick (2011) model has a floating section. The effect of additional backstress may be more significant on floating ice where the velocity is entirely opposed by lateral drag, than in grounded ice where basal drag can be the more significant component. More difficult to explain is the result of previous modelling on Helheim Glacier by Nick et al. (2009), who found strong sensitivity to backstress at the terminus in a grounded glacier model. However, the Nick et al. (2009) model, as discussed previously, is vertically integrated and is therefore likely to represent the stresses acting around the terminus less well than the vertically-resolved model presented here.

Although the results presented in this thesis suggest that grounded tidewater glaciers are insensitive to backstress applied at the terminus, it is possible that ice mélange may still have an effect on calving by another mechanism. It was hypothesized by Amundson and Truffer (2010) that the ice mélange is able to inhibit calving by preventing ice blocks which have separated from the main glacier body from tipping over. This would hold the blocks in direct contact with the glacier terminus until the break up of the ice mélange, and therefore the calved ice would still be able to exert backstress on the terminus through the winter months as if it had not calved at all. In a brief test of this type of mechanism on the Helheim Glacier model, calving was prevented from occurring over a winter period (Section 7.3.4). This produced a significant advance of the model's terminus, which also lowered below the flotation thickness meaning that further results were unreliable. This provided a proof of concept that this type of mechanism could have a significant effect on glacier behaviour, but at present no method has been developed for implementing it realistically in the calving model.

8.2.3 Comparison to observational studies

Although the insensitivity to oceanic forcing found in the modelling work presented in this thesis may generally be explained in the context of previous modelling studies, there is a wealth of observational data linking observed glacier retreat in Greenland to changes in ocean temperature (Section 1.2), which potentially contradicts the results of this modelling study. There are a number of reasons why observations may show a correlation between terminus behaviour and ocean temperature which are compatible with the results presented in this thesis. Firstly, most observations make no distinction between glaciers with grounded and floating termini, as in many cases the basal elevation is poorly known, making it difficult to determine if ice is floating or not. Although the model results presented here show that grounded glaciers should not be sensitive to ocean forcing, this is not likely to be true for those with floating sections. As mentioned previously, is well known from studies of ice shelves that basal melt of floating ice is important for ice dynamics (*e.g.* Rignot and Jacobs, 2002; Pritchard et al., 2012). Floating ice sections are also more likely to respond to changes in backstress at the terminus, as their velocity is entirely governed by lateral drag, and additional backstress is likely to provide a greater proportional change in resistance to flow than in grounded ice. In floating tongues, ice fracturing caused by tidal flexing is also significant, and ocean waves may be damped by the presence of fast-ice, decreasing fracturing. The presence of ice mélange can also protect the fjord waters from wind-mixing, decreasing the melt rate at the calving face, which can be significant for floating termini. The majority of observations linking tidewater behaviour to the presence of ice mélange have been made at glaciers with significant floating sections.

As mentioned above, the lack of basal elevation data around Greenland makes it difficult to distinguish floating and grounded termini. However, the presence of floating ice can be deduced from repeat measurements of surface elevation, which may identify the vertical motion in floating ice caused by tides (Rignot et al., 2004). In the case of Helheim Glacier, the terminus is known to have been grounded between

the summer of 2001 and 2005 during the glacier's retreat, but in 2006 when the front started to advance over a basal overdeepening the terminus began to float (Joughin et al., 2008b). In general, outlet glaciers in the north of Greenland frequently have large floating sections (Thomas et al., 2009), while in the southern regions many outlet glaciers are thought to be grounded (Rignot et al., 2004). The synchronous behaviour of the majority of glaciers in the South-East in recent years indicates that it is very likely that glaciers with both grounded and floating termini were responding simultaneously to external forcing (Howat et al., 2008).

Although the retreat of glaciers in south-east Greenland was synchronous, and coincided with a period of warm ocean temperature at the start of the retreat in 2003, this was also a year of very high coastal air temperatures (Howat et al., 2008; Murray et al., 2010). This is unsurprising given that ocean and atmosphere are in thermal contact, with ocean temperatures able to have a direct effect on local air temperatures and vice versa (Kagan, 1995). Air temperature can also affect ocean temperatures by the release of glacial runoff into proglacial fjords (Straneo et al., 2011). The high air temperatures could have caused a retreat in grounded ice, by increasing the level of water in crevasses around the front. The link to basal sliding velocity is more complex, as basal water pressure depends not only on the availability of water at the bed, but also the subglacial drainage system. The results presented by Murray et al. (2010) also show that 2003 was a year of low runoff, due to the high snowfall in the preceding winter. If the lower water availability meant that the glaciers failed to develop an efficient channelised drainage system this could have had the effect of increasing basal water pressure, which the model results presented in Section 7.3.2 indicate could cause retreat.

Ocean and air temperatures around the terminus of tidewater glaciers are likely to be strongly linked, and it is difficult to separate which may be the cause of glacier behaviour by observation alone, with the complicating factor that runoff levels may also have an effect and are not solely dependent on air temperature, but also on precipitation. In addition, the physical mechanisms relating ice dynamics to oceanic and atmospheric warming are also inter-related. As shown by the plume

models of O'Leary (2011) and Xu et al. (2012), undercutting rates at the terminus are affected not only by the surrounding water temperature, but also by the rate of subglacial discharge which is directly linked to glacier surface ablation and hence air temperatures. The mechanisms of environmental forcing of tidewater glaciers are inextricably linked. This is supported by work from Andresen et al. (2011) showing that reconstructed calving rates from sediment deposition correlate well over a long time-scale with both air and ocean temperatures. Examination of both atmospheric and ocean warming is important for understanding the future of the Greenland Ice Sheet, but the results presented in this thesis indicate that for grounded ice the factors related directly to ocean warming are relatively unimportant.

8.2.4 Calving statistics

A secondary aim of the thesis was to see if the different forcing mechanisms investigated could be distinguished by their effect on calving event size. The results showed that of the two forcing variables which had a significant effect on terminus behaviour, only changes in crevasse water depth caused a statistically significant change in calving event size. Increasing crevasse water depth up to 25 m caused a change in the typical event size from 500 m to less than 100 m. Further increases maintained a high number of small calving events, while extremely large events (>1000 m) also began to occur. Currently, measurements of terminus position are not frequent enough to make a full comparison to the model output. However, given a high temporal resolution record of terminus position, this result could be used to distinguish between retreat caused by acceleration or increased calving from pooling of water in crevasses.

8.3 Significance of Results

Although previous studies had concluded that changes in basal water pressure and sliding velocity can have an impact on the dynamics of tidewater glaciers (*e.g.* Kamb et al., 1994; Vieli et al., 2000), it had not generally been thought to be a significant factor in the behaviour of Greenland outlet glaciers, where the seasonal variations in velocity caused by changing basal water pressure are much smaller in tidewater glaciers than on land-terminating ice (Joughin et al., 2008a). The results presented in this thesis show that velocity changes on the scale of those observed by Joughin et al. (2008a) are sufficient to cause a significant change in terminus behaviour, and should not be disregarded as a potential cause of glacier retreat.

Work by Rignot et al. (2004) has shown that many of the outlet glaciers in south-east Greenland are likely to be grounded, and it is also known that Helheim Glacier was grounded prior to its retreat in 2003 (Joughin et al., 2008b). Given that prior to the retreat event in the early 2000s there was a year of very high air temperatures, it seems likely that the observed retreat event was caused by high air temperatures rather than ocean temperatures as hypothesized in previous studies. The mechanism could be via either increased sliding velocity or increased water in crevasses. Since 1979 there has been a trend of increasing surface melt observed in Greenland, with an exceptionally high melt extent observed in recent years (Fettweis et al., 2011). In the context of the results presented here, this trend seems likely to cause increased mass loss not only by surface ablation, but also through enhanced calving (by acceleration and increased fracturing) and consequently dynamic thinning. The effect of increased surface melt on the Greenland Ice Sheet could be more significant for mass loss than had previously been assumed.

Although the model presented in this thesis is limited in application to grounded tidewater glaciers, it is nevertheless relevant to many polar regions. There are known to be a significant number of grounded tidewater glaciers on the Antarctic Peninsula (Cook et al., 2005) and previous studies have shown that most tidewater glaciers on Svalbard are also grounded (Dowdeswell, 1989). The temperate tidewater glaciers

found in regions such as Alaska are also generally grounded, although in some cases it is possible they can develop floating sections (Walter et al., 2010). The results presented in this thesis indicate that these glaciers are also likely to be dominated by atmospheric rather than oceanic processes.

8.4 Model Limitations and Shortcomings

8.4.1 Validation

Ideally, the output of the model would be compared to observational data to determine if it is behaving in a physically realistic manner. Although the Columbia Glacier model could be tuned to match the observed retreat, for the Helheim Glacier model none of the experiments advanced as quickly as the observed glacier. This may be due to errors in the setup of the model (in the representation of 3D flux, basal conditions *etc.*) but may also indicate that the model over-predicts calving rates. The disparity should be viewed in the light of the large number of approximations made during the model set-up. Many of the model inputs such as ice temperature or basal water pressure are poorly known. Other input variables such as the inflow velocity and the flux arising from changes in channel width have been approximated due to the limitations of the model. The bed DEM is also of questionable quality, as radar measurements of bed elevation are always unreliable in the highly crevassed regions around the front of a tidewater glacier, and this is exacerbated by the interpolation required between flight lines. The sensitivity analysis performed in Section 5.5.9 indicates that the model is not sensitive to small errors in the bed DEM. However, the errors in the bed data are likely to be high, and as shown by Zwinger and Moore (2009) this can have important consequences for the modelled surface velocity and elevation change. The model produced is thus likely to behave in qualitatively the same manner as Helheim Glacier, but is not expected to represent accurately the observed short term variations in terminus position. Such a model can be used to help us improve our understanding of calving dynamics, but for a model to predict

accurately a glacier's terminus behaviour improved measurements of variables such as bed elevation, ice temperature and basal conditions are required.

As well as using the model to predict terminus behaviour, one of the aims of this thesis was to examine the modelled size distribution of calving events to see if it could distinguish different types of forcing. However, no data source is currently available which gives a high enough temporal resolution and a long enough record to provide a useful comparison. Most satellite measurements are made with a repeat period of around a month, and although some studies are now using cameras to observe calving fronts on short timescales, a record spanning years is really required to get a usefully large data set. The only study to publish data on calving event sizes at Helheim Glacier observed distinct calving episodes days to weeks apart, during which the terminus retreated by 0.5 to 1 km (Joughin et al., 2008b). This qualitatively agrees with the style of calving produced by the model of Helheim Glacier presented here, but the observational data are not sufficiently detailed to allow a full comparison. The model results show a strong response in calving event size to changes in crevasse water depth, which is absent in experiments with the other significant forcing variable (basal water pressure), but improved observational data are required before it can be determined if the model produces a realistic calving event size distribution or if changes in iceberg size can be distinguished in real life.

8.4.2 Sensitivity testing

Since validation against observed glacier behaviour is not possible, a series of experiments investigating the sensitivity of the Helheim Glacier model to its input variables were designed (Chapter 5). The model results were found to be particularly sensitive to errors in the applied ice temperature profile. The data used in the model were approximated from a previous modelling study by Funk et al. (1994) on Jakobshavn Glacier, with additional errors added by the approximations made when applying the results in the model. Testing showed that temperature changes of 5°C were sufficient to cause a significant change in terminus evolution

and calving behaviour. Since there have been very few studies of englacial temperatures in Greenland outlet glaciers, restricted mainly to the regions around the ice divide, temperatures must be approximated by modelling. However, the method used could be improved by designing a thermo-mechanical model of the glacier in question to find the most accurate temperature profile possible. This could be used as a preliminary test to set the ice temperature, which could then be applied to calving runs if it were too computer resource intensive to make all the calving runs thermo-mechanically coupled.

Given the unexpected insensitivity of the model to oceanic forcing, further testing was performed to check that ice temperature did not alter the sensitivity to undercutting or backstress at the terminus (Section 7.3.5). Two alternative temperature profiles, with the ice temperature shifted by $\pm 5°C$, were tested and were not found to have a strong effect on the sensitivity of terminus behaviour to oceanic forcing. However, there was some evidence that a model with warmer ice temperatures produced a greater change in iceberg size. The results presented in Section 7.3.5 showed that undercutting and backstress generally did not have a significant effect on modelled calving event size. In the light of these results, if the applied ice temperature is cooler than in the real glacier, the model may have underestimated this sensitivity. However, the lack of sensitivity in modelled terminus behaviour to oceanic forcing is not likely to arise from errors in the ice temperature profile.

Another input variable which had the potential to affect model behaviour was the inflow velocity, which can have an effect on terminus evolution. This is another large source of error in the model, as the model is currently restricted to a single velocity at the inflow boundary, whereas in a real glacier basal drag will mean that velocities at the bed are lower than at the surface. In a full length model of Helheim Glacier performed before the calving experiments, the basal velocity at 152 km (model cut-off location) was found to be around 3000 $\mathrm{m\,a^{-1}}$, while the observed surface velocity is approximately 4000 $\mathrm{m\,a^{-1}}$ at the same point. Thus the basal sliding velocity is a significant proportion of the surface velocity, and the approximation of no vertical velocity gradient should introduce relatively small errors to the model.

Other variables which had potential to affect the model's results were basal water pressure and the parameterisation of 3D flux. The implementation of basal water pressure is very basic, relying only on the depth of the bed below sea level. In observational studies it has been found to vary significantly due to precipitation (Kamb et al., 1994), supraglacial lake drainage events (Joughin et al., 2008a) or changes in the basal drainage system (Bartholomew et al., 2010; Howat et al., 2010), with consequent effects on the glacier's velocity. Although the sliding law used in the Helheim Glacier model is at the forefront of modelling techniques, the implementation of basal water pressure could be significantly improved upon. This would require improved observational data on basal water pressure and basal conditions at Helheim Glacier, which are not currently available, but are extremely important for improving future modelling work.

The parameterisation of 3D flux in the model was shown by sensitivity testing not to be a significant source of error in the model results, but is an area in which the model could certainly be improved. The current form makes very large assumptions about the shape of the glacier channel and the lateral velocity gradient which could be greatly improved upon by performing modelling in 3D, which would also improve the representation of lateral drag. This presents particular challenges not only in terms of the large requirement in computing resources, but also in the theoretical implementation of calving in such a model. The identification of a calving point in a two-dimensional model is conceptually simple; however, in three dimensions finding the new shape of a calving bay after a calving event takes place is far from a trivial problem. One potential solution has been developed by Otero et al. (2010), whereby a three dimensional flow model is coupled to a calving model which uses a number of separate flowlines throughout the glacier and identifies a calving point along each of them. This then creates an estimated shape for the new calving front. This approach would be compatible with the calving model presented in this thesis, and is a possible area of future development.

The remaining sensitivity tests determined that the glacier model is not sensitive to small changes in the bed DEM, surface accumulation/ablation, lateral drag or in

the period of the surface relaxation performed before model runs began and these are not considered to be large sources of error in the model. As noted previously, in some places errors in the bed DEM are likely to be high and these would be expected to have a significant effect on model behaviour.

8.4.3 Other limitations

Beyond the scope of the sensitivity tests, there are two other obvious shortcomings of the model in its current form. Although in most experiments presented in this thesis the model remained grounded, in some cases the terminus reached flotation point rendering further results unreliable. If the model were extended to be able to represent floating ice it would have a far wider applicability.

Secondly, the crevasse depth calving criterion used in the model is highly simplified and unlikely to represent accurately all the fracturing processes occurring in a real glacier. The Nye model does not allow for any interaction between crevasses and the surrounding stress distribution. This is generally considered a reasonable approximation where crevasses are closely spaced (which is the case near most calving fronts). However, using a linear elastic fracture mechanics approach could potentially improve the accuracy of predicted crevasse depths (see Section 3.2.1).

In addition, the dense field of crevasses near the calving front is likely to have a significant effect on large-scale stresses within the ice, and highly fractured regions are expected to have very different flow properties which the model is unable to account for. Some experiments into representing the interaction between crevassing and ice dynamics have been performed by reducing the viscosity in fractured ice regions (*e.g.* Vieli et al., 2006), which is a common approach in ice shelf models but would be difficult to apply in a flowline model as presented here. A more rigorous approach to representing crevasses in tidewater glaciers could use differing ice properties in different directions to properly represent crevassed regions which are able to support the weight of ice vertically, but have no horizontal connection. Another shortcom-

ing in the representation of crevasses is that the model uses only local stresses to determine ice fracture, whereas in real life crevasses will not open and close instantaneously and there will be some memory of fracture history upstream. An improved representation of ice fracturing could be achieved using damage mechanics methods, which track damage in the ice as it advects downstream (*e.g.* Jouvet et al., 2011). This would also provide another potential feedback effect with velocity affecting not only the degree of fracturing but also the rate at which the fractures are transported to the calving front.

8.5 Chapter Summary

Globally, large numbers of tidewater and outlet glaciers exist with grounded termini, with particular concentrations in the Antarctic Peninsula, Svalbard, Alaska and south Greenland. In recent years many (though not all) of these glaciers have been observed to retreat, with the changes in terminus position attributed often to changes in local environment (Cook et al., 2005; Vieli et al., 2002; Krimmel, 2001; Howat et al., 2008). In south-east Greenland, synchronous behaviour in glaciers with grounded and floating termini has also been observed (Howat et al., 2008), which many studies have attributed to an increase in local ocean temperatures, with the hypothesized mechanisms being an increase in subaqueous melt or a reduction in backstress from proglacial ice mélange (Murray et al., 2010; Christofferson et al., 2012).

The model results presented in this thesis indicate that these two mechanisms are unlikely to have a significant effect on grounded glacier ice. Neither undercutting by subaqueous melt or changes in backstress at the terminus had a significant effect on the position of the model's terminus, while changes in the depth of water in crevasses and basal water pressure produced substantial changes in behaviour.

In the specific context of Greenland glaciers, the wide speculation that changes in terminus position are driven directly by ocean temperatures may only be true

for floating glaciers. It is not well known how many of the glaciers in the south-east were floating prior to the terminus retreat of the early 2000s, and it is likely that any glaciers with floating termini could be affected directly by warmer ocean temperatures. The synchronous behaviour in grounded and floating termini observed in south-east Greenland may be explained through the strong feedback processes linking local ocean and air temperatures, and the inter-related processes by which these temperatures act on the glacier system (Section 8.2.3).

There are some cases in which grounded ice may respond to changes in ocean temperatures, for example if melting occurs at the waterline then this will have the effect of increasing fracturing in the unsupported ice block, as observed by Vieli et al. (2002) at Hansbreen, Svalbard. However, in general, if we are interested in interpreting observations of tidewater glaciers, whether the terminus is floating or grounded is likely to be a crucial factor governing the glacier's response to external forcing. This is a complex problem, as glaciers may of course have a floating or grounded terminus at different times. A change from grounded to floating terminus has been observed at both Columbia Glacier (Walter et al., 2010) and Helheim Glacier (Joughin et al., 2008b).

The strong dependence of the model results on variables dependent on surface ablation (basal water pressure and crevasse water depth) indicates the possibility that outlet glaciers on the Greenland Ice Sheet may respond much more strongly to the observed trend in surface melt than had previously been assumed, raising concerns over possible dynamic thinning of the margins of the ice sheet.

Chapter 9

Summary and Further Work

9.1 Summary

9.1.1 Motivation

The calving of icebergs has been found to be a significant mass loss contributor in a large number of ice masses worldwide, including both the Greenland and Antarctic Ice Sheets (Church et al., 2001; Rignot and Thomas, 2002), where changes in calving rate can contribute to dynamic thinning of the ice margin (Pritchard et al., 2009). Recent studies have shown that tidewater glaciers can be strongly sensitive to climate change (Howat et al., 2007; Larsen et al., 2007), with rapid changes in terminus position being observed in a number of glaciers (*e.g.* Howat et al., 2008; Krimmel, 2001). The processes governing calving in tidewater glaciers are complex, depending on a number of inter-related environmental factors (see Section 1.2) and the challenging working environment makes it difficult to obtain the observational data crucial to interpreting observations of terminus position change. Numerical ice flow modelling is a key tool in understanding the behaviour of such glaciers, as it provides the possibility of isolating individual forcing variables and testing their impact on glacier behaviour.

The work presented in this thesis used a novel finite element model of a tidewater glacier, including calving determined by penetration of surface crevasses to sea level. As discussed in Chapter 2, the crevasse-depth calving criterion has been applied in a number of glacier models (Otero et al., 2010; Vieli and Nick, 2011), but the model presented in this thesis is the first depth-resolved, prognostic model to use a crevasse-depth calving criterion. It is the first implementation of the crevasse-depth calving criterion to allow the prediction of discrete calving events, with the potential to provide insight into calving behaviour statistics. The model was applied to two grounded tidewater glaciers; Columbia Glacier, Alaska and Helheim Glacier, East Greenland.

The aims identified at the beginning of this thesis were to produce a realistic model which can adequately represent the tidewater glacier system and its interaction with its environment, to investigate the sensitivity of the model to various environmental forcing factors, to analyse the relative importance of these factors and make conclusions about the sensitivity of tidewater glacier systems to climatic change which may be used in application in wider research contexts. In order to achieve this the sensitivity of the model was tested to changes in four environmental variables: water in crevasses, basal water pressure, subaqueous melt and backstress from ice mélange, with experiments using both constant and seasonal forcing.

9.1.2 Main results

In applications to both Columbia and Helheim Glaciers a strong dependence of model behaviour on crevasse water depth was found, suggesting that tidewater glaciers may be highly sensitive to atmospheric warming. Increases in crevasse water depth were found to cause the modelled terminus to retreat, and also to significantly affect the size distribution of calving events produced by the model. Previous work by Vieli and Nick (2011) had found a similar dependence of terminus behaviour on water in crevasses, but this was hypothesized to be caused by the shallow terminus region. The Helheim Glacier model presented in this thesis remains firmly

grounded, without a particularly shallow terminus, but is still sensitive to crevasse water depth. These results indicate that any type of tidewater glacier, whether floating or grounded, may be strongly affected by increased surface ablation.

Changes in basal water pressure were applied to the Helheim Glacier model both constantly and seasonally. Modelled terminus behaviour was found to depend strongly on basal water pressure in experiments with seasonally applied forcing, although this result was not observed in the constantly forced experiments. These results indicate that changes in the velocity of a tidewater glacier can have a significant effect on the calving rate and terminus behaviour, and this effect should not be ruled out as an important factor in understanding the behaviour of Greenland outlet glaciers.

The Helheim Glacier model was also tested with a range of subaqueous melt rates and backstresses at the calving front, designed to represent the interaction of the glacier with the surrounding ocean. Undercutting by subaqueous melt was applied both constantly and seasonally, and although it was found to be capable of changing the behaviour of the model in terms of both terminus evolution and modelled calving event size, the rate of subaqueous melt required to cause these changes was significantly outside the range of previously estimated melt rates at Helheim Glacier. Similarly, applying a force to the calving face to simulate backstress from a proglacial ice mélange was able to affect the terminus behaviour of the model, but the magnitudes of force required were significantly greater than is likely to be physically realistic.

This insensitivity to oceanic forcing was unexpected in the context of previous studies of Greenland outlet glaciers, which had found that changes in glaciers coincided with periods of warm ocean temperatures (Howat et al., 2008; Murray et al., 2010). Previous models of tidewater glaciers had also indicated that they could be sensitive to changes in undercutting and backstress (Nick et al., 2009; Vieli and Nick, 2011; O'Leary, 2011). The disparity in results is likely to arise from two sources, firstly that atmospheric and ocean temperatures are strongly linked, as are the mechanisms by which they act on glacier-fjord systems. The inter-related nature of the

forcing means that it is very difficult to identify the cause of glacier change by observation alone. Secondly, many observations were made on glaciers with floating termini, which are likely to be much more sensitive to changes ocean temperatures. This study indicates that grounded tidewater glaciers are relatively insensitive to oceanic forcing mechanisms, with atmospheric forcing via surface melt much more important.

A secondary aim of the thesis was to examine the calving event size distribution produced by the model to see if different forcing variables could be distinguished by the size of calving event produced. Of the two variables found to affect terminus behaviour, changes in basal water pressure produced very little change in the modelled iceberg distribution, while changes in crevasse water depth strongly affected the shape of the distribution. Current observational records of terminus position are not detailed enough to make an analysis of observed calving event sizes possible, but in future this may be a possible method for identifying the causes behind glacier retreat.

9.2 Suggestions for Further Work

The key area for developing this work would be to improve the validation against observed data. The model as presented was unable to reproduce accurately the observed terminus behaviour of Helheim Glacier, which is most likely because of errors in the input geometry and ice temperature profile. In order to test robustly whether the model provides a valid representation of calving would require improved input data so that the output might realistically be compared to observed terminus behaviour. The aquisition of such input data is challenging because the terminus of a fast-flowing tidewater glacier is an extremely difficult working environment, due to the highly fractured nature of the ice. Likewise, studies of the proglacial fjord are made difficult by the density of brash ice and icebergs. Other areas where improved observational records would significantly benefit this modelling project include basal

water pressure, the depth of crevasses and water in them.

Another possible method of validation would be to compare the distribution of calving event sizes produced by the model to observed data, but at present no record has either the number of observation or the high temporal resolution required for such a comparison. A high temporal and spatial resolution record of calving events would also provide the opportunity to attempt to identify different forcing mechanisms acting on the calving front by their influence on calving event size.

As with any model, a number of approximations have been made in this study, as discussed in Section 8.4.2. There are a number of areas where the model could be significantly improved:

- **Floating ice.** The application of the model so far has been limited as it is unable to represent floating ice. One of the advantages of the crevasse depth calving criterion is that it is valid for both floating and grounded ice, and the model's relevance could be significantly extended by including representation of floating ice.

- **Crevasse implementation.** This could include the use of linear elastic fracture mechanics to improve crevasse depth predictions, damage mechanics methods to trace fractures as the advect through the model and anisotropic flow properties to represent the effect of crevassing on flow dynamics.

- **Three dimensional modelling.** Although this would have high computational resource requirements, modelling in three dimensions would significantly improve the representation of lateral drag and flux in the model.

- **Parallelisation.** As described in Section 3.2.2, even using the automated calving script the model has a long running time, which could be significantly shortened if the python wrapper-code were developed to be run in parallel. This would be necessary if the model were to be extended to three dimensions as the memory requirements would become too high for a single processor. It

would also improve running speed for other experiments, and allow a greater range of experiments to be run in a short time.

- **Thermo-mechanical coupling.** The approximated ice temperature profile was the largest source of error in the model presented. This could be improved by implementing a thermo-mechanically coupled model. The software in Elmer/Ice has already been developed to allow thermo-mechanical coupling, but it would also require further development of the python wrapper-code used for the calving model.

- **Basal sliding**. The basal sliding law used has a strong dependence on basal water pressure. This is poorly represented in the model, as observed basal water pressures tend to be highly variable due to surface ablation, precipitation, supraglacial lake drainage events and changes in the basal drainage system. An improved implementation of basal water pressure would require improved observational data availability, but would significantly improve the validity of the model results.

The output of the model also has potential to be used to improve the representation of calving in ice sheet models. Although it is unlikely that an ice sheet model will be developed with the fine spatial resolution required to include a crevasse depth calving criterion such as that presented here, the flowline model could potentially be used to derive relationships between calving rate and external variables. These could be used to adjust the calving rate applied on the boundaries of ice sheet models which would improve the response of ice sheet models to environmental variables, and hence provide more accurate predictions of future behaviour.

References

Abdalati, W., Krabill, W., Frederick, E., Manizade, S., Martin, C., Sonntag, J., Swift, R., Thomas, R., Wright, W., and Yungel, J. (2001). Outlet glacier and margin elevation changes: Near-coastal thinning of the Greenland Ice Sheet. *Journal of Geophysical Research*, 106(D24):33729–33742.

Amundson, J. and Truffer, M. (2010). A unifying framework for iceberg-calving models. *Journal of Glaciology*, 56(199):822–30.

Amundson, J. M., Fahnestock, M., Truffer, M., Brown, J., Lüthi, M. P., and Motyka, R. (2010). Ice mélange dynamics and implications for terminus stability, Jakobshavn Isbræ, Greenland. *Journal of Geophysical Research*, 115(F01005).

Andersen, M., Larsen, T. B., Nettles, M., and others, . (2010). Spatial and temporal melt variability at Helheim Glacier, East Greenland, and its effect on ice dynamics. *Journal of Geophysical Research*, 115(F04041):doi:10.1029/2010JF001760.

Andersen, M., Nettles, M., Elosegui, P., Larsen, T. B., Hamilton, G. S., and Stearns, L. A. (2011). Quantitative estimates of velocity sensitivity to surface melt variations at a large Greenland outlet glacier. *Journal of Glaciology*, 57(204):609–620.

Andresen, C. S., Straneo, F., Ribergaard, M. H., Bjørk, A. A., Andersen, T. J., Kuijpers, A., Nørgaard-Pedersen, N. N., Kjær, K. H., Schjøth, F., Weckström, K., and Ahlstrøm, A. P. (2011). Rapid response of Helheim Glacier in Greenland to climate variability over the past century. *Nature Geoscience*, 5:37–41.

Bamber, J. L., Layberry, R., and Gogenini, S. (2001). A new ice thickness and bed

data set for the Greenland Ice Sheet 1: Measurement, data reduction, and errors. *Journal of Geophysical Research*, 106(D24):33773–33780.

Bartholomew, I., Niewnow, P., Muir, D., Hubbard, A., King, M. A., and Sole, A. (2010). Seasonal evolution of subglacial drainage and acceleration in a Greenland outlet glacier. *Nature Geoscience*, 3:408–411.

Bassis, J. (2011). The statistical physics of iceberg calving and the emergence of universal calving laws. *Journal of Glaciology*, 57(201):3–16.

Benn, D. I., Hulton, N. R. J., and Mottram, R. H. (2007a). 'Calving laws', 'sliding laws' and the stability of tidewater glaciers. *Annals of Glaciology*, 46:123–130.

Benn, D. I., Warren, C. R., and Mottram, R. H. (2007b). Calving processes and the dynamics of calving glaciers. *Earth-Science Reviews*, 82:143–179.

Bevan, S. L., Luckman, A., and Murray, T. (2012). Glacier dynamics over the last quarter of a century at Helheim, Kangerdlugssuaq and 14 other major Greenland outlet glaciers. *The Cryosphere*, 6:1637–1672.

Bindschadler, R. A. (1983). The importance of pressurized subglacial water in separation and sliding at the glacier bed. *Journal of Glaciology*, 29(101):3–19.

Bindschadler, R. A. and Rasmussen, L. A. (1983). Finite-difference model predictions of drastic retreat of Columbia Glacier, Alaska. U.S. Geological Survey Professional Paper 1258-D.

Blaszczyk, M., Jania, J. A., and Hagen, J. O. (2009). Tidewater glaciers of Svalbard: Recent changes and estimates of calving fluxes. *Polish Polar Research*, 30(2):85–142.

Box, J. E., Bromwich, D. H., and Bai, L. (2004). Greenland ice sheet surface mass balance 1991 – 2000: Application of Polar MM5 mesoscale model and in situ data. *Journal of Geophysical Research*, 109(D16105):doi:10.1029/2003JD004451.

Brown, C. S., Meier, M. F., and Post, A. (1982). Calving speed of Alaska tidewater glaciers with application to the Columbia Glacier, Alaska. U.S. Geological Survey Professional Paper 1258-C.

Budd, W. F. and Keage, P. L. (1979). Empirical studies of ice sliding. *Journal of Glaciology*, 23(89):157–170.

Christofferson, P., O'Leary, M., van Angelen, J. H., and van den Broeke, M. (2012). Partitioning effects from ocean and atmosphere on the calving stability of Kangerdlugssuaq Glacier, East Greenland. *Annals of Glaciology*, 53(60):249–256.

Church, J. A., Church, J. G., Huybrechts, P., Kuhn, M., Lambeck, C., Nhuan, M. T., Qin, D., and Woodworth, P. L. (2001). *Changes in sea level, in Climate Change 2001: The Scientific BasisContribution of Working Group I to the Third Assessment Report of the Intergovernmental Panel on Climate Change*. Cambridge University Press, New York.

Cook, A. J., Fox, A. J., Vaughan, D. G., and Ferrigno, J. G. (2005). Retreating glacier fronts on the Antarctic Peninsula over the past half-century. *Science*, 308(5721):541–544.

Cook, S., Zwinger, T., Rutt, I. C., O'Neel, S., and Murray, T. (2012). Testing the effect of water in crevasses on a physically based calving model. *Annals of Glaciology*, 53(60):90–96.

Cuffey, K. and Paterson, W. S. B. (2010). *The physics of glaciers, 4th edition*. Elsevier.

Dahl-Jensen, D., Mosegaard, K., Gundestrup, N., Johnsen, G. D. C. S. J., Hansen, A. W., and Balling, N. (1998). Past temperatures directly from the Greenland Ice Sheet. *Science*, 282(5387):268–271.

DiMarzio, J., Brenner, A., Schutz, R., Shuman, C. A., and Zwally, H. J. (2007). GLAS/ICESat 1 km laser altimetry digital elevation model of Greenland. Digital Media. Boulder, Colorado USA: National Snow and Ice Data Center.

Dowdeswell, J. A. (1989). On the nature of Svalbard icebergs. *Journal of Glaciology*, 35(120):224–234.

Engel, C. (2008). Defining basal geometry and force balance at Columbia Glacier, Alaska. Master's thesis, University of Colorado.

Fettweis, X. (2007). Reconstruction of the 1976 – 2006 Greenland ice sheet surface mass balance using the regional climate model MAR. *The Cryosphere*, 1:123–168.

Fettweis, X., Tedesco, M., van den Broeke, M., and Ettema, J. (2011). Melting trends over the Greenland ice sheet (1958-2009) from spaceborne microwave data and regional climate models. *The Cryosphere*, 5:359–375.

Fowler, A. C. (1987). Sliding with cavity formation. *Journal of Glaciology*, 33(115):255–267.

Frederking, R. M. W. and Timco, G. W. (1984). Measurement of shear strength of granular/discontinuous-columnar sea ice. *Cold Regions Science and Technology*, 9(3):215–220.

Funk, M., Echelmeyer, K., and Iken, A. (1994). Mechanisms of fast flow in Jakobshavn Isbræ, West Greenland: Part II. Modelling of englacial temperatures. *Journal of Glaciology*, 40(136):569–85.

Funk, M. and Röthlisberger, H. (1989). Forecasting the effects of a planned reservoir that will partially flood the tongue of Unteraargletscher in Switzerland. *Annals of Glaciology*, 13:76–80.

Gagliardini, O., Cohen, D., Råback, P., and Zwinger, T. (2007). Finite-element modeling of subglacial cavities and related friction law. *Journal of Geophysical Research*, 112:F02027.

Gagliardini, O. and Zwinger, T. (2008). The ISMIP-HOM benchmark experiments performed using the finite-element code Elmer. *The Cryosphere*, 2(1):67–76.

Glen, J. W. (1955). The creep of polycrystalline ice. *Proc. R. Soc. London, Ser. A*, 228(1175):519–538.

Hanson, B. and Hooke, R. L. (2000). Glacier calving: a numerical model of forces in the calving-speed/water-depth relation. *Journal of Glaciology*, 46(153):188–196.

Hanson, B. and Hooke, R. L. (2003). Buckling rate and overhang development at a calving face. *Journal of Glaciology*, 49(167):577–86.

Haresign, E. C. (2004). *Glacio-limnological interactions at lake-calving glaciers*. PhD thesis, University of St Andrews.

Hasholt, B. and Christiansen, H. (2003). Rock Temperatures, Sermilik, Southeast Greenland. Digital Media. Boulder, Colorado USA: National Snow and Ice Data Center.

Holland, D. M., Thomas, R. H., de Young, B., Ribergaard, M. H., and Lyberth, B. (2008). Acceleration of Jakobshavn Isbræ triggered by warm subsurface ocean waters. *Nature Geoscience*, 1:38–42.

Hooke, R. L. (2005). *Principles of glacier mechanics*. Cambridge University Press, 2nd edition.

Howat, I., Joughin, I., Fahnestock, M., Smith, B., and Scambos, T. (2008). Synchronous retreat and acceleration of southeast Greenland outlet glaciers 2000 – 06: ice dynamics and coupling to climate. *Journal of Glaciology*, 54(187):646–60.

Howat, I. M., Box, J. E., Ahn, Y., Herrington, A., and McFadden, E. M. (2010). Seasonal variability in the dynamics of marine-terminating outlet glaciers in Greenland. *Journal of Glaciology*, 56(198):601–613.

Howat, I. M., Joughin, I., and Scambos, T. A. (2007). Rapid changes in ice discharge from Greenland outlet glaciers. *Science*, 315(5818):1559–1561.

Howat, I. M., Joughin, I., Tulaczyk, S., and Gogineni, S. (2005). Rapid retreat and acceleration of Helheim Glacier, East Greenland. *Geophysical Research Letters*, 32:L22502.

Hughes, T. (1992). Theoretical calving rates from glaciers along ice walls grounded in water of variable depths. *Journal of Glaciology*, 38(129):282–294.

Humphrey, N., Kamb, B., Fahnestock, M., and Engelhardt, H. (1993). Characteristics of the bed of the lower Columbia Glacier, Alaska. *Journal Geophysical Research*, 98(B1):837–846.

Iken, A. (1977). Movement of a large ice mass before breaking off. *Journal of Glaciology*, 19(8):595–604.

Johnsen, S. J., Dahl-Jensen, D., Dansgaard, W., and Gundestrup, N. (1995). Greenland palaeotemperatures derived from GRIP borehole temperature and ice core isotope profiles. *Tellus*, 47B:624–629.

Joughin, I., Abdalati, W., and Fahnestock, M. (2004). Large fluctuations in speed on Greenland's Jakobshavn Isbræ glacier. *Nature*, 432(7017):608–610.

Joughin, I., Das, S. B., King, M. A., Smith, B. E., Howat, I. M., and Moon, T. (2008a). Seasonal speedup along the western flank of the Greenland Ice Sheet. *Science*, 320:781–783.

Joughin, I., Howat, I., Alley, R. B., Eckstrom, G., Fahnestock, M., Moon, T., Nettles, M., Truffer, M., and Tsai, V. C. (2008b). Ice-front variation and tidewater behaviour on Helheim and Kangerdlugssuaq Glaciers, Greenland. *Journal of Geophysical Research*, 113:F01004.

Joughin, I., Howat, I. M., Fahnestock, M., Smith, B., Krabill, W., Alley, R. B., Stern, H., and Truffer, M. (2008c). Continued evolution of Jakobshavn Isbræ following its rapid speed up. *Journal Geophysical Research*, 113:F04006.

Joughin, I. and MacAyeal, D. R. (2005). Calving of large tabular icebergs from ice shelf rift systems. *Geophysical Research Letters*, 32(L02501):doi:10.1029/2004GL020978.

Jouvet, G., Picasso, M., Rappaz, J., Huss, M., and Funk, M. (2011). Modelling and numerical simulation of the dynamics of glaciers including local damage effects. *Mathematical modelling of natural phenomena*, 6(5):263–280.

Kagan, B. A. (1995). *Ocean-atmosphere interaction and climate modelling*. Cambridge University Press Atmospheric and Space Science Series.

Kamb, B., Engelhardt, H., Fahnestock, M. A., Humphrey, N., Meier, M., and Stone, D. (1994). Mechanical and hydrological basis for the rapid motion of a large tidewater glacier 2. Interpretation. *Journal of Geophysical Research*, 99(B8):15231–15244.

Kirkbride, M. P. and Warren, C. R. (1997). Calving processes at a grounded ice cliff. *Annals of Glaciology*, 24:116–121.

Krimmel, R. (2001). Photogrammetric data set, 1957-2000 and bathymetric measurements for Columbia Glacier, Alaska. USGS Water-Resour. Invest. Rep. 01-4089.

Larour, E., Seroussi, H., Morlighem, M., and Rignot, E. (2012). Continental scale, high order, high spatial resolution ice sheet modeling using the Ice Sheet System Model (ISSM). *Journal Geophysical Research*, 117(F01022):doi:10.1029/2011JF002140.

Larsen, C. F., Motyka, R. J., Arendt, A. A., Echelmeyer, K. A., and Geissler, P. E. (2007). Glacier changes in southeast Alaska and northwest British Columbia and contribution to sea level rise. *Journal of Geophysical Research*, 112(F01007):doi:10.1029/2006JF000586.

Lee, J., Jin, Y. K., Hong, J. K., Yoo, H. J., and Shon, H. (2008). Simulation of a tidewater glacier evolution in Marian Cove, King George Island, Antarctica. *Geosciences Journal*, 12(1):33–39.

Leuschen, C., Allen, C., Gogineni, P., Rodriguez, F., Paden, J., and Li, J. (2011). IceBridge MCoRDS L3 Gridded Ice Thickness, Surface, and Bottom. Digital Media. Boulder, Colorado USA: National Snow and Ice Data Center.

Levermann, A., Albrecht, T., Winkelmann, R., Martin, M. A., Haseloff, M., and Joughin, I. (2012). Kinematic first-order calving law implies potential for abrupt ice-shelf retreat. *The Cryosphere*, 6:273–286.

Lliboutry, L. (1958). Contribution á la théorie du frottement du glacier sur son lit. *Comptes rendus Hebdomadaires des Séances de l'Académie des Sciences*, 247(3):318320.

Luckman, A., Murray, T., de Lange, R., and Hanna, E. (2006). Rapid and synchronous ice-dynamic changes in East Greenland. *Geophysical Research Letters*, 33(3).

Mansell, D., Luckman, A., and Murray, T. (2012). Dynamics of tidewater surge-type glaciers in northwest Svalbard. *Journal of Glaciology*, 58(207):110–118.

Martin, M. A., Winkelmann, R., Haseloff, M., Albrecht, T., Bueler, E., Khroulev, C., and Levermann, A. (2011). The Potsdam Parallel Ice Sheet Model (PISM-PIK) Part 2: Dynamic equilibrium simulation of the Antarctic ice sheet. *The Cryosphere*, 5:727–740.

Meier, M., Lundstrom, S., Stone, D., Kamb, B., Engelhardt, H., Humphrey, N., Dunlap, W., Fahnestock, M., Krimmel, R., and Walters, R. (1994). Mechanical and hydrological basis for the rapid motion of a large tidewater glacier 1. Observations. *Journal of Geophysical Research*, 99(B8):15219–229.

Meier, M. F. and Post, A. (1987). Fast tidewater glaciers. *Journal of Geophysical Research*, 92:9051–9058.

Mernild, S. H., Howat, I. M., Ahn, Y., Liston, G. E., Steffen, K., Jakobsen, B. H., Hasholt, B., Fog, B., and van As, D. (2010). Freshwater flux to Sermilik Fjord, SE Greenland. *The Cryosphere*, 4:453–465.

Mottram, R. and Benn, D. (2009). Testing crevasse-depth models: a field study at Breiamerkulljökull, Iceland. *Journal of Glaciology*, 55(192):746–752.

Motyka, R. J., Hunter, L., Echelmeyer, K. A., and Connor, C. (2003). Submarine melting at the terminus of a temperate tidewater glacier, LeConte Glacier, Alaska, U.S.A. *Annals of Glaciology*, 36:57–65.

Murray, T., Scharrer, K., James, T., Dye, S., Hanna, E., Booth, A., Selmes, N., Luckman, A., Hughes, A., Cook, S., and Huybrechts, P. (2010). Ocean regulation hypothesis for glacier dynamics in southeast Greenland and implications for ice sheet mass changes. *Journal of Geophysical Research*, 115(F03026).

Nick, F., van der Veen, C., Vieli, A., and Benn, D. (2010). A physically based calving model applied to marine outlet glaciers and implications for the glacier dynamics. *Journal of Glaciology*, 56(199):781–794.

Nick, F. M. and Oerlemans, J. (2006). Dynamics of tidewater glaciers: comparison of three models. *Journal of Glaciology*, 52(177):183–190.

Nick, F. M., van der Kwast, J., and Oerlemans, J. (2007a). Simulation of the evolution of Breidamerkurjökull in the late Holocene. *Journal of Geophysical Research*, 112(B01103).

Nick, F. M., van der Veen, C. J., and Oerlemans, J. (2007b). Controls on advance of tidewater glacier: Results from numerical modelling applied to Columbia Glacier. *Journal of Geophysical Research*, 112.

Nick, F. M., Vieli, A., Howat, I. M., and Joughin, I. (2009). Large-scale changes in Greenland outlet glacier dynamics triggered at the terminus. *Nature Geoscience*, 2(2):110–114.

Noll, G. (2005). Report of equipment and methods to accompany data from project OPR-P132-RA-05, Eastern Prince William Sound, AK. Columbia Bay Hydrographic Survey Sheets H11493 & H11494, National Oceanographic and Atmospheric Administration.

Nye, J. (1955). Correspondence. Comments on Dr. Loewes letter and notes on crevasses. *Journal of Glaciology*, 2(17):512–514.

Nye, J. (1957). The distribution of stress and velocity in glacier and ice-sheets. *Proceedings of the Royal Society London, Series A*, 239(1216):113–133.

Oerlemans, J. (2001). *Glaciers and climate change*. Taylor and Francis.

Oerlemans, J. and Nick, F. (2005). A minimal model of a tidewater glacier. *Annals of Glaciology*, 42(1):1–6.

Oerlemans, J. and Nick, F. M. (2006). Modelling the advance-retreat cycle of a tidewater glacier with simple sediment dynamics. *Global and Planetary Change*, 50:148–160.

O'Leary, M. (2011). *Frontal processes on tidewater glaciers*. PhD thesis, University of Cambridge.

O'Neel, S., Echelmeyer, K. A., and Motyka, R. J. (2003). Short-term variations in the calving of a tidewater glacier: LeConte Glacier, Alaska, U.S.A. *Journal of Glaciology*, 49(167):587–598.

O'Neel, S., Pfeffer, W. T., Krimmel, R., and Meier, M. (2005). Evolving force balance at Columbia Glacier, Alaska during its rapid retreat. *Journal of Geophysical Research*, 110:F03012.

Otero, J., Navarro, F., Martin, C., Cuadrado, M., and Corcuera, M. (2010). A three-dimensional calving model: numerical experiments on Johnsons Glacier, Livingston Island, Antarctica. *Journal of Glaciology*, 56(196):200–214.

Paterson, W. (1994). *The Physics of Glaciers. Third Edition.* Oxford, etc., Elsevier.

Pattyn, F., Perichon, L., Aschwanden, A., Breuer, B., de Smedt, B., Gagliardini, O., Gudmundsson, G. H., Hindmarsh, R., Hubbard, A., Johnson, J. V., Kleiner, T., Konovalov, Y., Martin, C., Payne, A. J., Pollard, D., Price, S., Ruckamp, M., Saito, F., Soucek, O., Sugiyama, S., and Zwinger, T. (2008). Benchmark experiments for higher-order and full Stokes ice sheet models (ISMIP-HOM). *The Cryosphere*, 2:111151.

Pelto, M. S. and Warren, C. R. (1991). Relationship between tidewater glacier calving velocity and water depth at the calving front. *Annals of Glaciology*, 15:115–118.

Pralong, A. and Funk, M. (2005). Dynamic damage model of crevasse opening and application to glacier calving. *Journal of Geophysical Research*, 110(B01309).

Pralong, A., Funk, M., and Lüthi, M. P. (2003). A description of crevasse formation using continuum damage mechanics. *Annals of Glaciology*, 37:77–82.

Pritchard, H. D., Arthern, R. J., Vaughan, D. G., and Edwards, L. A. (2009). Extensive dynamic thinning on the margins of the Greenland and Antarctic ice sheets. *Nature*, 461:971–975.

Pritchard, H. D., Ligtenberg, S. R. M., Fricker, H. A., Vaughan, D. G., van den Broecke, M. R., and Padman, L. (2012). Antarctic ice-sheet loss driven by basal melting of ice shelves. *Nature*, 484:502–505.

Pritchard, H. D. and Vaughan, D. G. (2007). Widespread acceleration of tidewater glaciers on the Antarctic Peninsula. *Journal of Geophysical Research*, 112(doi:10.1029/2006JF000597):F03S29.

Rasmussen, L. A. (1989). Surface velocity variations of the lower part of Columbia Glacier, Alaska, 1977-1981. USGS Professional Paper 1258-H.

Rasmussen, L. A. and Meier, M. F. (1985). Surface topography of the lower part of Columbia Glacier, Alaska, 1974-1981. USGS Professional Paper 1258-E.

Reeh, N., Thomsen, H. H., Higgins, A. K., and Weidick, A. (2001). Sea ice and the stability of north and northeast Greenland floating glaciers. *Annals of Glaciology*, 33:474–480.

Rignot, E., Braaten, D., Gogineni, S. P., Krabill, W. B., and McConnell, J. R. (2004). Rapid ice discharge from southeast Greenland glaciers. *Geophysical Research Letters*, 31(doi:10.1029/2004GL019474):L10401.

Rignot, E. and Jacobs, S. S. (2002). Rapid bottom melting widespread near Antarctic Ice Sheet grounding lines. *Science*, 296(5575):2020–2023.

Rignot, E. and Kanagaratnam, P. (2006). Changes in the velocity structure of the Greenland Ice Sheet. *Science*, 311:986–990.

Rignot, E., Koppes, M., and Velicogna, I. (2010). Rapid submarine melting of the calving faces of West Greenland glaciers. *Nature Geoscience*, 3:187–191.

Rignot, E. and Thomas, R. H. (2002). Mass balance of polar ice sheets. *Science*, 297(5586):1502–1506.

Schoof, C. (2005). The effect of cavitation on glacier sliding. *Proceedings of the Royal Society London, Series A*, 461(2055):609–627.

Seale, A., Christofferson, P., Mugford, R. I., and O'Leary, M. (2011). Ocean forcing of the Greenland Ice Sheet: Calving fronts and patterns of retreat identified by automatic satellite monitoring of eastern outlet glaciers. *Journal of Geophysical Research*, 116(F03013):doi:10.1029/2010JF001847.

Sikonia, W. G. (1982). Finite element glacier dynamics model applied to Columbia Glacier, Alaska. USGS Professional Paper 1258-B.

Smith, L. M. and Andrews, J. T. (2000). Sediment characteristics in iceberg dominated fjords, Kangerlussuaq region, East Greenland. *Sedimentary Geology*, 130:11–25.

Smith, R. A. (1976). The application of fracture mechanics to the problem of crevasse penetration. *Journal of Glaciology*, 17:223–228.

Sohn, H.-G., Jezek, K. C., and van der Veen, C. (1998). Jakobshavn Glacier, West Greenland: 30 years of spaceborne observations. *Geophysical Research Letters*, 25(14):2699–2702.

Sole, A. J., Mair, D. W. F., Nienow, P. W., Bartholomew, I. D., King, M. A., Burke, M. J., and Joughin, I. (2011). Seasonal speedup of a Greenland marine-terminating outlet glacier forced by surface melt – induced changes in subglacial hydrology. *Journal Geophysical Research*, 116(F03014):doi:10.1029/2010JF001948.

Sorensen, L. S., Simonsen, S. B., Nielsen, K., Lucas-Picher, P., Spada, G., Adalgeirsdottir, G., Forsberg, R., and Hvidberg, C. S. (2011). Mass balance of the

Greenland ice sheet (2003 – 2008) from ICESat data the impact of interpolation, sampling and firn density. *The Cryosphere*, 5:173–186.

Straneo, F., Curry, R. G., Sutherland, D. A., Hamilton, G. S., Cenedese, C., Våge, K., and Stearns, L. A. (2011). Impact of fjord dynamics and glacial runoff on the circulation near Helheim Glacier. *Nature Geoscience*, 4:322–327.

Straneo, F., Hamilton, G. S., Sutherland, D. A., Stearns, L. A., Davidson, F., O'Hammill, M., Stenson, G. B., and Rosing-Asvid, A. (2010). Rapid circulation of warm subtropical waters in a major glacial fjord in East Greenland. *Nature Geoscience*, 3(33):182–186.

Sutherland, D. A. and Straneo, F. (2012). Estimating ocean heat transports and submarine melt rates in Sermilik Fjord, Greenland, using lowered acoustic Doppler current profiler (LADCP) velocity profiles. *Annals of Glaciology*, 53(60):50–58.

Tangborn, W. (1997). Using low-altitude meteorological observations to calculate the mass balance of Alaska's Columbia and relate it to calving and speed. In *Calving Glaciers: Report of a Workshop, February 28-March 2, 1997, BPRC Rep. 15*, pages 14–161. Byrd Polar Research Center, Ohio State University, Columbus.

Thomas, R. (2004). Force-perturbation analysis of recent thinning and acceleration of Jakobshavn Isbræ, Greenland. *Journal of Glaciology*, 50(168):57–66.

Thomas, R., Frederick, E., Krabill, W., Manizade, S., and Martin, C. (2009). Recent changes on Greenland outlet glaciers. *Journal of Glaciology*, 55(189):147–162.

van der Veen, C. (1998). Fracture mechanics approach to penetration of surface crevasses on glaciers. *Cold Regions Science and Technology*, 27:31–47.

van der Veen, C. J. (1996). Tidewater calving. *Journal of Glaciology*, 42(141):375–385.

van der Veen, C. J. (2002). Calving glaciers. *Progress in Physical Geography*, 26(1):96–122.

Venteris, E. R. (1999). Rapid tidewater glacier retreat: a comparison between Columbia Glacier, Alaska and Patagonian calving glaciers. *Global and Planetary Change*, 22:131–138.

Vieli, A., Funk, M., and Blatter, H. (2000). Tidewater glaciers: frontal flow acceleration and basal sliding. *Annals of Glaciology*, 31:217–221.

Vieli, A., Funk, M., and Blatter, H. (2001). Flow dynamics of tidewater glaciers: a numerical modelling approach. *Journal of Glaciology*, 47(159):595–606.

Vieli, A., Jania, J., and Kolondra, L. (2002). The retreat of a tidewater glacier: observations and model calculations on Hansbreen, Spitsbergen. *Journal of Glaciology*, 48:592–600.

Vieli, A. and Nick, F. (2011). Understanding and modelling rapid dynamic changes of tidewater outlet glaciers: issues and implications. *Surveys in Geophysics*, 32(4-5):437–458.

Vieli, A., Payne, A. J., Du, Z., and Shepherd, A. (2006). Numerical modelling and data assimilation of the Larsen B ice shelf, Antarctic Peninsula. *Phil. Trans. R. Soc.*, 364:1815–1839.

Walter, F., O'Neel, S., McNamara, D., Pfeffer, T., Bassis, J., and Fricker, H. (2010). Iceberg calving during transition from grounded to floating ice: Columbia Glacier, Alaska. *Geophysical Research Letters*, 37(1):L15501.

Walter, J. I., Box, J. E., Tulaczyk, S., Brodsky, E. E., Howat, I. M., Ahn, Y., and Brown, A. (2012). Oceanic mechanical forcing of a marine-terminating Greenland glacier. *Annals of Glaciology*, 53(60):181–192.

Weertman, J. (1957). On the sliding of glaciers. *Journal of Glaciology*, 3(21):33–38.

Xu, Y., Rignot, E., Menemenlis, D., and Koppes, M. (2012). Numerical experiments on subaqueous melting of Greenland tidewater glaciers in response to ocean warming and enhanced subglacial discharge. *Annals of Glaciology*, 53(60):229–234.

Zwally, H. J., Abdalati, W., Herring, T., Larson, K., Saba, K., and Steffen, K. (2002). Surface melt-induced acceleration of Greenland Ice-Sheet flow. *Science*, 297(5579):218–222.

Zwinger, T., Greve, R., Gagliardini, O., Shiraiwa, T., and Lyly, M. (2007). A full Stokes-flow thermo-mechanical model for firn and ice applied to the Gorshkov crater glacier, Kamchatka. *Annals of Glaciology*, 45(1):29–37.

Zwinger, T. and Moore, J. (2009). Diagnostic and prognostic simulations with a full Stokes model accounting for superimposed ice of Midtre Lovenbreen, Svalbard. *The Cryosphere*, 3:217–229.